

NASA Contractor Report 145281

Expansion of Flight Simulator Capability for Study and Solution of Aircraft Directional Control Problems on Runways — Appendixes

J. A. McGowan

McDonnell Douglas Corporation

Douglas Aircraft Company

CONTRACT NAS1-13981
JANUARY 1978



National Aeronautics and
Space Administration

Langley Research Center
Hampton, Virginia 23665

NASA CR-145281

EXPANSION OF FLIGHT SIMULATOR
CAPABILITY FOR STUDY AND SOLUTION
OF AIRCRAFT DIRECTIONAL CONTROL
PROBLEMS ON RUNWAYS

APPENDIXES

20 JANUARY 1978

PREPARED UNDER CONTRACT NO. NAS1-13981

FOR



LANGLEY RESEARCH CENTER
NATIONAL AERONAUTICS AND SPACE ADMINISTRATION
LANGLEY STATION, HAMPTON, VIRGINIA

MCDONNELL DOUGLAS CORPORATION
DOUGLAS AIRCRAFT COMPANY
LONG BEACH, CALIFORNIA

ii
Blank

TABLE OF CONTENTS

| | PAGE |
|--|------|
| CONVERSION FACTORS | iv |
| INTRODUCTION | 1 |
| APPENDIX A - Aircraft Simulation | 2 |
| Section 1 - Basic Airframe Equations of Motion | 7 |
| Section 2 - Aerodynamic and Control System Models | 23 |
| Section 3 - Engine Model. | 75 |
| Section 4 - Environmental Models | 79 |
| Section 5 - Struts Subroutine Implementation Notes | 85 |
| Section 6 - Auxiliary Equations | 111 |
| APPENDIX B - Software Antiskid | 122 |
| APPENDIX C - Analog/Hardware Antiskid | 125 |
| Section 1 - Introduction | 125 |
| Section 2 - Model Derivation | 127 |
| Section 3 - Program | 156 |
| Section 4 - Hardware | 161 |
| Section 5 - Analog Antiskid Simulator Validation | 203 |
| APPENDIX D - Cockpit Simulator | 209 |
| APPENDIX E - Programming Considerations | 216 |
| REFERENCES | 219 |

CONVERSION FACTORS

The following table gives conversion factors from the English system to SI units for those quantities used in this report.

The sign and first two digits of each numerical entry represent a power of 10.

| TO CONVERT FROM | TO | MULTIPLY BY |
|-------------------------------|---------------------------|--------------------------|
| Fahrenheit (temperature) | Celsius | $t_c = (5/9) (t_f - 32)$ |
| Foot | Meter | -01 3.048 |
| Inch | Meter | -02 2.54 |
| Knot (international) | Meter/Second | -01 5.144 444 |
| Mile (U.S. Statue) | Meter | +03 1.609 344 |
| Mile (U.S. Nautical) | Meter | +03 1.852 |
| Pound Force (lbf avoirdupois) | Newton | +00 4.448 222 |
| Slug | Kilograms | +01 1.459 390 |
| Foot/Second ² | Meter/Second ² | -01 3.048 |
| Free Fall, Standard (g's) | Meter/Second ² | +00 9.806 65 |
| Foot ² | Meter ² | -02 9.290 304 |
| lbf/Foot ² | Newton/Meter ² | +01 4.788 026 |
| psi(lbf/Inch ²) | Newton/Meter ² | +03 6.894 757 |
| Foot/second | Meter/Second | -01 3.048 |

The foregoing values were taken from Reference 11. Some of the values were rounded to six digits after the decimal point.

INTRODUCTION

The intention of this report is to present the models used implementing the DC-9-10 aircraft simulation for the Runway Direction Control study. The study was done on the Douglas Aircraft six-degree-of-freedom motion simulator at Long Beach.

The approach taken in documenting the models has been to describe them in algebraic form, to the extent possible. Furthermore, the effort has been directed toward presenting what was actually done rather than general forms.

The following Douglas personnel contributed to this report: P. L. Jernigan and R. E. Adams of the Systems Simulation group; G. W. Kibbee, R. A. Storley and R. P. Schiltz of Hydro-Mechanical group; and E. F. Admiral of Avionics group.

APPENDIX A
AIRCRAFT SIMULATION

The DC-9-10 aircraft was simulated using math models derived from information supplied by Aero Stability and Control, Power Plant and Hydro-Mechanical Controls groups. The supplied data was combined with classical kinematic and transformation equations to form the airframe model. The calculation flow of the airframe model is shown in Figure 1.

In developing the model it was assumed that the flight envelope would be in the low speed (mach 0-.3) and low altitude (0-500 feet) region. Also, since the runs were to be short (i.e., approach, landing and roll out), the aircraft weight was assumed to be constant and the C.G. position fixed at 25% MAC.

Three basic axes systems are used to represent the relative motions and orientations of the aircraft. The inertial system (called earth axes) has its origin at the "touchdown" point of the runway (see Figure 2). For the ground handling simulation the touchdown point was chosen to be 1000 feet in from the threshold. Another axes system called the Aircraft Body Axes System has its origin at the C.G. of the aircraft. (See Figure 3.) The sign conventions for these axes systems are as follows:

- X body axis velocity positive forward
- X earth axis velocity positive toward runway and position positive beyond touchdown point
- Y body axis velocity positive to right
- Y earth axis velocity positive to the right and position positive to the right
- Z body axis velocity positive down (negative up)
- Z earth axis velocity negative up and position negative above ground.

A third axes system used is called the Stability Axes. This system is closely related to the body axes system but is aligned with the longitudinal wind vector rather than the body of the aircraft. The stability axes are used in defining most of the aerodynamic data.

Validation of the aircraft simulation was accomplished in three phases. First, the individual sections (aero, engine, etc.) were checked to see that they were statically correct. Secondly, to the extent possible, the various models were checked dynamically using inputs which produce transient responses. These responses, recorded as time histories, were then compared with expected responses. Where direct time histories were not available comparative parameters such as frequency and time to damp were used.

The third phase of validation was to have test pilots familiar with the DC-9-10 aircraft "fly" the simulator through various maneuvers. Their comments were used to adjust some parameters to improve the "feel" of the simulation.

The data collected during some of the validation runs and the associated comparative data is part of the file of rolled charts and is labeled Validation Data.

For convenience the description of the aircraft simulation has been divided into six sections. Sections 1 and 2 cover aerodynamics and equations of motion; Section 3 describes the engine model used; Section 4 explains the environmental model (winds, and runway conditions); Section 5 covers the landing gear but does not include the antiskid system which is described in Appendices B and C; and Section 6 picks up other programs such as instrument drives, motion drives, visual system drives, etc.

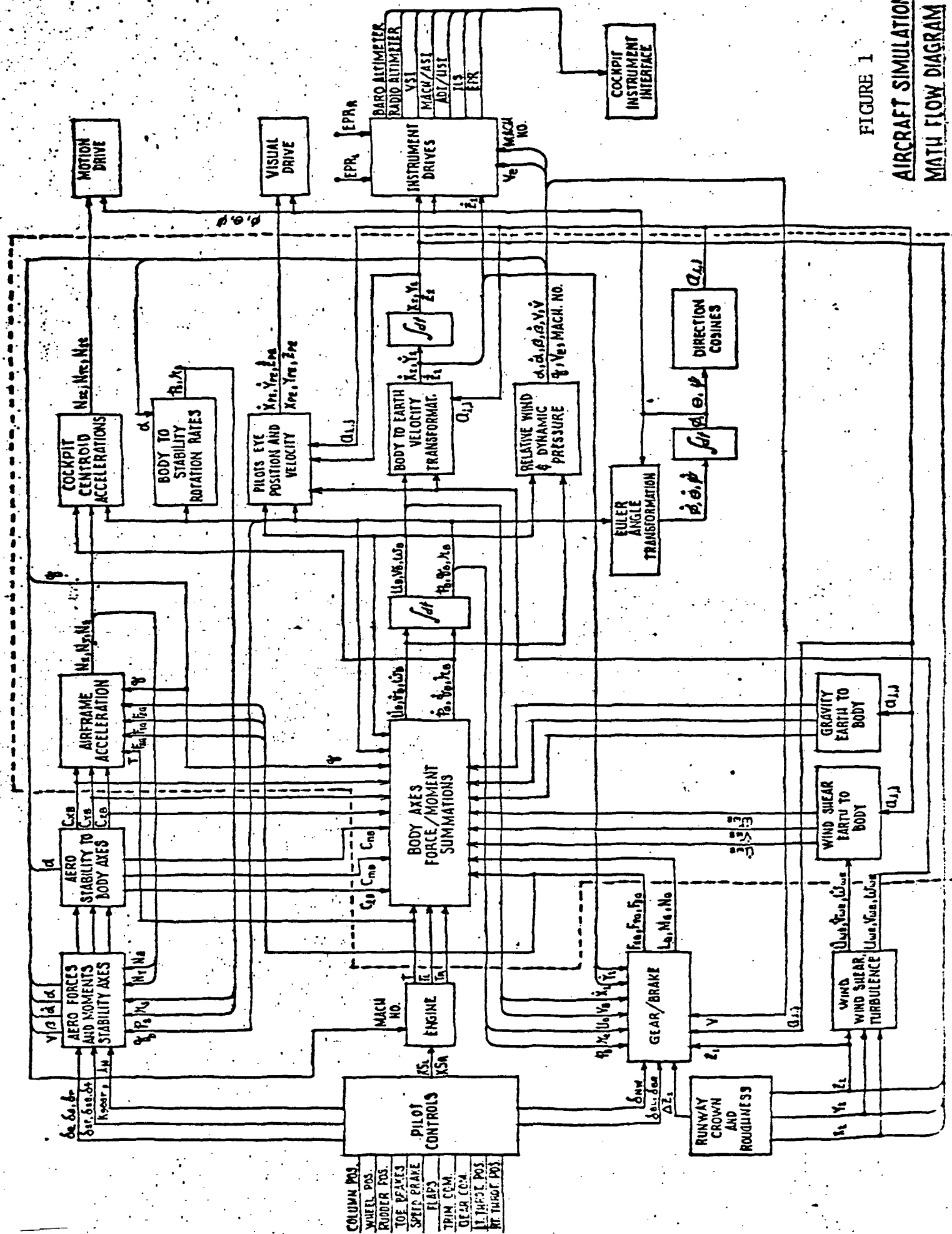
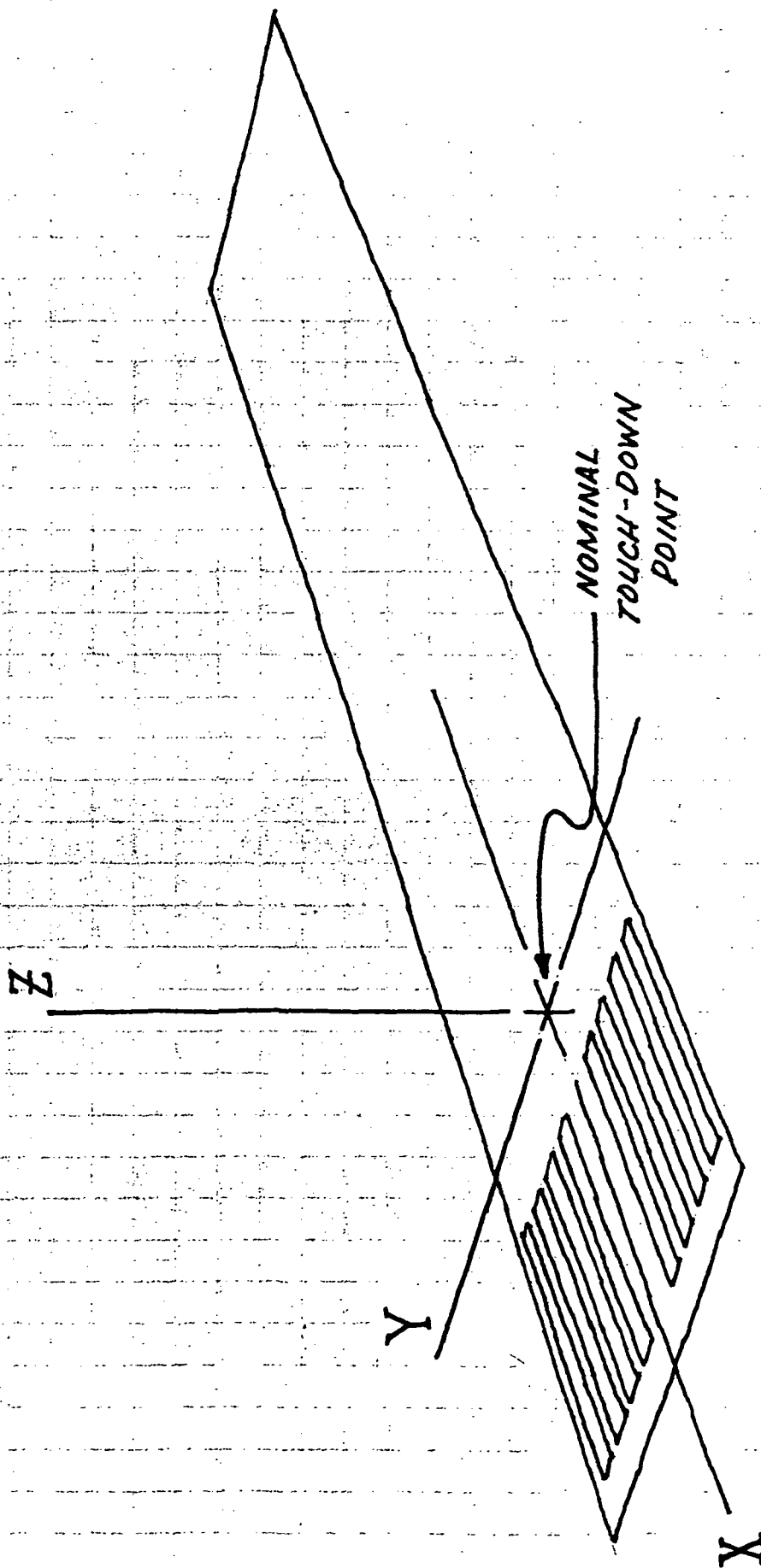


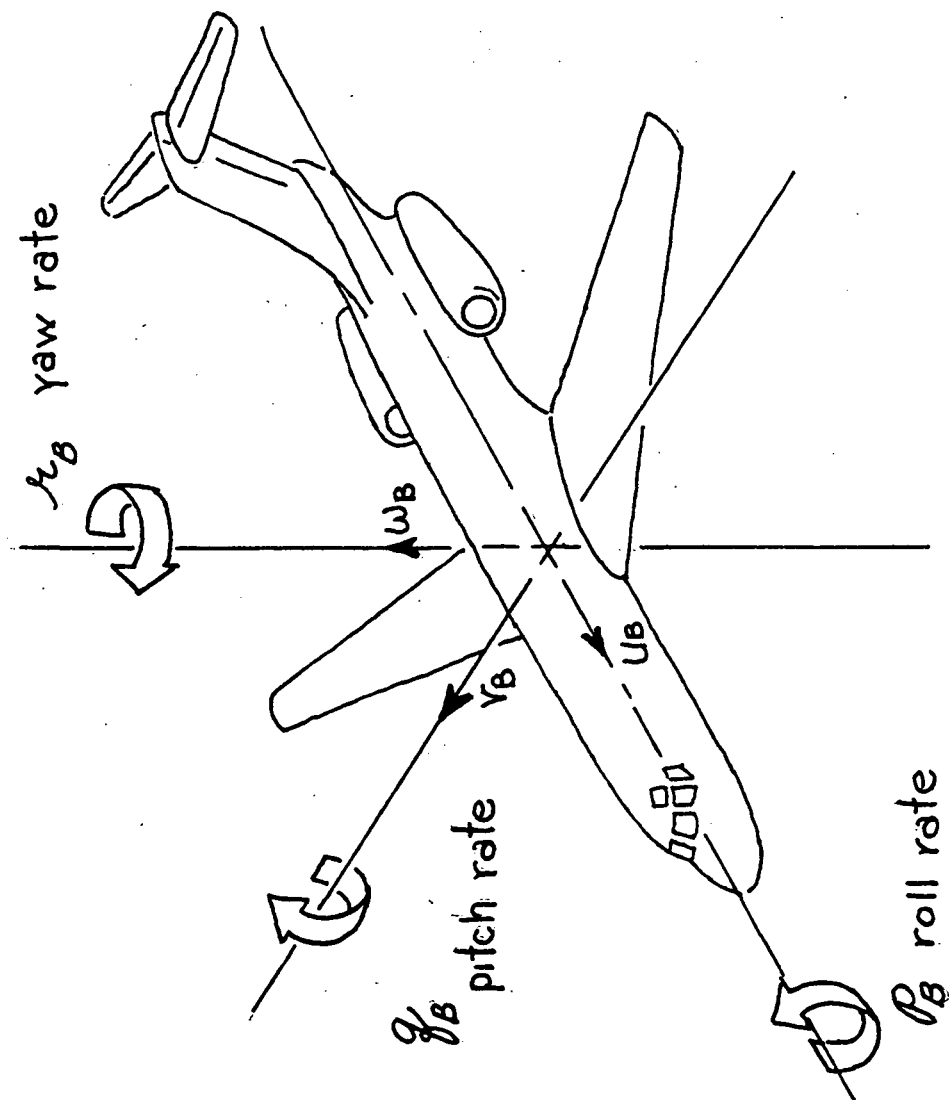
FIGURE 1

**AIRCRAFT SIMULATION
MATH FLOW DIAGRAM**



EARTH AXES

FIG. 2



AIRCRAFT BODY AXES

FIG. 3

Section 1

Basic Airframe Equations of Motion

The calculations covered in the Equations of Motion (EOM) are those which form the six independent variables of the airframe system and perform the appropriate axes transformations between the three axes systems used. Basically these equations are those needed to describe the motions of any rigid body. The derivations of these equations are covered in almost any text on aerodynamics or rigid body dynamics. Looking at Figure 1, this section covers all the boxes enclosed by the dashed line.

The associated equations for the EOM boxes are shown in Figures 1.1 - 1.9. Table 1.1 has descriptions of all the symbols used.

The EOM used for the Ground Handling Simulation are essentially the same for any aircraft using the same axes systems. The documentation of the equations should be fairly self sufficient, however, there are a few things that might be mentioned.

The 57.3 and $1/57.3$ factors show up because it was desired to have the angular state variables in units of degrees rather than radians. The method employed is to assume the angles to be in degrees and convert them back to radians for summation into the force and moment equations. The results of the summations are then converted back to degrees!

In Figure 1.4 the $1/1.69$ factor in the V_e equation is the ratio of knots to feet per sec. It is more convenient to have V_e in units of knots.

The fact that weight and C.G. position were constant in this simulation meant that mass, moments of inertia, and the lever arms only had to be calculated once at initialization and remained constant during real time runs.

These EOM are designed to handle winds and wind shears, i.e., time-rate-of-change of wind speed and/or direction. This is accomplished by first defining the wind profile in the inertial (earth) axes system. The steady state part of the wind components are then summed directly onto the inertial velocities. The time-rate-of-change parts are transformed to the body axes and summed directly into the force equations. (See Figures 1.1 and 1.7). This method allows a very versatile representation of the wind conditions without sacrificing the true inertial effects of a changing wind vector on the aircraft dynamics.

It should be noted that although a transformation matrix (direction cosines) is defined, and its elements are mentioned, the EOM program uses no matrix type operations. Using the individual matrix elements streamlines the calculations by eliminating any operation where the result would be zero anyway, e.g., the gravity vector transformation into the body axes.

Validation of the EOM program consisted mainly of checking to see that the proper parameters were entered for the DC-9-10. Further tests and check runs were not made on the EOM themselves for two reasons. First, this program has been used, in almost the same form, for numerous other transport type airframe simulations. Since the changes to the EOM for the DC-9-10 were minor it was felt that any more extensive checking would not be productive. Second, and foremost, the EOM are an integral part of the whole dynamic airframe simulation. For this reason it was felt that it would be more cost effective to validate the system as a whole and only do a detailed check if it was indicated. (Which, as it turned out, it was not.)

SYMBOL TABLE EQUATIONS OF MOTION
TABLE 1.1

| ALGEBRAIC SYMBOL | | DESCRIPTION | UNITS |
|--|---|--|----------------------|
| C_{NB} | CNB | COEFFICIENT OF YAWING MISMATCH BODY AXIS | UNITLESS |
| T, T_L, T_R | THT, THL, THR | TOTAL THRUST, LEFT AND RIGHT ENGINE THRUST | lbs |
| $\dot{\zeta}_T$ | - | ANGLE BETWEEN THRUST VECTOR AND PROP POSITIVE UP | deg |
| $F_{X_G}, F_{Y_G}, F_{Z_G}$ | F _{XG} , F _{YG} , F _{ZG} | FORCE DUE TO GRAV ALONG X, Y AND Z BODY AXES | lbs |
| L_G, M_G, N_G | ROLL PMG, YAWG | MOMENTS DUE TO GRAV ABOUT X, Y AND Z BODY AXES | ft-lb |
| I_x, I_y, I_z, I_{xz} | XIX, XIY, XIIZ, XIXZ | AIRCRAFT MOMENTS OF INERTIA BODY AXES | slug-ft ² |
| Z_{TCG} | ZCG | DISTANCE FROM CENTER OF THRUST TO C.G. | ft |
| C_w | CW | WING MEAN AERO DYNAMIC CHORD (MAC) | ft |
| $\dot{C}_{WB}, \dot{C}_{WBg}, \dot{C}_{WBg}$ | UDW, VDW, WDW | WIND SHEAR TERMS FOR X, Y AND Z BODY AXES | ft/sec ² |
| b_w | BW | WING SPAN | ft |
| Y_T | - | LATERAL DISTANCE FROM AIRCRAFT CENTER LINE TO CENTER OF THRUST | ft |

SYMBOL TABLE EQUATIONS OF MOTION

TABLE 1.1 (CONT.)

| ALGEBRAIC SYMBOL | | DESCRIPTION | UNITS |
|------------------|-----------------|---|---------------------|
| U_B, V_B, W_B | U_B, V_B, W_B | VELOCITY COMPONENTS ALONG THE X, Y, AND Z BODY AXES | ft/sec |
| P_B, Q_B, R_B | P_B, Q_B, R_B | ANGULAR VELOCITIES ABOUT THE X, Y AND Z BODY AXES | deg/sec |
| $S_{T,3}$ | RTD | NUMBER OF DEGREES PER RADIAN | |
| g | - | LOCAL ACCELERATION OF GRAVITY (NOMINALLY 32.2) | ft/sec ² |
| $a_{i,j}$ | $AT(i, j)$ | ELEMENT OF THE TRANSFORMATION MATRIX (DIRECTION COSINE) | UNITLESS |
| M | X_{MASS} | AIRCRAFT MASS | SLUGS |
| q | q | DYNAMIC PRESSURE | lb/ft ² |
| S_w | S_w | WING AREA | ft ² |
| C_{x_B} | C_{x_B} | COEFFICIENT OF DRAG BODY AXIS | UNITLESS |
| C_{y_B} | C_{y_B} | COEFFICIENT OF SIDE FORCE BODY AXIS | " |
| C_{z_B} | C_{z_B} | COEFFICIENT OF LIFT BODY AXIS | " |
| C_{l_B} | C_{l_B} | COEFFICIENT OF ROLLING MOMENT BODY AXIS | " |
| C_{m_B} | C_{m_B} | COEFFICIENT OF PITCHING MOMENT BODY AXIS | " |

SYMBOL TABLE EQUATIONS OF MOTION
TABLE 11 (CONT.)

| ALGEBRAIC SYMBOL | SYMBOL | DESCRIPTION | UNITS |
|------------------|--------|---|----------------------|
| α | ALF | ANGLE OF ATTACK, ANGLE BETWEEN AIRCRAFT FLIGHT PATH VELOCITY AND X BODY AXIS IN THE PLANE OF SYMMETRY | deg |
| β | BET | SWEEP ANGLE, ANGLE BETWEEN AIRCRAFT FLIGHT PATH VELOCITY AND AIRPLANE OF SYMMETRY | deg |
| V | VT | FLIGHT PATH VELOCITY, TRUE | ft/sec |
| V_e | VERT | EQUIVALENT AIRSPEED | knots |
| ρ | RHO | AIR DENSITY | slug/ft ³ |
| MACH | XMACH | AIRCRAFT MACH NUMBER | unitless |
| SOUND | SOUND | SPEED OF SOUND | ft/sec |
| h_{CG} | HCG | ALTITUDE OF C.G. ABOVE GROUND | ft |
| h_{WHEEL} | HWHEEL | ALTITUDE OF MAIN LANDING GEAR ABOVE GROUND | ft |
| $X_{W,CG}$ | XBWHL | LONGITUDINAL DISTANCE FROM MAIN GEAR TO C.G. | ft |
| $Z_{W,CG}$ | ZBWHL | VERTICAL DISTANCE FROM MAIN GEAR TO C.G. | ft |

SYMBOL TABLE EQUATIONS OF MOTION
TABLE 1.1 (CONT.)

| ALGEBRAIC SYMBOL | DESCRIPTION | UNITS |
|--|---|---------------------|
| $\dot{x}_I, \dot{y}_I, \dot{z}_I$ | AIRCRAFT VELOCITY IN INERTIAL (EARTH) AXES | ft/sec |
| U_{WE}, V_{WE}, W_{WE} | WIND VELOCITY IN EARTH AXES | ft/sec |
| $\dot{U}_{WE}, \dot{V}_{WE}, \dot{W}_{WE}$ | WIND ACCELERATIONS (SHEAR) IN EARTH AXES | ft/sec ² |
| ϕ, θ, ψ | EUCLER ANGLES OF ROTATION RELATING AIRCRAFT BODY AXES TO EARTH AXES (ROLL, PITCH AND YAW) | deg |
| $p, q, r, \dot{\gamma}_s$ | ANGULAR VELOCITIES (STABILITY AXES) | deg/sec |
| x_{PE}, y_{PE}, z_{PE} | POSITION OF PILOTS EYE IN EARTH AXES SYSTEM | ft |
| $\dot{x}_{PE}, \dot{y}_{PE}, \dot{z}_{PE}$ | VELOCITY OF PILOTS EYE IN EARTH AXES SYSTEM | ft/sec |
| U_{PE}, V_{PE}, W_{PE} | VELOCITY OF PILOTS EYE IN BODY AXES SYSTEM | ft/sec |
| $x_{PE,CG}, y_{PE,CG}, z_{PE,CG}$ | X, Y AND Z DISTANCES FROM C.G. TO PILOTS EYE | ft |
| $x_{CE,CG}, y_{CE,CG}, z_{CE,CG}$ | X, Y AND Z DISTANCES FROM C.G. TO COCKPIT CENTROID | ft |
| n_x, n_y, n_z | AIRCRAFT ACCELERATIONS ALONG X, Y AND Z AXES (BODY AXES LOAD FACTORS) | g's |
| n_{xc}, n_{yc}, n_{zc} | ACCELERATIONS OF COCKPIT CENTROID | g's |

FORCE AND MOMENT SEPARATIONS (LONGITUDINAL)

$$\dot{u}_B = \frac{1}{57.3} (V_B \dot{\theta}_B - \omega_B \dot{\theta}_B) + g_{1,3} \\ + \frac{1}{M} [75w C_{x_B} + T \cos \dot{\gamma} + F_{x_G}] - \dot{u}_{wB}$$

$$\dot{w}_B = \frac{1}{57.3} (u_B \dot{\theta}_B - V_B \dot{\theta}_B) + g_{3,3} \\ + \frac{1}{M} [75w C_{z_B} + T \sin \dot{\gamma} + F_{z_G}] - \dot{w}_{wB}$$

$$\dot{\theta}_B = \frac{1}{I_y} \left[\frac{1}{57.3} (\dot{I}_z - \dot{I}_x) \dot{\theta}_B \dot{\theta}_B + \frac{1}{57.3} (\dot{I}_{x2}) (\dot{\theta}_B^2 - \dot{\theta}_B^2) \right. \\ \left. + 57.3 Sw C_{w\dot{\gamma}} C_{m_B} + 57.3 Z_{Tc_G} T + 57.3 M_G \right]$$

FORCE AND MOMENT SUMMATIONS (LATERAL - DIRECTIONAL)

$$\dot{V}_B = \frac{1}{57.3} (\omega_B \dot{P}_B - \dot{\psi}_B \dot{\gamma}_B) + g_{a_{2,3}} \\ + \frac{1}{M} [g_{Sw} C_{YB} + F_{yG}] - \dot{V}_{wB}$$

$$\dot{P}_B = \frac{1}{I_x} \left[I_{xz} \dot{\gamma}_B + \frac{1}{57.3} (I_y - I_z) \dot{\gamma}_B \dot{\gamma}_B + \frac{1}{57.3} (I_{xz}) \dot{P}_B \dot{\gamma}_B \right. \\ \left. + 57.3 S_w b_w F C_{lB} + 57.3 L_G \right]$$

$$\dot{\gamma}_B = \frac{1}{I_z} \left[I_{xz} \dot{P}_B + \frac{1}{57.3} (I_x - I_y) \dot{P}_B \dot{\gamma}_B - \frac{1}{57.3} (I_{xz}) \dot{\gamma}_B \dot{\gamma}_B \right. \\ \left. + 57.3 S_w b_w F C_{nB} + 57.3 V_T (T_L - T_R) + 57.3 N_G \right]$$

ANGLE OF ATTACK AND ANGLE OF SWEEP

$$\dot{\alpha} = 57.3 (\dot{\omega}_B c_B - \dot{c}_B \omega_B) / (c_B^2 + \omega_B^2)$$

$$\dot{\beta} = 57.3 (\dot{V}_B - \dot{V}_B / V) / \sqrt{c_B^2 + \omega_B^2}$$

$$\sin \alpha = \omega_B / \sqrt{c_B^2 + \omega_B^2} ; \quad \sin \beta = \sqrt{c_B^2 + \omega_B^2} / V$$

$$\cos \alpha = c_B / \sqrt{c_B^2 + \omega_B^2} ; \quad \cos \beta = \sqrt{c_B^2 + \omega_B^2} / V$$

$$\alpha = \tan^{-1} \omega_B / c_B$$

$$\beta = \tan^{-1} V / \sqrt{c_B^2 + \omega_B^2}$$

FLIGHT PATH VELOCITY AND ACCELERATION

$$V = \sqrt{u_B^2 + v_B^2 + w_B^2} ; \quad \dot{V} = (\dot{u}_B u_B + \dot{v}_B v_B + \dot{w}_B w_B) / V$$

EQUIVALENT AIRSPEED, DYNAMIC PRESSURE AND MACH NO.

$$V_e = V \sqrt{\rho/\rho_0} \left(\frac{1}{1.69} \right)$$

$$q = \frac{1}{2} \rho V^2$$

$$MACH = V / \text{SOUND} ; \quad \text{SOUND} = 1116.89 - .003908 h_{CG}$$

CENTER OF GRAVITY ALTITUDE AND WHEEL HEIGHT

$$h_{CG} = -z_I$$

$$h_{WHEEL} = -(z_I + q_{1,3} X_{WHEEL} + q_{3,3} z_{WHEEL})$$

EULER ANGLE TRANSFORMATION

$$\dot{\psi} = (\dot{\chi}_B \cos \phi + \dot{\chi}_B \sin \phi) / \cos \theta$$

$$\dot{\phi} = \dot{\chi}_B + \dot{\psi} \sin \theta$$

$$\dot{\theta} = \dot{\chi}_B \cos \phi - \dot{\chi}_B \sin \phi$$

TRANSFORMATION OF BODY AXES RATES TO STABILITY AXES

$$\dot{\chi}_B = \dot{\chi}_B \cos \alpha + \dot{\chi}_B \sin \alpha$$

$$\dot{\chi}_B = \dot{\chi}_B \cos \alpha - \dot{\chi}_B \sin \alpha$$

EQUATIONS OF MOTION

FIG. 1.6

TRANSFORMATION ELEMENTS (DIRECTION COSINES)

$$a_{1,1} = \cos \phi \cos \theta$$

$$a_{2,1} = \sin \phi \sin \theta \cos \psi - \cos \phi \sin \psi$$

$$a_{3,1} = \sin \phi \sin \psi + \cos \phi \sin \theta \cos \psi$$

$$a_{1,2} = \cos \theta \sin \psi$$

$$a_{2,2} = \cos \phi \cos \psi + \sin \phi \sin \theta \sin \psi$$

$$a_{3,2} = \cos \phi \sin \theta \sin \psi - \sin \phi \cos \psi$$

$$a_{1,3} = -\sin \theta$$

$$a_{2,3} = \sin \phi \cos \theta$$

$$a_{3,3} = \cos \phi \cos \theta$$

BODY TO EARTH AIRCRAFT VELOCITY TRANSFORMATION

$$\dot{X}_I = a_{1,1} u_B + a_{2,1} v_B + a_{3,1} w_B + u_{WE}$$

$$\dot{Y}_I = a_{1,2} u_B + a_{2,2} v_B + a_{3,2} w_B + v_{WE}$$

$$\dot{Z}_I = a_{1,3} u_B + a_{2,3} v_B + a_{3,3} w_B + w_{WE}$$

EARTH TO BODY WIND SHEAR TRANSFORMATION

$$\dot{u}_{WB} = a_{1,1} \dot{u}_{WE} + a_{1,2} \dot{v}_{WE} + a_{1,3} \dot{w}_{WE}$$

$$\dot{v}_{WB} = a_{2,1} \dot{u}_{WE} + a_{2,2} \dot{v}_{WE} + a_{2,3} \dot{w}_{WE}$$

$$\dot{w}_{WB} = a_{3,1} \dot{u}_{WE} + a_{3,2} \dot{v}_{WE} + a_{3,3} \dot{w}_{WE}$$

PILOTS EYE POSITION AND VELOCITY FOR VISUAL SYSTEM

$$X_{PE} = X_I + a_{1,1} X_{PE,CG} + a_{3,1} Z_{PE,CG}$$

$$Y_{PE} = Y_I + a_{1,2} X_{PE,CG} + a_{3,2} Z_{PE,CG}$$

$$Z_{PE} = Z_I + a_{1,3} X_{PE,CG} + a_{3,3} Z_{PE,CG}$$

$$U_{PE} = U_B + \frac{1}{57.3} (q_B) Z_{PE,CG}$$

$$V_{PE} = V_B + \frac{1}{57.3} (X_{PE,CG} \gamma_B - Z_{PE,CG} p_B)$$

$$W_{PE} = W_B - \frac{1}{57.3} (q_B) X_{PE,CG}$$

$$\dot{X}_{PE} = U_{PE} a_{1,1} + V_{PE} a_{2,1} + W_{PE} a_{3,1} + U_{WE}$$

$$\dot{Y}_{PE} = U_{PE} a_{1,2} + V_{PE} a_{2,2} + W_{PE} a_{3,2} + V_{WE}$$

$$\dot{Z}_{PE} = U_{PE} a_{1,3} + V_{PE} a_{2,3} + W_{PE} a_{3,3} + W_{WE}$$

NOTE: PILOT IS ASSUMED
TO BE ON AIRCRAFT
CENTER LINE THEREFORE
 $Y_{PE,CG} = 0$

TRANSFORMATION OF AIRCRAFT ACCELERATIONS FROM C.G.

TO COCKPIT CENTROID FOR MOTION BASE.

$$N_{xc} = N_x - (\dot{p}_B^2 + \dot{q}_B^2) X_{c,cg} + (\dot{q}_B \dot{p}_B - \dot{r}_B \dot{q}_B) Y_{c,cg} + (\dot{r}_B \dot{p}_B + \dot{q}_B \dot{r}_B) Z_{c,cg}$$

$$N_{yc} = N_y + (\dot{p}_B \dot{q}_B + \dot{r}_B \dot{q}_B) X_{c,cg} + (\dot{p}_B^2 + \dot{q}_B^2) Y_{c,cg} + (\dot{r}_B \dot{q}_B - \dot{p}_B \dot{r}_B) Z_{c,cg}$$

$$N_{zc} = N_z + (\dot{p}_B \dot{r}_B - \dot{q}_B \dot{r}_B) X_{c,cg} + (\dot{q}_B \dot{r}_B + \dot{p}_B \dot{q}_B) Y_{c,cg} - (\dot{p}_B^2 + \dot{q}_B^2) Z_{c,cg}$$

WHERE: AIRCRAFT ACCELERATIONS

$$N_x = \frac{1}{m} g (\dot{q} \dot{r} \cos \psi_B + \dot{r} + F_{xg})$$

$$N_y = \frac{1}{m} g (\dot{q} \dot{r} \sin \psi_B + F_{yg})$$

$$N_z = -\frac{1}{m} g (\dot{q} \dot{r} \cos \psi_B + F_{zg})$$

EQUATIONS OF MOTION

FIG. 1.10

AIRCRAFT WEIGHT AND INERTIA VALUES USED FOR DC-9-10 SIMULATION

OPERATING WEIGHT EMPTY = 49,452 lbs.

PAYLOAD = 7,548 lbs.

FUEL = 17,000 lbs.

GROSS WEIGHT = 74,000 lbs.

INERTIAS

$$I_x = 3.3 \times 10^5 \text{ slug-ft}^2$$

$$I_y = 8.41 \times 10^5 \text{ "}$$

$$I_z = 1.09 \times 10^6 \text{ "}$$

$$I_{xz} = .69 \times 10^5 \text{ "}$$

Section 2

Aerodynamic and Control System Models

This section contains descriptions of the Pilot Controls and Aero Forces and Moments algorithms. The information is presented in two parts. The first part is called Pilot Control Inputs to Aero Equations and the second is called Aerodynamic Equations.

The primary source for the data and algorithms used in this section is the Douglas Aircraft Estimated Data for Stability and Control. (Reference 6). The references cited in the equations are to this document.

The aerodynamic equations were developed using the assumptions of low mach number and no weight change as stated. Aero elasticity terms were, however, included eventhough their value for this study is questionable.

PILOT CONTROL INPUTS TO AERO EQUATIONS

Along with the inputs from the EOM the aero force equations require eight pilot control inputs. These eight inputs are generated from seven pilot operated controls in the cockpit as follows:

Elevator Input:

$$\delta_e = (3.427 + 5.31 X_{CG}) \delta_{cc} \left| \begin{array}{l} 15 \\ -25 \end{array} \right.$$

Where:

X_{CG} is the C.G. position as a ratio of MAC.

δ_{cc} is the position of the control column in inches and has a dead band of .25 inch.

δ_e is elevator deflection in degrees and is limited to the range of 15° trailing edge down to 25° trailing edge up.

Aileron Input:

$$\delta_a = .25 \delta_w \left| \begin{array}{l} 20 \\ -20 \end{array} \right.$$

Where:

δ_w is wheel deflection in degrees limited to ± 113 degrees with a dead band of .25 degrees.

δ_a is aileron deflection in degrees limited to the range of 20° for both trailing edge up and down.

Rudder Input:

$$\delta_r = 6.28 \delta_{rp} + \delta_{yD} \left| \begin{array}{l} 30 \\ -30 \end{array} \right.$$

Where:

δ_{rp} is rudder pedal deflection in inches with stops at 4.78 inches left and right and a dead band of .25 inch.

δ_r is rudder deflection in degrees limited to 30 degrees trailing edge left and right.

δ_{yD} is rudder deflection due to yaw damper. This input is limited to approximately ± 1.6 degrees. (See Section 6 YAW DAMPER.)

Spoiler Input

On the DC-9-10 the spoiler surfaces are used for three areas of flight, 1) speed brakes, all spoilers go up at once as commanded by speed brake control, 2) ground spoilers, all spoilers go full up (60 degrees) automatically if armed and main gear spin up, and 3) lateral control spoilers, spoilers are deployed one side at a time to aid the ailerons in the rolling maneuver. In this simulation both the speed brake function and the ground spoiler function (symmetric spoiler deployment) are referred to as speed brakes.

Lateral Control Spoiler Input

$$\delta_{sp} = f(\delta_w)$$

Where:

δ_{sp} is spoiler deflection in degrees, positive for right wing down and negative for left wing down.

δ_w is control wheel deflection (same as drives the ailerons).

$f(\delta_w)$ is defined by the following table:

| δ_w | $f(\delta_w)$ |
|------------|---------------|
| 0 | 0 |
| 3 | 0 |
| 10 | .8 |
| 20 | 2.5 |
| 30 | 5.0 |
| 40 | 6.7 |
| 50 | 7.9 |
| 60 | 9.3 |
| 70 | 12.0 |
| 75 | 14.2 |
| 80 | 17.5 |
| 90 | 28.7 |
| 113 | 60.0 |

The table is entered using absolute value of wheel deflection. The direction of the wheel deflection is tested and the function value is returned with a positive value for right wing down and a negative value for left wing down. This accounts for the differential nature of roll control.

Speed Brakes/Ground Spoilers

δ_{SB} is speed brake deflection (symmetrical spoilers) from 0 to 60 degrees. The speed brakes move linearly with the speed brake control handle and produce 60 degrees of spoiler deflection for full control deflection.

- OR -

$\delta_{SB} = \delta_{SBC} \left(\frac{1}{.75 + 1} \right)$ with 150 degrees per second rate limit. If auto ground spoilers are armed and the main gear have spun up δ_{SBC} goes from 0 to 60.

It should be noted that all of the control surfaces mentioned above have some associated lags in the actual aircraft system. These lags are of the order of .1 to .3 of a second. These lags were not implemented in the ground handling simulation. It is felt that this omission does not significantly alter the overall fidelity of the simulation.

Horizontal Stabilizer Input

$\dot{\delta}_H$ is the angle of incidence of the horizontal stabilizer in degrees. $\dot{\delta}_H$ is limited to the range of 12 degrees trailing edge up and 1.5 degrees trailing edge down.

For the ground handling simulation $\dot{\delta}_H$ was controlled by a thumb switch on the left side of the wheel. Pushing the switch down caused $\dot{\delta}_H$ to move trailing edge up and pushing the switch up caused it to move in the opposite direction. The rate of $\dot{\delta}_H$ movement was 1/3 of a degree per second in both directions. The maximum displacement of $\dot{\delta}_H$ was limited to 12 degrees trailing edge up and 1.5 degrees trailing edge down represented as -12 and + 1.5 degrees.

PILOT CONTROL INPUTS TO AERO EQUATIONS

Flap Input

δ_f is the flap angle in degrees. δ_f is limited to the range of 0 to 50 degrees trailing edge down.

Only two flap positions were used during the ground handling study and the flap positions remained fixed during the runs. These two positions, 15 degrees and 50 degrees, represented nominal takeoff and landing configurations respectively.

If the flap handle had been changed during the runs δ_f would have moved toward the new commanded position at a rate of 2.2 degrees per second.

Landing Gear Position Input

K_{gear} represents the landing gear position

$K_{gear} = 0$ is gear up
 $K_{gear} = 1$ is gear down

The gear was always down for the ground handling simulation.

SYMBOL TABLE AERO DYNAMIC SECTION
TABLE 2.1

| ALGEBRAIC SYMBOL | COMPUTER SYMBOL | DESCRIPTION | UNITS |
|------------------------------------|-----------------|---|---------------------|
| $(C_{LTD})^R$ | CLTOR1 | STATIC COEFF. OF LIFT WITH TAIL OFF AND RIGID BODY | UNITLESS |
| $C_L(\alpha, \alpha_f)$ | CL1 | CONTRIBUTION OF ANGLE OF ATTACK AND FLAPS TO STATIC LIFT | " |
| $\Delta C_{LGE}(\alpha, \alpha_f)$ | DCLIGE | CONTRIBUTION OF GND. EFFECTS TO STATIC LIFT | " |
| K_{GE} | XKGE | GND. EFFECT FACTOR, FUNCTION OF GEAR ALT. (WHERE) | " |
| ΔC_{LGE} | — | CONTRIBUTION OF LANDING GEAR TO STATIC LIFT | " |
| K_{gear} | XKGEAR | FACTOR WHICH REPRESENTS GEAR POSITION ($u_p=0$, $u_w=1$) | " |
| ΔC_{LTD}^E | DCLTDE | INCREMENT TO ACCOUNT FOR STRUCTURAL ELASTICITY | " |
| C_{LTD}^{ER} | CLER | RATIO OF ELASTIC TO RIGID COEF. OF LIFT | " |
| q | q | DYNAMIC PRESSURE | lbs/ft ² |
| N_z | ANZ | NORMAL (VERTICAL) ACCELERATION | g's |

SYMBOL TABLE AERODYNAMIC SECTION TABLE 2.1 (CONT.)

| ALGEBRAIC SYMBOL | PROGRAM SYMBOL | DESCRIPTION | UNITS |
|--------------------------|----------------|--|-----------------|
| C_{LTO}^E | CLTOE | COEF. OF LIFT WITH TAIL OFF INCLUDING ELASTICITY | UNITLESS |
| $C_{L\dot{\gamma}TO}$ | CLQTO | COEF. OF LIFT DUE TO DITCH RATE | " |
| q_B | QB | DITCH RATE (SEE EOM SECTION) | DEG/SEC. |
| $C_{L\dot{\alpha}TO}$ | CLADTO | COEF. OF LIFT DUE TO ANGLE OF ATTACK RATE | UNITLESS |
| $\dot{\alpha}$ | ALPD | ANGLE OF ATTACK RATE (SEE EOM SECTION) | DEG/SEC. |
| C_w | CW | WING MEAN AERODYNAMIC CHORD (MAC) | FT. |
| V | VT | AIRCRAFT TOTAL VELOCITY (SEE EOM SECTION) | FT/SEC. |
| δ_f | FLAP | FLAP ANGLE FULL EXTEND 50° , UP 0° | DEG. |
| C_{T_i} | T | COEF. OF LIFT DUE TO THRUST | UNITLESS |
| T | THT | THRUST (SEE ENGINE SECTION) | LBS. |
| S_w | SW | WING AREA | FT ² |
| C_{ZS} | CZS | COEF. OF LIFT FORCE IN STABILITY AXIS | UNITLESS |
| $C_L(\dot{\gamma}_{sp})$ | CLGSP | COEF. OF LIFT DUE TO GND. SLOPERS | " |

SYMBOL TABLE AERO DYNAMIC SECTION

TABLE 2.1 (CONT.)

| ALGEBRAIC SYMBOL | PROGRAM SYMBOL | DESCRIPTION | UNITS |
|---|----------------|--|----------|
| $(C_{M,TD})^R_{STATIC}$ | CMTOR4 | STATIC COEF. OF PITCHING MOMENT WITH TAIL OFF AND RIGID BODY | UNITLESS |
| $C_m(\alpha, \sigma_f)$ | CM2 | CONTRIBUTION OF ALPHA AND FLAP TO STATIC PITCHING MOMENT | " |
| $\Delta C_{MGE}(\alpha, \sigma_f)$ | DCMIGE | CONTRIBUTION OF GND EFFECTS TO STATIC PITCHING MOMENT | " |
| ΔC_{MGR} | - | CONTRIBUTION OF GEAR TO STATIC PITCHING MOMENT | " |
| ΔC_{MTO}^E | DCMTOE | INCREMENT TO PITCHING MOMENT DUE STRUCTURAL ELASTICITY | " |
| C_{MTO}^E | CMT0E | COEF. OF PITCHING MOMENT INCLUDING ELASTIC EFFECTS | " |
| $f(XCG)$ | FXCG | NORMALIZED DISTANCE BETWEEN C.G. AND CENTER OF LIFT | FT. |
| C_{mqto} | CMQTO | COEF. OF PITCHING MOMENT DUE TO DITCH RATE | UNITLESS |
| $C_{m\dot{\alpha}to}$ | CMADTO | COEF. OF PITCHING MOMENT DUE TO ANGLE OF ATTACK RATE | UNITLESS |
| ϵ | EP | HORIZONTAL STABILIZER DOWN WASH ANGLE | DEG. |
| $\epsilon_1(\alpha, \sigma_f)$ | EPI | CONTRIBUTION TO ϵ DUE TO ALPHA AND FLAPS | DEG. |
| $\Delta \epsilon_{IGE}(\alpha, \sigma_f)$ | DEPIGE | DOWN WASH INCREMENT DUE GND. EFFECTS | DEG. |

SYMBOL TABLE AERO DYNAMIC SECTION

TABLE 2.1 (CONT.)

| ALGEBRAIC SYMBOL | PROGRAM SYMBOL | DESCRIPTION | UNITS |
|-------------------------|----------------|---|----------|
| α_H | AX | HORIZONTAL STABILIZER ANGLE OF ATTACK | DEG. |
| i_H | XIH | HORIZONTAL STABILIZER ANGLE OF INCIDENCE | DEG. |
| F_H | FH | FUSELAGE BENDING FACTOR (VERTICAL PLANE) | UNITLESS |
| $C_{L\alpha_H}^{EK}$ | CLHER | FACTOR WHICH TAKES INTO ACCOUNT THE EFFECT OF STRUCTURAL ELASTICITY | UNITLESS |
| C_{LH_H} | CLH | COEF. OF LIFT FOR HOR. STABILIZER | " |
| $C_{L\alpha_H}$ | CLAH | COEF. OF LIFT OF HOR. STAB. FOR α_H | UNITLESS |
| $(C_{Lq})_H$ | CLQH | COEF. OF LIFT OF HOR. STAB. FOR q | " |
| $(C_{L\dot{\alpha}})_H$ | CLADH | COEF. OF LIFT OF HOR. STAB. FOR $\dot{\alpha}$ | " |
| $C_{L\dot{\epsilon}}$ | CLDE | COEF. OF LIFT OF HOR. STAB. FOR $\dot{\epsilon}$ | " |
| $\bar{\epsilon}$ | DE | ELEVATOR ANGLE | DEG. |
| C_{MH} | CMH | COEF. OF PITCHING MOMENT ONE HOR. STAB. | UNITLESS |
| L_{HCG} | XLH | DISTANCE FROM C.G. TO HOR. STAB. | FT. |

SYMBOL TABLE AERODYNAMIC SECTION

TABLE 2.1 (CONT.)

| ALGEBRAIC SYMBOL | PROGRAM SYMBOL | DESCRIPTION | UNITS |
|----------------------------|----------------|--|-------|
| C_{ms} | CMS | COEF. OF PITCHING MOMENT FOR STABILITY AXIS | " |
| $\Delta C_m(\delta_{sp})$ | CMGSP | INCREMENT OF PITCHING MOMENT COEF. DUE TO GND SPOILERS | " |
| ΔC_{DGR} | CDIGR | INCREMENT OF DRAG COEF. DUE TO LANDING GEAR | " |
| ΔC_{DGR_0} | CDIGR0 | INTERCEPT POINT OF LINEAR FUNCTION | " |
| ΔC_{DGR_1} | CDIGR1 | SLOPE OF LINEAR FUNCTION | " |
| C_{DIGE} | CDIGE | COEF. OF INDUCED DRAG DUE TO GND REFLECTS | " |
| C_D | CD | COEF. OF DRAG | " |
| $C_{Dp}(\alpha, \delta_f)$ | CDO | COEF. OF PARASITIC DRAG | " |
| $C_{Di}(\alpha, \delta_f)$ | CDI | COEF. OF INDUCED DRAG | " |
| $\Delta C_D(\delta_{sp})$ | CDGSP | INCREMENT OF DRAG COEF. DUE TO GND SPOILERS | " |
| C_{xs} | CXS | COEF. OF DRAG IN STABILITY AXIS | " |

SYMBOL TABLE AERO DYNAMIC SECTION

TABLE 2.1 (CONT.)

| ALGEBRAIC SYMBOL | PROGRAM SYMBOL | DESCRIPTION | UNITS |
|--------------------------------|----------------|--|----------|
| C_{XB} | CXB | COEF. OF DRAG BODY AXIS | UNITLESS |
| C_{ZB} | CZB | COEF. OF LIFT BODY AXIS | " |
| C_{mB} | CMB | COEF. OF PITCHING MOMENT BODY AXIS | " |
| F_V | FV | EUSELAGE BENDING LATERAL PLANE | UNITLESS |
| $C_{l\beta_{TO}}$ | CLBTO | COEF. OF ROLLING MOMENT (TAIL OFF) DUE TO SIDE SLIP ANGLE (β_{ETA}) | UNITLESS |
| $C_{l\beta_1}$ | CLB1 | INTERLENT POINT FUNCTION OF ANGLE OF ATTACK AND FLAP ANGLE | UNITLESS |
| $C_{l\beta_2}$ | CLB2 | | UNITLESS |
| $C_{l\dot{p}}^{EIR}$ | CLPER | RATIO OF RIGID TO ELASTIC FORCE FOR THE EFFECT OF ROLL RATE ON THE COEF. OF ROLLING MOMENT | UNITLESS |
| $C_{l\dot{\delta}_{SP}}^{EIR}$ | CLSPER | RIGID TO ELASTIC FACTOR FOR THE EFFECT OF SPOILERS | UNITLESS |
| $C_{l\dot{\delta}_a}^{EIR}$ | DAER | RIGID TO ELASTIC FACTOR FOR THE EFFECT OF AILERONS | UNITLESS |
| $C_{l\dot{r}_{TO}}$ | CLRTO | COEF. OF ROLLING MOMENT DUE TO YAW RATE | " |
| $C_{l\dot{r}_{OS}}$ | CLTOS | COEF. OF ROLLING MOMENT IN STABILITY AXIS WITH TAIL OFF | " |

SYMBOL TABLE AERODYNAMIC SECTION

TABLE 2.1 (CONT.)

| ALGEBRAIC SYMBOL | PROGRAM SYMBOL | DESCRIPTION | UNITS |
|-----------------------------------|-------------------|---|----------|
| $C_{l\beta_0}$ | CLBTO | COEF. OF ROLLING MOMENT DUE TO SIDE SLIP ANGLE | UNITLESS |
| C_{lp} | CLPD | COEF. OF ROLLING MOMENT DUE TO ROLLING ACCELERATION | UNITLESS |
| $C_{l\dot{p}_0}$ | CLPTO | COEF. OF ROLLING MOMENT DUE TO ROLL RATE | " |
| b_w | BW | WING SPAN | FT. |
| CL_{δ_a} | CLDA | COEF. OF ROLLING MOMENT DUE TO AILERON DEFLECTION | UNITLESS |
| $C_l(\alpha, \delta_a, \delta_f)$ | CLSP | COEF. OF ROLLING MOMENT DUE TO SPOILER DEFLECTION, ANGLE OF ATTACK, AND FLAP | " |
| $C_{y\beta_0}$ | CYBTO | COEF. OF SIDE FORCE DUE TO ANGLE OF SIDE SLIP, TAKE OFF | " |
| $C_{y\dot{p}_0}$ | CYPTO | COEF. OF SIDE FORCE DUE TO ROLL RATE | " |
| $C_{y\delta_a}$ | CYDA | COEF. OF SIDE FORCE DUE TO AILERON DEFLECTION | " |
| $C_{y\delta_{sp}}$ | CYDSP | COEF. OF SIDE FORCE DUE TO SPOILER DEFLECTION | " |
| $C_{y\dot{p}_0}$ | CYTO | COEF. OF SIDE FORCE WITH TAKE OFF | " |
| β | BET | SIDE SLIP ANGLE (BETA) | DEG. |
| R_z | PS | ROLL RATE STABILITY AXIS | DEG/SEC |

SYMBOL TABLE AERO DYNAMIC SECTION

TABLE 2.1 (CONT.)

| ALGEBRAIC SYMBOL | PROGRAM SYMBOL | DESCRIPTION | UNITS |
|----------------------|----------------|---|----------|
| $C_{L\alpha}^{EL}$ | CLAEV | ELASTIC TO RIGID RATIO FOR | UNITLESS |
| $C_{y\beta}$ | CYBD | COEF. OF SIDE FORCE DUE TO SIDE SLIP ANGLE RATE | " |
| $C_{y\dot{\beta}}$ | CYPD | COEF. OF SIDE FORCE AT THE VERTICAL TAIL DUE TO ROLL ACCELERATION | " |
| $C_{y\ddot{\beta}}$ | CYBV | COEF. OF SIDE FORCE AT THE VERTICAL TAIL DUE TO SIDE SLIP ANGLE | " |
| $C_{y\dot{p}}$ | CYPD | COEF. OF SIDE FORCE AT THE VERTICAL TAIL DUE TO ROLL RATE | " |
| $C_{y\ddot{p}}$ | CYRV | COEF. OF SIDE FORCE AT THE VERTICAL TAIL DUE TO YAW RATE | UNITLESS |
| $C_{y\dot{r}}$ | CYRD | COEF. OF SIDE FORCE DUE TO YAW ACCELERATION | " |
| $C_{y\ddot{r}}$ | CYNY | COEF. OF SIDE FORCE DUE TO LATERAL ACCELERATION | UNITLESS |
| $C_{y\dot{v}}$ | CYV | COEF. OF SIDE FORCE ON VERTICAL TAIL | " |
| $C_{y\dot{v}}^{EL}$ | DRER | ELASTIC TO RIGID RATIO FOR EFFECT OF RUDDER ON SIDE LOAD | " |
| $C_{y\ddot{v}}$ | CYDR | COEF. OF SIDE LOAD DUE TO RUDDER | " |
| $C_{y(\dot{\beta})}$ | CYRV | TOTAL COEF. OF SIDE LOAD DUE TO RUDDER | " |

SYMBOL TABLE AERO DYNAMIC SECTION

TABLE 2.1 (CONT.)

| ALGEBRAIC SYMBOL | PROGRAM SYMBOL | DESCRIPTION | UNITS |
|---|----------------|---|----------|
| C_{np} | CNP TO | COEF. OF YAWING MOMENT DUE TO ROLL RATE | UNITLESS |
| C_{nr} | CNR TO | COEF. OF YAWING MOMENT DUE TO YAW RATE | " |
| C_{nda} | CNDA | COEF. OF YAWING MOMENT DUE AIRCRAFT DEFLECTION | " |
| C_{ntos} | CNTOS | TOTAL COEF. OF YAWING MOMENT FOR TAIL OFF STABILITY AXIS | " |
| $C_{n\beta}$ (α, δ_f) | CNB TO | COEF. OF YAWING MOMENT DUE SIDE SLIP ANGLE | " |
| C_n ($\alpha, \delta_{sp}, \delta_f$) | CNSP | COEF. OF YAWING MOMENT DUE TO SPOILER DEFLECTION ALSO FUNCTION OF ANGLE OF ATTACK AND FLAP ANGLE | " |
| D_s | PS | ROLL RATE STABILITY AXIS | DEG/SEC. |
| r_s | RS | YAW RATE STABILITY AXIS | " |
| Cl_R | CLB | TOTAL COEF. OF ROLLING MOMENT FOR BODY AXIS | UNITLESS |
| cl_{ug} | ZVCG | VERTICAL DISTANCE FROM C.G. TO AERO CENTER OF VERTICAL STABILIZER | FT. |
| cl_{ugr} | ZVCGU | VERTICAL DISTANCE FROM C.G. TO AERO CENTER OF RUDDER SURFACE | FT. |

SYMBOL TABLE AERO DYNAMIC SECTION

TABLE 2.1 (CONT.)

| ALGEBRIC SYMBOL | PROGRAM SYMBOL | DESCRIPTION | UNITS |
|-----------------|----------------|--|----------|
| C_{yB} | CYB | TOTAL COEF. OF SIDE FORCE IN BODY AXIS | UNITLESS |
| C_{nB} | CNB | TOTAL COEF. OF YAWING MOMENT IN BODY AXIS | " |
| $l_{v.c.g.}$ | XVCG | LONGITUDINAL DISTANCE FROM C.G. TO VERTICAL STABILIZER | FT. |
| $l_{v.c.g.v}$ | XVCGV | LONGITUDINAL DISTANCE FROM C.G. TO RUDDER SURFACE | " |
| $l_{x.c.g.}$ | FXCGZ | LONGITUDINAL DISTANCE FROM C.G. AT 25% MAC TO ACTUAL C.G. (TERM IS ZERO FOR C.G. AT 25% MAC) | " |
| δ_{sp} | PSP | SPOILER DEFLECTION DUE TO WHEEL MOTION | DEG |
| δ_{sb} | DSB | SPOILER DEFLECTION DUE TO SPEED BRAKE HANDLE | DEG |

LONGITUDINAL AERO FORCE COEFFICIENTS

COEFFICIENT OF LIFT (TAIL OFF WITH ELASTIC CORRECTIONS)

$$C_{LTO}^E = (C_{LTO})_{STATIC}^R + \Delta C_{LTO}^E + \left[(C_{Lq})_{TO} \dot{q} + (C_{L\dot{\alpha}})_{TO} \dot{\alpha} \right] C_T$$

$$+ \frac{\partial C_L}{\partial \dot{C}_T} (\dot{C}_T) C_T$$

WHERE:

$$(C_{LTO})_{STATIC}^R = C_L(\alpha, \sqrt{f}) + \Delta C_{LGE}(\alpha, \sqrt{f}) K_{GE} + \Delta C_{LGE} K_{gear}$$

$$\Delta C_{LTO}^E = -(C_{LTO})_{STATIC}^R \left(1 - C_{L\alpha}^{E/R} \right) + (C_{Lh})_{TO}^E N_z$$

$$C_T = T / 95W$$

$$C_{L\alpha}^{E/R} = 1 - .00034 \dot{q}$$

$$K_{GE} = f(h_{WHEEL}) \quad (\text{SEE TABLE 2.4})$$

$$\frac{\partial C_L}{\partial \dot{C}_T} (\dot{C}_T) = .36 - .001 \dot{C}_T$$

EQUATIONS AERODYNAMIC SECTION

FIG. 2.2

LONGITUDINAL AERO FORCE COEFFICIENTS

COEFFICIENT OF PITCHING MOMENT (TAKE OFF WITH ELASTIC CORRECTIONS)

$$C_{m_{TO}}^E = (C_{m_{TO}})^R + \Delta C_{m_{TO}}^E + C_{L_{TO}}^E f(X_{CG}) + [C_{m_{\dot{\alpha}_{TO}}} \dot{\alpha} + C_{m_{\dot{\alpha}_{TO}}} \dot{\alpha}] C_W/2V$$

WHERE:

$$(C_{m_{TO}})^R = C_m(\alpha, \sigma_f) + \Delta C_{m_{CE}}(\alpha, \sigma_f) K_{GE} + \Delta C_{m_{GR}} K_{gear}$$

$$\Delta C_{m_{TO}}^E = (\Delta C_{m_o})_{TO}^E \frac{q}{q} + \left(\frac{\partial C_m}{\partial C_L} \right)_{TO}^E \frac{q}{q} C_{L_{TO}}^E - (C_{m_n})_{TO}^E N_z$$

$$f(X_{CG}) = .25 - X_{CG} \quad (X_{CG} = .25 \text{ FOR THE GND HANDLING STUDY})$$

$$K_{GE} = f(h_{WHEEL}) \quad (\text{SEE TABLE 2.4})$$

EQUATIONS AERO DYNAMIC SECTION

FIG. 2.3

LONGITUDINAL AERO CONSTANTS

LIFT:

$$(C_{Lq})_{T0} = -104 \quad \text{REF: (DC9-A14.59, P.55)}$$

$$(C_{L\dot{x}})_{T0} = .012 \quad "$$

$$\Delta C_{LGR} = .026$$

$$(C_{L\eta})^E_{T0} = .01 \quad (\text{DC9-A5-185, P.200})$$

PITCHING MOMENT:

$$C_{mq_{T0}} = -.087 \quad (\text{DC9-A14.609, P.56}) (C_{m\eta})^E_{T0} = .003 \quad (\text{DC9-A5-185, P.200})$$

$$C_{m\dot{x}_{T0}} = -.017 \quad " \quad \Delta C_{mGR} = 0$$

$$(\Delta C_{m0})^E_{T0} = .00001 \quad (\text{DC9-A5-184, P.199})$$

$$\left(\frac{\partial C_m}{\partial C_L} \right)^E_{T0} = .000077 \quad "$$

LONGITUDINAL AERO COEFFICIENTS

HORIZONTAL STABILIZER (LIFT)

$$C_{LH} = F_H \left[\alpha_H C_{L\alpha_H} C_{L\alpha_H}^{E/R} + (C_{L\eta})_H^E \eta_z + C_{L\delta_e} C_{L\delta_e}^{E/R} \delta_e \right. \\ \left. + C_{L\dot{\alpha}_H}^{E/R} \left((C_{Lq})_H \dot{q}_B + (C_{L\dot{\alpha}})_H \dot{\alpha} \right) C_w/2v \right]$$

WHERE:

$$F_H = 1 - .00067 \dot{q}$$

REF: (DCLG-C4.776, P.203)

$$\alpha_H = \alpha - \epsilon + \dot{C}_H$$

$$\epsilon = \epsilon_1(\alpha, \delta_f) + \Delta \epsilon_{GE}(\alpha, \delta_f) K_{GE} + \Delta \epsilon(\delta_{SB})$$

$$C_{L\alpha_H}^{E/R} = 1 - .00035 \dot{q}$$

(DCLG-C4.880, P.204)

$$C_{L\delta_e}^{E/R} = 1 - .0007 \dot{q}$$

(DCLG-C4.775, P.205)

EQUATIONS AERODYNAMIC SECTION

FIG. 2.5

LONGITUDINAL AERO COEFFICIENTS

HORIZONTAL STABILIZER (PITCHING MOMENT)

$$C_{m_H} = -C_{L_H} L_{HCG}$$

WHERE:

$$L_{HCG} = L_{H/4} + (.25 - x_{cg})$$

TOTAL PITCHING MOMENT COEFFICIENT

$$C_{m_S} = C_{m_{T0}}^E + C_{m_H} + \Delta C_m (\delta_{SB})$$

TOTAL LIFT COEFFICIENT

$$C_{Z_3} = -(C_{L_{T0}}^E + C_{L_H}) - \Delta C_L (\delta_{SB})$$

EQUATIONS AERODYNAMIC SECTION

FIG. 2.6

LONGITUDINAL AERO CONSTANTS

HORIZONTAL STABILIZER:

$$\begin{aligned} C_{L\alpha_H} &= .0169 & \text{REF: (DC9-44964, P.41)} \\ (C_{L\alpha})_H^E &= .0035 & \text{(DC9-44-449, P.202)} \\ C_{L\delta_e} &= .00932 & \text{(DC9-44.964, P.41)} \\ (C_{Lq})_H &= .138 & \text{(DC9-A14-59, P.55)} \\ (C_{L\dot{\alpha}})_H &= .046 & \text{"} \end{aligned}$$

$$L_{H\frac{c}{4}} = X_{H,CG}/c_w = 3.969$$

GENERAL CONSTANTS:

$$\begin{aligned} b_w &= 89.35 \text{ ft.} \\ c_w &= 11.79 \text{ ft.} \\ S_w &= 934.3 \text{ ft.}^2 \end{aligned}$$

EQUATIONS AERODYNAMIC SECTION

FIG. 2.7

LONGITUDINAL AERO COEFFICIENTS

COEFFICIENT OF DRAG

$$C_D = C_{D_p}(\sigma_f) + C_{D_{IGE}}(C_{2s})^2 C_{Di}(\sigma_f) + \Delta C_{D_{GR}} K_{gear} + \Delta C_D(\sigma_{SB})$$

WHERE:

$$C_{D_{IGE}} = 1 - e^{[-2.48(2 h_{cg/bw})^{.768}]}$$

$$\Delta C_{D_{GR}} = .0249 - .0002732 \sigma_f$$

TOTAL DRAG COEFFICIENT

$$C_{XS} = -C_D$$

FUNCTION TABLE AERO DYNAMIC SECTION

TABLE 2.2

FUNCTION : $C_{Di} (df)$

| df | $C_{Di} (df)$ | df | $C_{Di} (df)$ |
|------|---------------|------|---------------|
| 0 | .044914 | 30 | .044430 |
| 5 | .044650 | 35 | .044401 |
| 10 | .044564 | 40 | .044371 |
| 15 | .044535 | 45 | .044349 |
| 20 | .044504 | 50 | .044322 |
| 25 | .044470 | | |

REF: (A-4 7149-4-63)

FUNCTION TABLE AERO DYNAMIC SECTION

TABLE 2.3

FUNCTION: $C_{Dp}(\alpha_f)$

| α_f | $C_{Dp}(\alpha_f)$ | α_f | $C_{Dp}(\alpha_f)$ |
|------------|--------------------|------------|--------------------|
| 0 | .0217 | 30 | .0677 |
| 5 | .0252 | 35 | .0810 |
| 10 | .0300 | 40 | .0970 |
| 15 | .0360 | 45 | .1160 |
| 20 | .0447 | 50 | .1391 |
| 25 | .0550 | | |

REF: (A-4 7149-4-63)

FUNCTION TABLE AERODYNAMIC SECTION

FUNCTION: K_{GE} (h_{WHEEL}) TABLE 2.4

| h_{WHEEL} | K_{GE} | h_{WHEEL} | K_{GE} | h_{WHEEL} | K_{GE} |
|-------------|----------|-------------|----------|-------------|----------|
| 0 | 1.0 | 25 | .13 | 50 | .01 |
| 5 | .61 | 30 | .09 | 55 | .008 |
| 10 | .39 | 35 | .06 | 60 | .007 |
| 15 | .26 | 40 | .04 | 65 | .004 |
| 20 | .185 | 45 | .015 | 70 | 0 |

REF: DC9-A28

THESE FUNCTIONS HAVE BEEN LINEARIZED

$$\Delta \epsilon (\delta_{SB}) = 0.0$$

$$\Delta C_m (\delta_{SB}) = -.00203 \delta_{SB}$$

$$\Delta C_L (\delta_{SB}) = -.01063 \delta_{SB}$$

$$\Delta C_D (\delta_{SB}) = .00198 \delta_{SB}$$

FLAP • •00

| ALF | CL | CL GE | CM | CM GE | EP | EP GE |
|----------|---------|---------|--------|--------|---------|---------|
| •4.00000 | •19000 | •15000 | •08085 | •02203 | •38000 | 1.00000 |
| •7.00000 | •10250 | •04625 | •07954 | •02208 | •68500 | 1.15000 |
| •2.00000 | •01500 | •05750 | •07823 | •02213 | •99000 | 1.30000 |
| •1.00000 | •07250 | •16125 | •07691 | •02218 | 1.29500 | 1.45000 |
| •00000 | •16000 | •26500 | •07560 | •02274 | 1.60000 | 1.60000 |
| 1.00000 | •25040 | •37000 | •07424 | •02361 | 1.93000 | 1.74286 |
| 2.00000 | •34080 | •47500 | •07289 | •02448 | 2.26000 | 1.88571 |
| 3.00000 | •43120 | •57500 | •07114 | •02531 | 2.59000 | 2.02857 |
| 4.00000 | •52160 | •67500 | •06866 | •02614 | 2.92000 | 2.17143 |
| 5.00000 | •61200 | •77000 | •06617 | •02692 | 3.25000 | 2.31429 |
| 6.00000 | •70240 | •86500 | •06368 | •02771 | 3.58000 | 2.45710 |
| 7.00000 | •79280 | •95750 | •06120 | •02786 | 3.91000 | 2.60000 |
| 8.00000 | •88320 | 1.05000 | •05767 | •02763 | 4.24000 | 2.74290 |
| 9.00000 | •97360 | 1.15000 | •05406 | •02795 | 4.57000 | 2.88570 |
| 10.00000 | 1.06400 | 1.21000 | •04916 | •02940 | 4.90000 | 3.02860 |
| 11.00000 | 1.15500 | 1.27750 | •04370 | •03210 | 5.25000 | 3.17140 |
| 12.00000 | 1.24600 | 1.34500 | •03755 | •03615 | 5.60000 | 3.31430 |
| 13.00000 | 1.32000 | 1.41333 | •03200 | •02875 | 6.00000 | 3.45710 |
| 14.00000 | 1.37500 | 1.02167 | •02787 | •02770 | 6.40000 | 3.60000 |
| 15.00000 | 1.41800 | •86000 | •02600 | •02767 | 6.85000 | 3.60000 |
| 16.00000 | 1.45000 | •86000 | •02600 | •02767 | 7.30000 | 3.60000 |
| 17.00000 | 1.33750 | •86000 | •03069 | •02767 | 7.30000 | 3.60000 |
| 18.00000 | 1.24500 | •86000 | •03762 | •02767 | 7.30000 | 3.60000 |
| 19.00000 | 1.15250 | •86000 | •04385 | •02767 | 7.30000 | 3.60000 |
| 20.00000 | 1.06000 | •86000 | •04940 | •02767 | 7.30000 | 3.60000 |

DELT CL GEAR • •00000 DELT CM GEAR • •00000

THIS TABLE CONTAINS THE FOLLOWING FUNCTIONS:

$$C_L(\alpha, \sigma_f), \Delta C_{LGE}(\alpha, \sigma_f), C_M(\alpha, \sigma_f), \Delta C_{MGE}(\alpha, \sigma_f)$$

$$C_E(\alpha, \sigma_f), \Delta C_{EGE}(\alpha, \sigma_f)$$

TABLE 2.5

FLAP • 5.00

| ALF | CL | CL GE | CM | CM GE | EP | EP GE |
|-----------|---------|---------|--------|--------|---------|---------|
| 4.000000 | .07500 | .00000 | .10150 | .07307 | .56000 | 1.25000 |
| 5.000000 | .01375 | .10187 | .10145 | .07304 | .90125 | 1.38750 |
| 6.000000 | .10250 | .20375 | .10112 | .07104 | 1.24250 | 1.52500 |
| 7.000000 | .19125 | .30563 | .10078 | .06942 | 1.58370 | 1.66245 |
| 8.000000 | .28000 | .40750 | .10045 | .06781 | 1.92500 | 1.80000 |
| 9.000000 | .37020 | .51000 | .10011 | .06618 | 2.28500 | 1.93482 |
| 10.000000 | .46040 | .61250 | .09902 | .06456 | 2.64500 | 2.06964 |
| 11.000000 | .55060 | .70625 | .09755 | .06311 | 3.00500 | 2.20446 |
| 12.000000 | .64080 | .80000 | .09588 | .06225 | 3.36500 | 2.33930 |
| 13.000000 | .73100 | .89000 | .09397 | .06143 | 3.72500 | 2.47410 |
| 14.000000 | .82120 | .98000 | .09176 | .06017 | 4.08500 | 2.60890 |
| 15.000000 | .91140 | 1.06625 | .08860 | .05913 | 4.44500 | 2.74380 |
| 16.000000 | 1.00160 | 1.15250 | .08542 | .05862 | 4.80500 | 2.87860 |
| 17.000000 | 1.09180 | 1.22875 | .08114 | .05857 | 5.16340 | 3.01340 |
| 18.000000 | 1.18200 | 1.30500 | .07686 | .05884 | 5.52190 | 3.14820 |
| 19.000000 | 1.27250 | 1.37375 | .07165 | .06004 | 5.89530 | 3.28300 |
| 20.000000 | 1.35800 | 1.44250 | .06652 | .06050 | 6.26880 | 3.41790 |
| 21.000000 | 1.43500 | 1.52167 | .06400 | .05868 | 6.67970 | 3.55270 |
| 22.000000 | 1.49750 | 1.60083 | .06400 | .05875 | 7.09060 | 3.68750 |
| 23.000000 | 1.55400 | .93000 | .06400 | .06090 | 7.53910 | 3.68750 |
| 24.000000 | 1.61800 | .93000 | .06400 | .06090 | 7.98750 | 3.68750 |
| 25.000000 | 1.42970 | .92995 | .06400 | .06090 | 7.98750 | 3.68750 |
| 26.000000 | 1.34150 | .93000 | .06751 | .06090 | 7.98750 | 3.68750 |
| 27.000000 | 1.25330 | .93005 | .07280 | .06090 | 7.98750 | 3.68750 |
| 28.000000 | 1.16500 | .93000 | .07766 | .06089 | 7.98750 | 3.68750 |

DELT CL GEAR • .00000 DELT CM GEAR • .00000

TABLE 2.5 (CONT.)

| ALF | CL | CL GE | CM | CM GE | EP | EP GE |
|----------|--------|--------|-------|-------|---------|---------|
| 4.00000 | 04000 | 15000 | 12530 | 12200 | 74000 | 1.50000 |
| 3.00000 | 13000 | 25000 | 12597 | 11799 | 1.11750 | 1.62500 |
| 2.00000 | 22000 | 35000 | 12665 | 11400 | 1.49500 | 1.75000 |
| 1.00000 | 31000 | 45000 | 12732 | 10999 | 1.87250 | 1.87500 |
| 0.00000 | 40000 | 55000 | 12800 | 10600 | 2.25000 | 2.00000 |
| 1.00000 | 49000 | 65000 | 12755 | 10200 | 2.64000 | 2.12679 |
| 2.00000 | 58000 | 75000 | 12710 | 09867 | 3.03000 | 2.25357 |
| 3.00000 | 67000 | 85750 | 12595 | 09633 | 3.42000 | 2.38040 |
| 4.00000 | 76000 | 92500 | 12460 | 09400 | 3.81000 | 2.50710 |
| 5.00000 | 85000 | 101000 | 12250 | 09180 | 4.20000 | 2.63390 |
| 6.00000 | 94000 | 109500 | 11980 | 09010 | 4.59000 | 2.76070 |
| 7.00000 | 103000 | 117500 | 11695 | 08850 | 4.98000 | 2.88750 |
| 8.00000 | 112000 | 125500 | 11480 | 08607 | 5.37000 | 3.01430 |
| 9.00000 | 121000 | 132750 | 11055 | 08354 | 5.75690 | 3.14110 |
| 10.00000 | 130000 | 140000 | 10650 | 08100 | 6.14370 | 3.26780 |
| 11.00000 | 139000 | 147000 | 10245 | 08217 | 6.54060 | 3.39460 |
| 12.00000 | 147000 | 154000 | 09780 | 08300 | 6.93750 | 3.52140 |
| 13.00000 | 155000 | 160000 | 09300 | 08240 | 7.33590 | 3.64820 |
| 14.00000 | 162000 | 168000 | 08840 | 08840 | 7.78120 | 3.77500 |
| 15.00000 | 169000 | 170000 | 08280 | 09200 | 8.22810 | 3.77500 |
| 16.00000 | 176000 | 170000 | 08952 | 09200 | 8.67500 | 3.77500 |
| 17.00000 | 182200 | 170000 | 09468 | 09200 | 8.67500 | 3.77500 |
| 18.00000 | 183800 | 170000 | 09972 | 09200 | 8.67500 | 3.77500 |
| 19.00000 | 185400 | 170000 | 10407 | 09200 | 8.67500 | 3.77500 |
| 20.00000 | 187000 | 170000 | 10785 | 09200 | 8.67500 | 3.77500 |

DELT CL GEAR • 00000 DELT CM GEAR • 00000

FLAP • 15.00

| ALF | CL | CL GE | CM | CM GE | EP | EP GE |
|----------|---------|---------|---------|---------|---------|---------|
| •4.00000 | •18500 | •30500 | ••16225 | ••16450 | •92000 | 1.75000 |
| •5.00000 | •27525 | •40313 | ••16441 | ••16435 | 1.33370 | 1.86245 |
| •2.00000 | •36550 | •50125 | ••16701 | ••15977 | 1.74750 | 1.97500 |
| •1.00000 | •45575 | •59938 | ••16870 | ••15518 | 2.16120 | 2.08745 |
| •0.00000 | •54600 | •69750 | ••16936 | ••15059 | 2.57500 | 2.20000 |
| 1.00000 | •63625 | •79250 | ••16932 | ••14677 | 2.99500 | 2.31875 |
| 2.00000 | •72650 | •88750 | ••16887 | ••14296 | 3.41500 | 2.43750 |
| 3.00000 | •81675 | •97150 | ••16816 | ••13959 | 3.83500 | 2.55630 |
| 4.00000 | •90700 | 1.05550 | ••16635 | ••13641 | 4.25500 | 2.67500 |
| 5.00000 | •99725 | 1.13525 | ••16455 | ••13348 | 4.67500 | 2.79380 |
| 6.00000 | 1.08750 | 1.21500 | ••16187 | ••13043 | 5.09500 | 2.91250 |
| 7.00000 | 1.17750 | 1.29125 | ••15917 | ••12706 | 5.51500 | 3.03130 |
| 8.00000 | 1.26750 | 1.36750 | ••15574 | ••12568 | 5.93500 | 3.15000 |
| 9.00000 | 1.35750 | 1.43500 | ••15207 | ••12105 | 6.35030 | 3.26870 |
| 10.00000 | 1.44750 | 1.50250 | ••14804 | ••11876 | 6.76560 | 3.38750 |
| 11.00000 | 1.53630 | 1.57005 | ••14451 | ••11820 | 7.18590 | 3.50620 |
| 12.00000 | 1.62000 | 1.63125 | ••13870 | ••11820 | 7.60620 | 3.62490 |
| 13.00000 | 1.69500 | 1.69500 | ••13383 | ••12369 | 8.03910 | 3.74380 |
| 14.00000 | 1.76000 | 1.76000 | ••13350 | ••13093 | 8.47190 | 3.86250 |
| 15.00000 | 1.75330 | 1.75330 | ••13350 | ••13698 | 8.91720 | 3.86250 |
| 16.00000 | 1.66970 | 1.66970 | ••13247 | ••13698 | 9.36250 | 3.86250 |
| 17.00000 | 1.58600 | 1.58600 | ••14077 | ••13698 | 9.36250 | 3.86250 |
| 18.00000 | 1.50230 | 1.50230 | ••14537 | ••13698 | 9.36250 | 3.86250 |
| 19.00000 | 1.41870 | 1.41870 | ••14943 | ••13698 | 9.36250 | 3.86250 |
| 20.00000 | 1.33500 | 1.33500 | ••15299 | ••13698 | 9.36250 | 3.86250 |

DELT CL GEAR • 00000 DELT CM GEAR • 00000

TABLE 2.5 (CONT.)

FLAP = 20.00

| ALF | CL | CL GE | CM | CM GE | EP | EP GE |
|----------|---------|---------|---------|---------|----------|---------|
| 4.00000 | .33000 | .46000 | ..20450 | ..21379 | 1.10000 | 2.00000 |
| 5.00000 | .42050 | .55625 | ..20862 | ..20865 | 1.55000 | 2.10000 |
| 6.00000 | .51100 | .65250 | ..21111 | ..20349 | 2.00000 | 2.20000 |
| 7.00000 | .60150 | .74875 | ..21201 | ..19834 | 2.45000 | 2.30000 |
| 8.00000 | .69200 | .84500 | ..21246 | ..19319 | 2.90000 | 2.40000 |
| 9.00000 | .78250 | .93500 | ..21291 | ..18837 | 3.35000 | 2.51071 |
| 10.00000 | .87300 | 1.02500 | ..21227 | ..18356 | 3.80000 | 2.62140 |
| 11.00000 | .96350 | 1.11550 | ..21136 | ..17925 | 4.25000 | 2.73210 |
| 12.00000 | 1.05400 | 1.18600 | ..20965 | ..17495 | 4.70000 | 2.84290 |
| 13.00000 | 1.14450 | 1.26050 | ..20739 | ..17097 | 5.15000 | 2.95360 |
| 14.00000 | 1.23500 | 1.33500 | ..20472 | ..16698 | 5.60000 | 3.06430 |
| 15.00000 | 1.32500 | 1.40750 | ..20142 | ..16287 | 6.05000 | 3.17500 |
| 16.00000 | 1.41500 | 1.48000 | ..19812 | ..15870 | 6.50000 | 3.28570 |
| 17.00000 | 1.50500 | 1.54250 | ..19475 | ..15160 | 6.94370 | 3.39640 |
| 18.00000 | 1.59500 | 1.60500 | ..19025 | ..14685 | 7.38750 | 3.50710 |
| 19.00000 | 1.68250 | 1.67000 | ..18587 | ..14489 | 7.83120 | 3.61780 |
| 20.00000 | 1.77000 | 1.72250 | ..17940 | ..13320 | 8.27500 | 3.72860 |
| 21.00000 | 1.84000 | 1.77500 | ..17380 | ..16484 | 8.71880 | 3.83930 |
| 22.00000 | 1.90000 | 1.82750 | ..16900 | ..17273 | 9.16250 | 3.95000 |
| 23.00000 | 1.81670 | 1.88003 | ..17567 | ..18062 | 9.60620 | 3.95000 |
| 24.00000 | 1.73330 | 1.90797 | ..18233 | ..18062 | 10.05000 | 3.95000 |
| 25.00000 | 1.65000 | 1.98000 | ..18750 | ..18062 | 10.05000 | 3.95000 |
| 26.00000 | 1.56670 | 1.98003 | ..19167 | ..18062 | 10.05000 | 3.95000 |
| 27.00000 | 1.48330 | 1.90797 | ..19561 | ..18062 | 10.05000 | 3.95000 |
| 28.00000 | 1.40000 | 1.98000 | ..19867 | ..18062 | 10.05000 | 3.95000 |

DELTA CL = 0.00000 DELTA CM GEAR = 0.00000

TABLE 2.5 (CONT.)

FLAP - 25.00

| ALF | CL | CL GE | CM | CM GE | EP | EP GE |
|----------|---------|---------|-------|-------|---------|---------|
| 4.00000 | 48000 | 61000 | 24950 | 21329 | 1.31670 | 2.16670 |
| 3.00000 | 57050 | 70063 | 24950 | 21329 | 1.77500 | 2.26667 |
| 2.00000 | 66100 | 79125 | 25057 | 21329 | 2.23330 | 2.36663 |
| 1.00000 | 75150 | 88187 | 25215 | 21329 | 2.69170 | 2.46670 |
| 0.00000 | 84200 | 97250 | 25310 | 21329 | 3.15000 | 2.56667 |
| 1.00000 | 93250 | 1.05750 | 25333 | 21329 | 3.61250 | 2.67321 |
| 2.00000 | 1.02300 | 1.14250 | 25315 | 21106 | 4.07500 | 2.77980 |
| 3.00000 | 1.11350 | 1.22025 | 25180 | 20700 | 4.53750 | 2.88630 |
| 4.00000 | 1.20400 | 1.29800 | 25039 | 20293 | 5.00000 | 2.99290 |
| 5.00000 | 1.29450 | 1.36900 | 24782 | 19920 | 5.46250 | 3.09940 |
| 6.00000 | 1.38500 | 1.44000 | 24526 | 19415 | 5.92500 | 3.20600 |
| 7.00000 | 1.47370 | 1.50745 | 24145 | 18838 | 6.38750 | 3.31250 |
| 8.00000 | 1.56250 | 1.57500 | 23697 | 18288 | 6.85000 | 3.41900 |
| 9.00000 | 1.65250 | 1.63500 | 23146 | 17923 | 7.30450 | 3.52560 |
| 10.00000 | 1.73500 | 1.69500 | 22536 | 17648 | 7.75900 | 3.63210 |
| 11.00000 | 1.81250 | 1.75000 | 21884 | 17625 | 8.21350 | 3.73860 |
| 12.00000 | 1.89000 | 1.80750 | 21167 | 18185 | 8.66810 | 3.84530 |
| 13.00000 | 1.95500 | 1.86500 | 21075 | 19544 | 9.12260 | 3.95180 |
| 14.00000 | 1.94290 | 1.86254 | 21075 | 20478 | 9.57710 | 4.05840 |
| 15.00000 | 1.85900 | 1.09995 | 21454 | 21329 | 9.57710 | 4.05840 |
| 16.00000 | 1.77520 | 1.09996 | 22204 | 21329 | 9.57710 | 4.05840 |
| 17.00000 | 1.69140 | 1.09997 | 22883 | 21329 | 9.57710 | 4.05840 |
| 18.00000 | 1.60760 | 1.09998 | 23449 | 21330 | 9.57710 | 4.05840 |
| 19.00000 | 1.52380 | 1.09999 | 23900 | 21329 | 9.57710 | 4.05840 |
| 20.00000 | 1.44000 | 1.10000 | 24300 | 21329 | 9.57710 | 4.05840 |

DELT CL GEAR - .00000 DELT CM GEAR - .00000

TABLE 2.5 (CONT.)

FLAP = 30.00

| ALF | CL | CL GE | CM | CM GE | EP | EP GE |
|----------|---------|---------|--------|--------|---------|---------|
| 4.00000 | .63000 | .76000 | .28790 | .24703 | 1.53330 | 2.33330 |
| 5.00000 | .72050 | .84500 | .29061 | .24703 | 2.00000 | 2.43333 |
| 6.00000 | .81100 | .93000 | .29316 | .24703 | 2.46670 | 2.53337 |
| 7.00000 | .90150 | 1.01500 | .29452 | .24703 | 2.93330 | 2.63330 |
| 8.00000 | .99200 | 1.10000 | .29588 | .24703 | 3.40000 | 2.73333 |
| 9.00000 | 1.08250 | 1.18000 | .29559 | .24294 | 3.87500 | 2.83570 |
| 10.00000 | 1.17300 | 1.26000 | .29513 | .23883 | 4.35000 | 2.93810 |
| 11.00000 | 1.26350 | 1.33500 | .29373 | .23500 | 4.82500 | 3.04050 |
| 12.00000 | 1.35400 | 1.41000 | .29192 | .23080 | 5.30000 | 3.14290 |
| 13.00000 | 1.44450 | 1.47750 | .28855 | .22495 | 5.77500 | 3.24520 |
| 14.00000 | 1.53500 | 1.54500 | .28557 | .21925 | 6.25000 | 3.34760 |
| 15.00000 | 1.62250 | 1.60750 | .27809 | .21421 | 6.72500 | 3.45000 |
| 16.00000 | 1.71000 | 1.67000 | .27065 | .21035 | 7.20000 | 3.55240 |
| 17.00000 | 1.80000 | 1.72750 | .26300 | .20850 | 7.66530 | 3.65480 |
| 18.00000 | 1.87500 | 1.78500 | .25512 | .20849 | 8.13060 | 3.75720 |
| 19.00000 | 1.94250 | 1.83000 | .24804 | .20850 | 8.59580 | 3.85950 |
| 20.00000 | 2.01000 | 1.85250 | .24071 | .21143 | 9.06110 | 3.96190 |
| 21.00000 | 2.07000 | 1.47500 | .23300 | .22517 | 9.52640 | 4.06430 |
| 22.00000 | 1.98570 | 1.29749 | .24350 | .23692 | 9.99170 | 4.16670 |
| 23.00000 | 1.90140 | 1.11997 | .25235 | .24601 | 9.99170 | 4.16670 |
| 24.00000 | 1.81710 | 1.11996 | .26120 | .24601 | 9.99170 | 4.16670 |
| 25.00000 | 1.73290 | 1.12004 | .26871 | .24601 | 9.99170 | 4.16670 |
| 26.00000 | 1.64860 | 1.12003 | .27587 | .24601 | 9.99170 | 4.16670 |
| 27.00000 | 1.56430 | 1.12001 | .28196 | .24600 | 9.99170 | 4.16670 |
| 28.00000 | 1.48000 | 1.12000 | .28660 | .24601 | 9.99170 | 4.16670 |

DELT CL GEAR * .00000 DELT CM GEAR * .00000

TABLE 2.5 (CONT.)

FLAP • 35.00

| ALF | CL | CL GE | CM | CM GE | EP | EP GE |
|----------|---------|----------|---------|---------|----------|---------|
| 4.00000 | .73000 | .86000 | ..32400 | ..28077 | 1.75000 | 2.50000 |
| 5.00000 | .82037 | .94062 | ..32400 | ..28077 | 2.22500 | 2.60000 |
| 6.00000 | .91075 | 1.02125 | ..32400 | ..28077 | 2.70000 | 2.70000 |
| 7.00000 | 1.00110 | 1.10185 | ..32402 | ..28068 | 3.17500 | 2.80000 |
| 8.00000 | 1.09150 | 1.18250 | ..32594 | ..27664 | 3.65000 | 2.90000 |
| 9.00000 | 1.18190 | 1.25878 | ..32705 | ..27283 | 4.13750 | 2.99820 |
| 10.00000 | 1.27220 | 1.33495 | ..32653 | ..26901 | 4.62500 | 3.09640 |
| 11.00000 | 1.36260 | 1.40623 | ..32531 | ..26520 | 5.11250 | 3.19460 |
| 12.00000 | 1.45300 | 1.47750 | ..32236 | ..25896 | 5.60000 | 3.29290 |
| 13.00000 | 1.54340 | 1.54190 | ..31830 | ..25344 | 6.08750 | 3.39110 |
| 14.00000 | 1.63370 | 1.60620 | ..31330 | ..24801 | 6.57500 | 3.48930 |
| 15.00000 | 1.71900 | 1.66563 | ..30712 | ..24341 | 7.06250 | 3.58750 |
| 16.00000 | 1.80420 | 1.72495 | ..30086 | ..24075 | 7.55000 | 3.68570 |
| 17.00000 | 1.88890 | 1.78065 | ..29314 | ..24075 | 8.02600 | 3.78390 |
| 18.00000 | 1.96220 | 1.83370 | ..28644 | ..24075 | 8.50210 | 3.88220 |
| 19.00000 | 2.02940 | 1.88202 | ..27973 | ..24075 | 8.97810 | 3.98030 |
| 20.00000 | 2.06030 | 1.924340 | ..27628 | ..24513 | 9.45420 | 4.07860 |
| | 2.08560 | 1.96479 | ..27520 | ..26008 | 9.93020 | 4.17680 |
| | 2.00260 | 1.28611 | ..28271 | ..27145 | 10.40600 | 4.27480 |
| | 1.91970 | 1.10752 | ..29033 | ..28040 | 10.40600 | 4.27480 |
| | 1.83670 | 1.10745 | ..29790 | ..28040 | 10.40600 | 4.27480 |
| | 1.75380 | 1.10749 | ..30460 | ..28040 | 10.40600 | 4.27480 |
| | 1.67090 | 1.10753 | ..31061 | ..28040 | 10.40600 | 4.27480 |
| | 1.58790 | 1.10746 | ..31629 | ..28040 | 10.40600 | 4.27480 |
| | 1.50500 | 1.10750 | ..32002 | ..28039 | 10.40600 | 4.27480 |

DELT CL GEAR • .00000 DELT CM GEAR • .00000

TABLE 2.5 (CONT.)

FLAP = 40.00

| ALF | CL | CL GE | CM | CM GE | EP | EP GE |
|----------|---------|---------|--------|--------|----------|---------|
| -4.00000 | .83000 | .96000 | .35200 | .31452 | 1.96670 | 2.66670 |
| -3.00000 | .92025 | 1.03625 | .35200 | .31452 | 2.45000 | 2.76667 |
| -2.00000 | 1.01050 | 1.11250 | .35250 | .31391 | 2.93330 | 2.86663 |
| -1.00000 | 1.10070 | 1.18870 | .35677 | .31017 | 3.41670 | 2.96670 |
| .00000 | 1.19100 | 1.26500 | .35925 | .30644 | 3.90000 | 3.06667 |
| 1.00000 | 1.28120 | 1.33745 | .35950 | .30289 | 4.40000 | 3.16070 |
| 2.00000 | 1.37150 | 1.41000 | .35878 | .29895 | 4.90000 | 3.25480 |
| 3.00000 | 1.46170 | 1.47745 | .35634 | .29299 | 5.40000 | 3.34880 |
| 4.00000 | 1.55200 | 1.54500 | .35318 | .28710 | 5.90000 | 3.44290 |
| 5.00000 | 1.64220 | 1.60620 | .34896 | .28174 | 6.40000 | 3.53690 |
| 6.00000 | 1.73250 | 1.66750 | .34355 | .27603 | 6.90000 | 3.63100 |
| 7.00000 | 1.81550 | 1.72375 | .33830 | .27300 | 7.40000 | 3.72500 |
| 8.00000 | 1.89850 | 1.78000 | .33187 | .27300 | 7.90000 | 3.81900 |
| 9.00000 | 1.97770 | 1.83370 | .32572 | .27300 | 8.38680 | 3.91310 |
| 10.00000 | 2.04950 | 1.88250 | .31933 | .27300 | 8.87360 | 4.00710 |
| 11.00000 | 2.11630 | 1.91405 | .31740 | .27300 | 9.36040 | 4.10120 |
| 12.00000 | 2.11060 | 1.93429 | .31740 | .27914 | 9.84720 | 4.19520 |
| 13.00000 | 2.10110 | 1.95449 | .31740 | .29502 | 10.33400 | 4.28930 |
| 14.00000 | 2.01950 | 1.97473 | .32216 | .30597 | 10.82100 | 4.38350 |
| 15.00000 | 1.93790 | 1.99496 | .32881 | .31452 | 10.82100 | 4.38350 |
| 16.00000 | 1.85630 | 1.99495 | .33513 | .31451 | 10.82100 | 4.38350 |
| 17.00000 | 1.77480 | 1.99504 | .34101 | .31451 | 10.82100 | 4.38350 |
| 18.00000 | 1.69320 | 1.99502 | .34591 | .31452 | 10.82100 | 4.38350 |
| 19.00000 | 1.61160 | 1.99501 | .35080 | .31451 | 10.82100 | 4.38350 |
| 20.00000 | 1.53000 | 1.99500 | .35595 | .31452 | 10.82100 | 4.38350 |

DELT CL GEAR = .00000 DELT CM GEAR = .00000

TABLE 2.5 (CONT.)

FLAP * 45.00

| ALF | CL | CL GE | CM | CM GE | EP | EP GE |
|----------|----------|---------|--------|--------|----------|---------|
| 4.00000 | 1.93000 | 1.06000 | 3.8000 | 3.4826 | 2.18330 | 2.83330 |
| 5.00000 | 1.02010 | 1.13185 | 3.8148 | 3.4673 | 2.67500 | 2.93333 |
| 2.00000 | 1.11020 | 1.20370 | 3.8782 | 3.4329 | 3.16670 | 3.03337 |
| 1.00000 | 1.20040 | 1.27565 | 3.9175 | 3.3986 | 3.65830 | 3.13330 |
| 0.00000 | 1.29050 | 1.34750 | 3.9265 | 3.3642 | 4.15000 | 3.23333 |
| 1.00000 | 1.38060 | 1.41622 | 3.9235 | 3.3247 | 4.66250 | 3.32320 |
| 2.00000 | 1.47070 | 1.48495 | 3.9048 | 3.2634 | 5.17500 | 3.41310 |
| 3.00000 | 1.56090 | 1.54878 | 3.8823 | 3.2070 | 5.68750 | 3.50300 |
| 4.00000 | 1.65100 | 1.61250 | 3.8483 | 3.1480 | 6.20000 | 3.59290 |
| 5.00000 | 1.74110 | 1.67060 | 3.8055 | 3.0846 | 6.71250 | 3.68270 |
| 6.00000 | 1.83130 | 1.72880 | 3.7576 | 3.0525 | 7.22500 | 3.77260 |
| 7.00000 | 1.91200 | 1.78187 | 3.7061 | 3.0525 | 7.73750 | 3.86250 |
| 8.00000 | 1.99270 | 1.83495 | 3.6546 | 3.0525 | 8.25000 | 3.95240 |
| 9.00000 | 2.06660 | 1.88685 | 3.5986 | 3.0525 | 8.74760 | 4.04230 |
| 10.00000 | 2.13670 | 1.93120 | 3.5960 | 3.0525 | 9.24510 | 4.13210 |
| 11.00000 | 2.20310 | 1.98097 | 3.5960 | 3.0525 | 9.74270 | 4.22200 |
| 12.00000 | 2.26080 | 1.62509 | 3.5960 | 3.1342 | 10.24000 | 4.31160 |
| 13.00000 | 2.311670 | 1.44428 | 3.5960 | 3.2997 | 10.73800 | 4.40190 |
| 14.00000 | 2.36640 | 1.26334 | 3.6219 | 3.4045 | 11.23500 | 4.49130 |
| 15.00000 | 1.95620 | 1.08251 | 3.6779 | 3.4825 | 11.23500 | 4.49130 |
| 16.00000 | 1.87600 | 1.08255 | 3.7291 | 3.4826 | 11.23500 | 4.49130 |
| 17.00000 | 1.79570 | 1.08249 | 3.7795 | 3.4825 | 11.23500 | 4.49130 |
| 18.00000 | 1.71550 | 1.08252 | 3.8176 | 3.4825 | 11.23500 | 4.49130 |
| 19.00000 | 1.63520 | 1.08246 | 3.8558 | 3.4826 | 11.23500 | 4.49130 |
| 20.00000 | 1.55500 | 1.08250 | 3.8837 | 3.4825 | 11.23500 | 4.49130 |

DELT CL GEAR * 0.0000 DELT CM GEAR * 0.0000

TABLE 2.5 (CONT.)

FLAP = 50.00

58

| ALF | CL | CL GE | CM | CM GE | EP | EP GE |
|----------|---------|---------|---------|---------|----------|---------|
| -4.00000 | 1.03000 | 1.16000 | ..41100 | ..37920 | 2.40000 | 3.00000 |
| -3.00000 | 1.12000 | 1.22750 | ..41920 | ..37605 | 2.90000 | 3.10000 |
| -2.00000 | 1.21000 | 1.29500 | ..42420 | ..37290 | 3.40000 | 3.20000 |
| -1.00000 | 1.30000 | 1.36250 | ..42600 | ..36975 | 3.90000 | 3.30000 |
| .00000 | 1.39000 | 1.43000 | ..42600 | ..36530 | 4.40000 | 3.40000 |
| 1.00000 | 1.48000 | 1.49500 | ..42480 | ..35945 | 4.92500 | 3.48570 |
| 2.00000 | 1.57000 | 1.56000 | ..42345 | ..35360 | 5.45000 | 3.57140 |
| 3.00000 | 1.66000 | 1.62000 | ..42090 | ..34750 | 5.97500 | 3.65710 |
| 4.00000 | 1.75000 | 1.68000 | ..41775 | ..34000 | 6.50000 | 3.74290 |
| 5.00000 | 1.84000 | 1.73500 | ..41400 | ..33312 | 7.02500 | 3.82860 |
| 6.00000 | 1.93000 | 1.79000 | ..40950 | ..32625 | 7.55000 | 3.91430 |
| 7.00000 | 2.00850 | 1.84000 | ..40549 | ..31900 | 8.07500 | 4.00000 |
| 8.00000 | 2.08700 | 1.89000 | ..40078 | ..31150 | 8.60000 | 4.08570 |
| 9.00000 | 2.15550 | 1.94000 | ..39500 | ..30159 | 9.10830 | 4.17140 |
| 10.00000 | 2.22400 | 1.98000 | ..38812 | ..29320 | 9.61670 | 4.25720 |
| 11.00000 | 2.29000 | 1.79800 | ..38020 | ..32525 | 10.12500 | 4.34290 |
| 12.00000 | 2.21110 | 1.61599 | ..38967 | ..34800 | 10.63300 | 4.42820 |
| 13.00000 | 2.13220 | 1.43398 | ..39710 | ..36494 | 11.14200 | 4.51460 |
| 14.00000 | 2.05330 | 1.25197 | ..40280 | ..37491 | 11.65000 | 4.60000 |
| 15.00000 | 1.97440 | 1.06996 | ..40728 | ..38200 | 11.65000 | 4.60000 |
| 16.00000 | 1.89560 | 1.07004 | ..41122 | ..38200 | 11.65000 | 4.60000 |
| 17.00000 | 1.81670 | 1.07003 | ..41517 | ..38200 | 11.65000 | 4.60000 |
| 18.00000 | 1.73780 | 1.07002 | ..41818 | ..38200 | 11.65000 | 4.60000 |
| 19.00000 | 1.65890 | 1.07001 | ..42094 | ..38200 | 11.65000 | 4.60000 |
| 20.00000 | 1.58000 | 1.07000 | ..42330 | ..38200 | 11.65000 | 4.60000 |

DELT CL GEAR * .00000 DELT CM GEAR * .00000

STOP 0

TABLE 2.5 (CONT.)

LONGITUDINAL AERODYNAMIC EQUATIONS

STABILITY TO BODY AXIS TRANSFORMATION

$$C_{XB} = C_{XS} \cos \alpha - C_{ZS} \sin \alpha$$

$$C_{ZB} = C_{XS} \sin \alpha + C_{ZS} \cos \alpha$$

$$C_{MB} = C_{MS}$$

EQUATIONS AERODYNAMIC SECTION

FIG. 2.9

LATERAL - DIRECTIONAL AERO COEFFICIENTS

COEFFICIENT OF ROLLING MOMENT:

$$C_{l_{\tau 0}} = C_{l_{\beta 0}} \beta + C_{l_{\dot{\beta}}} \dot{\beta} + (C_{l_{p 0}} C_{l_{p}}^{E/R} \rho_s + C_{l_{r 0}} \rho_s) b w / 2 V \\ + C_{l_{\delta a}} C_{l_{\delta a}}^{E/R} \delta_a + C_{l_{\delta \dot{a}}}^{E/R} \delta_{\dot{a}} + C_{l_{\delta \dot{a}}}^{E/R} C_{\ell} (\alpha, \delta_{s p}, \delta_{\dot{f}})$$

WHERE:

$$C_{l_{\beta 0}} = C_{l_{\beta}}(\delta_f) + (\Delta C_{l_{\beta}})_{C_{L 0} = 0}^E + (C_{l_{\beta}}(\delta_f) - (\Delta \frac{\partial C_{l_{\beta}}}{\partial C_L})_{\tau 0}^E) C_{L \tau 0}^E \\ + (\frac{\partial C_{l_{\beta}}}{\partial \alpha})_{\tau 0}^E N_z$$

$$C_{l_{\dot{\beta}}} = .00002$$

REF: (DC9-A10-432.1, P. 210)

$$C_{l_{p 0}} = -.0075$$

(DC9-C20-623.1, P. 68)

$$C_{l_{r 0}} = -.0000254 \delta_f + .00488 C_{L \tau 0}^E$$

(DC9-A11.74A, P. 70)

EQUATIONS AERODYNAMIC SECTION

FIG. 2.10

LATERAL - DIRECTIONAL AERO COEFFICIENTS

ROLLING MOMENT COEFF

$$C_{l_{\dot{\gamma}}} = .00093$$

REF: (D69-C2D-392, P. 73 & 79)

$$C_{l_{\dot{\gamma}}}^{E/R} = 1 - .001079$$

(D69-C2D-667, P. 212)

$$C_{l_{\dot{\gamma}}_{50}}^{E/R} = 1 - .000559$$

(D69-C2D-664, P. 213)

$$\left(\Delta C_{l_{\beta}} \right)_{\tau_0}^E = .00025$$

(D69-A9.67, P. 209)

$$\left(\Delta \frac{\partial C_{l_{\beta}}}{\partial C_L} \right)_{\tau_0}^E = .000059$$

"

$$\left(\frac{\partial C_{l_{\beta}}}{\partial \eta} \right)_{\tau_0}^E = .0001$$

"

$$C_{l_p}^{E/R} = 1 - .000589$$

(D69-C2D-665, P. 211)

FUNCTION TABLE AERO DYNAMIC SECTION
TABLE 2.6

FUNCTION: $C_e(\alpha, \delta_{sp}, \delta_f)$ FOR $\delta_f = 0$

| δ_{sp} | α | | | | |
|---------------|----------|-------|-------|-------|-------|
| | -4 | 0 | 4 | 8 | 12 |
| 0 | 0 | 0 | 0 | 0 | 0 |
| 20 | .0104 | .011 | .0114 | .0120 | .0120 |
| 35 | .0177 | .0187 | .0195 | .0204 | .0204 |
| 50 | .0244 | .0256 | .0269 | .0282 | .0282 |
| 60 | .0280 | .0295 | .0310 | .0326 | .0326 |

REF: DC-9-C20.803
LB-32322 A.82

FUNCTION TABLE AERODYNAMIC SECTION

TABLE 2.6 (CONT.)

FUNCTION: $C_e(\alpha, \delta_{sp}, \delta_f)$ FOR $\delta_f = 20$

| δ_{sp} | α | | | |
|---------------|----------|-------|-------|-------|
| | -4 | 0 | 4 | 8 |
| | 0 | 0 | 0 | 0 |
| 0 | .003 | .0031 | .0033 | .0035 |
| 5 | .0071 | .0075 | .0080 | .0085 |
| 10 | .0124 | .0131 | .0142 | .0149 |
| 15 | .0172 | .0182 | .0197 | .0207 |
| 20 | .0212 | .0225 | .0242 | .0255 |
| 25 | .0245 | .0260 | .0279 | .0293 |
| 30 | .0298 | .0319 | .0340 | .0358 |
| 40 | .0342 | .0367 | .0390 | .0412 |
| 50 | .0380 | .0410 | .0435 | .0460 |
| 60 | | | | |

REF: ibid.

FUNCTION TABLE AERODYNAMIC SECTION

TABLE 2.6 (CONT.)

FUNCTION: $C_e(\alpha, \delta_{sp}, \delta_f)$ FOR $\delta_f = 50$

| δ_{sp} | α | | | | |
|---------------|----------|-------|-------|-------|----|
| | -4 | 0 | 4 | 8 | 12 |
| 0 | 0 | 0 | 0 | 0 | |
| 4 | .0040 | .0042 | .0045 | .0048 | |
| 8 | .0150 | .0158 | .0173 | .0180 | |
| 16 | .0396 | .0410 | .0425 | .0444 | |
| 20 | .0470 | .0498 | .0522 | .0554 | |
| 25 | .0522 | .0575 | .0612 | .0665 | |
| 30 | .0558 | .0623 | .0674 | .0739 | |
| 35 | .0589 | .0654 | .0715 | .0780 | |
| 40 | .0616 | .0681 | .0745 | .0807 | |
| 50 | .0667 | .0734 | .0798 | .0855 | |
| 60 | .0715 | .0781 | .0846 | .0900 | |

REF: *ibid.*

FUNCTION TABLE AERODYNAMIC SECTION

TABLE 2.7

FUNCTION: $Cl_{P_2}(\alpha_f)$

| α_f | $Cl_{P_2}(\alpha_f)$ | α_f | $Cl_{P_2}(\alpha_f)$ |
|------------|----------------------|------------|----------------------|
| 0 | -.00225 | 30 | -.00242 |
| 5 | -.00230 | 35 | -.00244 |
| 10 | -.00232 | 40 | -.00245 |
| 15 | -.00235 | 45 | -.00247 |
| 20 | -.00238 | 50 | -.00250 |
| 25 | -.00240 | | |

FUNCTION TABLE AERO DYNAMIC SECTION

TABLE 2.8

FUNCTION: $C_{lp}(\alpha_f)$

| α_f | $C_{lp}(\alpha_f)$ | α_f | $C_{lp}(\alpha_f)$ |
|------------|--------------------|------------|--------------------|
| 0 | -.00004 | 30 | .00159 |
| 5 | .00020 | 35 | .00187 |
| 10 | .00045 | 40 | .00219 |
| 15 | .00073 | 45 | .00248 |
| 20 | .00100 | 50 | .00280 |
| 25 | .00128 | | |

LATERAL-DIRECTIONAL AERO COEFFICIENTS

COEFFICIENT OF YAWING MOMENT:

$$C_{n\beta_{TD}} = C_{n\beta_{TD}} \beta + C_{n\delta_a} \delta_a + C_n(\alpha, \delta_{sp}, \delta_f) + (C_{n\dot{p}} \dot{p}_s + C_{n\dot{r}} \dot{r}_s) \text{ bw/2V}$$

WHERE:

$$C_{n\beta_{TD}} = -.002 + .000011 \delta_f$$

REF: (DCA-A11.40, P.59)

$$C_{n\delta_a} = .000025 [\delta_f - 20]_{0}^{30} - .0000075 \alpha + .00001$$

(DCA-C20.496, P.80)

$$C_{n\dot{p}} = .0000084 \delta_f - .00148 C_{L\dot{E}}_{TD}$$

(DCA-A9.29, 30, P.64; 65)

$$C_{n\dot{r}} = -.00005 - .000011 \delta_f - .00019 (C_{L\dot{E}}_{TD})^2$$

(DCA-A11.69A, P.69)

FUNCTION TABLE AERODYNAMIC SECTION

TABLE 2.9

Function: $C_n(\alpha, \delta_{sp}, \delta_f)$ For $\delta_f = 0$

| δ_{sp} | α | | | | |
|---------------|----------|-------|-------|-------|-------|
| | -4 | 0 | 4 | 8 | 12 |
| 0 | 0 | 0 | 0 | 0 | 0 |
| 8 | .0006 | .0009 | .0006 | .0009 | .0006 |
| 12 | .0010 | .0014 | .0012 | .0014 | .0010 |
| 20 | .0018 | .0024 | .0022 | .0026 | .0018 |
| 60 | .0068 | .0080 | .0074 | .0086 | .0086 |

REF: DC9-C20.437
LB-31624 P. 113

FUNCTION TABLE AERODYNAMIC SECTION

TABLE 2.9 (CONT.)

FUNCTION: $C_n(\alpha, \delta_{sp}, \delta_f)$ FOR $\delta_f = 20$

| δ_{sp} | α | | | | |
|---------------|----------|-------|--------|-------|-------|
| | -4 | 0 | 4 | 8 | 12 |
| 0 | 0 | 0 | 0 | 0 | 0 |
| 5 | .0011 | .0010 | .0007 | .0004 | .0004 |
| 10 | .0030 | .0025 | -.0016 | .0010 | .0010 |
| 20 | .0058 | .0050 | .0037 | .0026 | .0026 |
| 40 | .0098 | .0090 | .0075 | .0061 | .0061 |
| 60 | .0136 | .0128 | .0111 | .0094 | .0094 |

Ref: ibid.

FUNCTION TABLE AERODYNAMIC SECTION

TABLE 2.9 (CONT.)

FUNCTION: $C_n(\alpha, \sigma_{sp}, \sigma_f)$ FOR $\sigma_f = 50$

| σ_{sp} | α | | | | |
|---------------|----------|-------|-------|-------|----|
| | -4 | 0 | 4 | 8 | 12 |
| 0 | 0 | 0 | 0 | 0 | |
| 5 | .0022 | .0017 | .0012 | .0009 | |
| 10 | .0051 | .0041 | .0030 | .0022 | |
| 15 | .0084 | .0070 | .0054 | .0041 | |
| 20 | .0112 | .0098 | .0080 | .0063 | |
| 25 | .0132 | .0117 | .0101 | .0080 | |
| 30 | .0146 | .0131 | .0114 | .0092 | |
| 40 | .0167 | .0150 | .0133 | .0110 | |
| 50 | .0184 | .0166 | .0149 | .0126 | |
| 60 | .0199 | .0180 | .0163 | .0138 | |

REF: ibid.

LATERAL-DIRECTIONAL AERO COEFFICIENTS

COEFFICIENT OF SIDE FORCE FOR FUSELAGE WITH TAIL OFF

$$C_{y\beta TO} = C_{y\beta TO} \beta + (C_{y\beta TO} (P_3)) \frac{bw}{2V}$$

WHERE:

$$C_{y\beta TO} = -.0051 - .000018 \sqrt{f}$$

REF: (DC9-A11.41, P.60)

$$C_{yP_{TO}} = .00115 - .0000068 \sqrt{f} + .00284 C_{L_{TO}}^E$$

(DC9-A9.22, P.23, P.66, P.67)

EQUATIONS AERODYNAMIC SECTION

FIG. 2.13

LATERAL-DIRECTIONAL AERO COEFFICIENTS

COEFFICIENT OF SIDE FORCE DUE TO VERTICAL TAIL WITHOUT RUDDER

$$C_{YV} = F_V \left[C_{L\alpha}^{ELR} C_{Y\beta} \beta + C_{Yi} \dot{r}_B + C_{Yny} N_Y + C_{L\alpha}^{ELR} (C_{Y\beta} \dot{\beta} + C_{Yp} p_B + C_{Yr} r_B + \frac{C_{Y\dot{r}}}{V} \dot{r}_B) \frac{w}{2V} \right]$$

WHERE:

$$F_V = 1 - .00016 f \quad (DC9-26.206, P.206) \quad C_{Yp} = -.00115 \quad (DC9-A9.22 \ddagger 23, P.66 \ddagger 67)$$

$$C_{L\alpha}^{ELR} = 1 - .00021 f \quad " \quad C_{Yr} = .0088 + .000032 \sqrt{f} \quad (DC9-A11.69 A, P.69)$$

$$C_{Yi} = -.000045 \quad (DC9-26.218, P.208) \quad C_{Y\dot{r}} = .0319 - .000058 \sqrt{f} \quad (DC9-A9.13, P.72)$$

$$C_{Yny} = .0014 \quad " \quad b_w = 89.35 ft.$$

$$C_{Y\beta} = .0003 + .000036 \sqrt{f} \quad (DC9-A15-194-1, P.71)$$

$$C_{Yp} = -.0106 - .000043 \sqrt{f} \quad (DC9-A11.41, P.60)$$

EQUATIONS AERODYNAMIC SECTION

FIG. 2.14

LATERAL-DIRECTIONAL AERO COEFFICIENTS

COEFFICIENT OF SIDE FORCE DUE TO RUDDER

$$C_y(\delta_r) = F_v C_{y_{\delta_r}}^{E/R} C_{y_{\delta_r}} C_{y_{\delta_r}} \delta_r$$

WHERE:

$$C_{y_{\delta_r}}^{E/R} = 1 - .00035 \delta_r$$

REF: (DLG-C6.219, P. 207)

$$C_{y_{\delta_r}} = .00492 - .000024 \alpha + .0000116 \delta_r \quad (\text{DLG-C6.166, P. 120})$$

COEFFICIENT OF TOTAL SIDE FORCE, BODY AXIS

$$C_{y_B} = C_{y_{T0}} + C_{y_v} + C_y(\delta_r)$$

EQUATIONS AERODYNAMIC SECTION

FIG. 2.15

LATERAL - DIRECTIONAL AERO COEFFICIENTS

COEFFICIENTS OF ROLLING AND YAWING MOMENT, BODY AXIS

$$C_{\ell_B} = C_{\ell_{TOS}} \cos \alpha - C_{n_{TOS}} \sin \alpha + a_{\ell_{CG}} C_{Yr} + a_{\ell_{CGr}} C_Y(\sigma_r)$$

$$C_{n_B} = C_{n_{TOS}} \cos \alpha + C_{\ell_{TOS}} \sin \alpha - \ell_{\ell_{CG}} C_{Yr} - \ell_{\ell_{CGr}} C_Y(\sigma_r) - \ell_{x_{CG}} C_{Yr}$$

WHERE:

$$a_{\ell_{CG}} = \bar{z}_{\ell_{CG}}/b_w = .1394$$

$$a_{\ell_{CGr}} = \bar{z}_{\ell_{CGr}}/b_w = .134$$

$$\ell_{\ell_{CG}} = \ell_{\ell_{CG}c/4} + (.25 - x_{CG}) c_w/b_w \quad ; \quad \ell_{\ell_{CGr}c/4} = x_{\ell_{CGr}}/b_w = .407$$

$$\ell_{\ell_{CGr}} = \ell_{\ell_{CGr}c/4} + (.25 - x_{CG}) c_w/b_w \quad ; \quad \ell_{\ell_{CGr}c/4} = x_{\ell_{CGr}}/b_w = .407$$

$$\ell_{x_{CG}} = (.25 - x_{CG}) c_w/b_w$$

Section 3
Engine Model

The simulation model for the JT8D DC-9 engine was developed from static and dynamic data provided by Pratt & Whitney and Douglas Flight Test. The static data for forward and reverse thrust were formed into a table with mach number and E.P.R. as arguments. (See Table 3.1) Likewise, a table of E.P.R. versus cross shaft angle was formed. (See Table 3.2) Table 3.2 was taken directly from the published engine performance data for the sea level static case. The values of E.P.R. were taken from the 59 degree F curve with the exception that the reverse E.P.R.'s were made negative to facilitate entry into the thrust vs. E.P.R./mach no. table, Table 3.1. The dynamic data (consisting of typical engine acceleration and deceleration time histories) was used to estimate a representative time constant.

The engine model was configured as shown in Figure 3.1. The sensor on the cockpit throttle pedestal provides a positive signal for the position of the main throttle handles and a negative signal for the position of the reverse thrust levers. When this plus/minus signal reaches the computer it is biased and scaled to represent cross shaft angle (XS) which has a range of 2.5 to 90 degrees. A cross shaft angle between 2.5 and 20 degrees indicates reverse thrust and an XS angle between 45 and 90 degrees indicates forward thrust. The idle position is 38.4 degrees of XS.

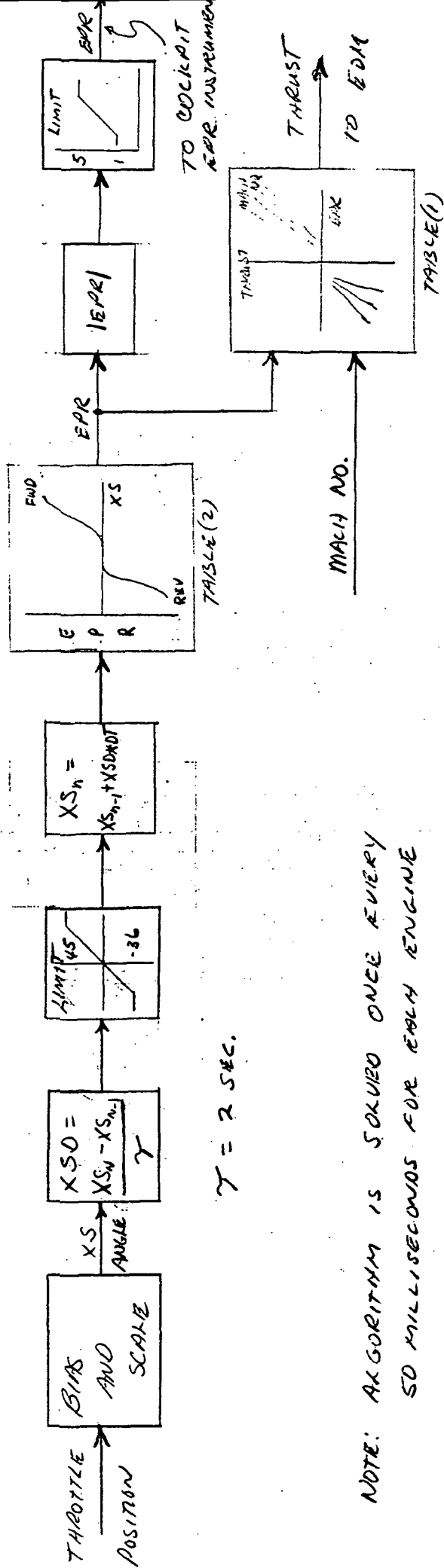
The past value of XS is subtracted from the current XS value to form a differential. After limiting the differential is integrated to form a new current value of XS angle. This process results in a first order lag which approximates the engine dynamics. The lagged XS position is then used as an argument in Table 3.2 to find E.P.R. and E.P.R. along with mach number is used to find thrust from Table 3.1. The absolute value of E.P.R. is limited and sent to the E.P.R. instrument in the cockpit and thrust is made available to the equations of motion for force calculations.

With the main throttle handles in the idle position, "reverse thrust" is commanded by pulling the reverse thrust levers up to a detent. At the detent the amber "UNLOCK" light is lit and a logic signal is sent to the engine program which starts a 2 second timer. After 2 seconds the computer returns a logic signal which causes the green "REVERSE THRUST" light to be lit and at the same time causes the detent to be retracted allowing the levers to move on up, thus increasing reverse thrust.

Returning the reverse thrust levers to the stowed position turns out the amber light and causes the computer to turn out the green light and reset the detent.

The engine model was validated by first comparing E.P.R. and thrust values for various cross shaft angles with supplied data. Secondly, the dynamic response of the engine model was adjusted using pilot comments and comparisons to supplied data.

NOTE: The actual engine acceleration and deceleration responses are not simple lags as used in the model. The deceleration of the engine is fairly close to a first order lag while the acceleration is more akin to a second order type response. Nevertheless, it has been found in past simulations, that a first order lag gives a very acceptable representation of engine dynamics. The data indicated a time constant of about 3 seconds, however, pilots seemed to prefer something a little less than 2 seconds. A time constant of 2 seconds was used in the simulation.



ENGINE MODEL BLOCK DIAGRAM

FIGURE 3.1

ENGINE MODEL FUNCTION TABLES

TABLE 3.1
THRUST VS. EPR AND MACH NO.

| -2.2 1. | -1.8 1.3 | -1.4 1.6 | -1 1.9 | -.6 2.2 | EPR EPR |
|-----------------|------------------|-----------------|------------------|--------------|-------------------|
| -7150. 0. | -4360. 5250. | -1920. 9520. | -100. 13200. | 0. 16400. | M = 0. M = 0 . |
| -9200. 0. | -6230. 4750. | -3400. 8750. | -820. 12320. | 0. 15400. | M = .1 M = .1 |
| -11920. 90. | -8510. 4400. | -5130. 8240. | -1880. 11780. | 0. 14890. | M = .2 M = .2 |
| -15200. 200. | -11400. 4300. | -7600. 8000. | -3740. 11470. | 0. 14700. | M = .3 M = .3 |

TABLE 3.2
EPR VS. CROSS SHAFT ANGLE

| 2.5 45. -2.13 1.03 | 10. 55. -1.60 1.03 | 15. 73.5 -1.27 1.70 | 20. 90. -1.03 2.16 | 35. -1.03 | 36. 1.03 | XS XS EPR EPR |
|-----------------------------|-----------------------------|------------------------------|-----------------------------|--------------|-------------|------------------------|
|-----------------------------|-----------------------------|------------------------------|-----------------------------|--------------|-------------|------------------------|

Section 4
Environmental Models

This section covers the runway condition models (crown, roughness and friction), the wind model and the turbulence model.

The crown, roughness and friction models are fully described in MCAIR report - titled "DC-9 Landing Gear Math Model for Directional Control On Runway Flight Simulation", by Harry Passmore, Reference 4. The crown model is the same as that in the report and the roughness and friction models are essentially the same except for the following changes:

- 1) The runway roughness table used was the same as the table 7-1 of the Passmore report except that all the bump heights were multiplied by 2. Also, the starting point of the table was set 500 feet "in" from the threshold to allow a "smooth" area for trimming the airframe simulation on the ground.
- 2) The DC-9 Nose Tire Cornering Coefficient (see figure 7-4 of the Passmore report) was multiplied by a factor of 5/7. This was done to reduce nose wheel steering sensitivity but did not take the resulting cornering force outside of an acceptable range. The main gear curves were the same as in the report.
- 3) The patchy runway condition profiles used in the study were essentially the same as cases 3 and 4 of figure 7-3 of the Passmore report. The exception is that in case 4, the patchy asymmetric profile, the "ICE"

segments were replaced with "WET" or "FLOODED" segments (see figure 4.1 below).

Turbulence Model:

The air turbulence model used for the ground handling study was developed from the Dryden* spectra (as opposed to the von Karman spectra). The independent longitudinal, lateral and vertical gust components are generated by filtering Gaussian random signals with the following three filters:

$$\begin{aligned}
 \text{Longitudinal} \quad F_u(s) &= \sigma_u \sqrt{\frac{L_u}{2\pi V}} \frac{1}{1 + \frac{L_u}{V} s} \\
 \text{Lateral} \quad F_v(s) &= \sigma_v \sqrt{\frac{L_v}{2\pi V}} \frac{1 + \sqrt{3} \frac{L_v}{V} s}{(1 + \frac{L_v}{V} s)^2} \\
 \text{Vertical} \quad F_w(s) &= \sigma_w \sqrt{\frac{L_w}{2\pi V}} \frac{1 + \sqrt{3} \frac{L_w}{V} s}{(1 + \frac{L_w}{V} s)^2}
 \end{aligned}$$

where:

$\sigma_u, \sigma_v, \sigma_w$ = RMS gust intensities.

These sigma values are a function of altitude.

| ALT | σ_u AND σ_v | σ_w |
|-----|---------------------------|------------|
| 20 | .65 | 0 |
| 75 | 1.63 | .15 |
| 150 | 3.61 | .25 |
| 300 | 4.75 | .31 |
| 450 | .5 | .09 |
| 600 | .25 | .06 |

*See, for example, Reference 7.

PATCHY RUNWAY CONDITION PROFILES

| RUNWAY DISTANCE, FT | PATCHY SYMMETRIC | | | | | PATCHY UNSYMMETRIC | | |
|---------------------------|------------------|---------|---------|---|----|--------------------|-----|---------|
| | LMG | NG | RMG | | | LMG | NG | RMG |
| 0-500 | WET | WET | WET | A | 1 | WET | WET | WET |
| 500-1000 | WET | WET | WET | B | 2 | WET | WET | WET |
| 1000-1500 | WET | WET | WET | C | 3 | WET | WET | WET |
| 1500-2000 | WET | WET | WET | D | 4 | WET | WET | WET |
| 2000-2500 | WET | WET | WET | E | 5 | WET | WET | WET |
| 2500-3000 | WET | WET | WET | F | 6 | WET | WET | WET |
| 3000-3500 | WET | WET | WET | G | 7 | WET | WET | WET |
| 3500-4000 | WET | WET | WET | H | 8 | WET | WET | WET |
| 4000-4500 | FLOODED | FLOODED | FLOODED | I | 9 | FLOODED | WET | WET |
| 4500-5000 | WET | WET | WET | J | 10 | WET | WET | DRY |
| 5000-5050 | FLOODED | FLOODED | FLOODED | K | 11 | DRY | DRY | WET |
| 5050-5100 | WET | WET | WET | L | 12 | WET | WET | FLOODED |
| 5100-5150 | FLOODED | FLOODED | FLOODED | M | 13 | DRY | DRY | WET |
| 5150-5200 | WET | WET | WET | N | 14 | WET | WET | FLOODED |
| 5200-5250 | DRY | DRY | DRY | O | 15 | FLOODED | WET | WET |
| 5250-5300 | FLOODED | FLOODED | FLOODED | P | 16 | WET | WET | DRY |
| 5300-5350 | WET | WET | WET | Q | 17 | DRY | DRY | WET |
| 5350-5400 | FLOODED | FLOODED | FLOODED | A | 18 | WET | WET | FLOODED |
| 5400-5450 | WET | WET | WET | B | 19 | DRY | DRY | WET |
| 5450-5500 | DRY | DRY | DRY | C | 20 | WET | WET | FLOODED |
| 5500-5600 | WET | WET | WET | D | 21 | FLOODED | WET | WET |
| 5600-5700 | FLOODED | FLOODED | FLOODED | E | 22 | WET | WET | FLOODED |
| 5700-5800 | WET | WET | WET | F | 23 | FLOODED | WET | WET |
| 5800-5900 | DRY | DRY | DRY | G | 24 | WET | WET | FLOODED |
| 5900-6000 | WET | WET | WET | H | 25 | FLOODED | WET | WET |
| 6000-6500 | FLOODED | FLOODED | FLOODED | I | 26 | WET | WET | FLOODED |
| 6500-7000 | WET | WET | WET | J | 27 | FLOODED | WET | WET |
| 7000-7500 | DRY | DRY | DRY | K | 28 | WET | WET | FLOODED |
| 7500-8000 | WET | WET | WET | L | 29 | FLOODED | WET | WET |
| 8000-8500 | FLOODED | FLOODED | FLOODED | M | 30 | WET | WET | FLOODED |
| 8500-9000 | WET | WET | WET | N | 31 | FLOODED | WET | WET |
| 9000-9500 | WET | WET | WET | O | 32 | WET | WET | FLOODED |
| 9500-10000 | WET | WET | WET | P | 33 | FLOODED | WET | WET |

NOTE: Patchy symmetrical same as Case #3 used in McAir simulator runs

FIGURE 4.1

L_u, L_v, L_w = scale lengths. These are normally functions of altitude, however, for the ground handling study they were held constant.

$$L_u = L_v = 400, \quad L_w = 200$$

V = the true airspeed of the aircraft. For this study the used for the filters was held constant at 100 f.p.s.

S = the Laplace transform variable.

The turbulence model was activated by using a numerical Gaussian random number generator to supply the inputs to the filters. The outputs of the filters are then considered to be the X, Y and Z gust components.

$$GUST_x = RAN(1) * F_u(S)$$

$$GUST_y = RAN(2) * F_v(S)$$

$$GUST_z = RAN(3) * F_w(S)$$

where:

$GUST_x, GUST_y, GUST_z$ = gust velocity components in feet per second.

$RAN(1), RAN(2), RAN(3)$ = three Gaussian random numbers which range from zero to +1 and are generated in series from a common seed.

$F_u(S), F_v(S), F_w(S)$ = the three filters shown above.

The actual digital algorithm was patterned after that in a NASA-Ames Program Specification, titled "Wind," by R. E. McFarland. (Reference 8). The algorithm used in the ground handling simulation did not include the rotational terms and had $1/\sqrt{2}$ less gain than the "Wind" algorithm.

Wind Model:

The wind model allowed for the specification of the wind components in the earth axes system. The X, Y and Z wind components could be specified as constants or functions of either range or altitude. Several of these tables of winds could be stored and the particular table desired could be called up before a run. Actually the tables for the gust parameters were also handled by the wind routine making it the complete definer of the wind conditions.

After calculating the various elements these elements were summed to form the total wind component for each axes.

$$U_{WE} = \text{SHEAR}_x + \text{STEADY}_x + \text{GUST}_x$$

$$V_{WE} = \text{SHEAR}_y + \text{STEADY}_y + \text{GUST}_y$$

$$W_{WE} = \text{SHEAR}_z + \text{STEADY}_z + \text{GUST}_z$$

These wind components are then differentiated to form the wind acceleration components.

$$\dot{U}_{WE}, \dot{V}_{WE} \text{ AND } \dot{W}_{WE}$$

The six wind velocities and accelerations are picked up in the EOM where the velocity components are added to the inertial velocity components and the acceleration components are transformed to the body axis where they are added to the body axis

force equations. See Figures 1.1, 1.2 and 1.7 of the EOM section.

The ground handling study only required a constant side wind and turbulence so that all terms except $STEADY_Y$ and the three GUST terms were zero. Note that \overline{w} was zero below 20 feet so that $GUST_z$ was zero on the ground. See description of turbulence model above.

Section 5
Struts Subroutine Implementation Notes

The STRUTS subroutine, written in FORTRAN, is an implementation of the mathematical model defined in Ref. 4, "DC-9 Landing Gear Math Model for Directional Control on Runway Flight Simulation." Most of the FORTRAN names defined in that report are used in STRUTS. The basic structure of STRUTS is similar to the subroutine LNDGR mentioned in the above report. Figure E1 is a general flow chart of STRUTS with line number references to the listing of STRUTS. The differences between STRUTS and LNDGR occur in the implementation of coordinate transformations, strut dynamic model and antiskid model. Most of the changes were made to decrease compute time.

An examination of the numerous coordinate transformations required in the gear model indicates that many of the transformation matrices are sparse. (They have several elements which are zero.) Therefore, compute time can be saved by coding the transform equations directly rather than using a general matrix multiply subroutine. Compute time is saved by eliminating the overhead required for a subroutine linkage.

Simulation of the strut dynamics (strut plus wheel mass dynamics) as defined in the above report consumes a lot of compute time. The natural frequency of that mass suspended between the tire spring and the strut spring is 15-20 Hz. Therefore, these equations must be solved approximately 200 times each second.

In the RDC simulation, STRUTS was called 20 times each second and these high frequency equations were solved 7 times for each pass through STRUTS. Satisfactory results were obtained with this solution rate of 140 times a second.

Compute time can be substantially reduced by minimizing the number of operations performed in the iterative loop used to solve for the strut dynamics. This was accomplished in STRUTS by expanding the dynamic equations and collecting all terms which are constant. All constant terms were moved outside the iterative loop and computed once for each pass through STRUTS to initialize the iterative loop.

Included in this initialization are calculations designed to minimize the step inputs to the strut dynamics. If the aircraft lands with a vertical velocity of 10 FPS and the simulation is solved 20 times a second, the step input to the landing

gear can be 6 inches. This is a large step when compared to the total tire and strut movement. Therefore, the step change in height input to STRUTS is divided by the number of passes through the strut dynamics. This makes each step into the strut dynamics less than 1 inch. No investigation was made of the efficacy of this technique.

It is recommended that elimination of the strut dynamics be investigated in future RDC programs. Adequate results can probably be obtained by allowing the aircraft mass to land on a non linear spring with a combined characteristic of the strut and tire. The savings in coding complexity and, therefore, compute time in the strut routine would be substantial.

See Appendix B for a detailed description of the software antiskid system.

A great deal of time was spent developing the low speed taxiing characteristics of the simulation. During checkout, the pilots had the sensation of skidding too much at low speeds. Also, after coming to a complete halt, an oscillation would occur which was very unreal. Adjustments of tire and strut damping did not affect the oscillation. Since the very low speed regime was not considered important in this program, speed logic and simple geometric relations were added to remedy these irregularities.

The following equations were added to the equations of motion (see subroutine EOM, lines 135-39 & 196-201).

$$VE = \text{SQRT} (VIX*VIX + VIY*VIY) = \sqrt{VIX^2 + VIY^2}$$

$$\text{ROLLG} = \text{YAWG} = 0.0$$

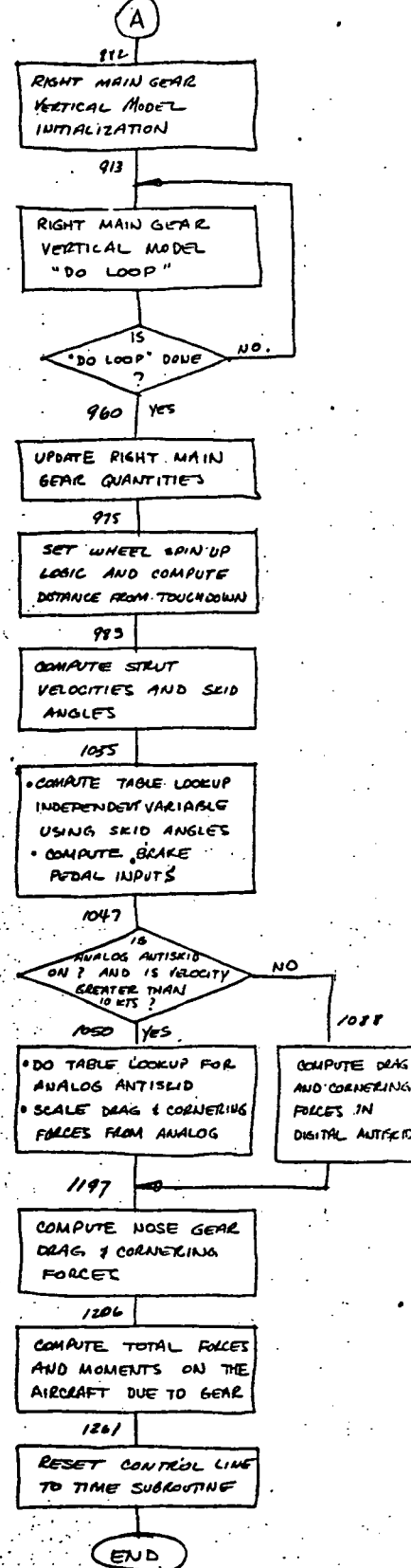
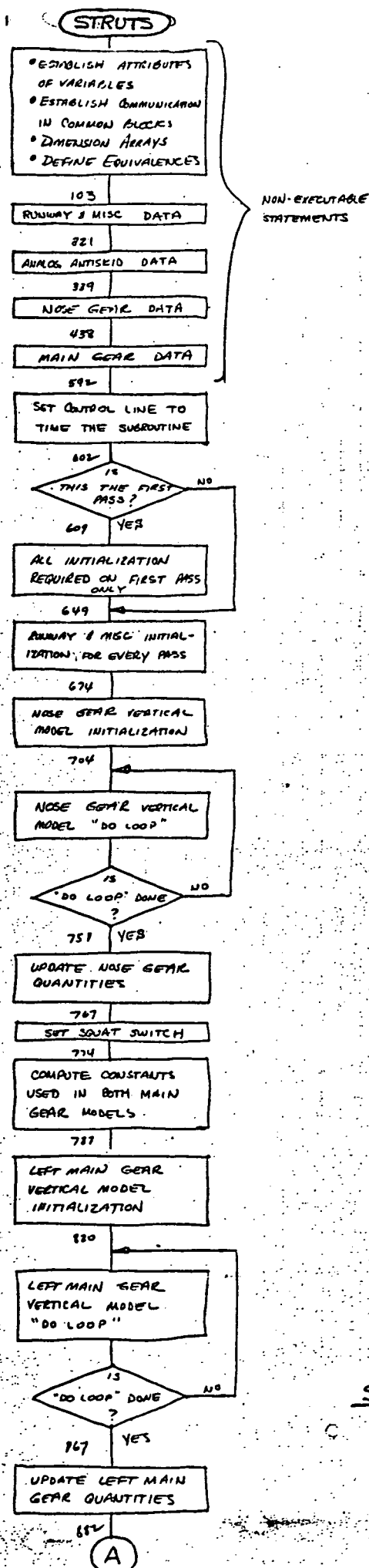
$$\text{FYG} = \text{XMASS} * (\text{UB} * \text{RB} * \text{DTR} - \text{QSM} * \text{CYB} - 32.2 * \text{AT}(2,3))$$

$$\text{RB} = \text{VE} * \text{INS} * .0229$$

$$\text{PB} = -\text{PHI}$$

$$\text{ANY} = \text{VE} * \text{RB} * .000542$$

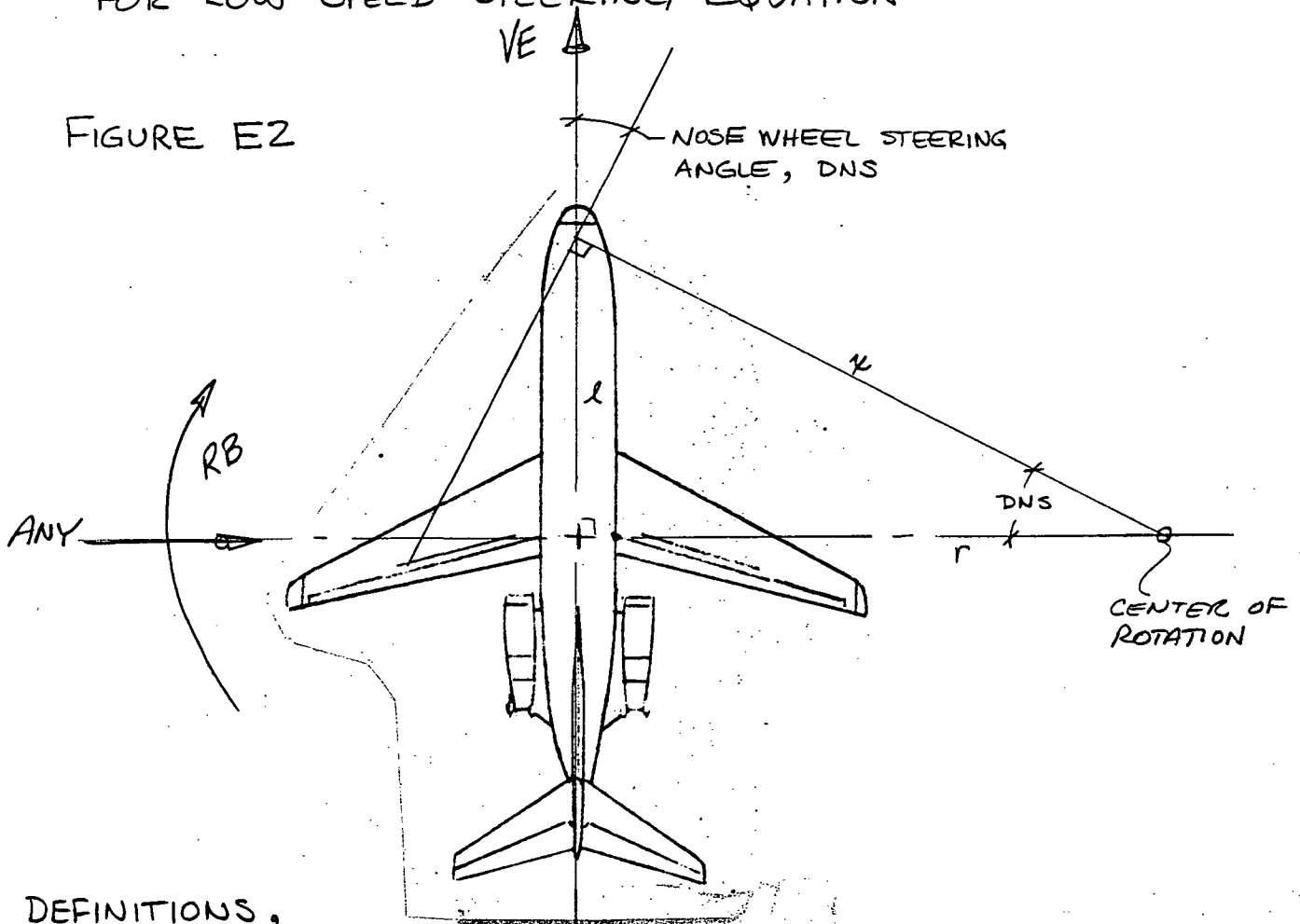
VE is the ground velocity of the aircraft in feet per second. When VE is less than 20 these simplified equations are used. The roll and yaw moments due to the gear are zeroed. The lateral force due to the gear, FYG, is set to a value that balances the aircraft side force equation. Body yaw rate, RB, is computed as simple circular motion based on the nose wheel steering angle, DNS, and VE. See Figure E2 for a derivation of the simplified RB equation. Body roll rate, PB, is set equal to negative roll angle to washout any roll angle that exists when the low speed logic is entered. Lateral acceleration, ANY, is also computed based on simple circular motion.



STRUTS SUBROUTINE
FLOW CHART WITH LINE NUMBER REFERENCES

FIGURE E1

DERIVATION OF YAW RATE DUE TO NOSE WHEEL STEERING FOR LOW SPEED STEERING EQUATION



DEFINITIONS,

- DNS = NOSE WHEEL STEERING ANGLE, DEG
- X = NORMAL FROM NOSE WHEEL PLANE TO CENTER OF ROTATION
- l = DISTANCE FROM CG TO NOSE WHEEL, FT ≈ 44.6
- r = RADIUS OF ROTATION, FT
- VE = AIRCRAFT SPEED, FPS
- RB = AIRCRAFT BODY YAW RATE, DEG/SEC
- ANY = AIRCRAFT LATERAL ACCELERATION, g's

FROM TRIGONOMETRIC RELATIONS

$$r = X \cos DNS$$

$$l = X \sin DNS$$

$$\therefore r = l / \tan DNS$$

$$= (44.6 / \tan DNS) 57.3 \text{ FT FOR SMALL ANGLES}$$

FROM SIMPLE CIRCULAR MOTION,

$$RB = 57.3 VE / r ; ANY = VE \times RB \times \frac{1}{57.3 \times 32.2}$$

| |
|---|
| $\therefore RB = VE \times DNS \times .0224 \text{ DEG/SEC.}$ $ANY = VE \times RB \times .000542 \text{ g's}$ |
|---|

DEFINITIONS FOR NAMES USED IN FORTRAN SUBROUTINE STRUTS

| NAME | DEFINITION | UNITS |
|----------|--|-----------------|
| \$COFRBL | LEFT TIRE BRAKING COEFFICIENT, ARRAY OF SIZE 4, EACH ELEMENT IS A DIFFERENT RUNWAY CONDITION, (1)= DRY, (2)= WET, (3)= FLOODED, (4)= ICY | LB |
| \$COFRBR | RIGHT TIRE BRAKING COEFFICIENT, ARRAY SIMILAR TO \$COFRBL | LB |
| \$COFRSL | LEFT TIRE. SIDEFORCE COEFFICIENT, ARRAY SIMILAR TO \$COFRBL | LB |
| \$COFRSN | NOSE TIRE SIDEFORCE COEFFICIENT, ARRAY SIMILAR TO \$COFRBL | LB |
| \$COFRSR | RIGHT TIRE SIDEFORCE COEFFICIENT, ARRAY SIMILAR TO \$COFRBL | LB |
| \$DATA | DUMMY ARRAY TO PAD COMMON BLOCK \$DATA | |
| \$UMAXL | LEFT TIRE MAXIMUM COEFFICIENT OF FRICTION | |
| \$UMAXR | RIGHT TIRE MAXIMUM COEFFICIENT OF FRICTION | |
| \$VARB | ARRAY THROUGH WHICH MAJORITY OF DATA IS TRANSMITTED TO AND FROM STRUTS | |
| ABRK | EFFECTIVE BRAKE AREA | IN ² |
| ABS | FORTRAN FUNCTION FOR FINDING ABSOLUTE VALUE | |
| ACMT | MAIN GEAR TIRE VISCOUS DAMPING COEFFICIENT | LB/IN/SEC |

DEFINITIONS (cont)

| NAME | DEFINITION | UNITS |
|---------|---|-----------|
| ACNT | NOSE GEAR TIRE VISCOUS DAMPING COEFFICIENT | LB/IN/SEC |
| AEA | AUXILLARY EULER ANGLE FOR TRANSFORMATION BETWEEN GEAR AXES AND AIRCRAFT BODY AXES. | RAD. |
| AKMT | MAIN GEAR TIRE LINEAR SPRING CONSTANT | LB/IN |
| AKNT | NOSE GEAR TIRE LINEAR SPRING CONSTANT | LB/IN |
| AMAX | FORTRAN FUNCTION FOR FINDING THE MAXIMUM OF TWO REAL VALUES. | |
| AMIN | FORTRAN FUNCTION FOR FINDING THE MINIMUM OF TWO REAL VALUES | |
| AMOD | FORTRAN FUNCTION FOR FINDING THE REMAINDER IN THE QUOTIENT OF TWO GIVEN REAL VALUES | |
| ARPTALT | AIRPORT ALTITUDE | FT. |
| AT | TRANSFORMATION MATRIX, INERTIAL AXES TO AIRCRAFT BODY AXES | |
| BPEDL | LEFT BRAKE PEDAL POSITION, NORMALIZED | |
| BPEDR | RIGHT BRAKE PEDAL POSITION, NORMALIZED | |
| CAEA | COSINE OF ANGLE AEA | |

DEFINITIONS (cont)

| NAME | DEFINITION | UNITS |
|--------|--|--------------------------|
| CBAR | LENGTH OF MEAN AERODYNAMIC CHORD (MAC) | IN |
| CFSTK | CONVERSION FACTOR, FPS TO KNOTS | KNOTS/FPS |
| CG | AIRCRAFT CENTER OF GRAVITY AS A FRACTION OF MAC | |
| CKTFS | CONVERSION FACTOR, KNOTS TO FPS | FPS/KNOT |
| CMD | MAIN GEAR STRUT VISCOUS DAMPING COEFFICIENT | LB/IN/SEC |
| CMVL | LEFT MAIN GEAR STRUT V^2 DAMPING COEFFICIENT | LB/(IN/SEC) ² |
| CMVN | NOSE GEAR STRUT V^2 DAMPING COEFFICIENT | LB/(IN/SEC) ² |
| CMVR | RIGHT MAIN GEAR STRUT V^2 DAMPING COEFFICIENT | LB/(IN/SEC) ² |
| CND | NOSE GEAR STRUT VISCOUS DAMPING COEFFICIENT | LB/IN/SEC |
| COFEBT | TABLE OF MAIN TIRE EFFECTIVE BRAKING COEFFICIENT | |
| COFRBL | LEFT TIRE BRAKING COEFFICIENT | |
| COFRBR | RIGHT TIRE BRAKING COEFFICIENT | |
| COFRSL | LEFT TIRE SIDEFORCE COEFFICIENT | |
| COFRSN | NOSE TIRE SIDEFORCE COEFFICIENT | |

DEFINITIONS (cont)

| NAME | DEFINITION | UNITS |
|---------|---|-------|
| COFRSNT | TABLE OF NOSE TIRE SIDEFORCE COEFFICIENT | |
| COFRSR | RIGHT TIRE SIDEFORCE COEFFICIENT | |
| COFSBT | TABLE OF MAIN TIRE SIDEFORCE COEFFICIENT | |
| COFSNT | TABLE OF NOSE TIRE SIDEFORCE COEFFICIENT | |
| COSKAL | COSINE OF LEFT TIRE SKID ANGLE | |
| COSKAN | COSINE OF NOSE TIRE SKID ANGLE | |
| COSKAR | COSINE OF RIGHT TIRE SKID ANGLE | |
| CPGCAE | PRODUCT OF COSINES OF PGM AND AEA | |
| CPGM | COSINE OF PGM | |
| CPGN | COSINE OF PGN | |
| CPHI | COSINE OF AIRCRAFT ROLL ANGLE | |
| CPHSTH | PRODUCT OF COSINE OF AIRCRAFT ROLL ANGLE AND SINE OF AIRCRAFT PITCH ANGLE | |
| CPL | LEFT GEAR ANTISKID CYCLE PERIOD | SEC. |
| CPR | RIGHT GEAR ANTISKID CYCLE PERIOD | SEC. |
| CPSI | COSINE OF AIRCRAFT HEADING | |

DEFINITIONS (cont)

| NAME | DEFINITION | UNITS |
|--------|--|-------|
| CRGM | COSINE OF RGM | |
| CTBLI | DIFFERENCE EQUATION COEFFICIENT FOR BRAKE HYDRAULIC PRESSURE LAG | |
| CTHE | COSINE OF AIRCRAFT PITCH ANGLE | |
| CTL | LEFT GEAR ANTISKID CYCLE DUTY (FRACTION OF TIME BRAKE IS ON) | |
| CTNWSI | DIFFERENCE EQUATION COEFFICIENT FOR NOSE WHEEL STEERING LAG | |
| CTR | RIGHT GEAR ANTISKID CYCLE DUTY (FRACTION OF TIME BRAKE IS ON) | |
| CXB | AIRCRAFT EQUATIONS OF MOTION LONGITUDINAL COEFFICIENT | |
| CYB | AIRCRAFT EQUATIONS OF MOTION LATERAL COEFFICIENT | |
| DEADZ | FUNCTION TO SIMULATE DEADZONE | |
| DELT | SIMULATION STEP SIZE (NOT ZERO DURING RESET) | SEC |
| DH | ALTITUDE OF AIRCRAFT CG ABOVE THE AIRPORT | FT. |
| DHUBHL | CHANGE IN LEFT GEAR HUB HEIGHT FOR EACH PASS THROUGH THE VERTICAL MODEL ITERATIVE LOOP | IN. |

DEFINITIONS (con't)

| NAME | DEFINITION | UNITS |
|--------|---|----------------|
| DHUBHN | SIMILAR TO DHUBHL FOR NOSE GEAR | IN. |
| DHUBHR | SIMILAR TO DHUBHR FOR RIGHT GEAR | IN. |
| DIN | TABLE OF CONTROL INPUTS FROM COCKPIT | 10 VOLTS/UNITY |
| DME | LENGTH OF MAIN STRUT EXTENDED | FT. |
| DML | LEFT STRUT LENGTH | FT. |
| DMR | RIGHT STRUT LENGTH | FT. |
| DN | NOSE STRUT LENGTH | FT. |
| DNE | LENGTH OF NOSE STRUT EXTENDED | FT. |
| DRCCG | DISTANCE FROM RUNWAY CENTERLINE TO AIRCRAFT CG | FT. |
| DRCLM | DISTANCE FROM RUNWAY CENTERLINE TO LEFT MAIN WHEEL | FT. |
| DRCNW | DISTANCE FROM RUNWAY CENTERLINE TO NOSE WHEEL | FT. |
| DRCRM | DISTANCE FROM RUNWAY CENTERLINE TO RIGHT MAIN WHEEL | FT. |
| DRTCG | X DISTANCE FROM GLIDESLOPE SHACK TO AIRCRAFT CG | FT |
| DRTLm | X DISTANCE FROM GLIDESLOPE SHACK TO LEFT MAIN WHEEL + 500 | FT |

DEFINITIONS (cont)

| NAME | DEFINITION | UNITS |
|--------|--|---------|
| DRTNW | X DISTANCE FROM GLIDESLOPE SHACK TO NOSE WHEEL + 500 | FT. |
| DRTRM | X DISTANCE FROM GLIDESLOPE SHACK TO RIGHT MAIN WHEEL + 500 | FT. |
| DT | INTEGRATION STEP SIZE | SEC. |
| DTONP | INTEGRATION STEP SIZE USED IN VERTICAL STRUT MODEL ITERATIVE LOOP | SEC |
| DTR | CONVERSION FACTOR, DEGREES TO RADIANS | RAD/DEG |
| DXMALE | DISTANCE FROM THE LEADING EDGE OF THE MAC TO MAIN STRUT ATTACH POINT | FT |
| DXNALE | DISTANCE FROM THE LEADING EDGE OF THE MAC TO NOSE STRUT ATTACH POINT | FT |
| EXP | FORTTRAN FUNCTION FOR FINDING e^x | |
| EXTRA | GENERAL PURPOSE ARRAY FOR PASSING DATA TO AND FROM SUBROUTINE, PART OF \$VARB. | |
| FBLCOM | LEFT MAIN WHEEL COMMANDED BRAKING FORCE | LB. |
| FBLMAX | LEFT MAIN WHEEL MAXIMUM AVAILABLE BRAKING FORCE | LB. |
| FBRCOM | RIGHT MAIN WHEEL COMMANDED BRAKING FORCE | LB. |

DEFINITIONS (cont)

| NAME | DEFINITION | UNITS |
|--------|---|--------|
| FBRMAX | RIGHT MAIN WHEEL MAXIMUM AVAILABLE BRAKING FORCE | LB. |
| FCON | SLOPE OF UNBRAKED CORNERING FORCE FUNCTION IN ANALOG ANTISKID | LB/DEG |
| FCOL | LEFT MAIN WHEEL UNBRAKED CORNERING FORCE IN ANALOG ANTISKID | LB |
| FCOR | RIGHT MAIN WHEEL UNBRAKED CORNERING FORCE IN ANALOG ANTISKID | LB |
| FDAMPL | LEFT MAIN STRUT TOTAL DAMPING FORCE | LB |
| FDAMPN | NOSE STRUT TOTAL DAMPING FORCE | LB |
| FDAMPR | RIGHT MAIN STRUT TOTAL DAMPING FORCE | LB. |
| FGML | LEFT MAIN TIRE FORCES ALONG STRUT Z-AXIS | LB. |
| FGMR | RIGHT MAIN TIRE FORCES ALONG STRUT Z-AXIS | LB. |
| FGN | NOSE TIRE FORCES ALONG STRUT Z-AXIS | LB. |
| FLE | LEFT MAIN TIRE FORCE \perp GROUND | LB. |
| FLEMUM | PRODUCT OF FLE & $\$UMAXL$ DIVIDED BY 2, USED IN ANALOG ANTISKID | LB. |
| FLV | LEFT MAIN TIRE FORCES IN GEAR VELOCITY AXES, AN ARRAY OF 3, (1)= X-FORCE, (2)= Y-FORCE & (3)= Z-FORCE | LB |

DEFINITIONS (con't)

| NAME | DEFINITION | UNITS |
|---------|--|-------------------|
| FML | LEFT MAIN TIRE FORCES IN AIRCRAFT BODY AXES, AN ARRAY OF 3; (1)= X-FORCE, (2)= Y-FORCE, (3)= Z-FORCE | LB |
| FMR | RIGHT MAIN TIRE FORCES IN AIRCRAFT BODY AXES, SIMILAR TO ARRAY FML | LB |
| FN | NOSE TIRE FORCES IN AIRCRAFT BODY AXES, SIMILAR TO ARRAY FML | LB |
| FNE | NOSE TIRE FORCE \perp GROUND | LB |
| FNV | NOSE TIRE FORCES IN GEAR VELOCITY AXES, SIMILAR TO ARRAY FLV | LB |
| FRE | RIGHT MAIN TIRE FORCE \perp GROUND | LB |
| FREMUM | PRODUCT OF FRE & \$UMAXR DIVIDED BY 2, USED IN ANALOG ANTISKID | LB |
| FRV | RIGHT MAIN TIRE FORCES IN GEAR VELOCITY AXES, SIMILAR TO ARRAY FLV | LB |
| FS | ARRAY OF SCALE FACTORS TO CONVERT ARRAY DIN INTO ENGINEERING UNITS | VARIOUS |
| FSL | LEFT MAIN STRUT NONLINEAR SPRING FORCE | LB |
| FSMCMVM | TABLE OF MAIN STRUT NONLINEAR SPRING FORCES AND V^2 DAMPING COEFFICIENT | LB & LB/IN/SEC |

DEFINITIONS (con't)

| NAME | DEFINITION | UNITS |
|---------|---|----------------|
| FSN | NOSE STRUT NONLINEAR SPRING FORCE | LB |
| FSNCMVN | TABLE OF NOSE STRUT NONLINEAR SPRING FORCES AND V^2 DAMPING COEFFICIENT | LB & LB/IN/SEC |
| FSR | RIGHT MAIN STRUT NONLINEAR SPRING FORCE | LB |
| FUNID | FORTTRAN SUBROUTINE FOR FINDING A FUNCTION OF ONE VARIABLE | |
| FXG | GEAR FORCES ALONG AIRCRAFT BODY X-AXIS | LB. |
| FYG | GEAR FORCES ALONG AIRCRAFT BODY Y-AXIS | LB |
| FZG | GEAR FORCES ALONG AIRCRAFT BODY Z-AXIS | LB |
| F3CL | EMPIRICAL FUNCTION USED TO REDUCE LEFT BRAKED DRAG FORCE AS A FUNCTION OF SKID ANGLE IN ANALOG ANTISKID | LB |
| F3CR | SAME AS F3CL FOR RIGHT WHEEL | LB |
| F3CT | TABLE OF VALUES FOR F3CL & F3CR | LB |
| GEOCON | ARRAY OF GEOMETRIC CONSTANTS | VARIOUS |
| HBUMP | RUNWAY BUMPS, AN ARRAY OF SIZE 3, (1)= NOSE GEAR, (2)= LEFT GEAR & (3)= RIGHT GEAR | IN. |

DEFINITIONS (cont)

| NAME | DEFINITION | UNITS |
|--------|--|-------|
| HCROWN | RUNWAY CROWN, AN ARRAY SIMILAR TO HBUMP | IN. |
| HUBHL | LEFT MAIN WHEEL HUB ALTITUDE | IN |
| HUBHLD | LEFT MAIN STRUT ATTACH POINT ALTITUDE CHANGE FOR EACH PASS THROUGH THE VERTICAL MODEL ITERATIVE LOOP | IN |
| HUBHLP | LEFT MAIN STRUT ATTACH POINT ALTITUDE PAST VALUE | IN |
| HUBHLO | LEFT MAIN STRUT ATTACH POINT INITIAL ALTITUDE FOR ITERATIVE LOOP | IN |
| HUBHN | NOSE STRUT EQUIVALENT OF HUBHL | IN |
| HUBHND | NOSE STRUT EQUIVALENT OF HUBHLD | IN |
| HUBHNP | NOSE STRUT EQUIVALENT OF HUBHLP | IN |
| HUBHNO | NOSE STRUT EQUIVALENT OF HUBHLO | IN |
| HUBHR | RIGHT MAIN STRUT EQUIVALENT OF HUBHL | IN |
| HUBHRD | RIGHT MAIN STRUT EQUIVALENT OF HUBHLD | IN |
| HUBHRP | RIGHT MAIN STRUT EQUIVALENT OF HUBHLP | IN |
| HUBHRO | RIGHT MAIN STRUT EQUIVALENT OF HUBHLO | IN |
| I | GENERAL PURPOSE INTEGER | |

DEFINITIONS (con't)

| NAME | DEFINITION | UNITS |
|----------|--|-------|
| I1140 | DUMMY ARRAY TO PAD COMMON BLOCK I1140 | |
| J | GENERAL PURPOSE INTEGER | |
| JCASE | RUNWAY CONDITION CASE NUMBER, 1 = SYMMETRICAL PATCHY, 2 = ASYMMETRICAL PATCHY, 3 = DRY, 4 = WET, 5 = FLOODED | |
| JDFRT | INTEGER DISTANCE FROM RUNWAY THRESHOLD TO AIRCRAFT CG | FT. |
| JPRWY | RUNWAY CONDITION CODE | |
| JPRWYD | TABLE OF RUNWAY CONDITION CODES | |
| JRWYCLM | RUNWAY CONDITION AT LEFT MAIN WHEEL, 1 IS DRY, 2 IS WET, 3 IS FLOODED | |
| JRWYCNG | RUNWAY CONDITION AT NOSE WHEEL | |
| JRWYCRM | RUNWAY CONDITION AT RIGHT MAIN WHEEL | |
| JRWYD | SUBSCRIPT FOR TABLE JPRWYD DERIVED FROM JDFRT | |
| K | GENERAL PURPOSE INTEGER | |
| KOUNT | DUMMY VARIABLE IN COMMON BLOCK \$TIME | |
| K1 to K8 | TEMPORARY CONSTANTS USED IN BOTH MAIN STRUTS, PART OF TRANSFORMATIONS | |
| LOG | LOGIC SWITCHES, AN ARRAY OF SIZE 30 | |

DEFINITIONS (con't)

| NAME | DEFINITION | UNITS |
|--------|--|-------|
| MAX | FORTRAN FUNCTION FOR FINDING THE MAXIMUM OF TWO OR MORE INTEGERS | |
| MFSL | MEMORY FOR LEFT STRUT NONLINEAR SPRING TABLE LOOKUP , FSL | |
| MFSN | MEMORY FOR FSN TABLE LOOKUP | |
| MFSR | MEMORY FOR FSR TABLE LOOKUP | |
| MF3CL | MEMORY FOR F3CL TABLE LOOKUP | |
| MF3CR | MEMORY FOR F3CR TABLE LOOKUP | |
| MIN | FORTRAN FUNCTION FOR FINDING THE MINIMUM OF TWO OR MORE INTEGERS | |
| MMUL | MEMORY FOR MUMAXL TABLE LOOKUP | |
| MMUR | MEMORY FOR MUMAXR TABLE LOOKUP | |
| MOD | INTEGER VERSION OF AMOD (see above) | |
| MSKBL | MEMORY FOR \$COFRBL TABLE LOOKUP | |
| MSKBR | MEMORY FOR \$COFRBR TABLE LOOKUP | |
| MSKN | MEMORY FOR \$COFRSN TABLE LOOKUP | |
| MSKSBL | MEMORY FOR \$COFRSL TABLE LOOKUP | |
| MSKSBR | MEMORY FOR \$COFRSR TABLE LOOKUP | |

DEFINITIONS (cont)

| NAME | DEFINITION | UNITS |
|--------|---|-------|
| MSKSNL | MEMORY FOR \$COFRSL TABLE LOOKUP | |
| MSKSNR | MEMORY FOR \$COFRSR TABLE LOOKUP | |
| MUMAXL | LEFT MAIN WHEEL MAXIMUM COEFFICIENT OF FRICTION, AN ARRAY OF SIZE 4, (1) = DRY, (2) = WET, (3) = FLOODED, (4) = ICY | |
| MUMAXR | RIGHT MAIN WHEEL MAXIMUM COEFFICIENT OF FRICTION, AN ARRAY SIMILAR TO MUMAXL | |
| MUMAXT | TABLE OF VALUES FOR MUMAXL & MUMAXR | |
| MVFG1 | FORTLAN SUBROUTINE TO FIND A FUNCTION OF ONE VARIABLE | |
| MVFG2 | FORTLAN SUBROUTINE TO FIND A FUNCTION OF TWO VARIABLES | |
| MVTBL | MEMORY FOR \$COFRBL TABLE LOOKUP | |
| MVTBR | MEMORY FOR \$COFRBR TABLE LOOKUP | |
| MVTN | MEMORY FOR \$COFRSN TABLE LOOKUP | |
| MVTSBL | MEMORY FOR \$COFRSL TABLE LOOKUP | |
| MVTSBR | MEMORY FOR \$COFRSR TABLE LOOKUP | |
| MVTSNL | MEMORY FOR \$COFRSL TABLE LOOKUP | |
| MVTSNR | MEMORY FOR \$COFRSR TABLE LOOKUP | |

DEFINITIONS (con't)

| NAME | DEFINITION | UNITS |
|-------|---|---------|
| NFSM | NUMBER OF STRUT POINTS IN FSMCMVM | |
| NFSN | NUMBER OF STRUT POINTS IN FSNCMVN | |
| NF3C | NUMBER OF SKID ANGLE POINTS IN F3CT | |
| NMU | NUMBER OF VELOCITY POINTS IN MUMAXT | |
| NPASS | NUMBER OF PASSES THROUGH VERTICAL STRUT MODEL ITERATIVE LOOPS | |
| NSKB | NUMBER OF SKID ANGLE POINTS IN COFEBT | |
| NSKN | NUMBER OF SKID ANGLE POINTS IN COFRSNT | |
| NSKSB | NUMBER OF SKID ANGLE POINTS IN COFSBT | |
| NSKSN | NUMBER OF SKID ANGLE POINTS IN COFSNT | |
| NVTB | NUMBER OF VELOCITY POINTS IN COFEBT | |
| NVTN | NUMBER OF VELOCITY POINTS IN COFRSNT | |
| NVTSB | NUMBER OF VELOCITY POINTS IN COFSBT | |
| NVTSN | NUMBER OF VELOCITY POINTS IN COFSNT | |
| OUTIN | DUMMY ARRAY TO PAD COMMON BLOCK \$OUTIN | |
| PB | AIRCRAFT BODY ROLL RATE | DEG/SEC |
| PGM | ANGLE BETWEEN THE AIRCRAFT STATION LINE AND MAIN STRUT CENTERLINE | DEG |

DEFINITIONS (cont)

| NAME | DEFINITION | UNITS |
|--------|---|---------|
| PGN | NOSE STRUT EQUIVALENT TO PGM | DEG. |
| PMG | AIRCRAFT BODY AXIS PITCHING MOMENT DUE TO GEARS | FT-LB. |
| PRWY | POSITION ON A 2400 FOOT SEGMENT OF RUNWAY, USED TO FIND HBUMP | FT. |
| QSM | AIRCRAFT EQUATIONS OF MOTION COEFFICIENT | LB/SLUG |
| RB | AIRCRAFT BODY AXIS YAW RATE | DEG/SEC |
| RFLATM | MINIMUM RADIUS OF MAIN TIRE | IN |
| RFLATN | MINIMUM RADIUS OF NOSE TIRE | IN |
| RGM | ANGLE BETWEEN AIRCRAFT BUTT LINE AND MAIN STRUT CENTER LINE | DEG |
| RMLA | LEFT MAIN STRUT ATTACH POINT LOCATION IN BODY AXES, AN ARRAY OF 3, (1) = X-POSITION, (2) = Y-POSITION, (3) = Z-POSITION | FT |
| RMLW | LEFT MAIN WHEEL HUB LOCATION IN BODY AXES, AN ARRAY OF 3 SIMILAR TO RMLA | FT |
| RMRA | RIGHT MAIN STRUT EQUIVALENT TO RMLA | FT |
| RMRW | RIGHT MAIN WHEEL EQUIVALENT TO RMLW | FT |

DEFINITIONS (con't)

| NAME | DEFINITION | UNITS |
|---------|--|----------|
| RNA | NOSE STRUT EQUIVALENT TO RMLA | FT. |
| RNW | NOSE WHEEL EQUIVALENT TO RMLW | FT. |
| ROLLG | AIRCRAFT BODY AXIS ROLL MOMENT DUE TO GEARS | FT-LB. |
| RTD | CONVERSION FACTOR, RADIANS TO DEGREES | DEG/RAD. |
| RTIM | RADIUS OF UNDEFLECTED MAIN TIRE | IN. |
| RTIN | RADIUS OF UNDEFLECTED NOSE TIRE | IN. |
| RWYBUMP | TABLE OF VALUES FOR HBUMP | IN. |
| SAEA | SINE OF AEA | |
| SFBUMP | SCALE FACTOR ON HBUMP | |
| SFCROWN | SCALE FACTOR ON HCROWN | |
| SIGN | FORTTRAN FUNCTION FOR ATTACHING THE SIGN OF ONE VARIABLE TO ANOTHER | |
| SINCOS | FORTTRAN SUBROUTINE FOR FINDING THE SINE AND COSINE OF AN ANGLE | |
| SISKAL | SINE OF SKANGL | |
| SISKAN | SINE OF SKANGN | |
| SISKAR | SINE OF SKANGR | |

DEFINITIONS (cont)

| NAME | DEFINITION | UNITS |
|--------|------------------------------------|---------------------|
| SKANGL | LEFT MAIN TIRE SKID ANGLE | DEG |
| SKANGN | NOSE TIRE SKID ANGLE (NO STEERING) | DEG |
| SKANGR | RIGHT MAIN TIRE SKID ANGLE | DEG |
| SKANGT | TOTAL NOSE TIRE SKID ANGLE | DEG |
| SL | LEFT MAIN STRUT DEFLECTION | IN |
| SLD | LEFT MAIN STRUT DEFLECTION RATE | IN/SEC |
| SLDD | LEFT MAIN STRUT DEFLECTION ACCEL. | IN/SEC ² |
| SMMAX | MAIN STRUT MAXIMUM DEFLECTION | IN |
| SN | NOSE STRUT DEFLECTION | IN |
| SND | NOSE STRUT DEFLECTION RATE | IN/SEC |
| SNDD | NOSE STRUT DEFLECTION ACCEL. | IN/SEC ² |
| SNMAX | NOSE STRUT MAXIMUM DEFLECTION | IN |
| SPGCAE | PRODUCT OF SPGM AND CAEA | |
| SPGM | SINE OF PGM | |
| SPGN | SINE OF PGN | |
| SPHI | SINE OF AIRCRAFT ROLL ANGLE | |
| SPHSTH | PRODUCT OF SPHI AND STHE | |

DEFINITIONS (con't)

| NAME | DEFINITION | UNITS |
|-------------|--|-------------------------|
| SPSI | SINE OF AIRCRAFT HEADING | |
| SQRT | FORTRAN FUNCTION FOR FINDING SQUARE ROOT | |
| SR | RIGHT MAIN STRUT DEFLECTION | IN |
| SRD | RIGHT MAIN STRUT DEFLECTION RATE | IN/SEC |
| SRDD | RIGHT MAIN STRUT DEFLECTION ACCEL | IN/SEC ² |
| SRGM | SINE OF RGM | |
| STHE | SINE OF AIRCRAFT PITCH ANGLE | |
| STRANG | NOSE WHEEL STEERING ANGLE | DEG |
| THT | ENGINE THRUST ALONG AIRCRAFT X-AXIS | LB |
| TI ML | LEFT WHEEL ANTISKID TIMER | SEC. |
| TIMR | RIGHT WHEEL ANTISKID TIMER | SEC. |
| TRIG | FORTRAN SUBROUTINE FOR FINDING THE ARCTANGENT GIVEN TWO VALUES | |
| TO to T9 | TEMPORARY STORAGE LOCATIONS FOR INTERMEDIATE VALUES. | |
| UB | AIRCRAFT VELOCITY, BODY X-AXIS | FT/SEC |
| USMM | UNSPRUNG MASS OF MAIN STRUT + WHEEL | LB-SEC ² /IN |

DEFINITIONS (cont)

| NAME | DEFINITION | UNITS |
|-------|---|-------------------------|
| USMN | UNSPRUNG MASS OF NOSE STRUT + WHEEL | LB-SEC ² /IN |
| VB | AIRCRAFT VELOCITY, BODY Y-AXIS | FT/SEC |
| VDW | WIND ACCELERATION, AIRCRAFT BODY Y-AXIS | FT/SEC ² |
| VE | AIRCRAFT EQUIVALENT AIRSPEED | FT/SEC |
| VIX | AIRCRAFT VELOCITY, INERTIAL X-AXIS | FT/SEC |
| VIY | AIRCRAFT VELOCITY, INERTIAL Y-AXIS | FT/SEC |
| VT LW | LEFT WHEEL TOTAL VELOCITY IN GROUND PLANE | FT/SEC |
| VT NW | NOSE WHEEL TOTAL VELOCITY IN GROUND PLANE | FT/SEC |
| VT RW | RIGHT WHEEL TOTAL VELOCITY IN GROUND PLANE | FT/SEC |
| VWL | LEFT WHEEL VELOCITY, INERTIAL AXES, AN ARRAY OF 3, (1) = X-AXIS, (2) = Y-AXIS, (3) = NOT USED | FT/SEC |
| VWN | NOSE WHEEL VELOCITY. SIMILAR TO VWL | FT/SEC |
| VWR | RIGHT WHEEL VELOCITY SIMILAR TO VWL | FT/SEC |
| XCG | SAME AS CG | |
| XMASS | AIRCRAFT MASS | SLUGS |

DEFINITIONS (cont)

| NAME | DEFINITION | UNITS |
|------|---------------------------------------|-------|
| XRO | ROLLOUT DISTANCE | FT |
| XTD | TOUCHDOWN POINT FROM GLIDESLOPE SHACK | FT |
| YAWG | AIRCRAFT YAW MOMENT DUE TO GEARS | FT-LB |
| ZI | AIRCRAFT POSITION, INERTIAL Z-AXIS | FT |

Section 6

Auxiliary Equations

This section contains descriptions of the models for the ILS and marker beacons; the instrument drive algorithms; and the yaw damper model. Also included are short descriptions of the interfaces to the motion base and the visual system.

ILS (Instrument Landing System):

The ILS consists of a glide slope beam (G/S) and a localizer beam (LOC). The G/S provides a descending path to the runway touch-down point which is about 1000' in from the threshold. Typically this path is about 3 degrees. The LOC provides lateral guidance by defining a path down the center of the runway. The origins of the LOC beam is at the far end of the runway.

The ILS model essentially does two things: 1) establish the position of the ILS receivers, on the aircraft, with respect to the transmitters on the ground, and 2) calculates the angular errors from the fixed beams.

The positions of the ILS sensors are transformed to the earth axes by the following equations:

G/S

$$\begin{aligned} X_{GI} &= X_I + X_{BGS}A_{1,1} + Z_{BGS}A_{3,1} \\ Z_{GI} &= Z_I + X_{BGS}A_{1,3} + Z_{BGS}A_{3,3} + AP_{ALT} \end{aligned}$$

LOC

$$\begin{aligned} X_{LI} &= X_I + X_{BL}A_{1,1} + Z_{BL}A_{3,1} \\ Y_{LI} &= Y_I + X_{BL}A_{1,2} + Z_{BL}A_{3,2} \end{aligned}$$

Where:

- X_{BGS}, Z_{BGS} = the body axes coordinates of the G/S antenna.*
- X_{BL}, Y_{BL} = The body axes coordinates of the LOC antenna.*
- $A_{i,j}$ = Elements of the body to earth transformation matrix (direction cosines).
- X_I, Y_I, Z_I = Earth axes coordinates of the aircraft.
- AP_{ALT} = Airport altitude
- X_{GI}, Z_{GI} = Earth axes coordinates of the G/S antenna.
- X_{LI}, Y_{LI} = Earth axes coordinates of the LOC antenna.

* NOTE: Body axes coordinates are based on a longitudinal C.G. position at the quarter chord and on the aircraft center line.

The earth axes positions of the ILS sensors on the aircraft are used to calculate the voltage errors as follows:

$$E_{G/S} = [G/S \text{ X} - (\text{Arctan } Z_{GI}/X_{GI}) 57.3] .214$$

$$E_{LDC} = [(\text{Arctan } Y_{LI}/X_{LI} - RWY_L) 57.3] .075$$

Where:

$G/S \text{ X}$ = The fixed glide path angle defined by the glide slope transmitter.

RWY_L = The length of the runway from the touch-down point to the far end (position of the localizer transmitter).

57.3 = Numbers of degrees in radian. Used here to convert from radians to degrees.

.214 = Volts per degree of G/S error.

.075 = Volts per degree of LOC error.

$E_{G/S}$ = Glide slope error in volts.

E_{LOC} = Localizer error in volts.

The glide slope and localizer error signals are sent to the indicators in the ADI and HSI instruments. The ILS displays are scaled in "DOTS" where .075 volts equals one dot for both G/S and LOC.

Marker Beacons:

Two marker beacons were simulated for the RDC study. Typically airports will have 2 or 3 of these beacons spaced out along the runway approach. These beacons activate a beeper and lights in the cockpit. There is a light for each beacon.

The simulation model consisted of using comparisons on longitudinal and lateral aircraft displacement to define two rectangles within which the beeper and appropriate light are activated.

For the RDC study the following dimensions were used:

Outer Marker:

-35856 $<X_I$ <-33456 range out from touch down point in feet
-2100 $<Y_I$ $<+2100$ lateral displacement in feet

Middle Marker:

-4640 $<X_I$ <-3440 range out from touch-down point in feet
-1000 $<Y_I$ $<+1000$ lateral displacement in feet

The rectangle sizes are the approximate size of the beacon radiation pattern if the aircraft were following a 3 degree glide slope.

Instrument Drives:

The six primary flight instruments were active at both the Captain's and First Officer's positions. The Captain's instruments were DC-9 types and the First Officer's were DC-10 types. In addition the center panel contained two DC-9 type Engine Pressure Ratio (EPR) instruments. Both the DC-9 and DC-10 instruments were driven with the same parameters, for the most part.

ADI (Attitude and Director Indicator)

Artificial horizon - driven by pitch and roll (θ and ϕ).

ILS indicators - driven by the ILS parameters $E_{G/S}$ and E_{LOC} .

The flight director bars, speed command bug and skid ball were not driven.

HSI (Horizontal Situation Indicator)

Compass - driven by heading (ψ)

ILS - same as ADI

DME (Distance Measuring Equipment) indicator was not used.

BARO altimeter - driven by C.G. attitude (h_{CG})

Radio altimeter - The altitude of the radio altimeter antenna is found as follows:

$$h_{RA} = -h_{RABIAS} - (Z_I + X_{BRA}A_{1,3} + Z_{BRA}A_{3,3} + AP_{ALT})$$

Where:

h_{RA} = radio altimeter altitude

h_{RABIAS} = Bias such that the radio altimeter will read zero when the main gear just touch the ground and the aircraft pitch angle is 6 degrees.

Z_I = earth axes Z component ($-h_{CG}$).

X_{BRA} = X body axes component of radio altimeter antenna position.*

Z_{BRA} = Z body axes component of radio altimeter antenna position.*

$A_{i,j}$ = elements of body to earth transformation matrix.

AP_{ALT} = airport altitude

*NOTE: Body axes coordinates are based on a longitudinal C.G. position at the quarter chord and on the aircraft center line.

In order to drive the radio altitude indicator h_{RA} must be changed to a voltage. The h_{RA} voltage relationship is non-linear as follows:

| h_{RA} | VOLTS |
|----------|--------|
| 0 | .4 |
| 200 | 4.4 |
| 400 | 8.4 |
| 600 | 12.151 |
| 800 | 14.947 |
| 1000 | 17.130 |
| 1200 | 18.920 |
| 1400 | 20.438 |
| 1600 | 21.756 |
| 1800 | 22.920 |
| 2000 | 23.962 |
| 2200 | 24.907 |
| 2400 | 25.769 |
| 2600 | 26.6 |
| 2800 | 32. * |

* This point is used to drive the DC-10 tape instrument display out of sight.

VSI (Vertical Speed Indicator)

The VSI instrument was driven with a first order lag as shown.

$$\text{VSI drive} = \dot{z}_I / \gamma S + 1$$

Where:

\dot{z}_I = aircraft vertical rate component in earth axes

γ = .5 second

IAS (Indicated Air Speed)

IAS was driven with equivalent airspeed (V_e) as calculated by EOM.

EPR (Engine Pressure Ratio)

EPR indicators were driven with EPR as calculated in the engine algorithm (see Section 3).

Yaw Damper

The DC-9 model used for the RDC study included a yaw damper. The yaw damper model used was optimized for the approach configuration. A block diagram of the yaw damper algorithm is shown in Figure 6.1.

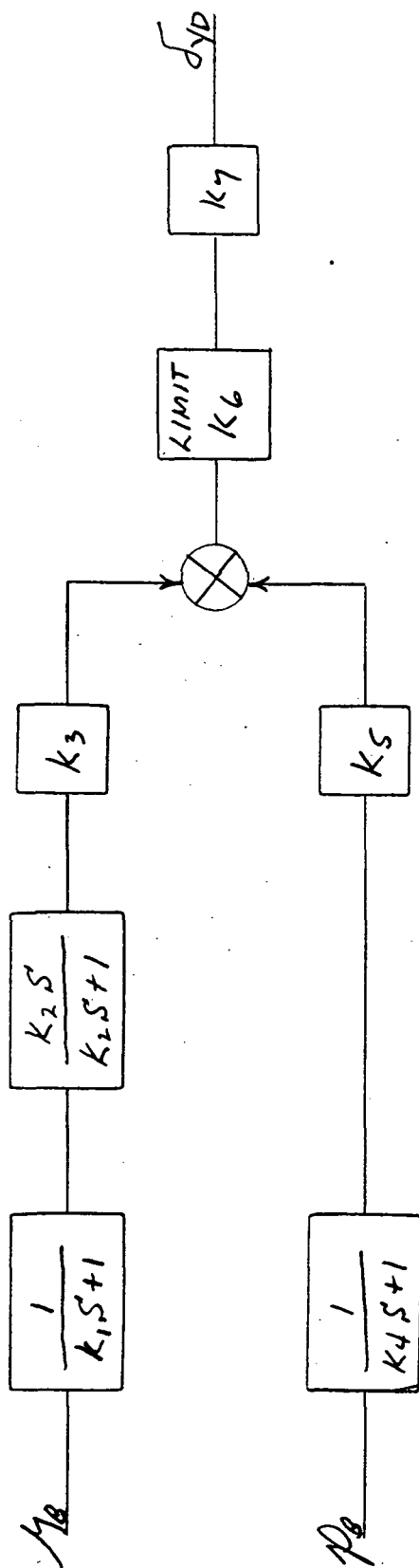
The body axes yaw rate (r_B) is the primary damping loop while the body axes roll rate (P_B) provides some turn coordination. The limiter is used to limit the authority of the yaw damper. K_7 is needed to change the commanded rudder deflection in hinge coordinates to stream coordinates. Stream coordinates are used in the computation of aero forces.

Motion Base Drive

The algorithms for the motion base drive have been taken from NASA report TN D-7350 (Reference 3). The only changes made by Douglas to the algorithms, other than those which relate to the geometry of the platform, were as follows:

- 1) The braking acceleration circuit was not used.
- 2) The lead compensation was applied directly to the jack signals and not to the centroid position as shown in the report.
- 3) The washout parameters used are very similar to those shown in Table 2 of a NASA paper presented at an AIAA conference (Reference 9). Table 6.1 below shows the actual values used for the Douglas motion base.

DC-9 YAW DAMPER and TURN COORDINATION MANUAL APPROACH MODE



$$k_1 = .05$$

$$k_2 = 1.45$$

$$k_3 = 2.5$$

$$k_4 = .01$$

$$k_5 = -.34$$

$$k_6 = \pm 2.12 \text{ degrees}$$

$$k_7 = .7692 \text{ degrees stream/degrees hinge}$$

FIG. 6.1

MOTION BASE WASHOUT PARAMETERS

TABLE 6.1

| VARIABLE | COMPUTER | UNITS | VALUE |
|------------------------|----------|----------|----------|
| MATH | | | |
| HIGH PASS FILTER | | | |
| $K_{Z,1}$ | C1(3) | - | 0.8 |
| $\epsilon_{Z,1}$ | ZET1(3) | - | 0.7 |
| $\omega_{n,Z,1}$ | OM1(3) | rad/sec | 2.0 |
| $K_{Z,2}$ | C2(3) | - | 1.0 |
| LOW PASS FILTER | | | |
| $K_{\theta,1}$ | C1(1) | - | 0.5 |
| ϵ_{θ} | ZET1(1) | - | 0.7 |
| $\omega_{n,\theta}$ | OM1(1) | rad/sec | 5.0 |
| $K_{\theta,2}$ | C2(1) | - | 0 |
| $K_{\phi,1}$ | C1(2) | - | 0.05 |
| ϵ_{ϕ} | ZET1(2) | - | 0.7 |
| $\omega_{n,\phi}$ | OM1(2) | rad/sec | 5.0 |
| $K_{\phi,2}$ | C2(2) | - | 0 |
| SIGNAL-SHAPING NETWORK | | | |
| $K_{q,T,1}$ | C3(1) | per ft. | 0.001 |
| $K_{q,T,2}$ | C3(1) | sec | 30.0 |
| $K_{q,T,3}$ | C5(1) | per sec. | 0.05 |
| $K_{p,T,1}$ | C3(2) | per ft. | -0.001 * |
| $K_{p,T,2}$ | C4(2) | sec | 30.0 |
| $K_{p,T,3}$ | C5(2) | per sec | 0.05 |
| $K_{r,1}$ | C3(3) | per ft. | 0.004 |
| $K_{r,2}$ | C4(3) | sec | 3.8 |
| $K_{r,3}$ | C5(3) | per sec. | 0.05 |

* The minus value takes the place of the minus signs in the ϕ_T equation.
(See page 21 of NASA report.)

MOTION BASE WASHOUT PARAMETERS

TABLE 6.1 (Cont'd)

| VARIABLE | COMPUTER | UNITS | VALUE |
|----------|------------------------------|---------|-------|
| MATH | SCALE AIRPLANE ANGULAR RATES | | |
| K_p | C6(1) | - | 0.7 |
| K_q | C6(2) | - | 0.5 |
| K_r | C6(3) | - | 0.2 |
| | TRANSLATIONAL WASHOUT | | |
| a_1 | C7(1) | rad/sec | 1.414 |
| a_2 | C7(2) | rad/sec | 2.1 |
| a_3 | C7(3) | rad/sec | 2.1 |
| b_1 | C8(1) | rad/sec | 1.0 |
| b_2 | C8(2) | rad/sec | 2.25 |
| b_3 | C8(3) | rad/sec | 2.25 |

Visual System Drive

The visual system used during the RDC study was a T.V. viewed model type called a Visual Flight Attachment (VFA), made by Redifon of England.

The VFA T.V. camera is mounted on a moving platform which can be moved over the model. The moving platform is driven by servos with the controlling signals originating in a "mini" digital computer. The drive algorithms, which were supplied by Redifon*, are calculated in the mini computer. The basic aircraft position, rate and orientation signals are calculated and transformed to the pilot's eye position in the main simulation computer. These signals are then transmitted to the mini over an analog link.

The main simulation computer calculates the input signals for the VFA at a frame rate of 20 per second. The mini does its calculations at a frame rate of 50 per second.

It should be mentioned that the analog link is just that, the signals from the main computer are put through digital to analog converters (DAC's) and transmitted over analog trunk lines to the VFA area where they are re-digitized by an analog-to-digital converter (ADC) and sent to the mini. It also should be mentioned that it is generally felt that an analog link is probably not the best way to interface two digital computers!

* See Reference 10.

APPENDIX B
SOFTWARE ANTISKID

The software antiskid model defined in Ref. 4, "DC-9 Landing Gear Math Model For Directional Control on Runway Flight Simulation", pages 36-38, was changed slightly to simplify the logic, decrease compute time and obtain the desired performance. This appendix will document those changes. The same notation is used here except the subscript, j , has been deleted in this appendix with the understanding that the equations and diagrams apply to both right and left main gears.

Figure B1 is a flow chart of the antiskid system as implemented in STRUTS, the Douglas subroutine implementation of the above report. Figure B2 is a typical time history of braking force with period C_p and duty C_t . In the original model, when $F_{BCOM} > F_{BON}$ (see Figure B1) antiskid cycling is started. In STRUTS, this decision point was made independent of C_t because at high speeds on wet runways C_t is small which makes F_{BON} large and the antiskid did not cycle as desired. In STRUTS, F_{BCOM} is compared to the product of the effective coefficient of friction, μ_D , normal tire load, F_E , and a constant, 1.35, to determine the onset of antiskid cycling. F_{BCOM} was also increased by changing the effective braking area from 5 to 8 square inches. In retrospect, this value of F_{BCOM} was probably too high. However, since maximum performance stops were used on most test runs, the high command level was not obvious. The precise onset of antiskid cycling was not investigated.

During checkout of the simulation, the antiskid system was evaluated by Douglas pilots and compared with the analog (hardware) antiskid system. The result of this check was a modification to the period and duty of the antiskid cycling. This change is illustrated in Figure B3. The period, C_p , was increased 0.8 seconds over the entire speed range and the duty, C_t , was increased for wet and flooded runway conditions.

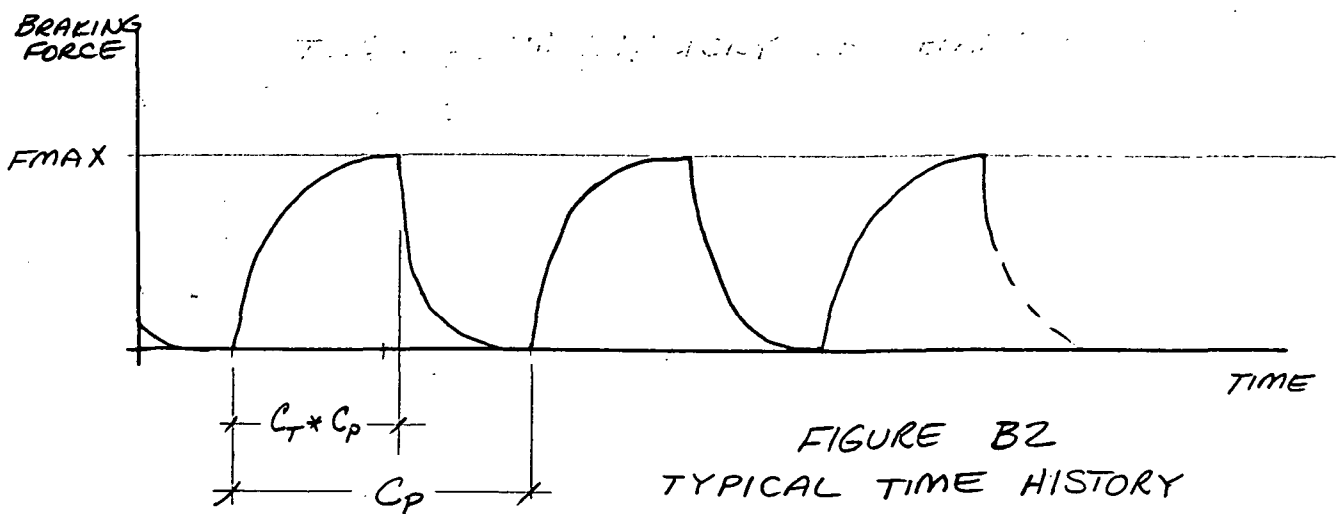
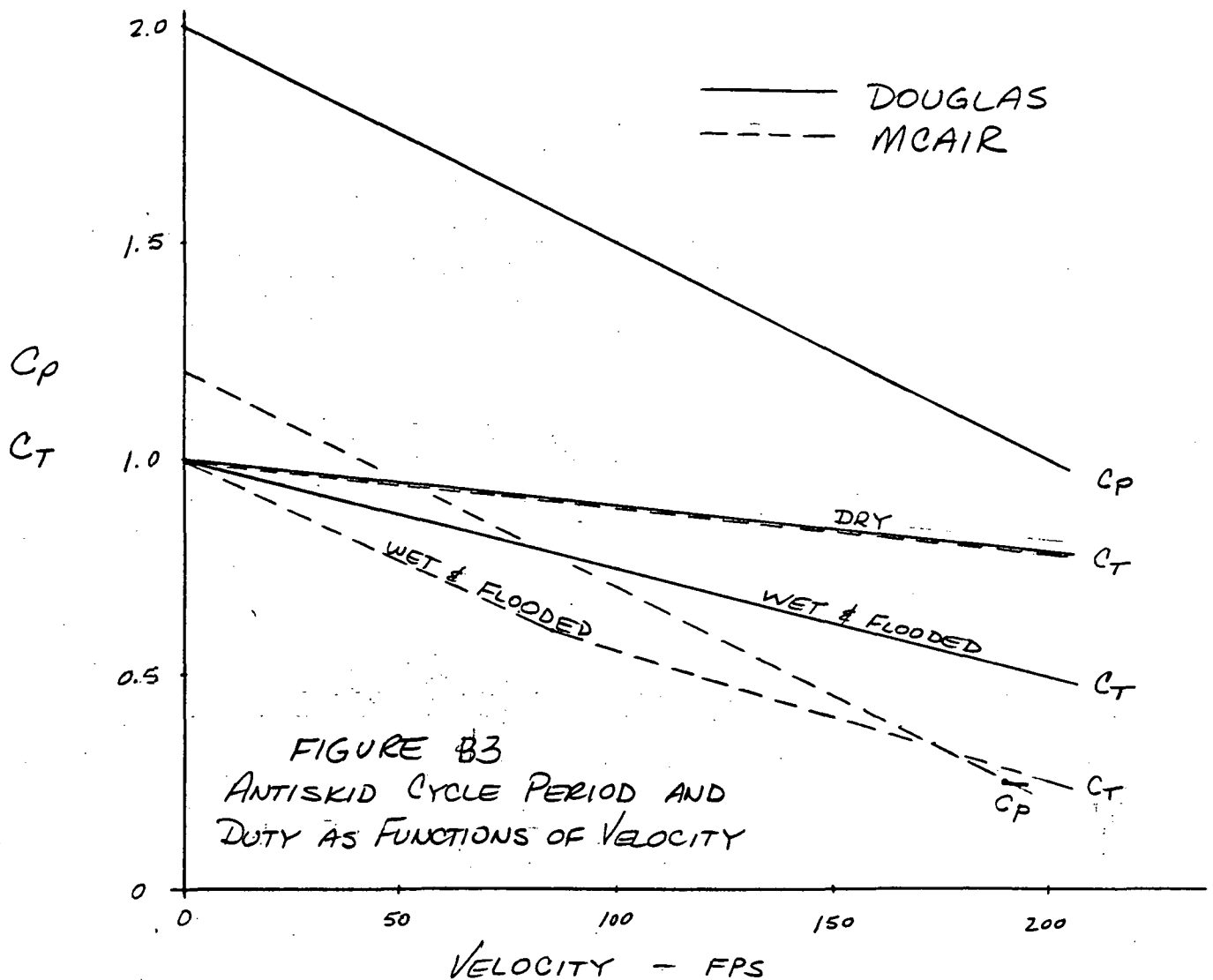
μ_D = EFFECTIVE COEFFICIENT OF FRICTION
 F_E = NORMAL LOAD ON STRUT
 A_{BRK} = EFFECTIVE AREA WORKED BY HYDRAULIC PRESSURE
 BK_L = BRAKE PEDAL DEFLECTION ($\neq 1.0$)
 C_T = FRACTION OF ANTISKID CYCLE BRAKES ARE ON
 C_p = PERIOD OF ANTISKID CYCLE
 DT = SIMULATION STEP SIZE
 TIM = CYCLE TIMER
 TO, TI = TEMPORARY VARIABLES.



RDC PROGRAM - DIGITAL ANTISKID

C_p - PERIOD OF ANTISKID CYCLES

C_T - FRACTION OF PERIOD BRAKES ARE ON (DUTY)



APPENDIX C

ANALOG/HARDWARE ANTISKID

Section 1. INTRODUCTION

The analog/hardware antiskid simulator is a system that produces real time drag and cornering tire forces for the aircraft simulation. The system consists of an analog computer and actual aircraft hardware implemented as shown in Figure C-1.

The analog computer receives inputs from the digital aircraft simulation and brake pressure from the hydraulics and calculates in real time the tire drag and cornering forces and wheel speed. The wheel speed is output to the antiskid control box and the forces are output to the aircraft simulation. The antiskid control box produces an antiskid control valve signal that controls brake pressure.

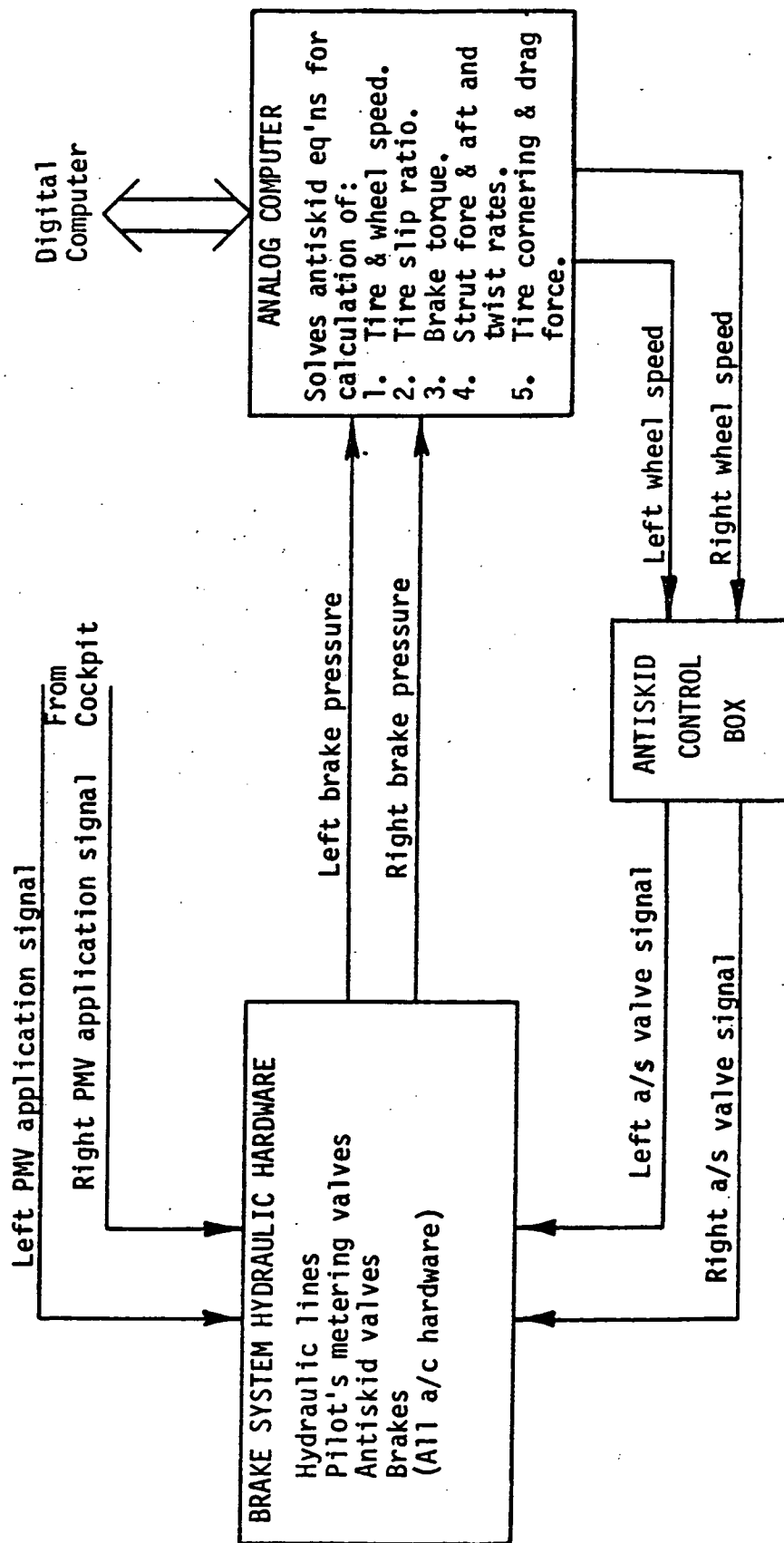


FIGURE C-1 ANALOG ANTISKID BLOCK DIAGRAM

Section 2. MODEL DERIVATION

The math flow diagram of the model for one strut is shown in Figure C-2. Both strut mechanizations are identical. These equations are implemented on an analog computer because of the high frequencies involved.

PRIMARY TIRE CORNERING AND DRAG FORCE

Originally it was planned to generate tire cornering and drag forces similarly to the method developed in Exhibit A of Reference 2. However, the method gave excessive side loads in the unbraked condition. Figure C-3 illustrates this problem. A new empirical method was developed based on data from Reference 5. This new method is developed in Primary Tire Cornering and Drag Force Analysis.

SECOND TIRE CORNERING AND DRAG FORCES, STRUT FORE-AFT AND TWIST RATES, BRAKE TORQUE, TIRE AND WHEEL SPEED, AND TIRE SLIP RATIO

The remainder of the items shown in Figure C-3 are developed in the above named analysis.

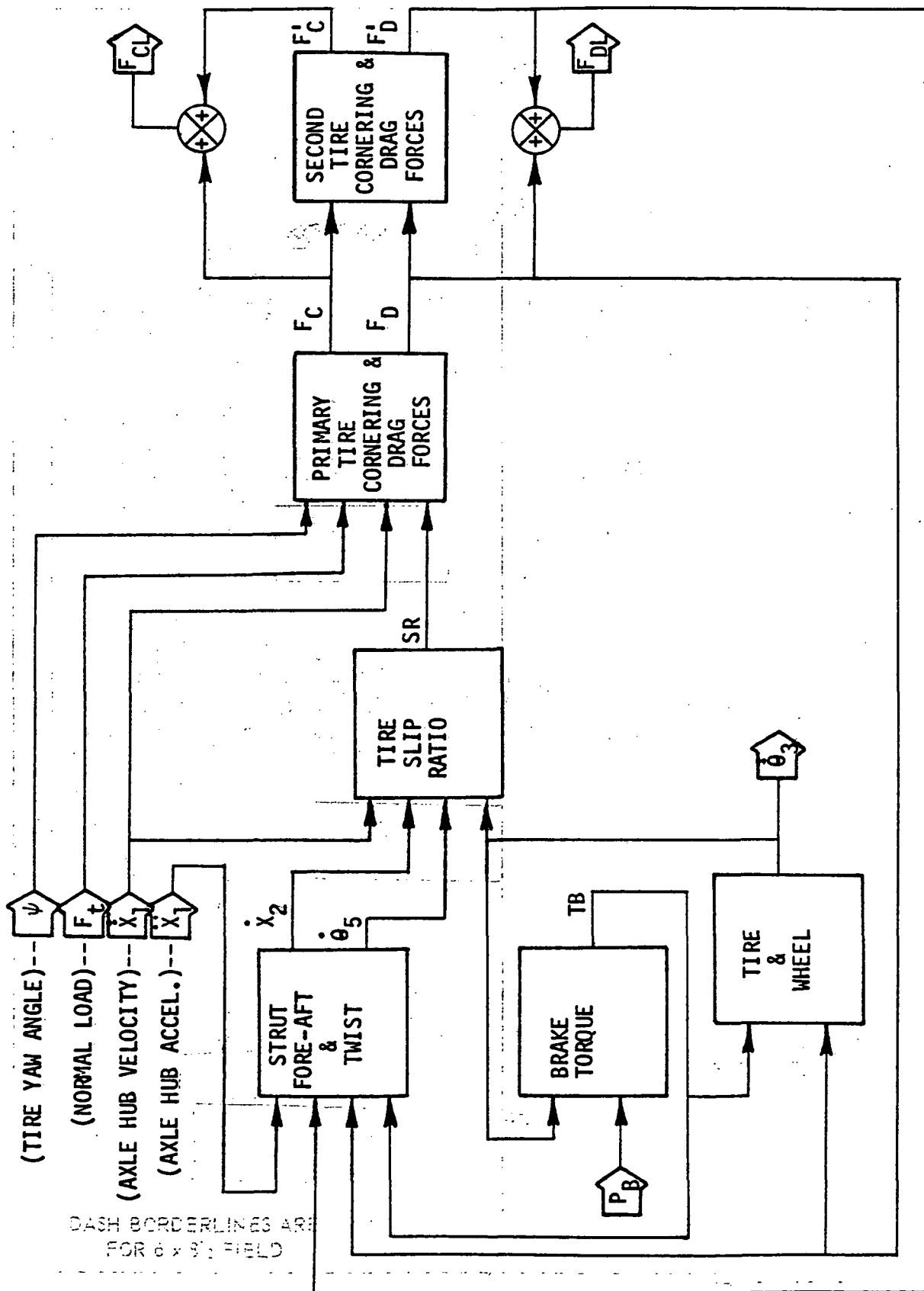


FIGURE C-2 MATH FLOW BLOCK DIAGRAM - STRUT EQUATIONS

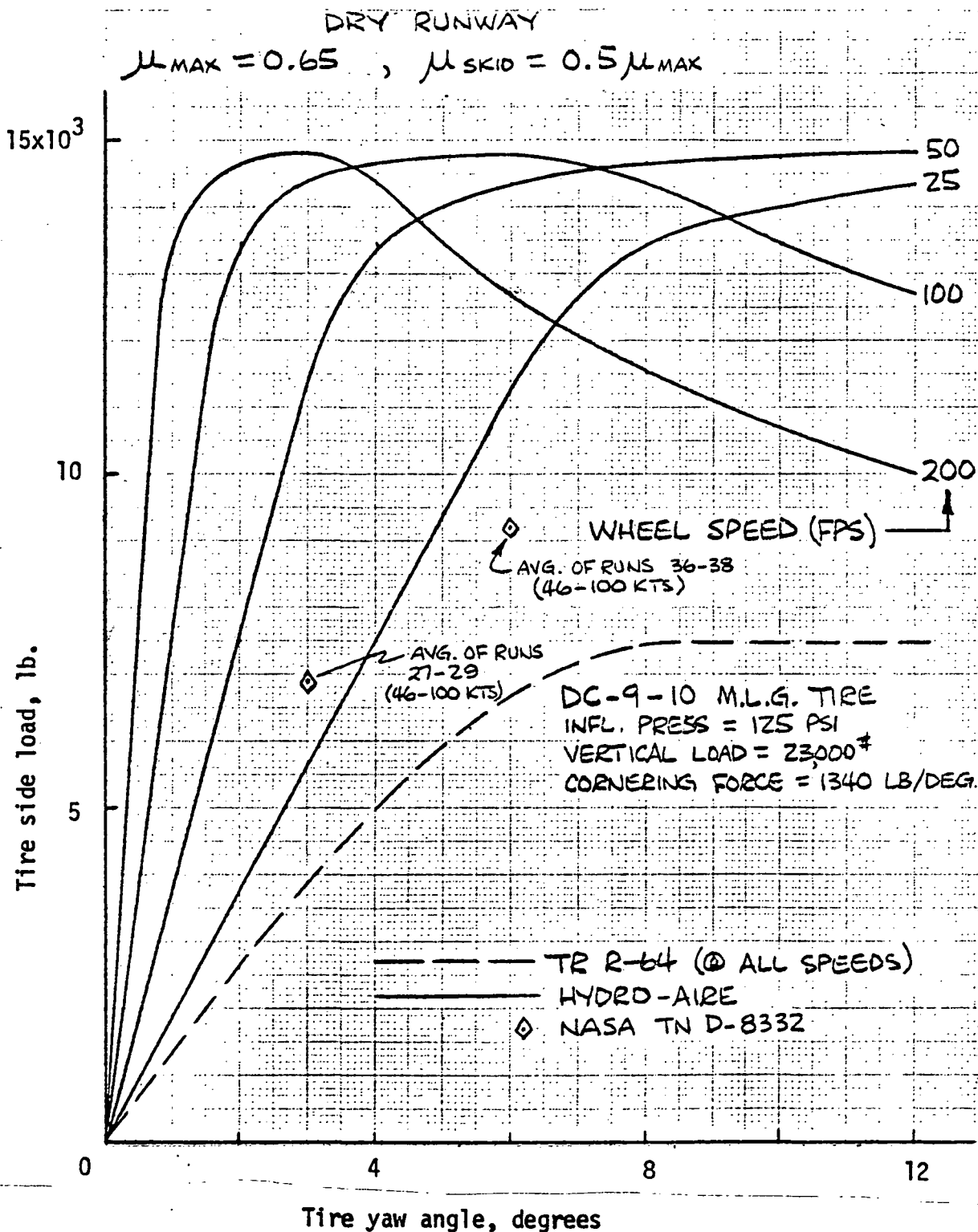


FIGURE C-3 COMPARISON OF HYDRO AIRE'S TIRE CORNERING THEORY WITH THAT OF NASA TR R-64 --- WITHOUT BRAKING

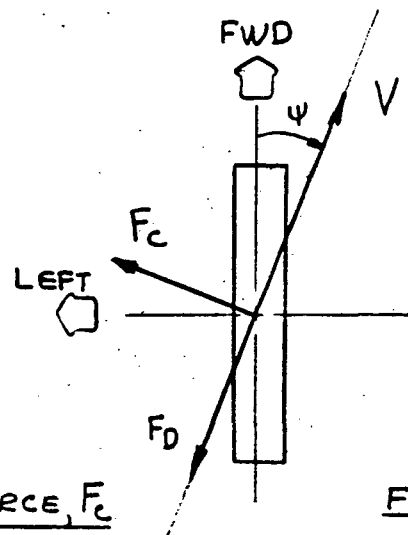
INTRODUCTION

THIS SECTION DEVELOPS, DESCRIBES, AND CORRELATES THE FRICTION FORCE MODELS USED FOR CORNERING AND DRAG IN THE ANALOG ANTISKID SIMULATION.

THE MODEL WAS DEVELOPED TO EXHIBIT THE TRENDS SHOWN IN TESTING CONDUCTED AT NASA LANGLEY AIRCRAFT LANDING LOADS AND DOCUMENTED IN REFERENCE 1. THE MODEL ALSO EXHIBITS EXPECTED LARGE ANGLE PERFORMANCE.

THE MODEL BASICALLY REDUCES THE UNBRAKED CORNERING FORCE AS A FUNCTION OF SLIP RATIO AND REDUCES THE DRAG FRICTION FORCE WITH INCREASING TIRE YAW ANGLE.

MODEL DEFINITION



CORNERING FRICTION FORCE, F_c

FIGURE 1

TIRE FORCES

THE CORNERING FRICTION FORCE IS DETERMINED BY REDUCING THE UNBRAKED CORNERING FORCE AS A FUNCTION OF INCREASING SLIP RATIO.

UNBRAKED CORNERING FORCE, F_{c0}

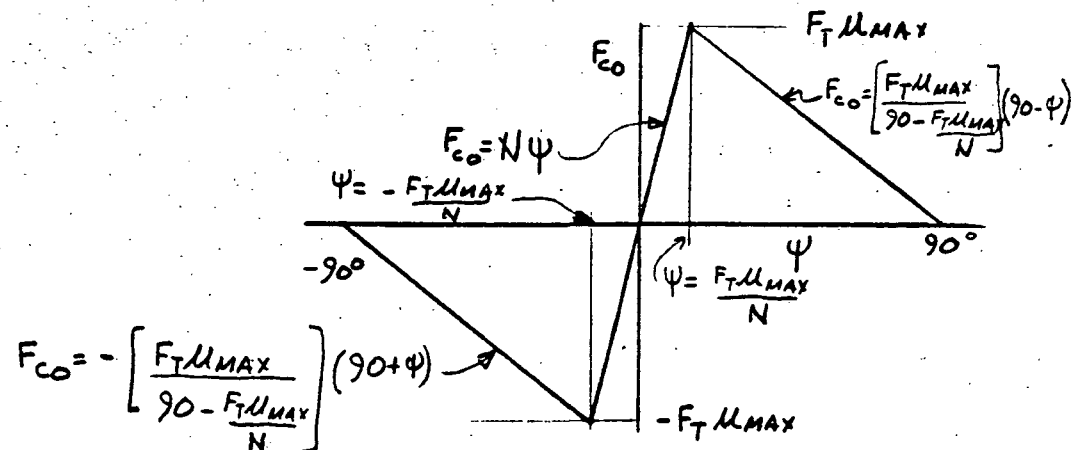


FIGURE 2 UNBRAKED

CORNERING FORCE

FOR SMALL YAW ANGLES

$$\text{EQN 1} \quad F_{c0} = N\psi \quad \left(-\frac{F_T \mu_{\max}}{N} < \psi < \frac{F_T \mu_{\max}}{N} \right)$$

WHERE N = TIRE CORNERING POWER

ψ = TIRE YAW ANGLE

μ_m = MAXIMUM TIRE FRICTION COEFFICIENT

F_T = TIRE NORMAL LOAD

FOR LARGE POSITIVE YAW ANGLES

$$\text{EQN 2} \quad F_{Co} = \left(\frac{F_T \mu_{MAX}}{90 - \frac{F_T \mu_{MAX}}{N}} \right) (90 - \psi) \quad \left(\frac{F_T \mu_{MAX}}{N} \leq \psi \leq 90^\circ \right)$$

FOR LARGE NEGATIVE YAW ANGLES

$$\text{EQN 3} \quad F_{Co} = - \left(\frac{F_T \mu_{MAX}}{90 - \frac{F_T \mu_{MAX}}{N}} \right) (90 + \psi) \quad \left(-90 < \psi \leq -\frac{F_T \mu_{MAX}}{N} \right)$$

NOTE: THIS REPRESENTATION IS A SIMPLIFICATION OF A PROCEDURE THAT CAN BE DEVELOPED USING RELATIONSHIPS GIVEN IN REFERENCE 2. THIS PROCEDURE WOULD BE AS FOLLOWS: (EQN NUMBERS ARE FOR REF 2)

1. DETERMINE TIRE DEFLECTION δ FROM NORMAL LOAD F_z USING EQNS 23 & 24.
2. DETERMINE CORNERING POWER N FROM TIRE DEFLECTION WITH EQN 82.
3. DETERMINE TIRE NORMAL FORCE $F_{\psi, n}$ FROM TIRE YAW ANGLE, ψ AND CORNERING POWER WITH EQNS 79 & 80.
4. DETERMINE CORNERING FORCE F_c FROM NORMAL FORCE WITH EQN 81.

THE CORNERING FORCE F_c IS DETERMINED BY REDUCING F_{c0} WITH INCREASING SLIP RATIO.

$$\text{EQN 4} \quad F_c = F_{c0} \cdot f_5(SR)$$

WHERE SR = SLIP RATIO

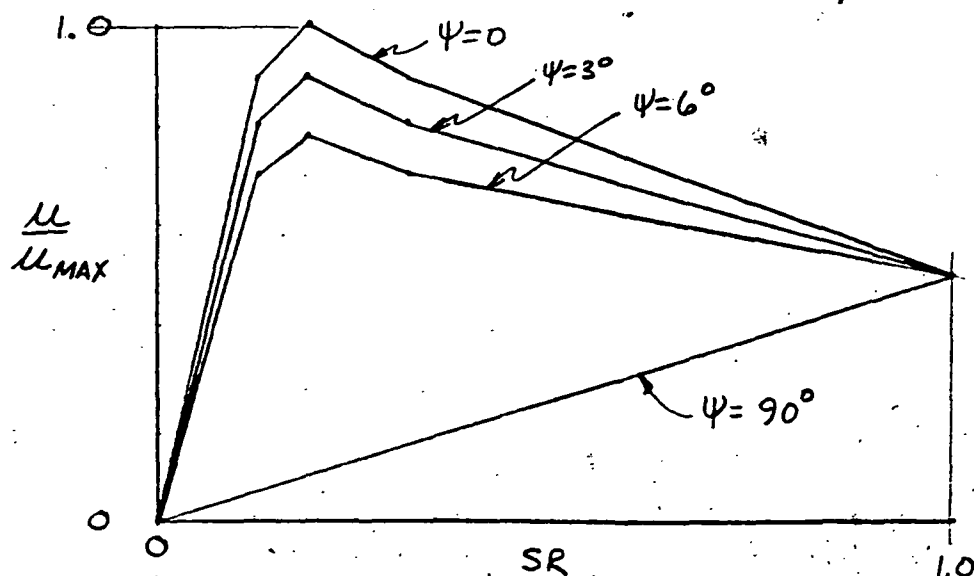
$f_5(SR)$ = MONOTONICALLY DECREASING FUNCTION WITH A VALUE OF 1. AT $SR=0$, 0 AT $SR=1$, AND ADJUSTED TO DUPLICATE EXPERIMENTAL RESULTS BETWEEN. (FIGURE 3)

DRAG FRICTION FORCE

THE DRAG FRICTION COEFFICIENT RATIO $\frac{\mu}{\mu_{MAX}}$ IS

$$\text{EQN 5} \quad \frac{\mu}{\mu_{MAX}} = f_3(SR, \psi)$$

WHERE $f_3(SR, \psi)$ IS AN EXPERIMENTALLY DETERMINED FUNCTION AS SHOWN IN FIGURE 4.



$$f_3(SR, \psi) = f_{3B}(SR) + f_{3A}(SR) \times f_{3C}(\psi)$$

WHERE, $f_{3A}(SR)$ IS AS SHOWN IN FIGURE 5,

$f_{3B}(SR)$ " " " " " 6, &

$f_{3C}(\psi)$ " " " " " 7.

THE DRAG FRICTION FORCE IS

EQN 6
$$F_D = \frac{\mu}{\mu_{MAX}} \times F_T \mu_{MAX}$$

MAXIMUM FRICTION COEFFICIENT

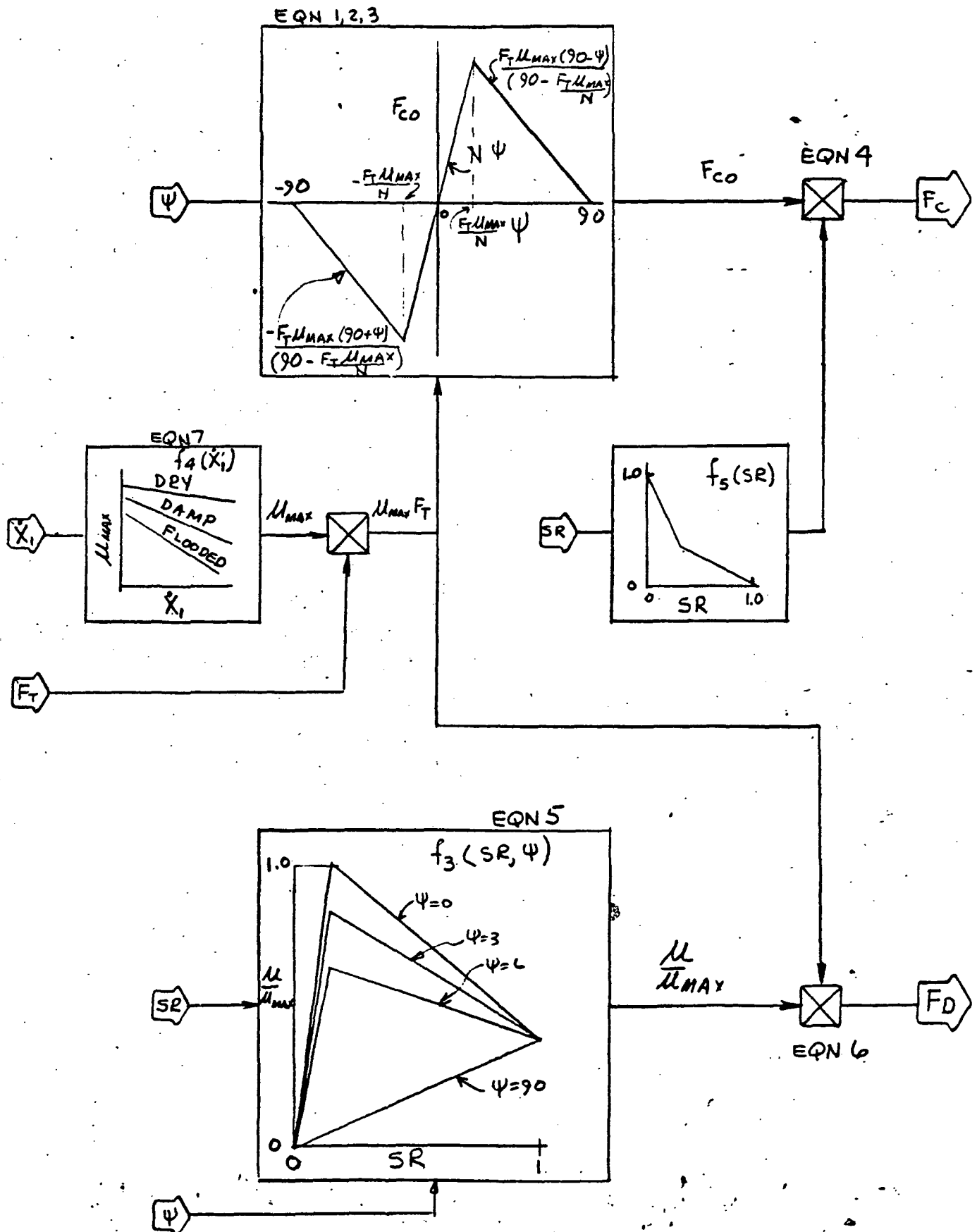
THE MAXIMUM FRICTION COEFFICIENT IS EXPRESSED AS A FUNCTION OF VELOCITY

EQN 7
$$\mu_{MAX} = f_4(\dot{X}_i)$$

WHERE \dot{X}_i = TOTAL VELOCITY

$f_4(\dot{X}_i)$ = FIGURE 19 OF REFERENCE 1
(SHOWN HERE IN FIGURE 8)

BLOCK DIAGRAM



SYMBOLS

| SYMBOL | CONSTANT | VARIABLE | NUMERICAL VALUE | UNITS | DESCRIPTION |
|-------------------------|----------|----------|--------------------|---------|--|
| F_c | | X | — | LBS | TIRE CORNERING FORCE PERPENDICULAR TO VELOCITY |
| F_{c0} | | X | — | LBS | ZERO SLIP CORNERING FORCE |
| F_D | | X | — | LBS | TIRE DRAG FORCE PARALLEL TO VELOCITY |
| F_T | | X | — | LBS | VERTICAL TIRE LOAD |
| $f_3(s, \psi)$ | X | | SEE PG 138 | — | NORMALIZED μ -SLIP CURVE |
| $f_4(\dot{x})$ | X | | SEE PG 141 | — | μ_{MAX} - VELOCITY CURVES |
| $f_5(s)$ | X | | SEE PG 139 | — | CORNER FORCE REDUCTION VS SLIP RATIO |
| N | X | | 1491 | LBS/DEG | CORNERING POWER |
| SR | | X | — | — | SLIP RATIO |
| \dot{x}_1 | | X | — | FT/SEC | TOTAL VELOCITY |
| ψ | | X | — | DEG | TIRE YAW ANGLE |
| μ_{MAX} | | X | — | — | MAXIMUM FRICTION COEFFICIENT |
| $\frac{\mu}{\mu_{MAX}}$ | | X | — | — | 'DRAG FRICTION COEFFICIENT RATIO |

$f_s(SR)$ - CORNER FORCE REDUCTION

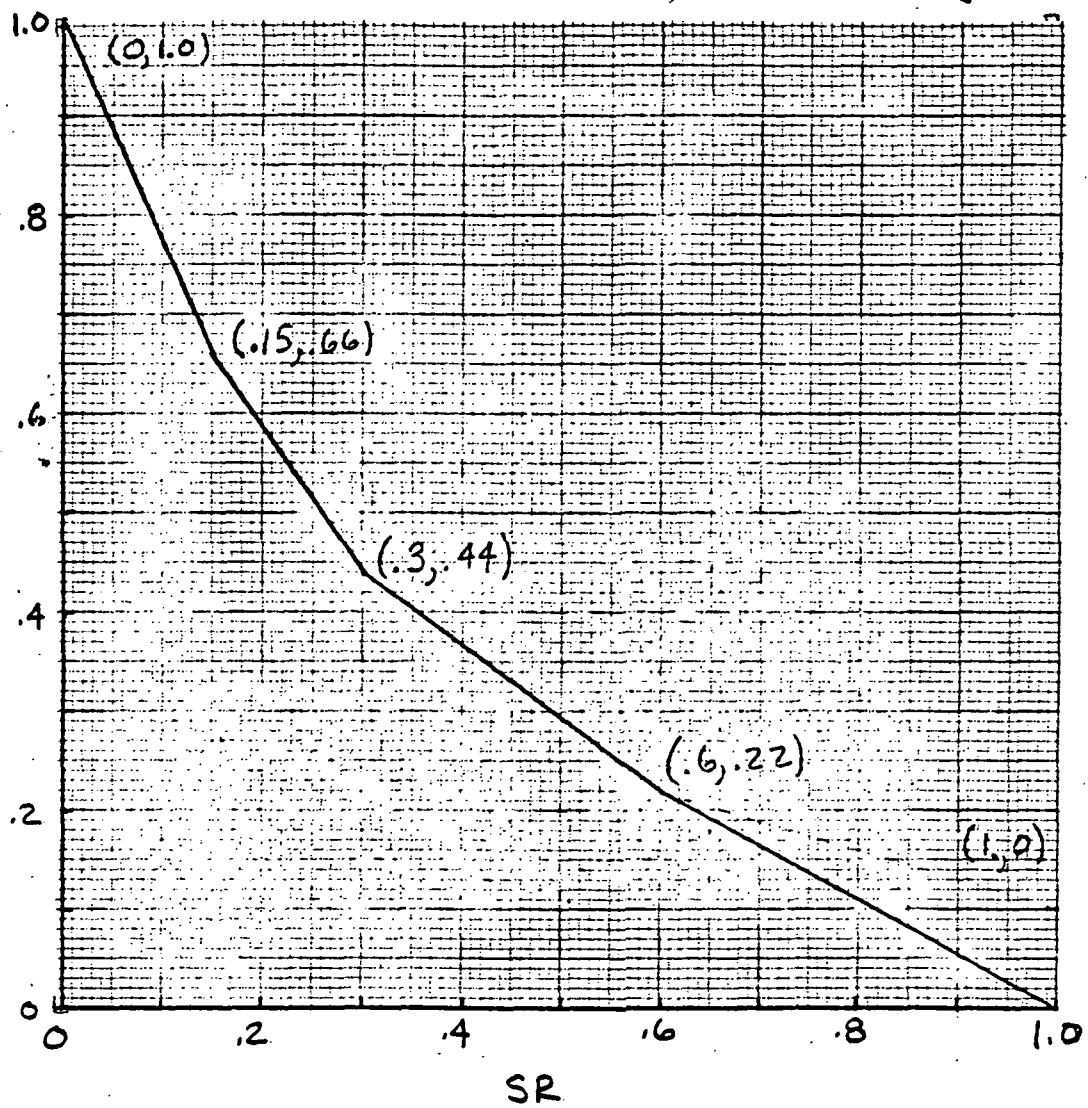


FIGURE 3

$f_3(SR, \psi)$ NORMALIZED μ -SLIP CURVE

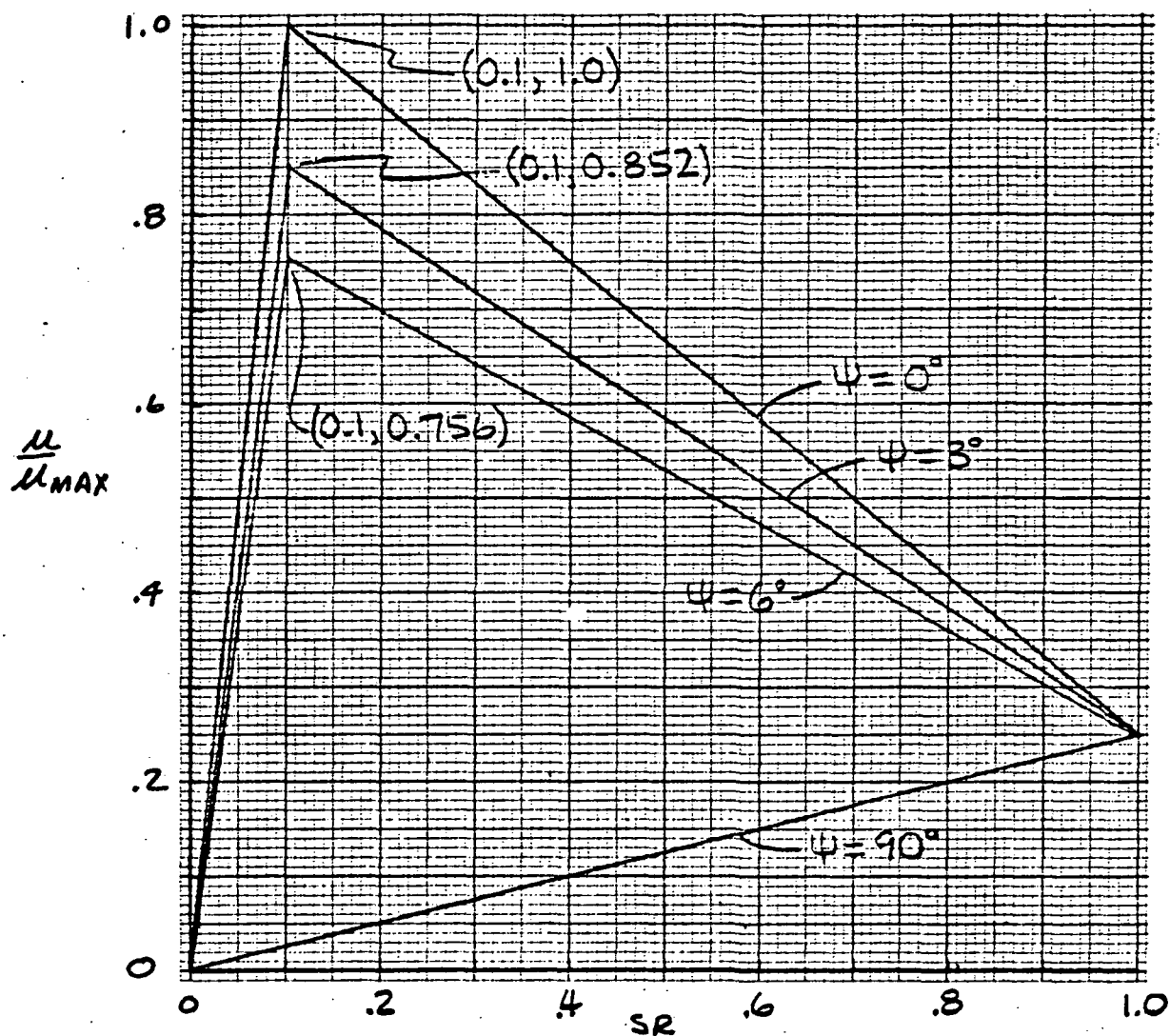


FIGURE 4

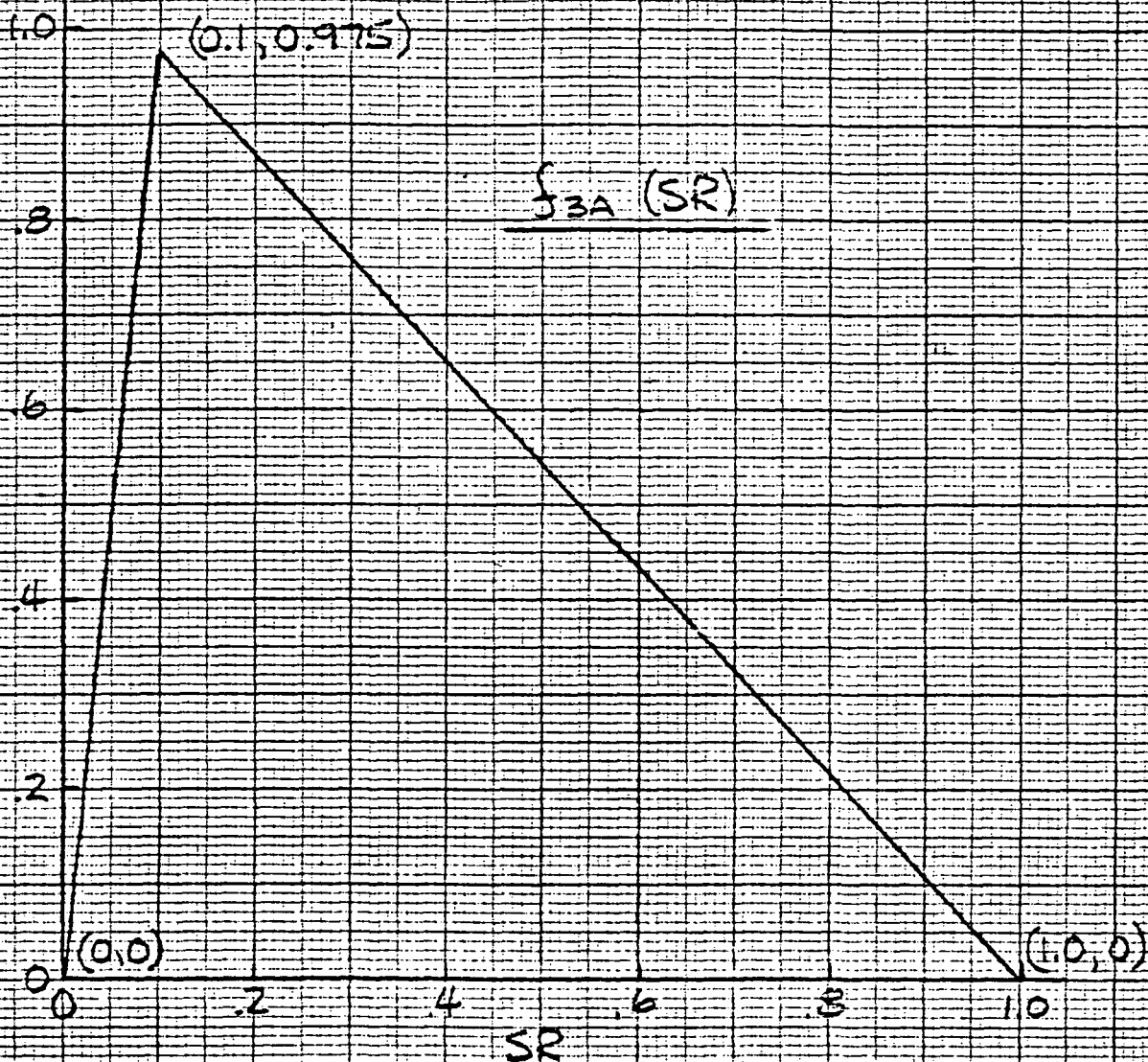


FIGURE 5

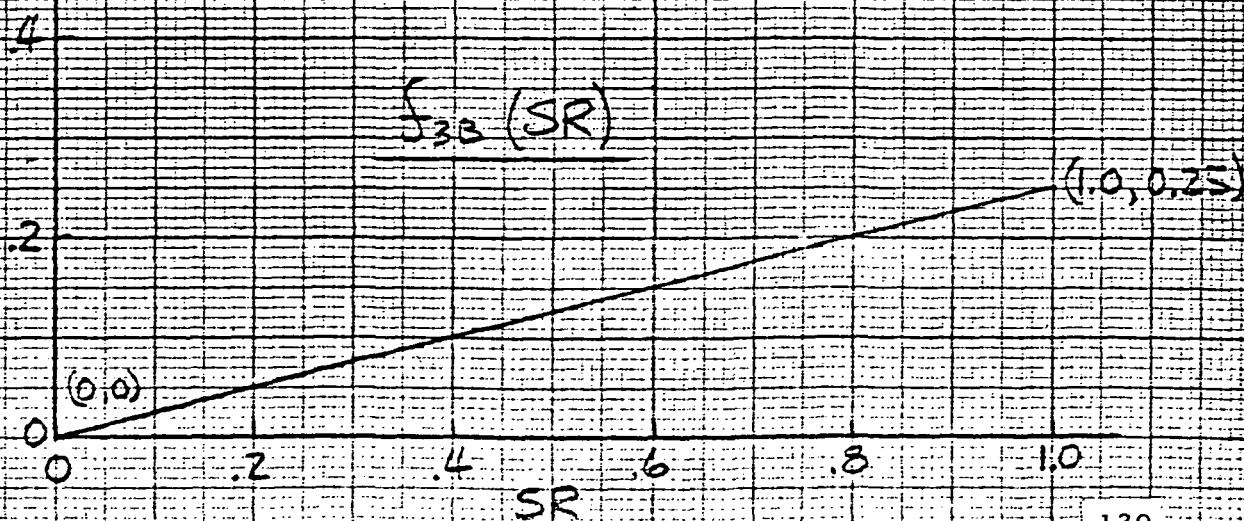


FIGURE 6

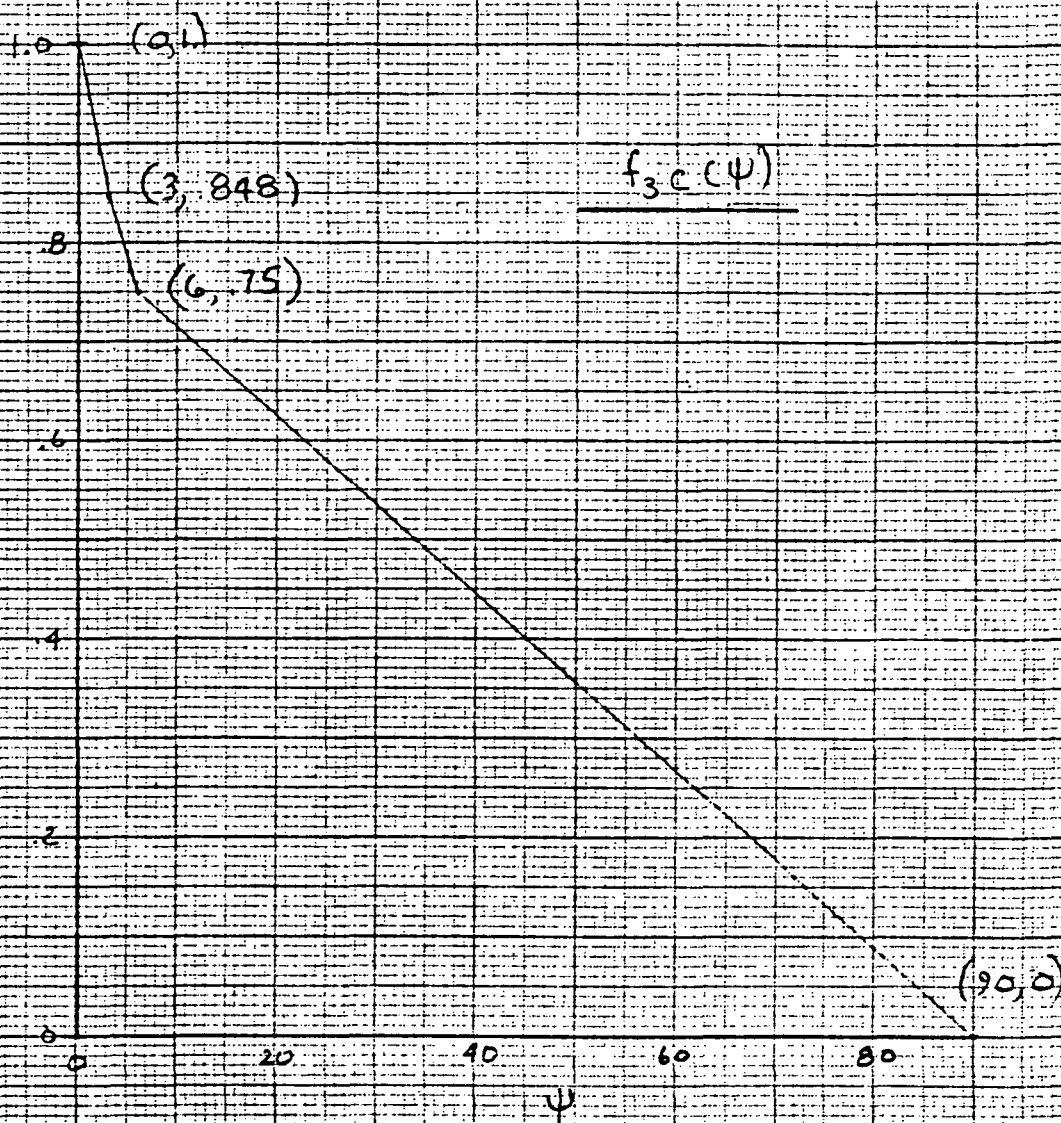


FIGURE 7

μ_{MAX} VERSUS VELOCITY (REF FIG 19)

$f_4(\dot{X}_1)$

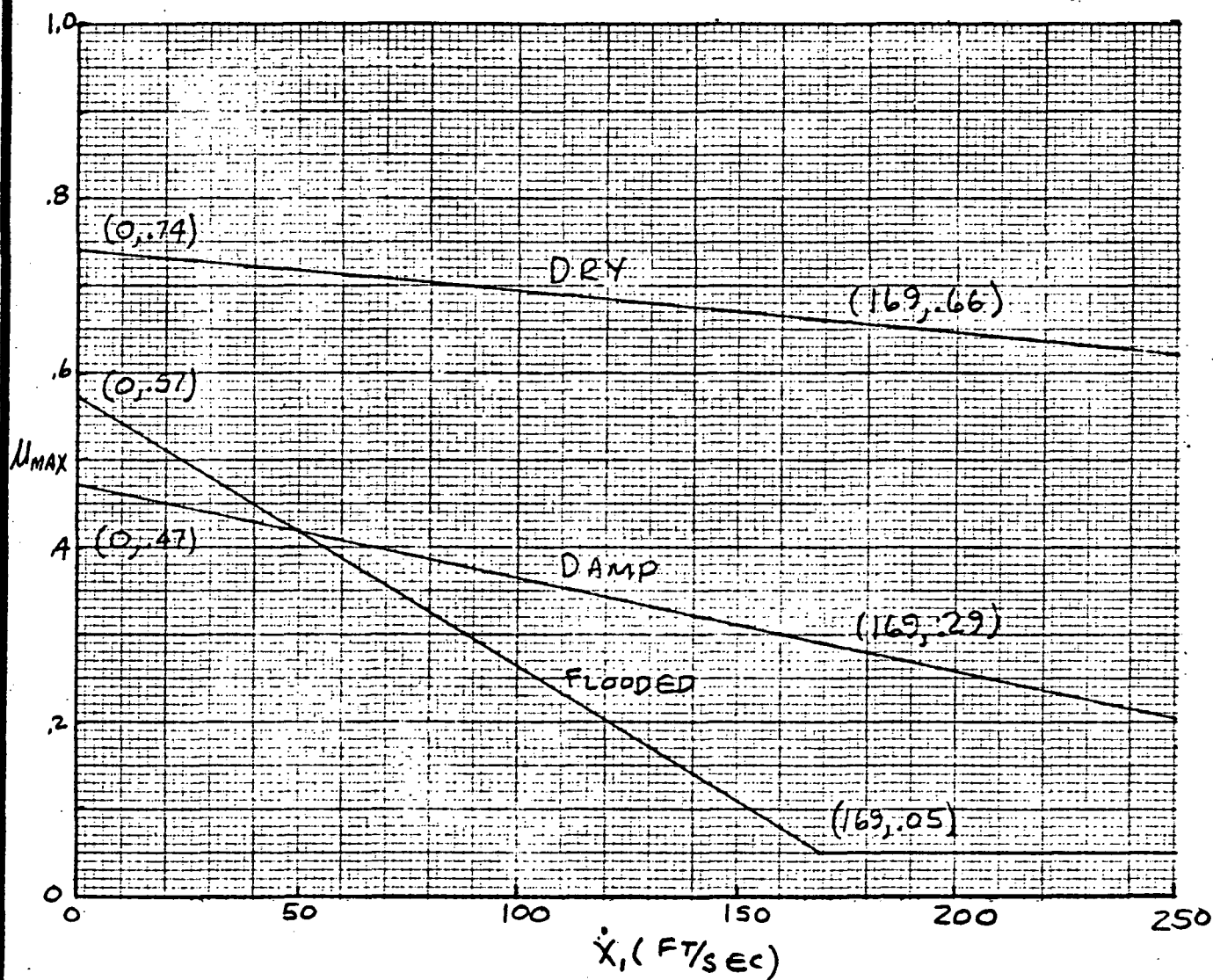


FIGURE 8

MODEL CORRELATION

TO ASSESS THE MODEL ACCURACY, PLOTS OF CORNERING AND DRAG FORCE VERSUS SLIP RATIO WERE MADE USING THE MODEL FOR 6 TEST CONDITIONS TESTED IN REFERENCE 1. TEST DATA IS THEN PLOTTED IN THE PROPER PLOT.

TEST DATA FROM REF 1

| CONDITIONS | | | | | | EXPERIMENTAL VALUES | | | |
|------------|-------------|-----------------------|--------------|-------------|-----|---------------------|--------------|-------|--------------|
| RUN | ψ ° | \dot{X}_1 FT/SEC | F_t LBS | TIME SEC | SR | μ_s | F_c LBS | M_d | F_D LBS |
| 1 | 0 | 78 | 12300 | 1.4 | .02 | - | - | .57 | 7011 |
| | | | | 2.0 | .04 | - | - | .61 | 7503 |
| | | | | 2.5 | .08 | - | - | .65 | 7995 |
| | | | | 3.0 | .09 | - | - | .70 | 8610 |
| | | | | 3.5 | .10 | - | - | .75 | 9225 |
| | | | | 3.9 | .12 | - | - | .76 | 9348 |
| | | | | 4.05 | .9 | - | - | .2 | 2460 |
| 27 | 3 | 78 | 13900 | .5 | 0 | .32 | 4448 | .05 | 695 |
| | | | | 1.2 | .04 | .3 | 4170 | .4 | 5560 |
| | | | | 1.5 | .09 | .29 | 4031 | .59 | 8201 |
| | | | | 2.0 | .10 | .28 | 3892 | .55 | 7645 |
| | | | | 2.5 | .10 | .24 | 3336 | .6 | 8340 |
| | | | | 3.0 | .12 | .22 | 3058 | .64 | 8896 |
| | | | | 3.2 | .9 | .05 | 695 | .2 | 2780 |
| 36 | 6 | 78 | 18800 | 2.0 | 0 | .45 | 8460 | .08 | 1504 |
| | | | | 3.5 | .04 | .4 | 7520 | .5 | 9400 |
| | | | | 4.0 | .08 | .37 | 6956 | .5 | 9400 |
| | | | | 4.8 | .72 | .05 | 940 | .25 | 4700 |
| | | | | 6.0 | .09 | .38 | 7144 | .48 | 9024 |
| | | | | 7.0 | .10 | .31 | 5828 | .52 | 9776 |
| | | | | 8.0 | .13 | .3 | 5640 | .58 | 10904 |
| | | | | 8.5 | .18 | .26 | 4883 | .6 | 11280 |

TEST DATA FROM REF 1

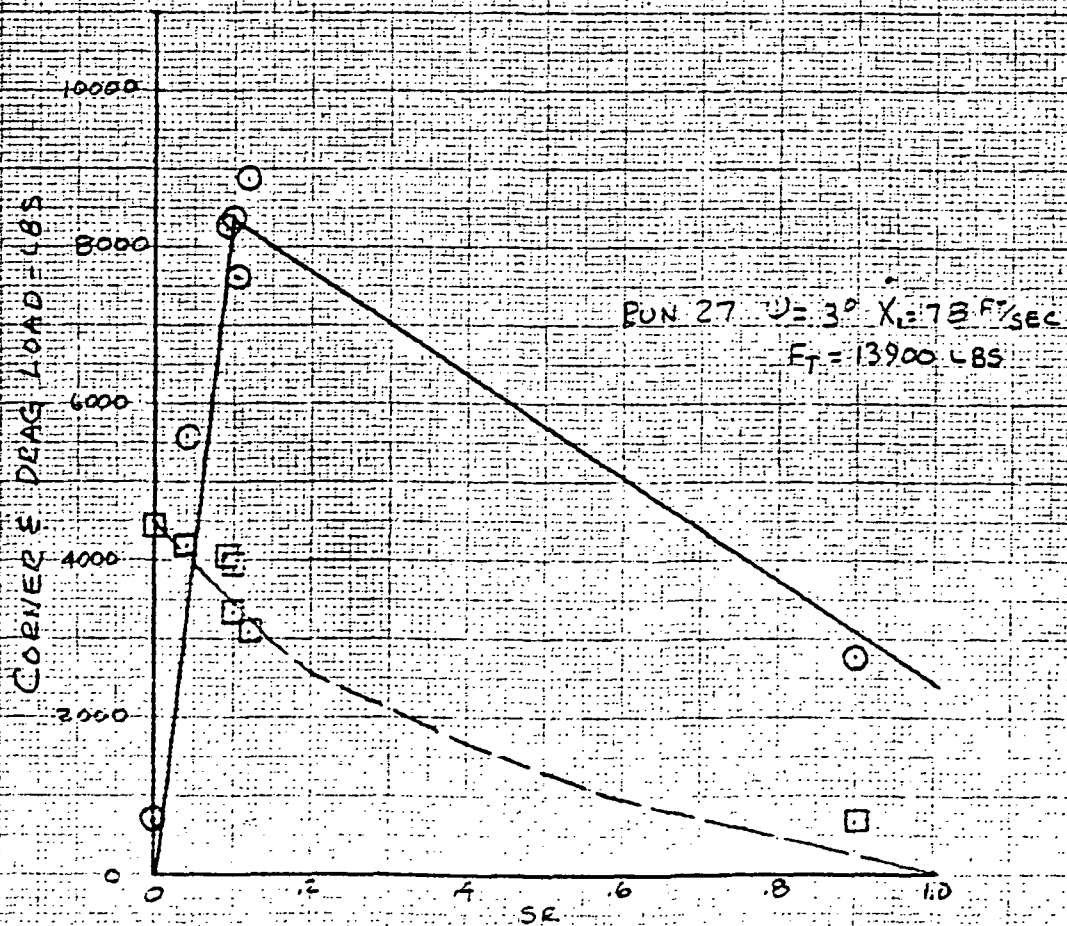
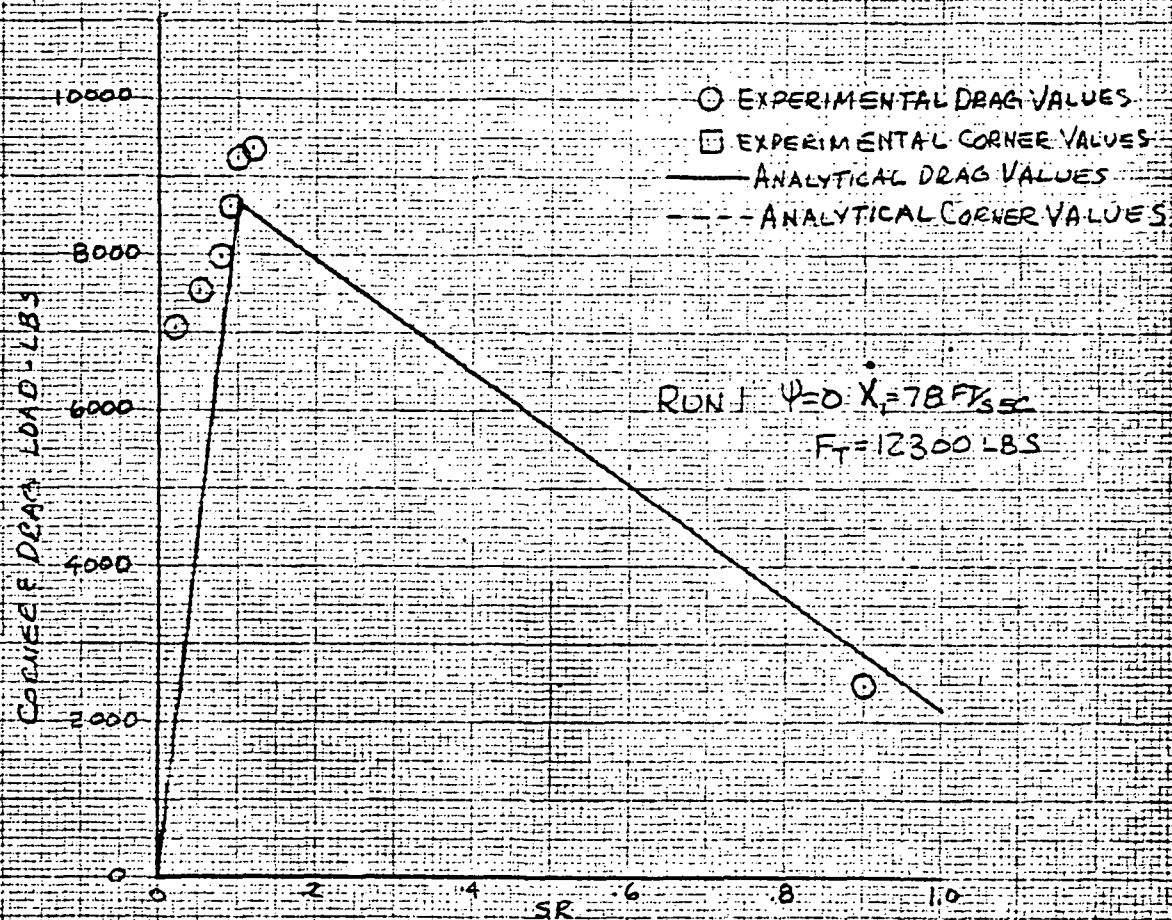
| CONDITIONS | | | | | | EXPERIMENTAL VALUES | | | |
|------------|--------|-------|-------|------|-----|---------------------|-------|------------------------|-------|
| RUN | ψ | V_i | F_T | TIME | SR | μ_s | F_c | M_d | F_D |
| | ° | F/SEC | LBS | SEC | | | LBS | | LBS |
| 4 | 0 | 166 | 13700 | 1.3 | .05 | - | - | .38 | 5206 |
| | | | | 1.6 | .09 | - | - | .55 | 7535 |
| | | | | 2.0 | .10 | - | - | .58 | 7946 |
| | | | | 2.6 | .18 | - | - | .68 | 9316 |
| | | | | 3.0 | .90 | - | - | .32 | 4384 |
| | | | | 3.5 | .03 | - | - | .2 | 2740 |
| | | | | 4.0 | .06 | - | - | .38 | 5206 |
| | | | | 5.0 | .08 | - | - | .5 | 6850 |
| | | | | 6.0 | .10 | - | - | .6 ^(.55-.7) | 8220 |
| 29 | 3 | 169 | 17000 | 7.0 | .11 | - | - | .65 ^(.5-.7) | 8905 |
| | | | | 1.0 | .01 | .3 | 5100 | .05 | 850 |
| | | | | 2.5 | .02 | .31 | 5270 | .14 | 2380 |
| | | | | 2.7 | .05 | .30 | 5100 | .28 | 4760 |
| | | | | 2.8 | .08 | .30 | 5100 | .38 | 6460 |
| | | | | 3.0 | .09 | .31 | 5270 | .42 | 7140 |
| | | | | 3.5 | .09 | .30 | 5100 | .48 | 8160 |
| | | | | 4.0 | .10 | .31 | 5270 | .50 | 8500 |
| | | | | 4.5 | .11 | .29 | 4930 | .52 | 8840 |
| 38 | 6 | 169 | 18700 | 5.0 | .12 | .28 | 4760 | .56 | 9520 |
| | | | | 1.0 | .04 | .43 | 8041 | .07 | 1309 |
| | | | | 2.6 | .09 | .40 | 7480 | .27 | 5049 |
| | | | | 2.75 | .12 | .34 | 6358 | .40 | 7480 |
| | | | | 3.0 | .13 | .31 | 5797 | .45 | 8415 |
| | | | | 3.5 | .18 | .28 | 5236 | .45 | 8415 |
| | | | | 4.0 | .20 | .20 | 3740 | .45 | 8415 |
| | | | | 4.25 | .22 | .18 | 3366 | .50 | 9350 |
| | | | | 4.4 | .50 | .08 | 1496 | .40 | 7480 |

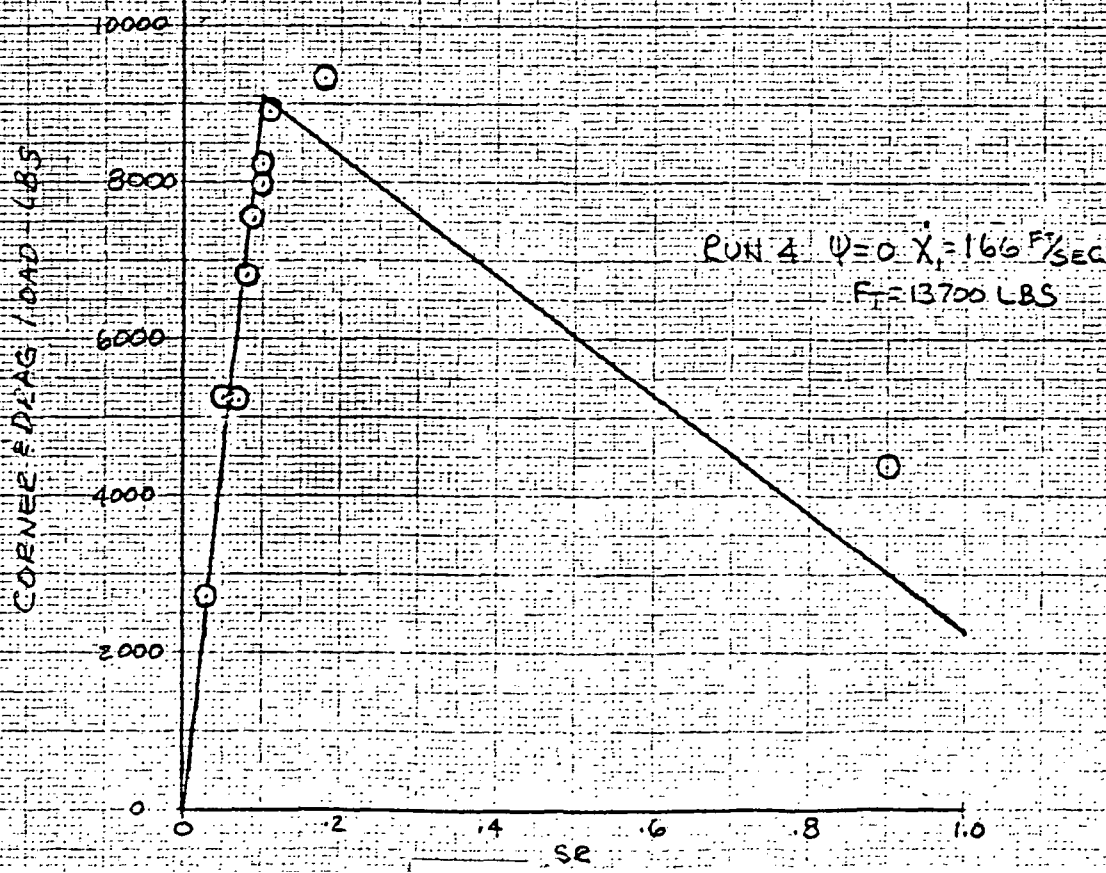
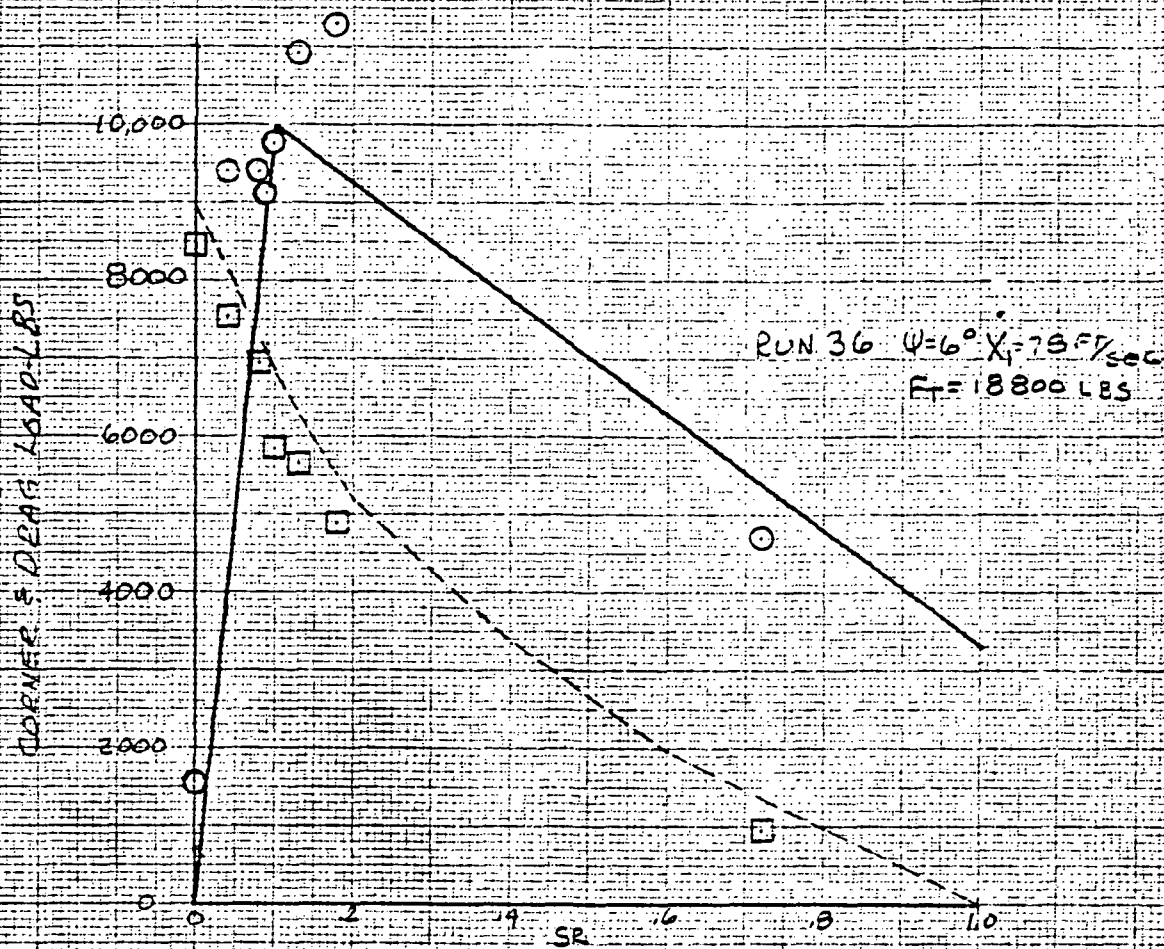
ANALYTICAL VALUES COMPUTED BY MODEL

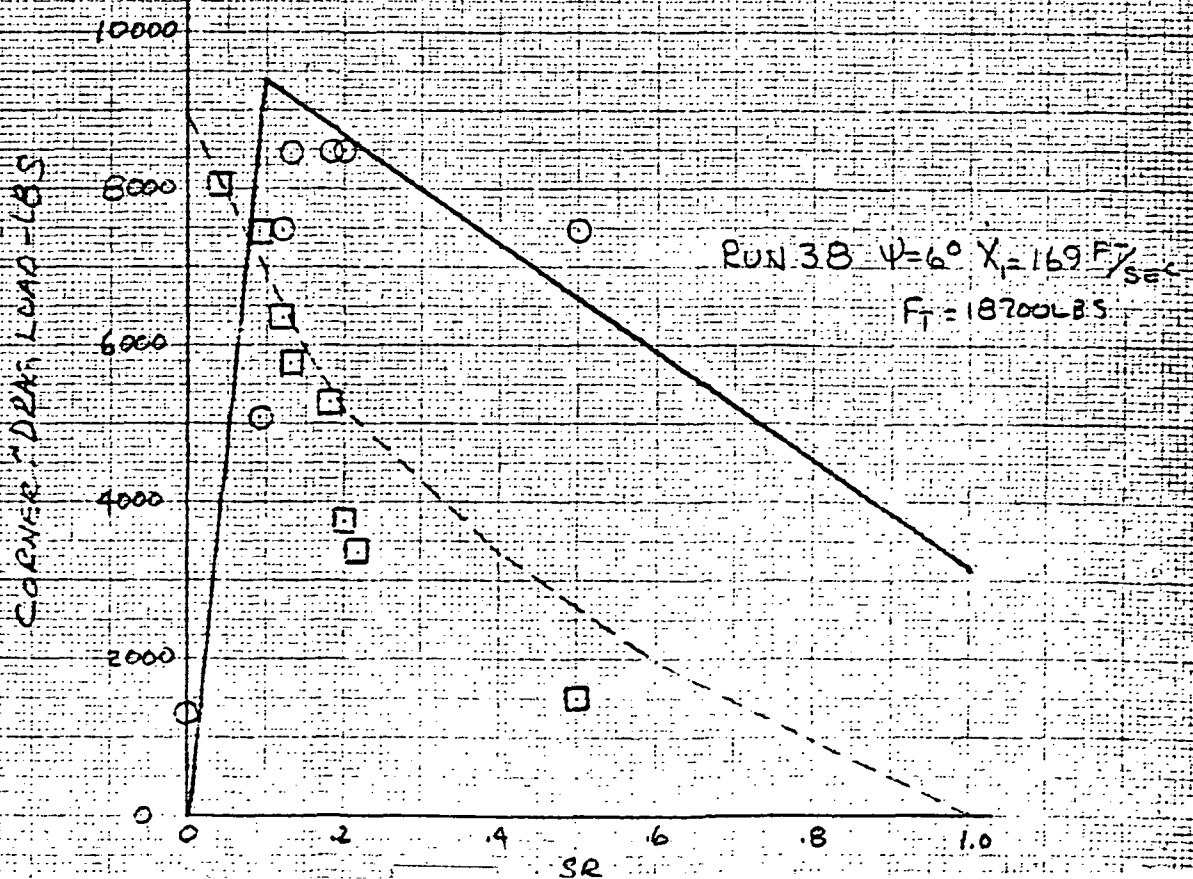
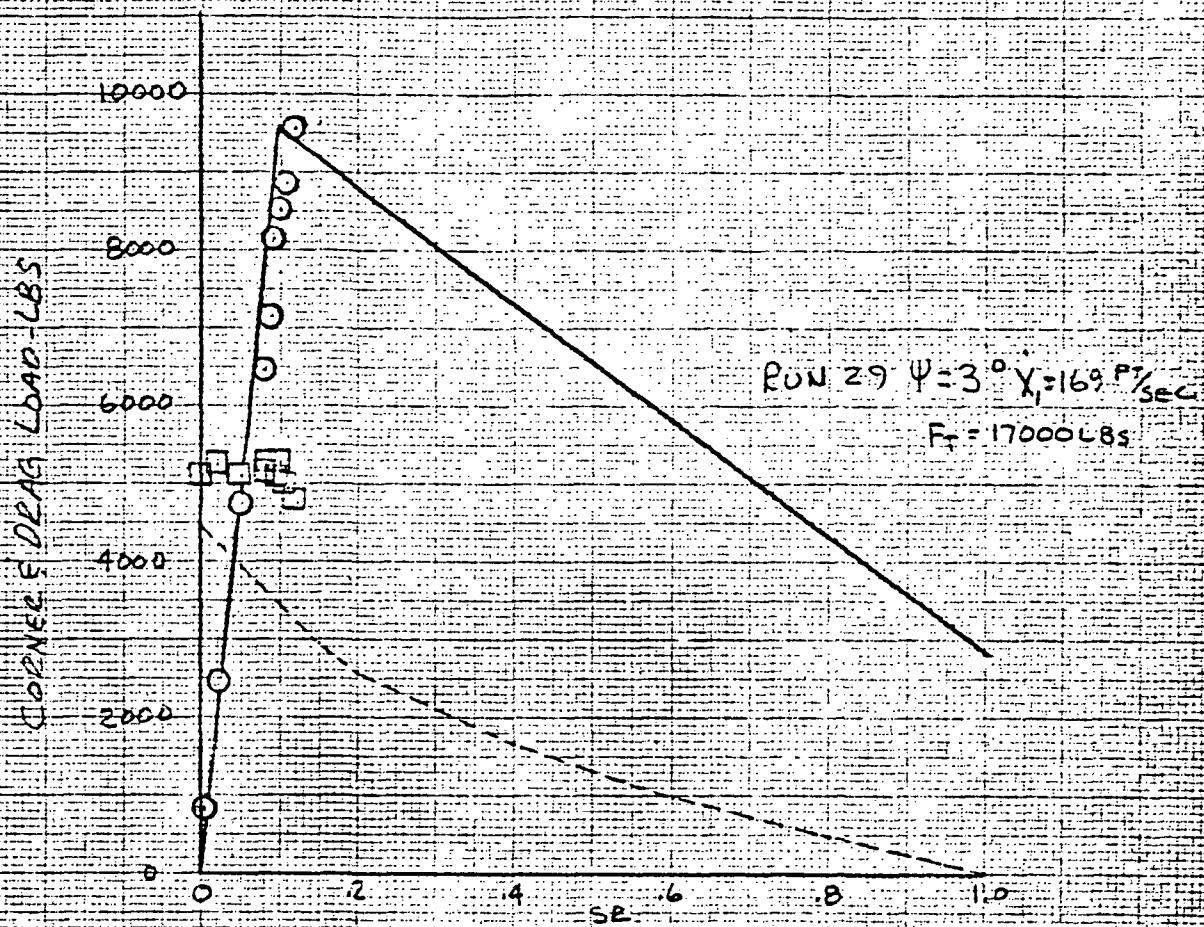
| RUN | Ψ ° | N/Ψ LBS | $F_T \mu_{MAX}$ LBS | \dot{X}_1 FT/SEC | $f_q(V)$ μ_{MAX} | F_T LBS | SR | $f_2(SR, \Psi)$ μ_{MAX} | $f_5(SR)$ | F_C LBS | F_D LBS |
|-----|-------------|------------|------------------------|-----------------------|-------------------------|--------------|------|--------------------------------|-----------|--------------|--------------|
| 1 | 0 | 0 | 8610 | 78 | .7 | 12300 | 0 | 0 | 1.00 | 0 | 0 |
| | | | | | | | .05 | .50 | .89 | 0 | 4305 |
| | | | | | | | .10 | 1.00 | .77 | 0 | 8610 |
| | | | | | | | .15 | .96 | .66 | 0 | 8266 |
| | | | | | | | .20 | .915 | .58 | 0 | 7878 |
| | | | | | | | .40 | .75 | .37 | 0 | 6458 |
| | | | | | | | .60 | .58 | .22 | 0 | 4994 |
| | | | | | | | .80 | .415 | .11 | 0 | 3573 |
| | | | | | | | 1.00 | .25 | 0 | 0 | 2152 |
| 27 | 3 | 4473 | 9730 | 78 | .7 | 13900 | 0 | 0 | 1.00 | 4473 | 0 |
| | | | | | | | .05 | .426 | .89 | 3981 | 4145 |
| | | | | | | | .10 | .852 | .77 | 3444 | 8290 |
| | | | | | | | .15 | .82 | .66 | 2952 | 7979 |
| | | | | | | | .20 | .78 | .58 | 2594 | 7589 |
| | | | | | | | .40 | .65 | .37 | 1655 | 6154 |
| | | | | | | | .60 | .515 | .22 | 984 | 5011 |
| | | | | | | | .80 | .38 | .11 | 492 | 3697 |
| | | | | | | | 1.00 | .25 | 0 | 0 | 2433 |
| 36 | 6 | 8946 | 13160 | 78 | .7 | 18800 | 0 | 0 | 1.00 | 8946 | 0 |
| | | | | | | | .05 | .378 | .89 | 7962 | 4975 |
| | | | | | | | .10 | .756 | .77 | 6888 | 9949 |
| | | | | | | | .15 | .725 | .66 | 5904 | 9541 |
| | | | | | | | .20 | .70 | .58 | 5189 | 9210 |
| | | | | | | | .40 | .585 | .37 | 3310 | 7699 |
| | | | | | | | .60 | .47 | .22 | 1968 | 6185 |
| | | | | | | | .80 | .36 | .11 | 984 | 4738 |
| | | | | | | | 1.00 | .25 | 0 | 0 | 3290 |

ANALYTICAL VALUES COMPUTED BY MODEL

| RUN | ψ ° | N ψ LBS | $F_T \mu_{max}$ LBS | \dot{X}_1 FT/SEC | $f_q(V)$ μ_{max} | F_T LBS | SR | $f_3(SR, \psi)$ | $f_5(SR)$ | F_c LBS | F_D LBS |
|-----|-------------|-----------------|------------------------|-----------------------|-------------------------|--------------|------|-----------------|-----------|--------------|--------------|
| 4 | 0 | 0 | 9042 | 166 | .66 | 13700 | 0 | 0 | 1.00 | 0 | 0 |
| | | | | | | | .05 | .50 | .89 | 0 | 4521 |
| | | | | | | | .10 | 1.00 | .77 | 0 | 9042 |
| | | | | | | | .15 | .96 | .66 | 0 | 8680 |
| | | | | | | | .20 | .915 | .58 | 0 | 8273 |
| | | | | | | | .40 | .75 | .37 | 0 | 6781 |
| | | | | | | | .60 | .58 | .22 | 0 | 5244 |
| | | | | | | | .80 | .415 | .11 | 0 | 3752 |
| | | | | | | | 1.00 | .25 | 0 | 0 | 2261 |
| 29 | 3 | 4473 | 11220 | 169 | .66 | 17000 | 0 | 0 | 1.00 | 4473 | 0 |
| | | | | | | | .05 | .426 | .89 | 3981 | 4780 |
| | | | | | | | .10 | .852 | .77 | 3444 | 9559 |
| | | | | | | | .15 | .82 | .66 | 2952 | 9200 |
| | | | | | | | .20 | .78 | .58 | 2594 | 8752 |
| | | | | | | | .40 | .65 | .37 | 1655 | 7293 |
| | | | | | | | .60 | .515 | .22 | 984 | 5778 |
| | | | | | | | .80 | .38 | .11 | 492 | 4264 |
| | | | | | | | 1.00 | .25 | 0 | 0 | 2805 |
| 38 | 6 | 8946 | 12408 | 169 | .66 | 18800 | 0 | 0 | 1.00 | 8946 | 0 |
| | | | | | | | .05 | .378 | .89 | 7962 | 4690 |
| | | | | | | | .10 | .756 | .77 | 6888 | 9380 |
| | | | | | | | .15 | .725 | .66 | 5904 | 8996 |
| | | | | | | | .20 | .70 | .58 | 5189 | 8686 |
| | | | | | | | .40 | .585 | .37 | 3310 | 7259 |
| | | | | | | | .60 | .47 | .22 | 1968 | 5832 |
| | | | | | | | .80 | .36 | .11 | 984 | 4467 |
| | | | | | | | 1.00 | .25 | 0 | 0 | 3102 |







INTRODUCTION

THIS SECTION DEVELOPS THE EQUATIONS FOR STRUT
AXLE DEFORMATIONS, BRAKE TORQUE, TIRE AND
WHEEL DYNAMICS, AND TIRE SLIP RATIO COMPUTATION.

MODEL DEFINITION

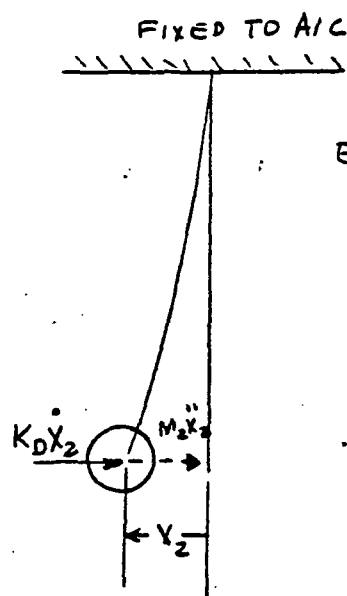
AXLE DEFLECTION

DURING BRAKING THE WHEEL AXLE DEFLECTS. THE DEFLECTIONS ARE LARGE ENOUGH THAT THE DEFLECTION VELOCITIES ARE IMPORTANT CONSIDERATIONS TO THE ANTISKID OPERATION. THE WHEEL AXLE DEFLECTION IS THE SUM OF THE FORE-AFT DEFLECTION OF THE STRUT AND THE AXLE TWIST ABOUT THE STRUT.

STRUT FORE-AFT DEFLECTION

INFLUENCE COEFFICIENTS ARE USED TO DERIVE THE STRUT FORE-AFT EQUATIONS OF MOTION. THE FORCES BENDING THE STRUT ARE DRAG FORCES, BRAKE TORQUE, INERTIA FORCES, AND STRUT DAMPING FORCES.

STRUT DAMPING FORCE - VISCOUS DAMPING IS ASSUMED IN THE MODEL. THE EXPRESSION FOR THE FORCE IS DERIVED AS FOLLOWS:



FROM FIGURE 1

$$\text{EQN 1} \quad X_2 = -M_2 \ddot{X}_2 \delta_{11} - K_D \dot{X}_2 \delta_{11}$$

WHERE $X_2, \dot{X}_2, \ddot{X}_2$ = STRUT DISP, VEL, ACC REL TO A/C

δ_{11} = INFLUENCE COEFF - DEFLECTION AT STRUT DUE TO 1 LB LOAD

M_2 = EFFECTIVE STRUT MASS

K_D = EFFECTIVE STRUT DAMPING COEF.

REARRANGING EQN 1 GIVES

FIG 1 DAMPING FORCE

$$\text{EQN 2} \quad \ddot{X}_2 + \frac{K_D}{M_2} \dot{X}_2 + \frac{1}{M_2 \delta_{11}} X_2 = 0$$

BY EQUATING LIKE COEFFICIENTS TO A SINGLE DEGREE OF FREEDOM EQUATION OF MOTION GIVES

$$\text{EQN 3} \quad K_D = 2 \zeta \sqrt{\frac{M_2}{\delta_{11}}}$$

WHERE ζ = CRITICAL DAMPING RATIO

INERTIA FORCE = $M_2(\ddot{X}_1 + \ddot{X}_2)$ SEE FIG 2

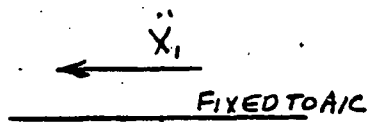
WHERE \ddot{X}_1 = AIRCRAFT LONGITUDINAL ACCELERATION

DRAG FORCE = $F_D + F_D'$

WHERE F_D = PRIMARY TIRE DRAG FORCE

F_D' = SECOND TIRE DRAG FORCE

BRAKE TORQUE - FOR SIMPLIFICATION, THE ASSUMPTION
 IS MADE THAT THE ^{TOTAL} BRAKE TORQUE ACTING
 ON THE STRUT IS TWICE THE PRIMARY BRAKE
 TORQUE T_B .



THE STRUT DISPLACEMENT IS

$$\text{EQN 4 } \ddot{X}_2 = -(F_D + F_D') \delta_{11} - 2T_B \delta_{12} - M_2 (\ddot{X}_1 + \ddot{X}_2) \delta_{11} - 2\sqrt{M_2 \delta_{11}} \dot{X}_2$$

WHERE δ_{12} = INFLUENCE COEFF - DEFLECTION
 AT STRUT DUE TO A 1 FT-LB
 TORQUE

REARRANGING EQN 4 GIVES

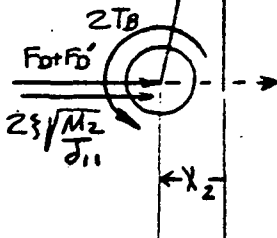


FIG-2 STRUT FORCES

$$\text{EQN 5 } \ddot{X}_2 = -\frac{X_2}{M_2 \delta_{11}} - \frac{(F_D + F_D')}{M_2} - \frac{2T_B \delta_{12}}{M_2 \delta_{11}} - \frac{2\sqrt{M_2 \delta_{11}}}{M_2 \delta_{11}} \dot{X}_2 - \ddot{X}_1$$

$$\text{EQN 6 } \dot{X}_2 = \dot{X}_2(0) + \int_0^t \ddot{X}_2 dt$$

$$\text{EQN 7 } X_2 = X_2(0) + \int_0^t \dot{X}_2 dt$$

INITIAL CONDITIONS $\dot{X}_2(0)$ AND $X_2(0)$ ARE ZERO.

AXLE TORSIONAL DEFLECTION

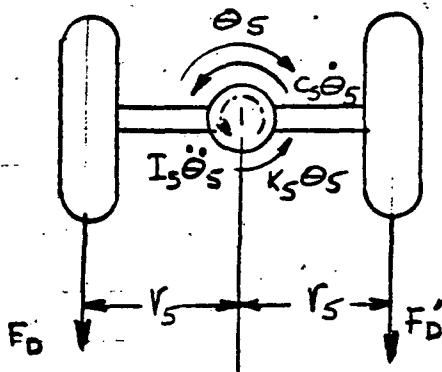


FIGURE 3 STRUT TWIST

THE STRUT TORSION MOMENT EQUATION IS

$$\text{EQN 8 } I_s \ddot{\theta}_s + c_s \dot{\theta}_s + k_s \theta_s = r_s (F_D - F_D')$$

WHERE $\theta_s, \dot{\theta}_s, \ddot{\theta}_s$ ARE AXLE ROTATIONAL DISPLACEMENT, VELOCITY AND ACCELERATION

I_s = MOMENT OF INERTIA

c_s = ROTATIONAL DAMPING FACTOR

k_s = ROTATIONAL SPRING FACTOR

r_s = DISTANCE FROM STRUT TO TIRE

BRAKE TORQUE MODEL

BRAKE TORQUE IS ASSUMED TO BE THE PRODUCT OF TWO FUNCTIONS

$$\text{EQN 9 } T_B = f_1(\dot{\theta}_3) \times f_2(\bar{P}_B)$$

WHERE

$f_1(\dot{\theta}_3)$ IS AN EMPIRICAL FUNCTION THAT INTRODUCES THE EFFECT OF BRAKE TORQUE VARIATION WITH BRAKE ROTATIONAL SPEED WHEN BRAKE PRESSURE IS HELD CONSTANT. A DIFFERENT FUNCTION IS USED FOR LANDINGS AND TAKEOFFS.

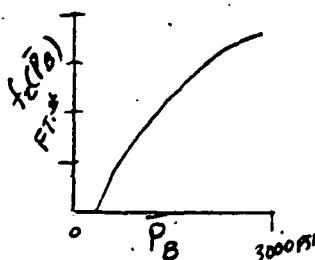
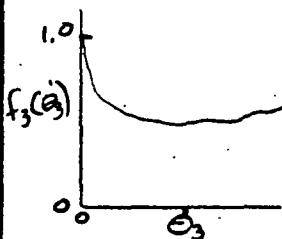


FIG 4 BRAKE FUNCTIONS

$f_2(\bar{P}_B)$ IS AN EMPIRICAL FUNCTION THAT INTRODUCES THE NON LINEAR RELATIONSHIP BETWEEN BRAKE TORQUE AND BRAKE PRESSURE WHEN ROTATIONAL SPEED, IS HELD CONSTANT.

\bar{P}_B FILTERED BRAKE PRESSURE

TO ACCOUNT FOR A TIME DELAY BETWEEN BRAKE TORQUE CHANGE AND BRAKE PRESSURE CHANGE, \bar{P}_B IS DETERMINED FROM THE RELATIONSHIP

EQN 10
$$\dot{\bar{P}}_B = \frac{1}{\tau_B} (P_B - \bar{P}_B)$$

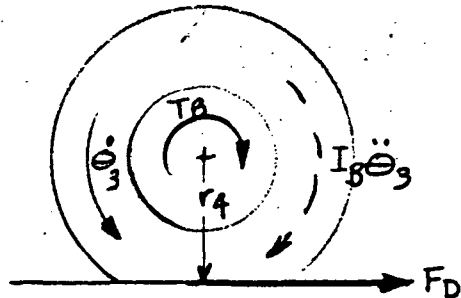
WHERE P_B IS THE MEASURED BRAKE PRESSURE AT THE BRAKE

τ_B TIME CONSTANT FOR BRAKE

EQN 11
$$\bar{P}_B = \bar{P}_B(0) + \int_0^T \dot{\bar{P}}_B dt$$

WHERE THE INITIAL CONDITION $\bar{P}_B(0)$ IS ZERO

TIRE AND WHEEL DYNAMICS



SUMMING MOMENTS GIVES

EQN 12
$$I_B \ddot{\theta}_3 + T_B - r_4 F_D = 0$$

WHERE

I_B = INERTIA OF TIRE, WHEEL & BRAKE

r_4 = AXLE HEIGHT

FIG 6 TIRE AND WHEEL

OR

EQN 13
$$\ddot{\theta}_3 = \frac{r_4 F_D - T_B}{I_B}$$

EQN 14
$$\dot{\theta}_3 = \dot{\theta}_3(0) + \int_0^T \ddot{\theta}_3 dt$$

WHERE $\dot{\theta}_3(0)$ IS THE INITIAL TIRE ROTATIONAL SPEED.

TIRE SLIP RATIO

THE SLIP RATIO OF THE PRIMARY TIRE IS

EQN 15

$$V_{SB} = \frac{(\dot{X}_1 + \dot{X}_2 - r_5 \dot{\Theta}_5 - r_r \dot{\Theta}_3)}{\dot{X}_1 + \dot{X}_2 - r_5 \dot{\Theta}_5}$$

WHERE r_r = EFFECTIVE ROLLING RADIUS

SECOND TIRE CORNERING & DRAG FORCES

THE SECOND TIRE FORCES ARE ASSUMED TO BE LAGGED FROM THE PRIMARY FORCES BY THE RELATION

EQN 16

$$\dot{F}_c' = \frac{1}{\tau_c} (F_c - F_c')$$

EQN 17

$$\dot{F}_d' = \frac{1}{\tau_d} (F_d - F_d')$$

WHERE F_c' AND F_d' ARE THE SECONDARY CORNERING AND DRAG FORCES RESPECTFULLY

τ_c = CORNERING TIME CONSTANT

τ_d = DRAG TIME CONSTANT

EQN 18

$$F_c' = F_c'(0) + \int_0^T \dot{F}_c' dt$$

EQN 19

$$F_d' = F_d'(0) + \int_0^T \dot{F}_d' dt$$

WHERE $F_c'(0)$ AND $F_d'(0)$ ARE INITIAL CONDITIONS

Section 3. PROGRAM

ANALOG PROGRAM

The analog computer program is shown in Figure C-4. The program was set up so that it could be used in either the stand alone or normal mode. This allowed the program to be developed independently of the total simulator.

INTERFACE AND PROGRAMMING CONSIDERATIONS

The simulation was interfaced with the digital simulation and hardware as illustrated in the Analog Antiskid Interface Description.

Analog computer to Hardware Interface - Wheel speed from the computer drove voltage controlled oscillators. The oscillator outputs were impressed on the antiskid control box to simulate the signal from each tire. The frequency corresponded to 40 pulses per wheel revolution.

The squat signal was 28 vdc when the nose gear was fully extended and zero when the gear compressed one and one half inches.

The PMV servos drove the PMV in response to brake pedal position.

Brake pressure was monitored by pressure transducers connected to amplifiers with appropriate gains for the analog circuit.

Digital Computer to Analog Computer Interface - The signal from the digital computer was processed by a Digital-to-Analog converter. To take advantage of the digital computer capabilities the product of normal load and maximum friction coefficient was formed in the digital computer. The unbraked cornering force and $f_{3c}(\psi)$ were also calculated in the digital computer because of nature of the computations and the relatively slow changes experienced by these parameters. Aircraft axle velocities and aircraft acceleration were also input to the analog computer. Cornering and drag loads were impressed on analog-to-digital converters for communication with the digital computer.

MACH. C = LEFT WHEEL
MACH. D = RIGHT "

RDC ANTISKID SIMULATION ~ ONE WHEEL

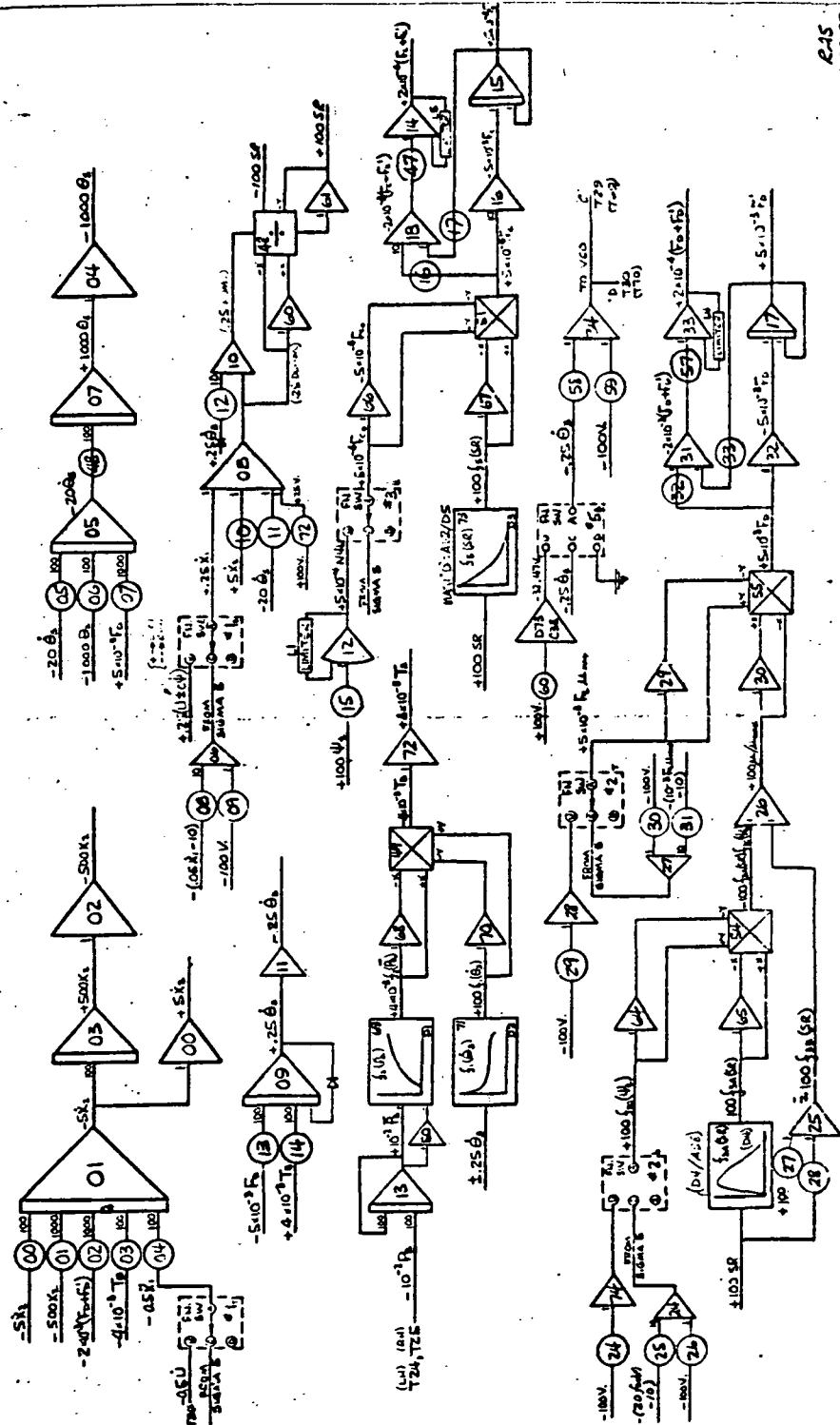


FIGURE C-4 WIRING DIAGRAM -- ANALOG ANTISKID SIMULATOR

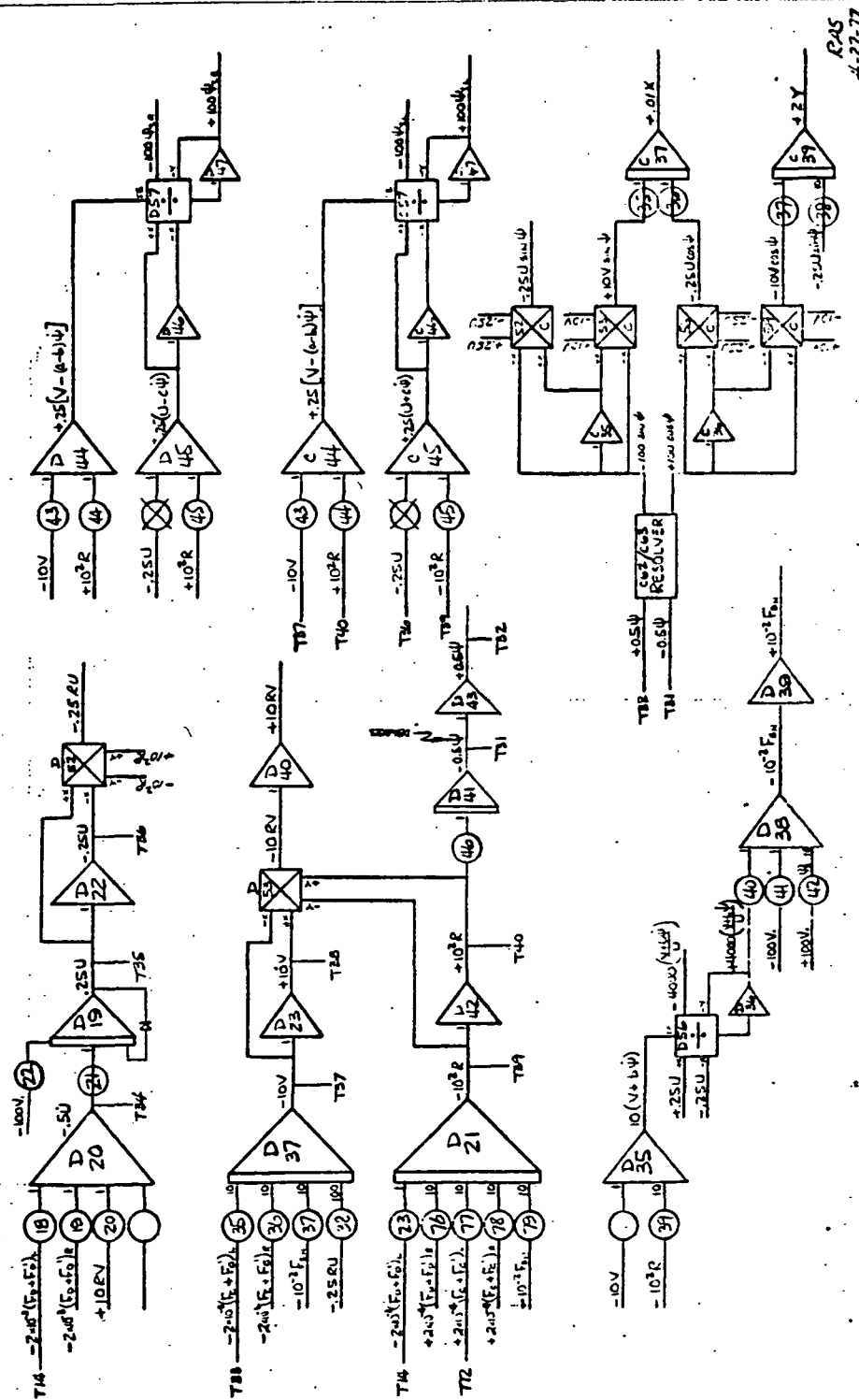


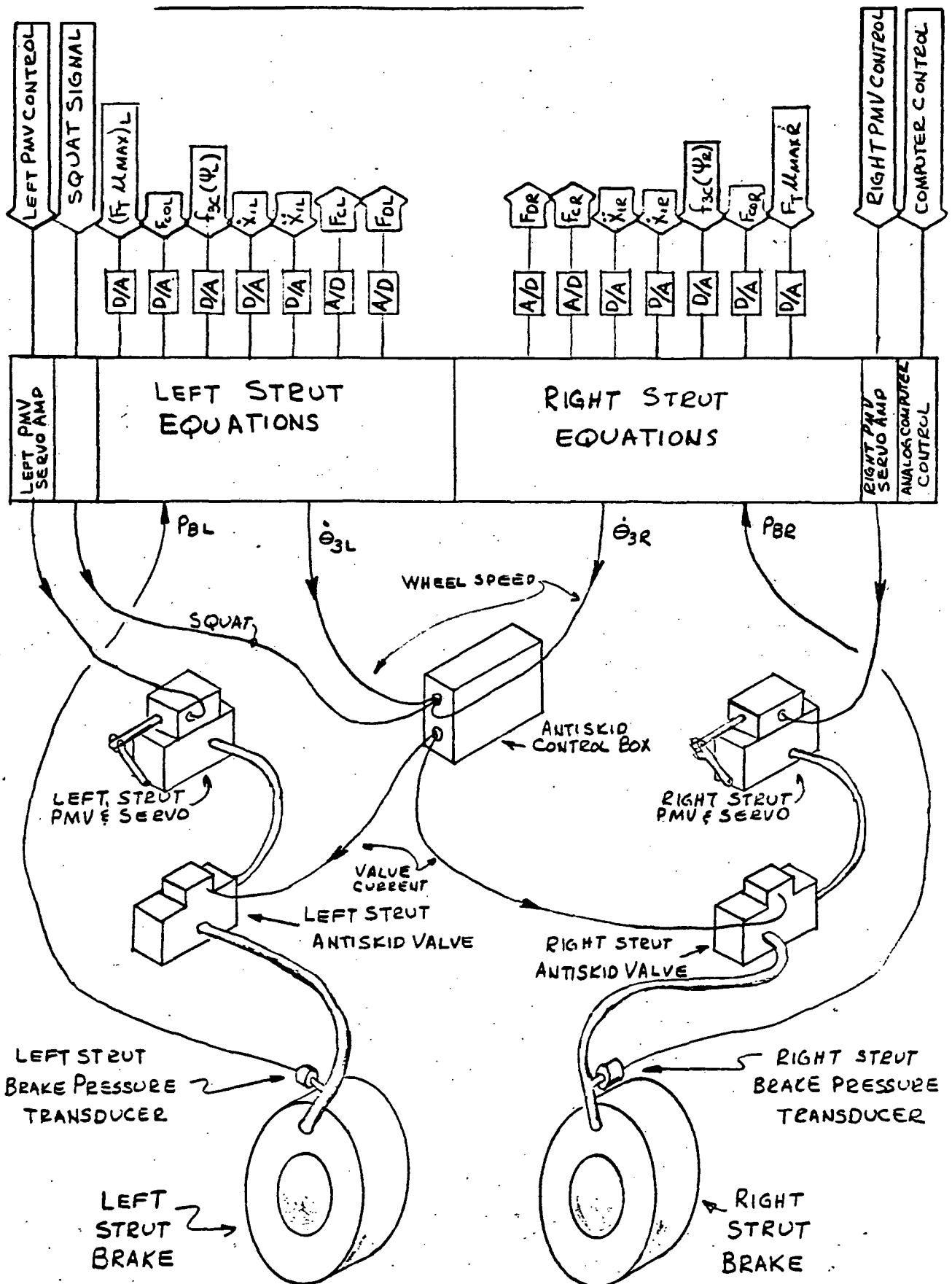
FIGURE C-4 WIRING DIAGRAM -- ANALOG ANTISKID SIMULATOR (CONCLUDED)

ANALOG ANTISKID SIMULATION INTERFACE DESCRIPTION

THE PHYSICAL BLOCK DIAGRAM FOR THE SIMULATION IS SHOWN ON THE NEXT PAGE. ITEMS WITH ARROWS TOWARD SIMULATION COME TO THE SIMULATION FROM THE AIRFRAME SIMULATION WITH THE EXCEPTION OF THE PMV CONTROLS WHICH COME FROM THE COCKPIT. ITEMS WITH ARROWS AWAY FROM SIMULATION GO TO THE AIRFRAME SIMULATION. THE FOLLOWING TABLE DEFINES THE VARIABLES.

| SYMBOL | DEFINITION |
|---------------------------------|--|
| LEFT/RIGHT PMV CONTROL | LEFT/RIGHT PILOTS METERING VALVE COMMAND - PROPORTIONAL TO BRAKE PEDAL POSITION |
| SQUAT SIGNAL | INDICATION THAT NOSE GEAR HAS COMPRESSED 3 INCHES - NECESSARY FOR ANTISKID BOX OPERATION |
| $(F_T \mu_{MAX})_{LR}$ | VALUE OF LEFT/RIGHT GEAR NORMAL LOAD MULTIPLIED BY MAXIMUM FRICTION COEFFICIENT |
| F_{C0LR} | LEFT/RIGHT UNBRAKED CORNERING FORCE |
| $f_{3C}(\Psi_{LR})$ | EMPIRICAL FUNCTION USED TO REDUCE BRAKED DRAG FORCE AS A FUNCTION OF YAW ANGLE. |
| $\dot{x}_{1LR}, \ddot{x}_{1LR}$ | LEFT/RIGHT AXLE VELOCITY, ACCELERATION |
| F_{CLR} | LEFT/RIGHT CORNERING FORCE |
| F_{D4R} | LEFT/RIGHT DRAG FORCE |
| COMPUTER CONTROL | SIGNAL TO ANALOG COMPUTER TO RESET, HOLD, COMPUTE |

ANALOG ANTISKID SIMULATION



Section 4. HARDWARE

The hardware needed for this program is outlined in the Task Assignment Drawing Z7802765. Details of the hardware are given in Drawing Z7935344.

Equipment serial numbers used in the simulation were as follows:

| | | |
|--------------|------------------|--------------|
| LH A/S Valve | P/N 39-101 | S/N 797C |
| RH A/S Valve | P/N 39-101 | S/N 799C |
| LH PMV | P/N 7920966-5503 | S/N 416309A |
| RH PMV | P/N 7920966-5503 | S/N 416308A |
| Control Box | P/N 42-089-5 | S/N 256 |
| LH Brake | P/N 9560788 | S/N MAY66-8E |
| RH Brake | P/N 9560788 | S/N NOV66-31 |

REVISIONS

| LTR | DESCRIPTION | DATE | APPROVED |
|-----|-------------|----------|----------|
| A | SEE E.O. | 5-6-77 | K.A.S. |
| B | SEE E.O. | 10-14-77 | K.A.S. |
| | | | |

TEST 0971 MAR 30 1977

McDONNELL DOUGLAS CORPORATION PROPRIETARY RIGHTS ARE INCLUDED IN THE INFORMATION DISCLOSED HEREIN. RECIPIENT BY ACCEPTING THIS DOCUMENT AGREES THAT NEITHER THIS DOCUMENT NOR THE INFORMATION DISCLOSED HEREIN NOR ANY PART THEREOF SHALL BE REPRODUCED OR TRANSFERRED TO OTHER DOCUMENTS OR USED OR DISCLOSED TO OTHERS FOR MANUFACTURING OR FOR ANY OTHER PURPOSE EXCEPT AS SPECIFICALLY AUTHORIZED IN WRITING BY McDONNELL DOUGLAS CORPORATION.

SCHEDULE INFORMATION

DATE

TEST INITIATED

FINAL REPORT SUBMITTAL

DESIGN APPROVAL

DATE

LAB TEST

STRENGTH

PR ENGR

GR ENGR

PREP BY

L.J. McLean

G.W. KIBBEE

R. A. Storley

3/25/77

3-25-77

3-17-77

DOUGLAS AIRCRAFT COMPANY

McDONNELL DOUGLAS

LONG BEACH, CALIFORNIA

TITLE

ANTISKID SIMULATION - RUNWAY DIRECTIONAL
CONTROL SIMULATOR DC-9 SERIES 10

TASK ASSIGNMENT DRAWING

SIZE

A

TAD Z7802765

EWO

S.O.

SHEET 1



TABLE OF CONTENTS AND REVISION LETTER RECORD

| TABLE OF CONTENTS | SHEET NUMBER | LETTER | | | | | | | | | | | |
|--------------------|--------------|--------|---|--|--|--|--|--|--|--|--|--|--|
| TITLE PAGE | 1 | A | B | | | | | | | | | | |
| TABLE OF CONTENTS | 2 | A | B | | | | | | | | | | |
| INTRODUCTION | 3 | | | | | | | | | | | | |
| PURPOSE | 4 | | | | | | | | | | | | |
| REQUIRED EQUIPMENT | 5 | | B | | | | | | | | | | |
| TEST REQUIREMENTS | 6 | | | | | | | | | | | | |
| FIELD WORK ITEMS | 7 | | B | | | | | | | | | | |
| SCHEDULE | 8 | | | | | | | | | | | | |
| FIGURE 1 | 9 | | | | | | | | | | | | |
| FIGURE 2 | 10 | A | | | | | | | | | | | |
| | | | | | | | | | | | | | |
| | | | | | | | | | | | | | |
| | | | | | | | | | | | | | |
| | | | | | | | | | | | | | |
| | | | | | | | | | | | | | |
| | | | | | | | | | | | | | |
| | | | | | | | | | | | | | |
| | | | | | | | | | | | | | |

DOUGLAS

SIZE
A

CODE IDENT NO.
88277

Z7802765

REV LTR

B

SHEET 2.

163

INTRODUCTION

This Task Assignment Drawing details the requirements for an analog/hardware antiskid simulation to be interfaced with the motion-base flight simulator. Actual brake and antiskid system hardware will be used, operating in conjunction with an analog computer.

DOUGLAS
AIRCRAFT COMPANY

TAD

SIZE

A**Z7802765**

EWO

S.O.

SHEET 3

PURPOSE

The purpose of these tests is to extend existing flight simulator capability for the study and solution of aircraft directional control problems on runways. A man-in-loop DC-9 aircraft ground handling simulator will be developed, correlated and then demonstrated to NASA personnel. A realistic simulation would be very useful in evaluating factors which influence aircraft ground handling performance up to and beyond the operational limits of the aircraft without risk to equipment and pilot.

DOUGLAS
AIRCRAFT COMPANY

TAD

SIZE

A**Z 7802765**

165

EWO

S.O.

SHEET 4

REQUIRED EQUIPMENT

1. Hydro-Aire DC-9 Hydraulic Brake System Simulator
2. Hydraulic Power Supply (Skydrol, 3000 psi, 15 GPM min.)
3. Brake Application Servo (two required)
4. Six Strain Gage Power Supplies
5. Six Channel Bridge Balance
6. Six Preston Model 8300 DO Amplifiers
7. Two Comcor Ci-175 Analog Computers
8. DC-9 Transformer/Rectifier
9. Two VCO's (HP 3310A or equivalent)
- *10. Function Generator (HP 3300A), with "Offset" plug-in (HP 3304A)
- *11. Electronic Counter (HP 5512A or equivalent)
- *12. X-Y Plotter
13. Beckman Six Channel Recorder
- *14. Scope
15. Two Pressure Gages (0-5000 psi)
16. Six Pressure Transducers (0-5000 psi)
17. Two Break-out Boards (Z7935344-13 and -15)
18. Connector Cables (Z7935344-17, -19, -21, -23)
19. Six Amplifier Pressure Monitoring Board (No identification) - Available on DC-10 Antiskid Simulator

A general layout of the required equipment is shown in Figure 1.

*Not required full time

DOUGLAS

AIRCRAFT COMPANY

TAD

SIZE

A

Z 7802765

EWO

S.O.

SHEET 5

TEST REQUIREMENTS

The following tests will be conducted:

1. A predemonstration evaluation of the simulator will be made, utilizing a FAA and a Douglas pilot. Corrective action will be taken to resolve any problem areas.
2. The complete simulation will be evaluated by both a FAA and a Douglas pilot. This demonstration program will be designed to qualitatively evaluate:
 - a. The benefits of using the antiskid simulation in conjunction with the aircraft simulator.
 - b. The degree of correlation between the simulator and the pilot's experience and available DC-9 flight test data.

DOUGLAS
AIRCRAFT COMPANY

TAD

SIZE

A**Z 7802765**

167

EWO

S.O.

SHEET 6

F&LD WORK ITEMS

1. Obtain^{*} and install Hydro-Aire DC-9 hydraulic brake system simulator.
2. Install hydraulic piping between hydraulic power supply and brake system simulator.
3. Develop and install brake application system.
4. Install pressure transducers and gages on brake system simulator (see Figure 2).
5. Operate hydraulic system as required.
6. Restore hydraulic brake system simulator to original condition and return to Hydro-Aire upon completion of test.
7. Obtain and install pressure instrumentation (strain gage power supplies, bridge balance, and Preston amplifiers) per drawing # Z7935344 (-501 rack assembly).
8. Fabricate two break-out boards per drawing # Z7935344 (-13 and -15 panel assemblies).
9. Fabricate and install connector cables. Fabricate per drawing # Z7935344-17, -19, -21, -23. Install per drawing # Z7935344.
10. Set up instrumentation rack per drawing # Z7935344 (-503 rack assembly).
11. Set up and maintain two Comcor Ci-175 computers and the Beckman recorder (setup in enclosed platform adjacent to motion-base).
12. Obtain VCO's, function generators, electronic counter, X-Y plotter and scope. Place near Comcor computers.
13. Return all instruments to stockroom at completion of test.

*Write consignment purchase order and provide transportation. Unit will be available from 1 May 1977 until 29 July 1977.

DOUGLAS**AIRCRAFT COMPANY****TAD**

SIZE

A**Z 7802765**

EWO

S.O.

SHEET **7**

SYM

SCHEDULE

Set-up of the Comcor Ci-175 computers is required by 22 April 1977 so that programming can be started. Fabrication and/or installation of all other required equipment is to be complete by 6 May 1977. System integration (with the flight simulator), checkout and demonstration will continue through 29 July 1977.

DOUGLAS**AIRCRAFT COMPANY****TAD**

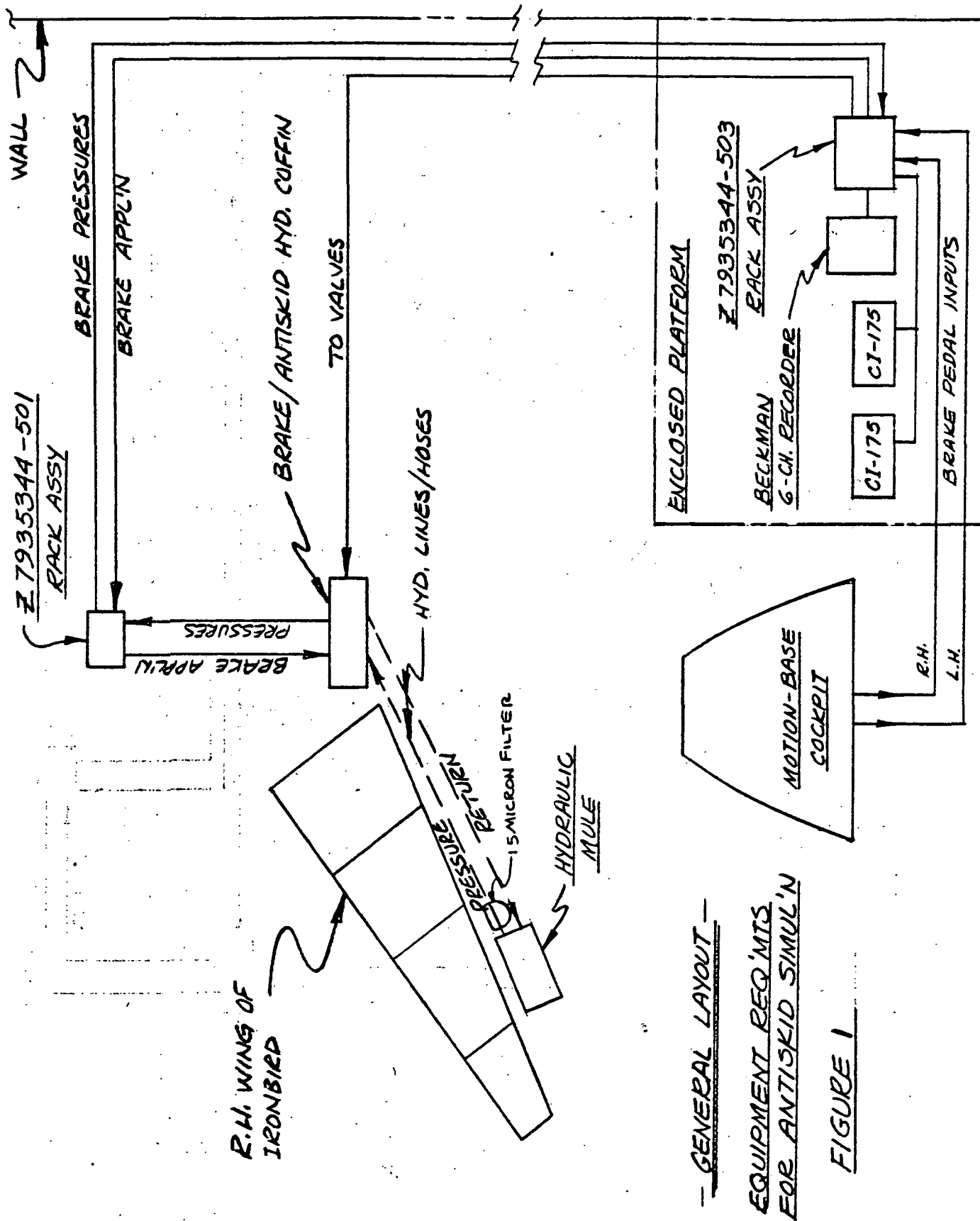
SIZE

A**Z 7802765**

EWO.

S.O.

SHEET 8



DOUGLAS

SIZE

A

CODE IDENT NO.

88277

Z7802765

REV LTR

SHEET 9

SYM A

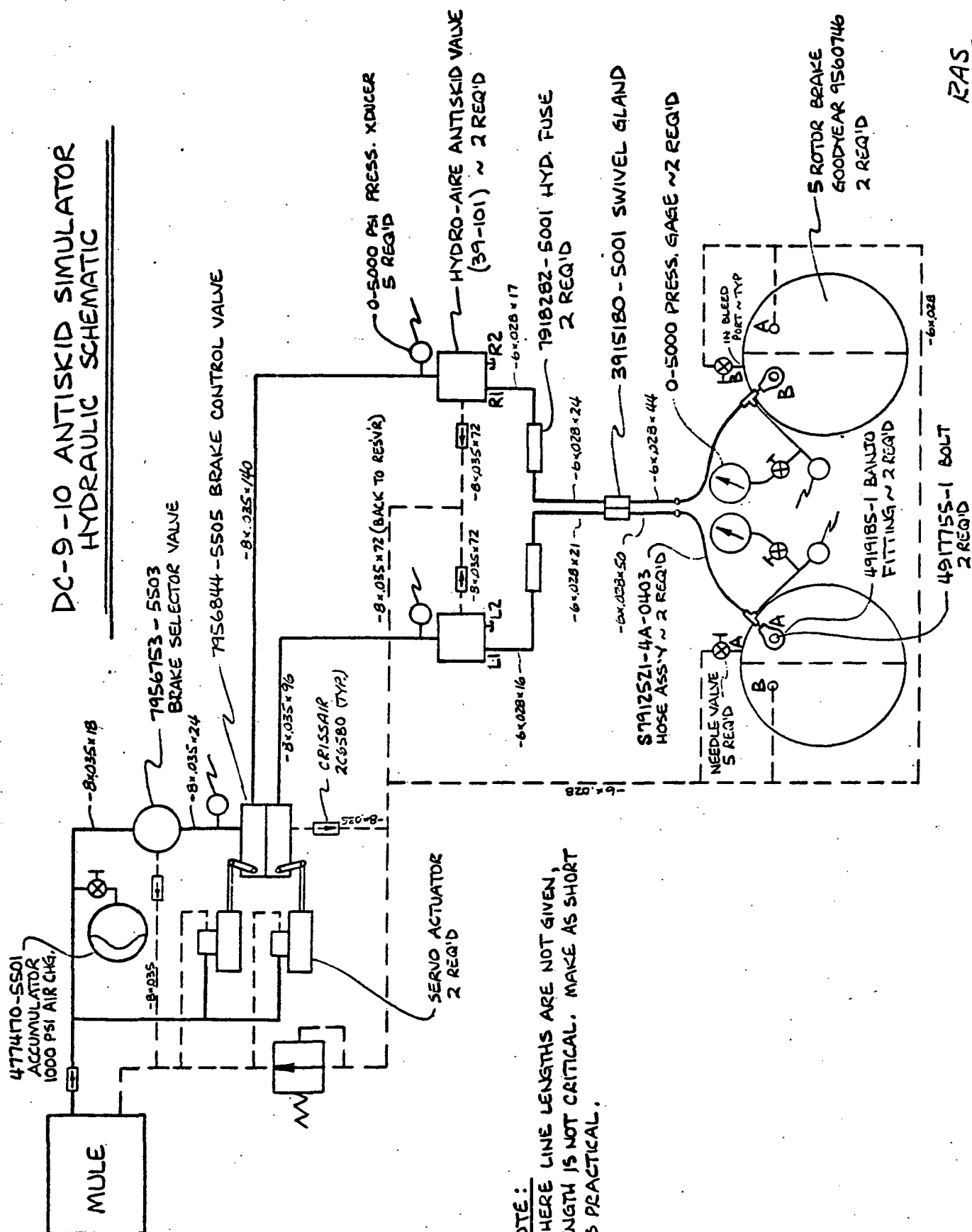
RAS
6-2-76DC-9-10 ANTISKID SIMULATOR
HYDRAULIC SCHEMATIC

FIGURE 2

DOUGLAS
AIRCRAFT COMPANY

TAD

SIZE

A

Z 7802765

EWO

S.O.

SHEET

10

ENGINEERING ORDER

DOUGLAS AIRCRAFT COMPANY
1800 S. MAIN, CALIFORNIA
MCDONNELL DOUGLAS CORPORATION
DOWNSHIFT NO. 00000

DAC 25-1700K (REV. 6-75)

| | | | | | | | | | | | |
|---|----|----|----|----|-------------------|----------------|----------------|-----------------|------------------|---------------------------|---------------|
| RC | MI | NW | AW | FS | OTHER MODEL USAGE | DESIGN SECTION | TYPE RELEASE | | MAJOR SUB MDC | TOTAL NO. PI INPUT SHEETS | |
| | | | | | | | DEVELOPMENT | A | | | |
| | | | | | | | PRODUCTION | B | | | |
| | | | | | | | NON PROD. | C | | | |
| HANDLING INSTRUCTIONS (HI) | | | | | TITLE | | SIZE | | | | |
| 0. INTERCHANGEABILITY OF PARTS NOT TO BE ASSUMED UNLESS SPECIALLY NOTED. | | | | | 1600 | | DRAWING NUMBER | | | | |
| 2. PARTS MUST CONFORM AT NOTED EFFECTIVITY. | | | | | 1402 | | Z7935344 | | | | |
| 3. PARTS MUST CONFORM AT NOTED EFFECTIVITY. PARTS MADE FOR PARTS MADE INCLUDED. | | | | | | | 1 | | | | |
| 4. SCRAP. | | | | | | | 2 | | | | |
| 5. NOTED. | | | | | | | 3 | | | | |
| 6. RETROFIT IDENTIFIED ARTICLES. | | | | | | | 4 | | | | |
| 7. MADE BY 10-11-77 DESIGN APPROVAL BY RA. STORLEY | | | | | | | 5 | | | | |
| 8. DNG MADE CHGO BY SPEC COMPLIANCE | | | | | | | R | | | | |
| EWO | | | | | DOG | WRO | ROUTING CODE | CHS CLASS | SEQ REWORK DNG | DWG REPLACES | DATE |
| SYS | | | | | COE | | | | REPLACES BY | RELEASE STOP ORDER | |
| CHECK EO | | | | | WEIGHTS | PROJ ENGR | CHANGE CONTROL | PRODUCT SUPPORT | PATTERN DIE MOLD | YES | NO |
| CHECK DNG | | | | | STRESS | | | | AFFECTED | YES | NO |
| 1ST FUS AFF | | | | | HI NO | RELEASE CCN | SECTION | MODEL | 12 LTR | CONFIGURATION | REPER ARTICLE |
| | | | | | | | | | | | NEW |
| | | | | | | | | | | | FORMER |
| | | | | | | | | | | | U |
| | | | | | | | | | | | CD |
| | | | | | | | | | | | 1 |
| | | | | | | | | | | | 2 |
| | | | | | | | | | | | 3 |
| | | | | | | | | | | | 4 |
| | | | | | | | | | | | 5 |

FOR RECORD PURPOSES ONLY.

THIS E.O. DOCUMENTS CORRECTIONS MADE TO THE DC-9 ANTISKID SYSTEM SIMULATION WHICH WAS A PART OF THE MOTION-BASE RUNWAY DIRECTIONAL CONTROL SIMULATOR.

SHEET 11 - IDENTIFIED WIRING CONNECTION POINTS ON ELEMENTS 2N2324 & 2N2647.

SHEET 13 - IDENTIFIED RATING ON RESISTORS (BETWEEN BRAKE PEDALS & COCKPIT/LOCAL SWITCH)

SHEET 20 - ADDED WIRING BETWEEN PTS. 33, 36, 37, 38 & 39 ON J1 CONNECTOR & -7 PANEL.

SHEET 30 - ADDED RESISTORS TO B/M (REF. SHEET 13)

| DATE AFF | YES | NO |
|------------------|-----|----|
| SCHEMATICS AFF | | |
| FINISH SPEC AFF | | |
| DANS & DRAWS AFF | | |
| VENTILATION AFF | | |
| SEALING AFF | | |
| ELEC BORDING AFF | | |
| LUBRICATION AFF | | |

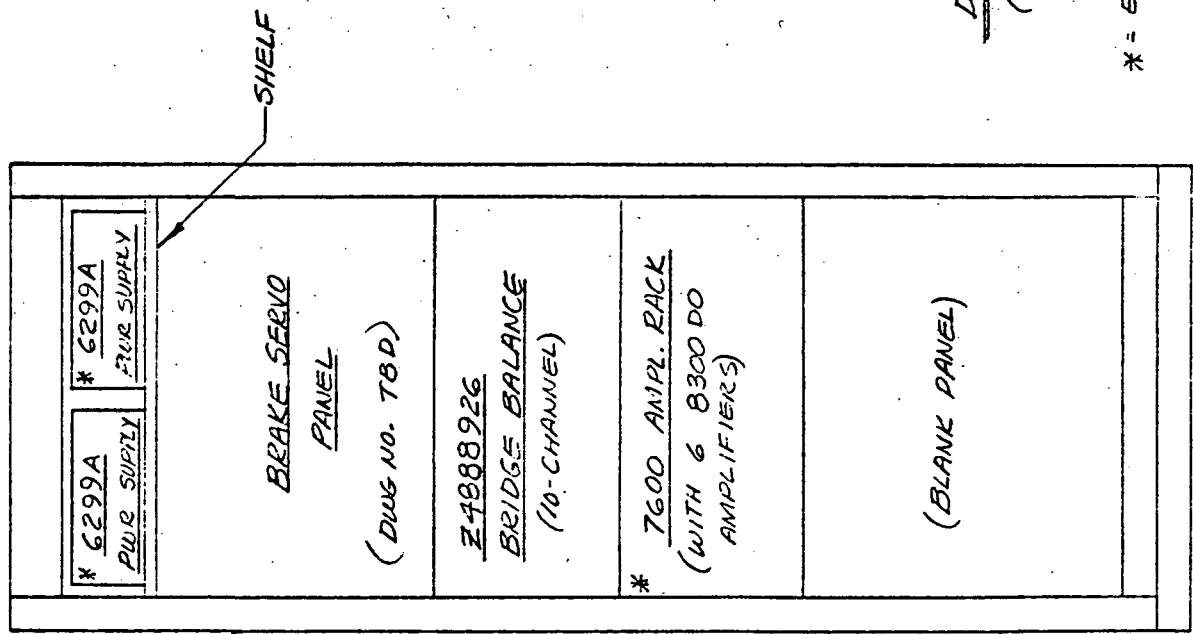
| | | |
|--|----------|----|
| PRINT DISTRIBUTION | Yes | No |
| DEVELOPMENT | | |
| Orig at | | |
| Dup at | | |
| SUPPLIER RELEASE WITH DDC PLANNING ACTION REQUIRED | | |
| DRAWING NUMBER | Z7935344 | |

ENGINEERING ORDER

DAC 25-17098 (6-71)

DOUGLAS AIRCRAFT COMPANY
1800 ROCK BLVD
BECOMMELL DOUGLAS
STANDARD NO. 26279

| 2 | | Z7935344 | |
|-------|------|---------------------|----------------|
| SHEET | | SIZE | DRAWING NUMBER |
| 1 | DATE | DRAWING CHANGED | |
| 2 | DATE | ADVANCE DWG CHG | |
| 3 | DATE | SERIAL EQ | |
| 4 | DATE | NEW/REVISED RELEASE | NEW |
| 5 | DATE | REISSUE TO REVISE | R |



DETAIL -501 RACK ASSY
(SEE CABLE DIAGRAM, SHEET 3)

* = EXISTING EQUIP.

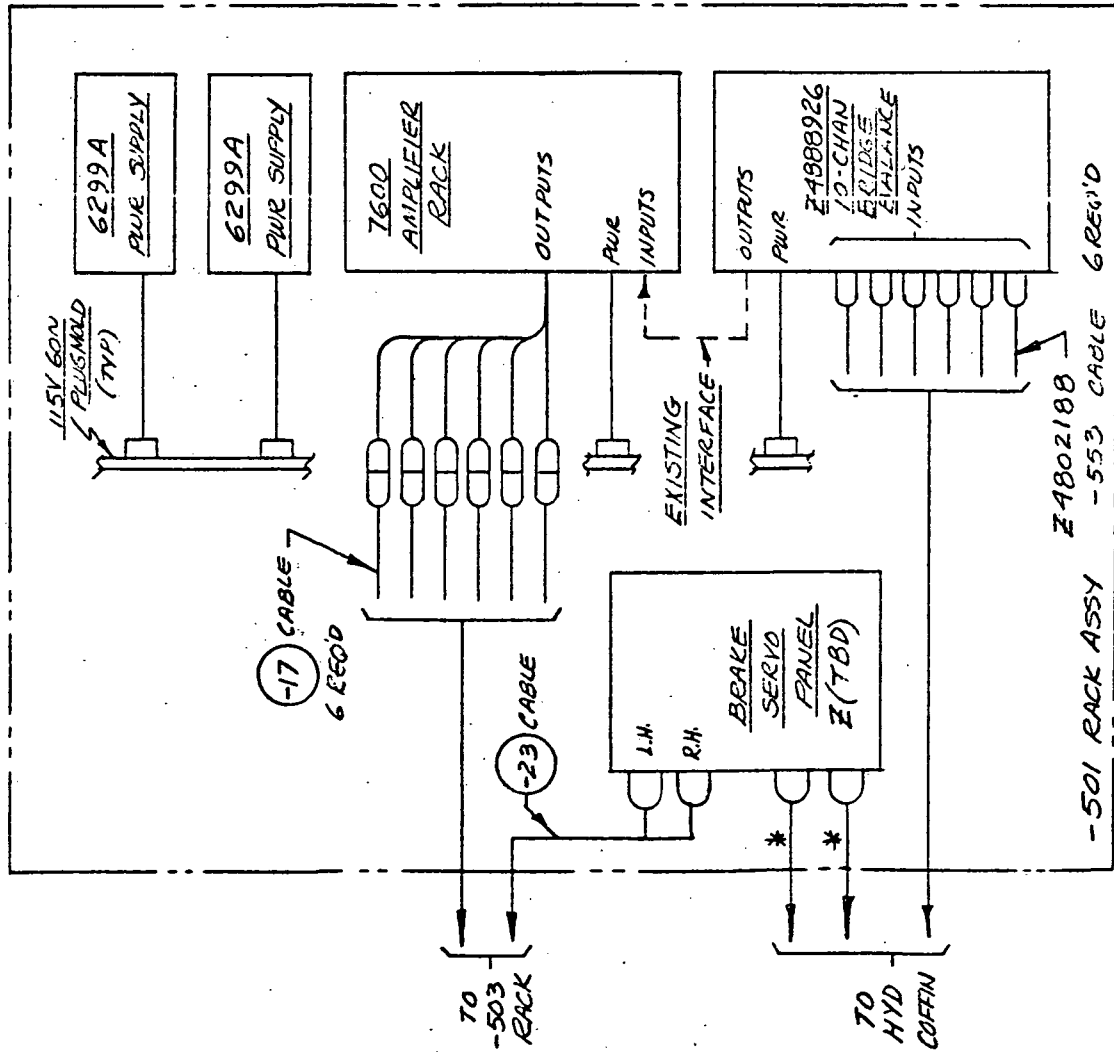
ENGINEERING ORDER

DAC 25-17089 (8-71)

DOUGLAS AIRCRAFT COMPANY
1400 SOUTH CALIFORNIA
MCDONNELL DOUGLAS
FORM ORBIT NO. 0817

| SHEET | 3 | SIZE | DRAWING NUMBER |
|-------|---|---------------------|----------------|
| DATE | 1 | DRAWING CHANGED | |
| DATE | 2 | ADVANCE DWG CHG | |
| DATE | 3 | SERIAL EO | |
| DATE | 4 | NEW/REVISED RELEASE | NEW |
| DATE | 5 | REISSUE TO REVISE | R |

Z 7935344



DETAIL -501 RACK ASSY

* THESE CABLES TO BE PART OF E (TBD) DWG.
CONTACT R. ECKWEILER X 39788 FOR FURTHER INFO.

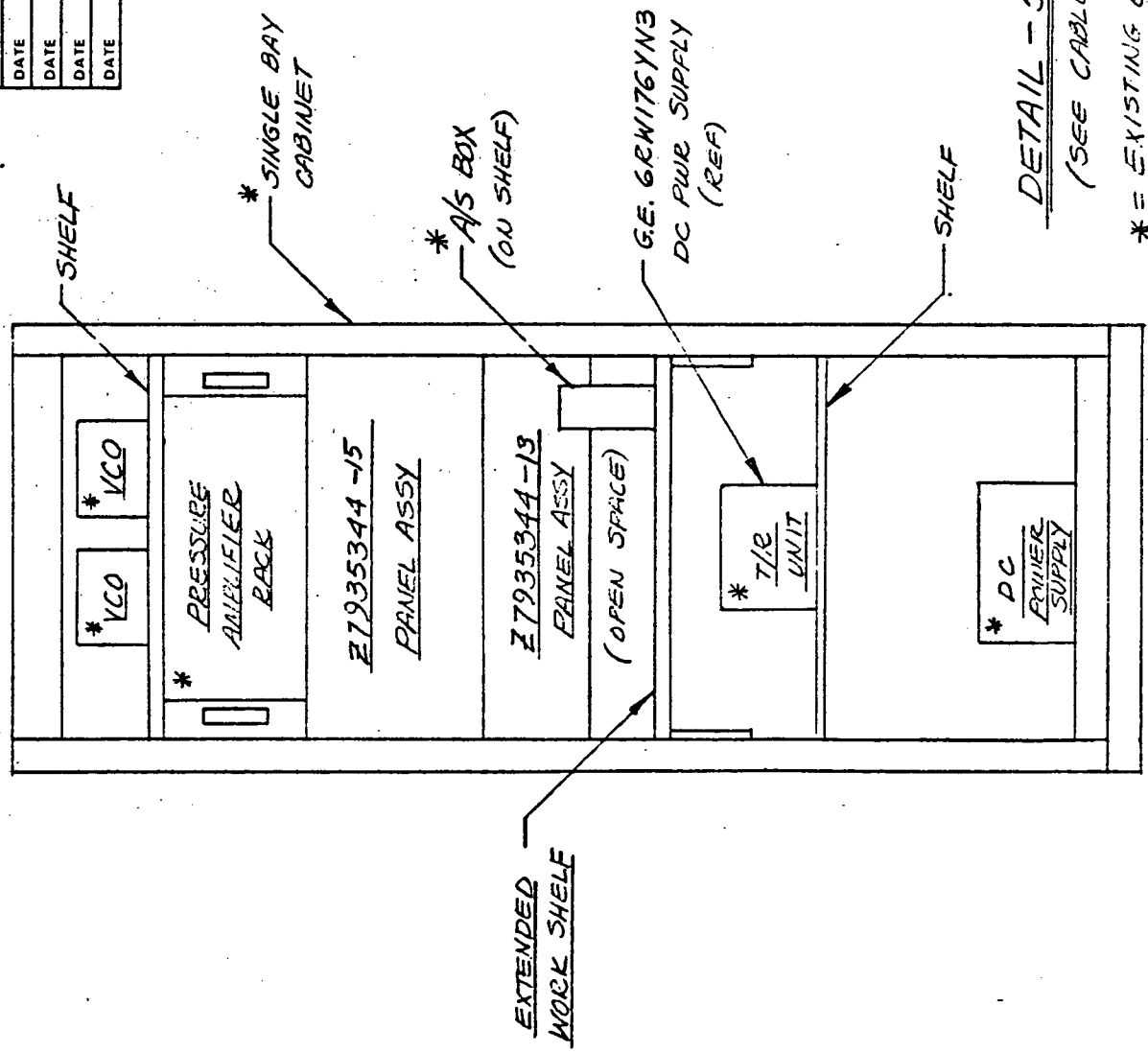
DWG NO. Z 7935344

ENGINEERING ORDER

DAC 25-17098 (8-71)

DOUGLAS AIRCRAFT COMPANY
 LONG BEACH, CALIFORNIA
 HUGHES AIRCRAFT COMPANY
 BOSTON, MASSACHUSETTS
 READ INSTRUCTIONS

| DATE | SHEET | SIZE | DRAWING NUMBER |
|------|-------|---------------------|----------------|
| | 4 | | Z7935344 |
| DATE | 1 | DRAWING CHANGED | |
| DATE | 2 | ADVANCE DWG CHG | |
| DATE | 3 | SERIAL EO | |
| DATE | 4 | NEW/REVISED RELEASE | NEW |
| DATE | 5 | REISSUE TO REVISE | R |



DETAIL - 503 RACK ASSY
 (SEE CABLE DIAGRAM, SHEET 5)

* = EXISTING EQUIP.
 DWG NO. Z7935344

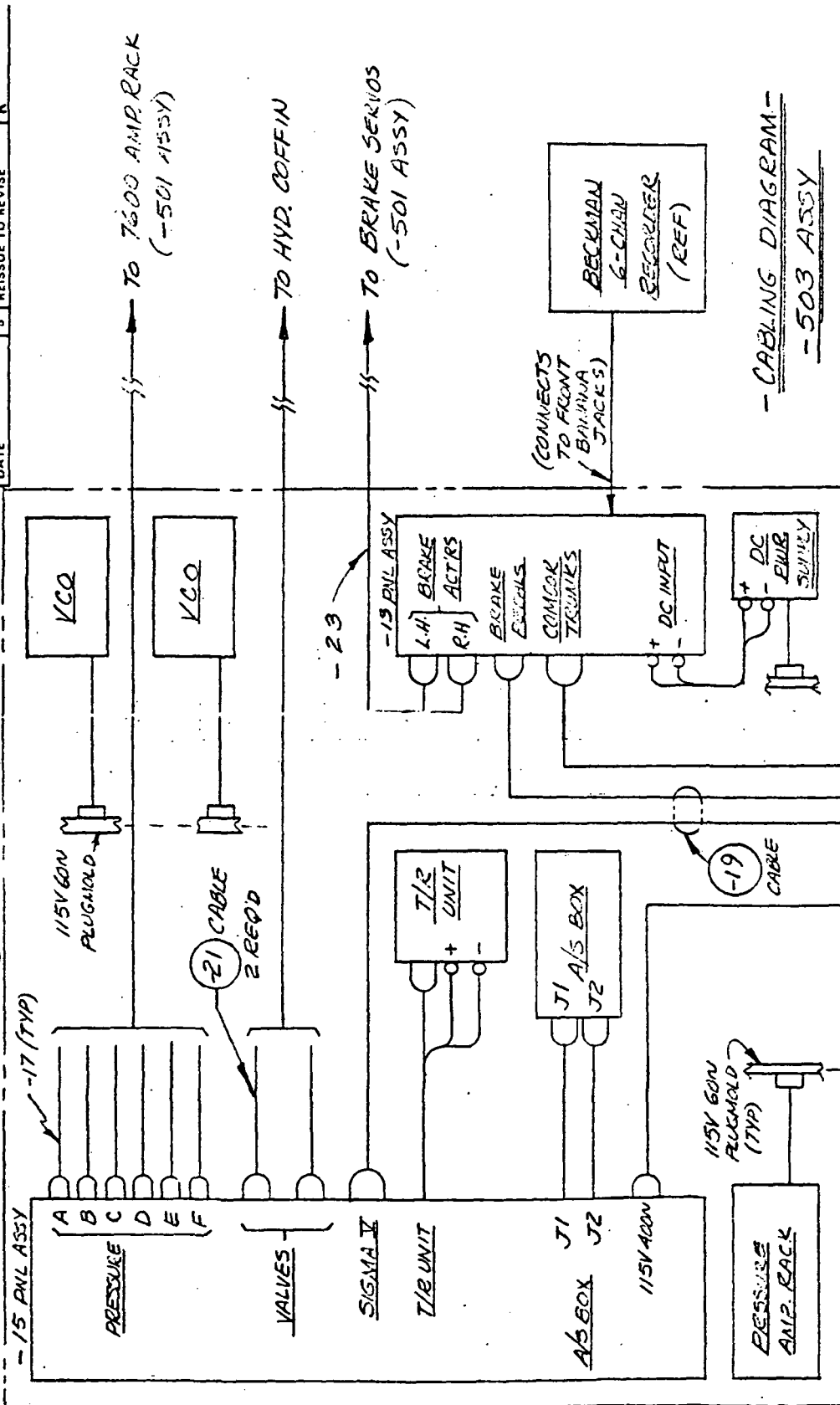
ENGINEERING ORDER

DAC 35-17098 (8-71)

DOUGLAS AIRCRAFT COMPANY
4400 SANTA MONICA
BENTONVILLE, ARKANSAS
FORM NO. 10-577

| SHEET | 5 | SIZE | DRAWING NUMBER |
|-------|---------------------|------|----------------|
| 1 | DRAWING CHANGED | | |
| 2 | ADVANCE DWG CHG | | |
| 3 | SERIAL EO | | |
| 4 | NEW/REVISED RELEASE | | NEW |
| 5 | REISSUE TO REVISE | | R |

-503 RACK ASSY



-CABLING DIAGRAM-
-503 ASSY

DWG NO. Z7935344

ENGINEERING ORDER

DAC 25-17098 (8-71)

DOUGLAS AIRCRAFT COMPANY
LONG BEACH, CALIFORNIA
MCDONNELL DOUGLAS
CORPORATION
GRAPHIC UNIT NO. 60277

6

SHEET SIZE DRAWING NUMBER

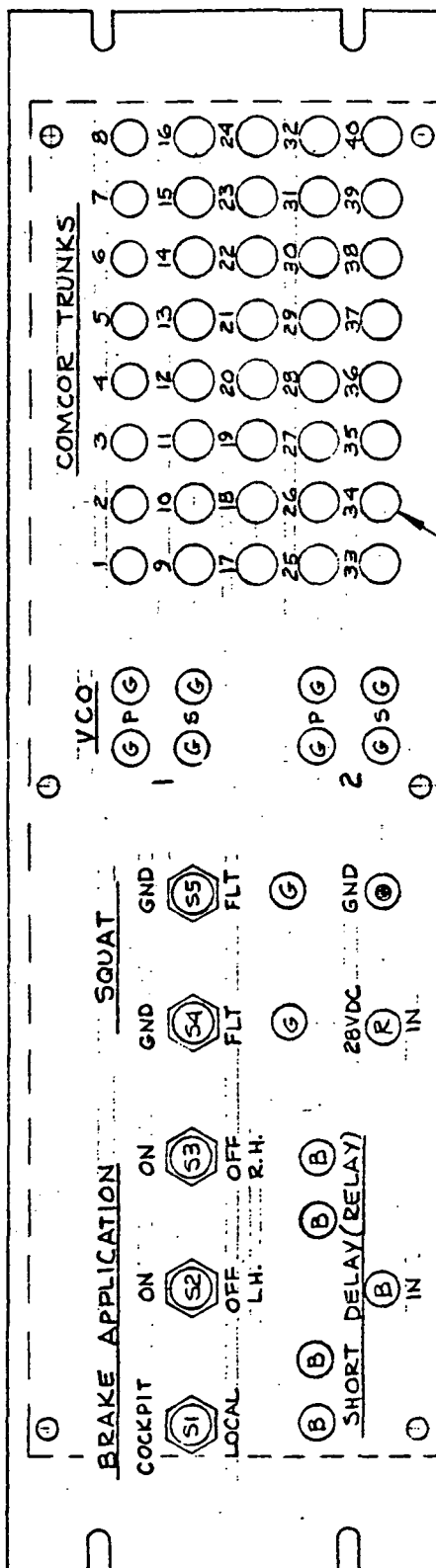
Z7935344

| DATE | 1 | DRAWING CHANGED |
|------|---|---------------------|
| DATE | 2 | ADVANCE DWG CHG |
| DATE | 3 | SERIAL ED |
| DATE | 4 | NEW/REVISED RELEASE |
| DATE | 5 | REISSUE TO REVISE |

NOTES: 1. SEE PARTS LIST FOR TABULATION OF PART NO.'S VS. LOCATION.

2. APPLY APPROPRIATE SIZE BLACK DRY-TRANSFER LETTERS & FIGURES APPROX AS SHOWN. OVERSPRAY WITH CLEAR ACRYLIC LACQUER.

⊙ = GREEN ⊙ = BLACK ⊙ = RED ⊙ = BLUE ⊙ = BROWN



NO. 1498 BANANA JACK 57 REQ'D
(SEE COLOR CODE ABOVE)

DETAIL - LETTERING & PARTS LOCATION (FRONT)

-13 PANEL ASSY

DWD
NO.

Z7935344

ENGINEERING ORDER

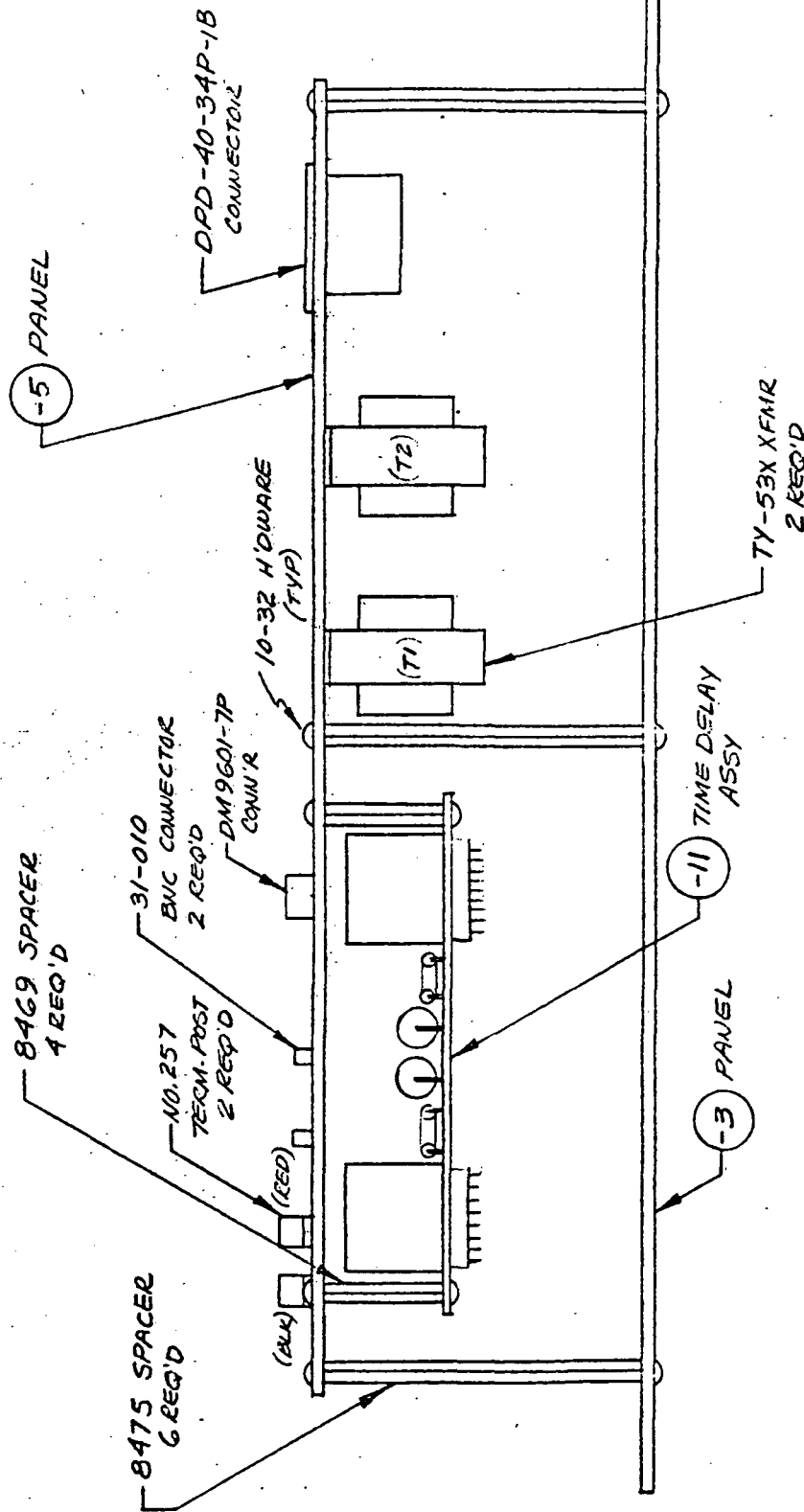
DAC 25-17098 (8-71)

DOUGLAS AIRCRAFT COMPANY
1800 MAIN CALIFORNIA
RECONSTRUCTION DOUGLAS
COMPANY

7 7935344

| DATE | 1 | DRAWING CHANGED |
|------|---|---------------------|
| DATE | 2 | ADVANCE DWG CHG |
| DATE | 3 | SERIAL EO |
| DATE | 4 | NEW/REVISED RELEASE |
| DATE | 5 | REISSUE TO REVISE |

NOTE: WIRE PER SHEETS 12 & 13.



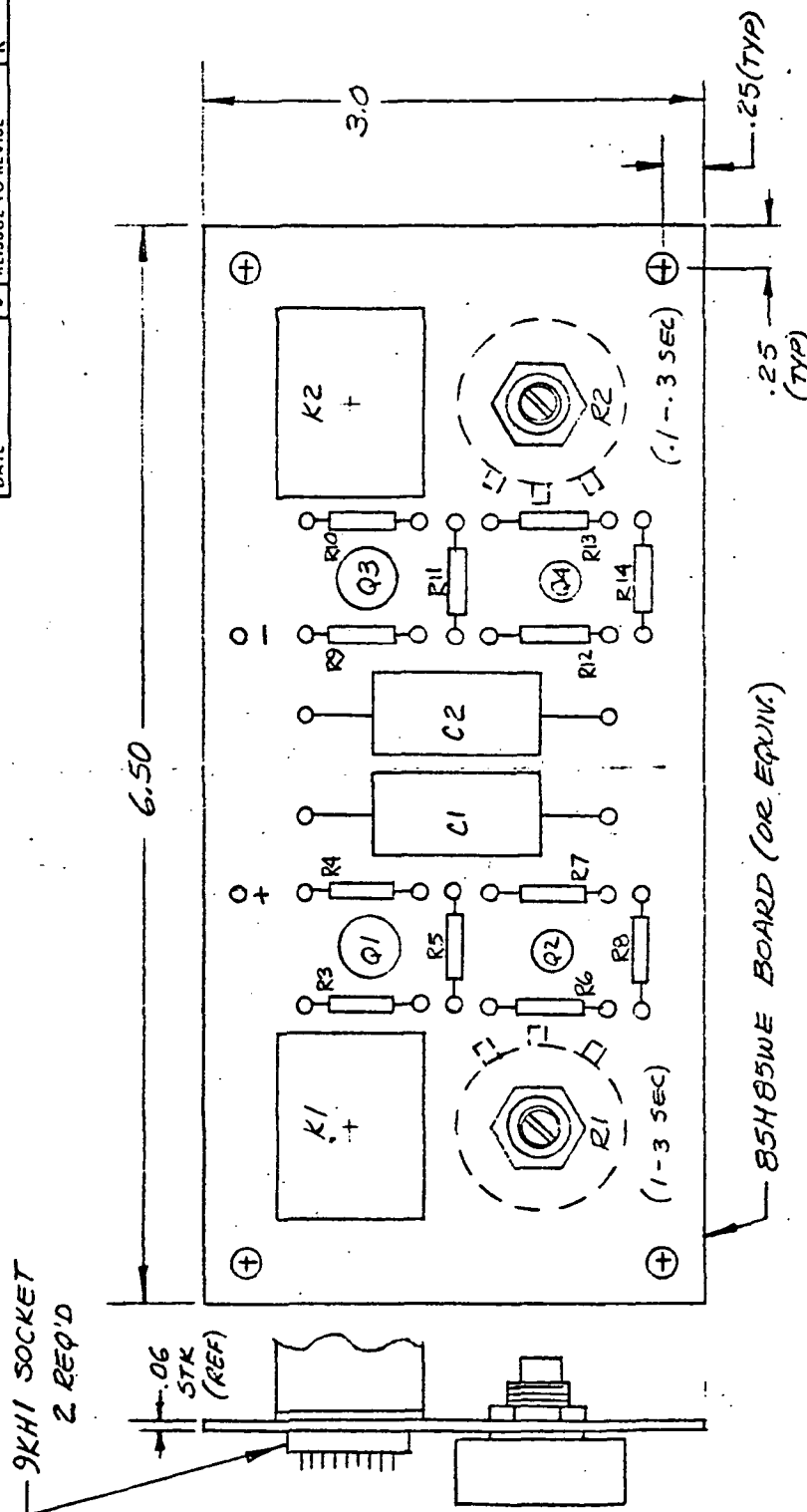
ASSY DETAIL -13 PANEL (TOP VIEW)

DWG NO. 7935344

Z7935344

DRAWING NUMBER

| | | |
|------|---|---------------------|
| DATE | 1 | DRAWING CHANGED |
| DATE | 2 | ADVANCE DWG CHG |
| DATE | 3 | SERIAL ED |
| DATE | 4 | NEW/REVISED RELEASE |
| DATE | 5 | REISSUE TO REVISE |



DETAIL - II TIME DELAY ASSY

- NOTES:
1. LOCATE COMPONENTS APPROX. AS SHOWN; USE TERMINALS TO MOUNT CAP'S & RESISTORS.
 2. IDENTIFY EACH COMPONENT FOR REFERENCE.
 3. WIRE PER SHEET 11.
 4. SEE PARTS LIST FOR PART NO.'S. NOT SHOWN.

DWG NO. E7935344

DOUGLAS AIRCRAFT COMPANY
LONG BEACH, CALIFORNIA
MCDONNELL DOUGLAS
2000 WIGHT RD. 90777
DOUGLASHILL 10

2000 JULY NO. 00077

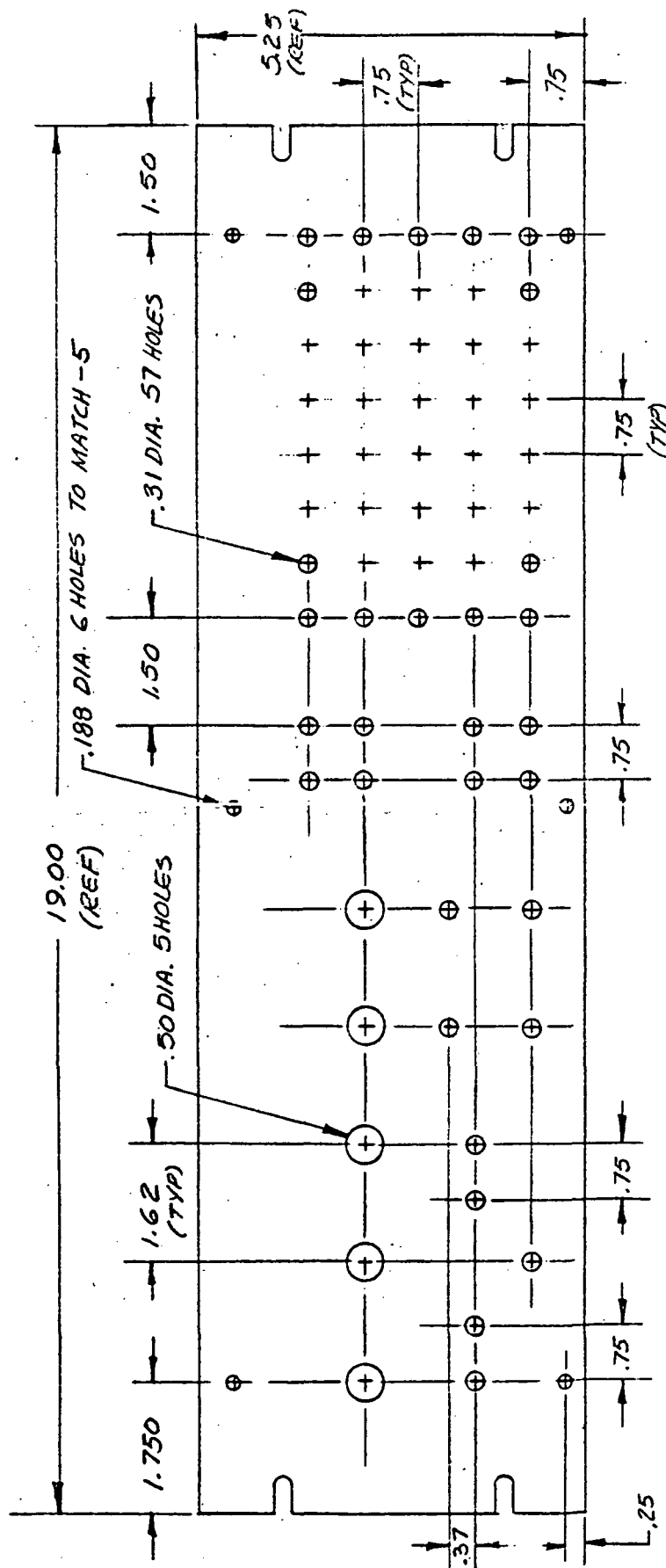
| | | | |
|------|---|---------------------|-----|
| DATE | 2 | ADVANCE DWG CHG | |
| DATE | 3 | SERIAL EO | |
| DATE | 4 | NEW/REVISED RELEASE | NEW |
| DATE | 5 | REISSUE TO REVISE | R |

Z 7935344

9

SIZE DRAWING NUMBER

| | | |
|------|---|---------------------|
| DATE | 1 | DRAWING CHANGED |
| DATE | 2 | ADVANCE DWG CHG |
| DATE | 3 | SERIAL E.O |
| DATE | 4 | NEW-REVISED RELEASE |
| DATE | 5 | REISSUE TO REVISE |



DETAIL - 3 PANEL

DWG
NO. Z 7935344

ENGINEERING ORDER

DAC 28-17088 (8-71)

DOUGLAS AIRCRAFT COMPANY
1800 AVENUE OF THE STARS
WASHINGTON, D.C. 20045

10

SHEET

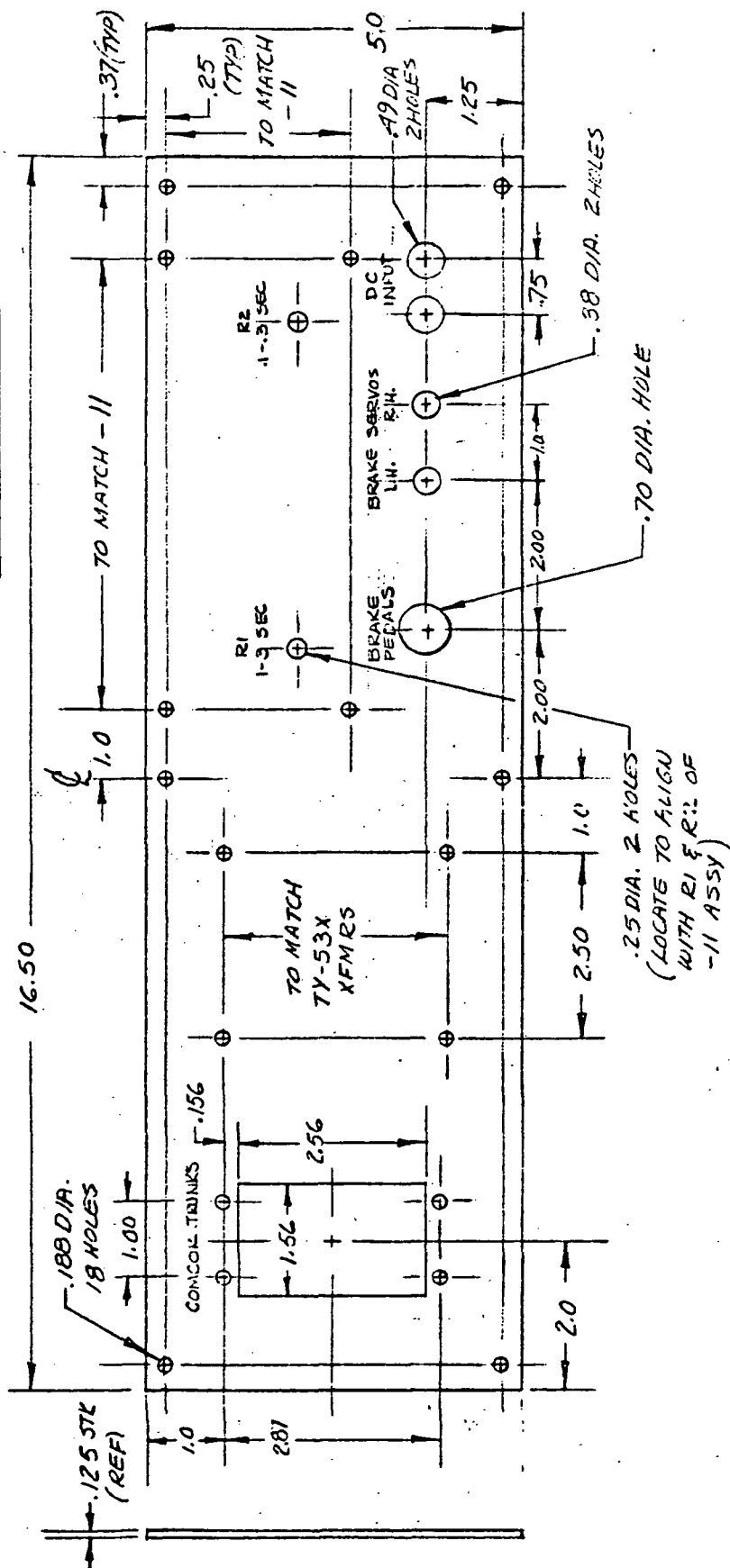
SIZE

DRAWING NUMBER

Z 7935344

| DATE | 1 | DRAWING CHANGED |
|------|---|---------------------|
| DATE | 2 | ADVANCE DWG CHG |
| DATE | 3 | SERIAL EO |
| DATE | 4 | NEW-REVISED RELEASE |
| DATE | 5 | REISSUE TO REVISE |

NOTES: 1. APPLY BLACK DRY-TRANSFER LETTERING APPROX.
AS SHOWN; OVERSPRAY WITH CLEAR ACRYLIC LACQUER.



DETAIL - 5 PANEL
(MATERIAL: 6061-T6 ALUM.)

DWG NO. Z 7935344

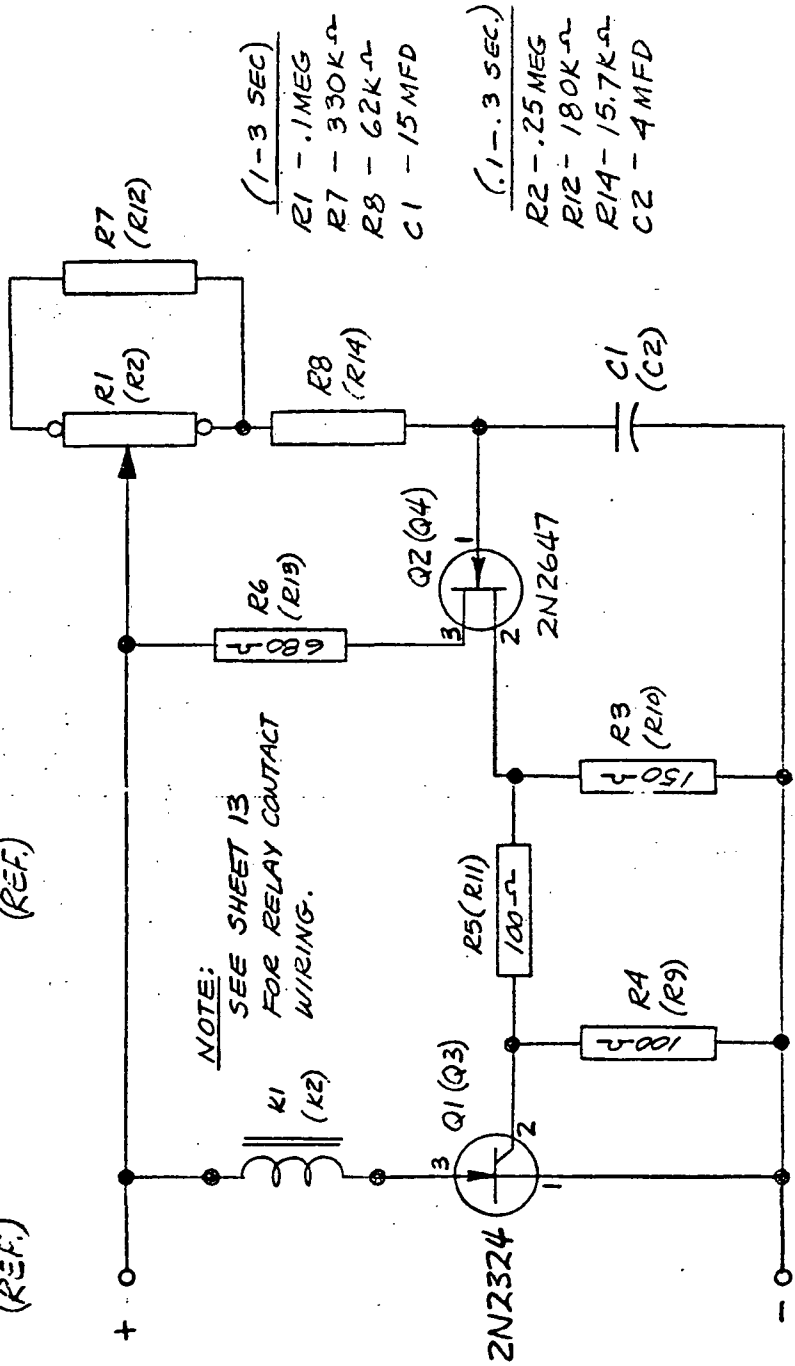
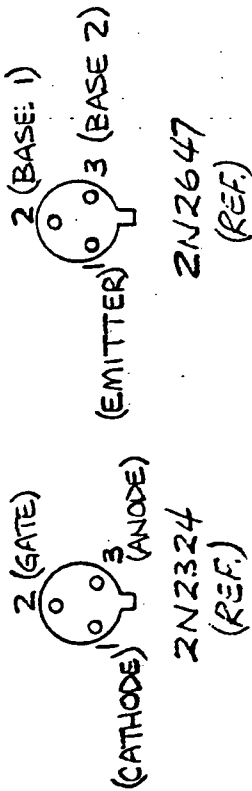
ENGINEERING ORDER

DAC 25-17088 (8-71)

DOUGLAS AIRCRAFT COMPANY
NEW BARK, CALIFORNIA
MCDONNELL DOUGLAS
FORM 100-100-100

11 Z 7935344

| DATE | SHEET | SIZE | DRAWING NUMBER |
|------|-------|---------------------|----------------|
| DATE | 1 | DRAWING CHANGED | |
| DATE | 2 | ADVANCE DWG CHG | |
| DATE | 3 | SERIAL EO | |
| DATE | 4 | NEW/REVISED RELEASE | NEIU |
| DATE | 5 | REISSUE TO REVISE | R |



WIRING DIAGRAM - 11 TIME DELAY ASSY

DWG NO. Z 7935344

ENGINEERING ORDER

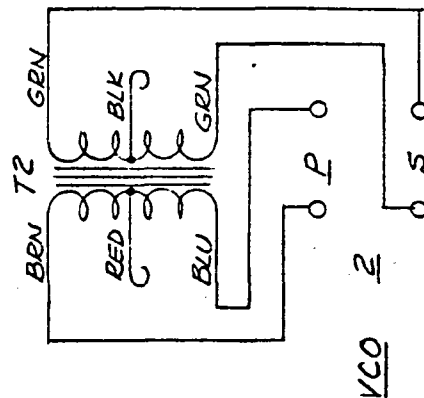
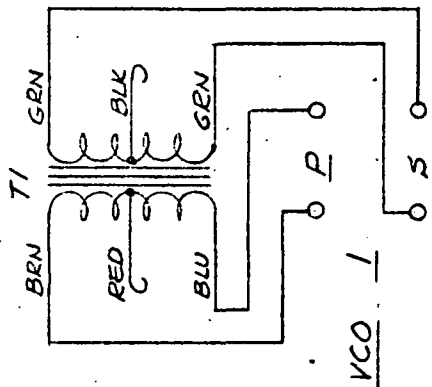
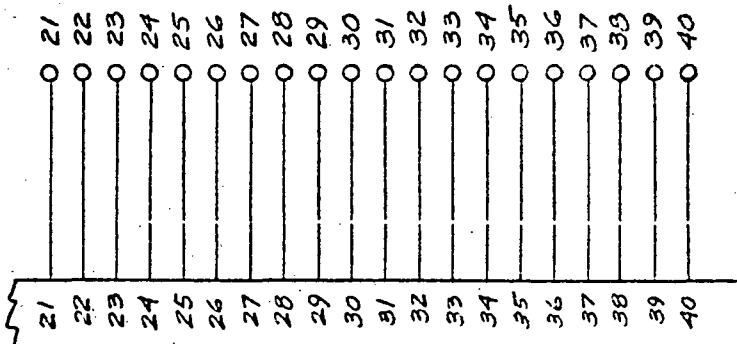
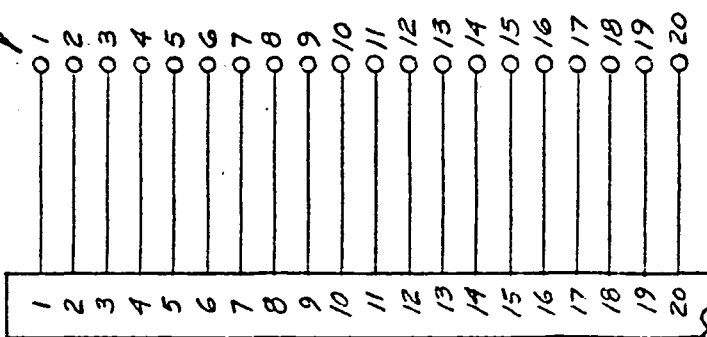
DAC 28-17008 (8-71)

DOUGLAS AIRCRAFT COMPANY
1400 WEST ALHAMBRA
MCDONNELL DOUGLAS
ENGINEERING DEPT. 4007

12 Z7935344

| SHEET | SIZE | DRAWING NUMBER |
|-------|---------------------|----------------|
| 1 | DRAWING CHANGED | |
| 2 | ADVANCE DWG CHG | |
| 3 | SERIAL EO | |
| 4 | NEW/REVISED RELEASE | NEW |
| 5 | REISSUE TO REVISE | R |

"COMCOR TRUNKS"



WIRING DIAGRAM - 13 PANEL ASSY

(CONT'D ON SHEET 13)

DWG NO. Z7935344

ENGINEERING ORDER

DAC 25-17098 (8-71)

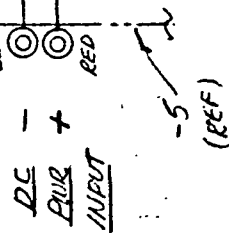
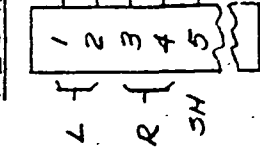
DOUGLAS AIRCRAFT COMPANY
1800 MAIN AVENUE
MCKINNEY, TEXAS 75069
FORM NO. 10-10-10

13 SHEET SIZE

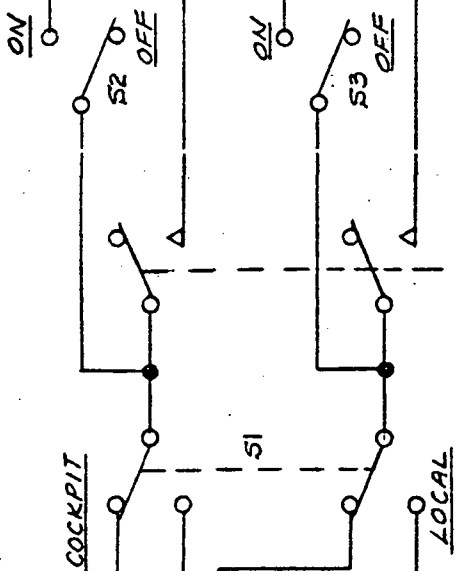
DRAWING NUMBER

| DATE | 1 | DRAWING CHANGED |
|------|---|---------------------|
| DATE | 2 | ADVANCE DWG CHG |
| DATE | 3 | SERIAL EO |
| DATE | 4 | NEW/REVISED RELEASE |
| DATE | 5 | REISSUE TO REVISE |

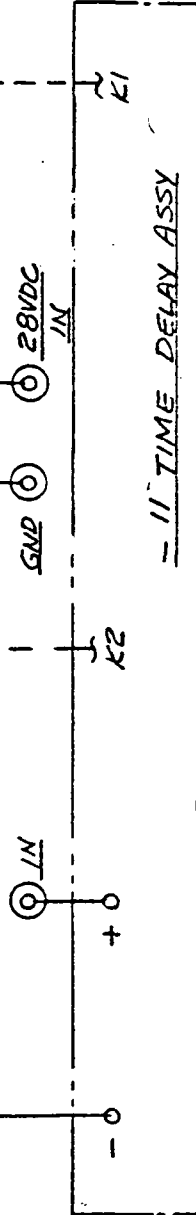
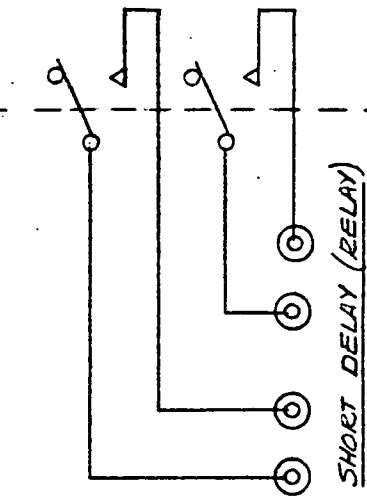
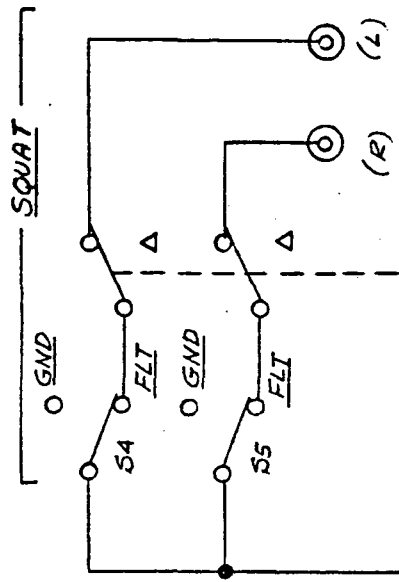
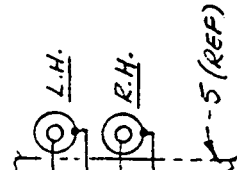
BRAKE PEDALS



BRAKE APPLICATION



BRAKE ACTUATORS



DWG NO. Z 7935344

WIRING DIAGRAM - 13 PANEL ASSY (CONT'D)

ENGINEERING ORDER

DAC 25-17098 (6-71)

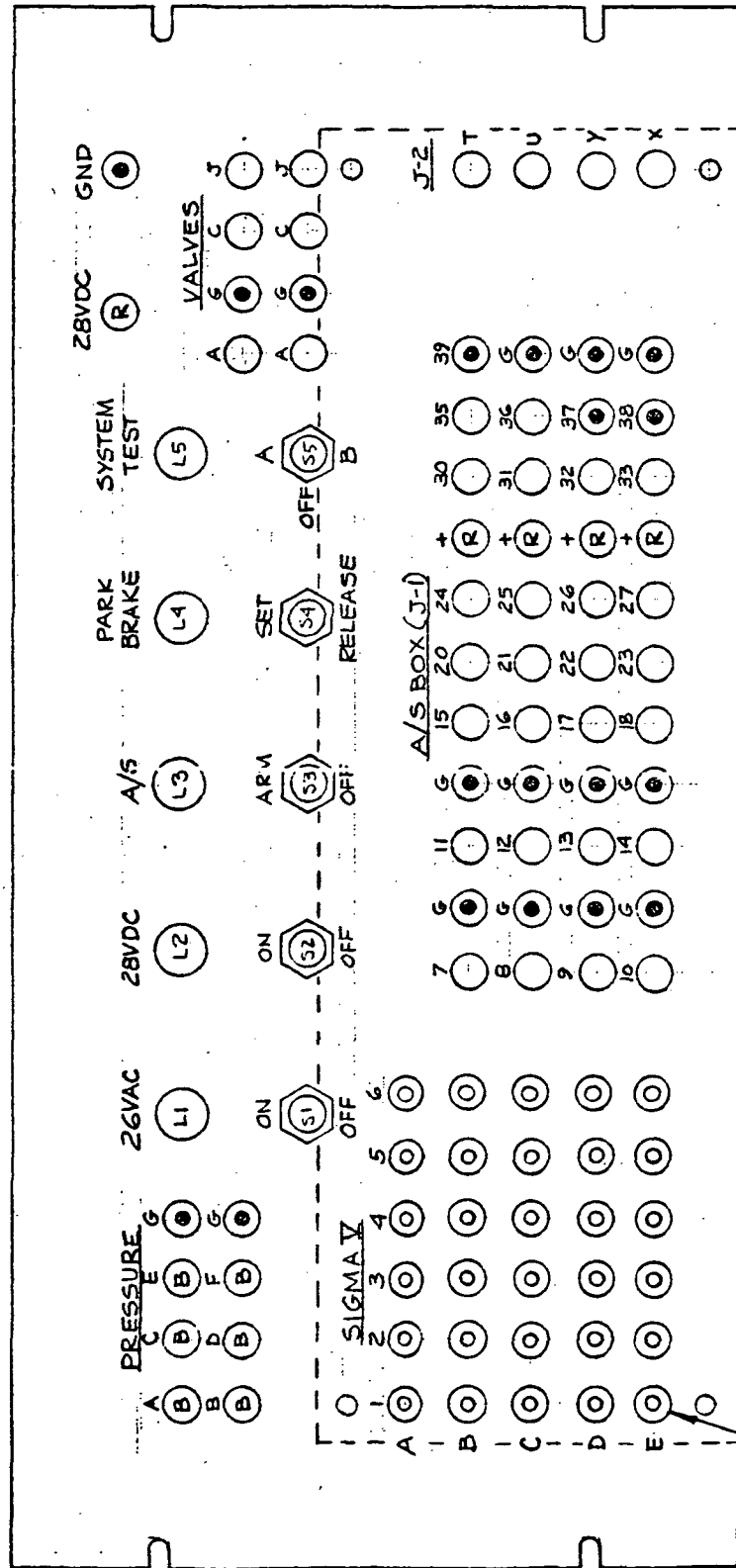
DOUGLAS AIRCRAFT COMPANY
1000 MAIN BUILDING
MCDONNELL DOUGLAS
ST. LOUIS, MO. 63117

14 Z 7935344

| SHEET | SIZE | DRAWING NUMBER |
|-------|---------------------|----------------|
| 1 | DRAWING CHANGED | |
| 2 | ADVANCE DWG CHG | |
| 3 | SERIAL EO | |
| 4 | NEW/REVISED RELEASE | NEW |
| 5 | REISSUE TO REVISE | R |

- NOTES: 1. SEE PARTS LIST FOR TABULATION OF PART NUMBERS VS. LOCATION.
2. APPLY APPROPRIATE SIZE BLACK DRY-TRANSFER LETTERS & FIGURES APPROX. AS SHOWN. OVERSPRAY WITH CLEAR ACRYLIC LACQUER.

3. ○ = GREEN ○ = YELLOW ○ = BLACK ○ = RED ○ = BLUE



NO. 1498 BANANA JACK 91 REQ'D (SEE NOTE 3 FOR COLOR)

DETAIL - LETTERING & PARTS LOCATION (FRONT)

-15 PANEL ASSY

DWG NO. Z 7935344

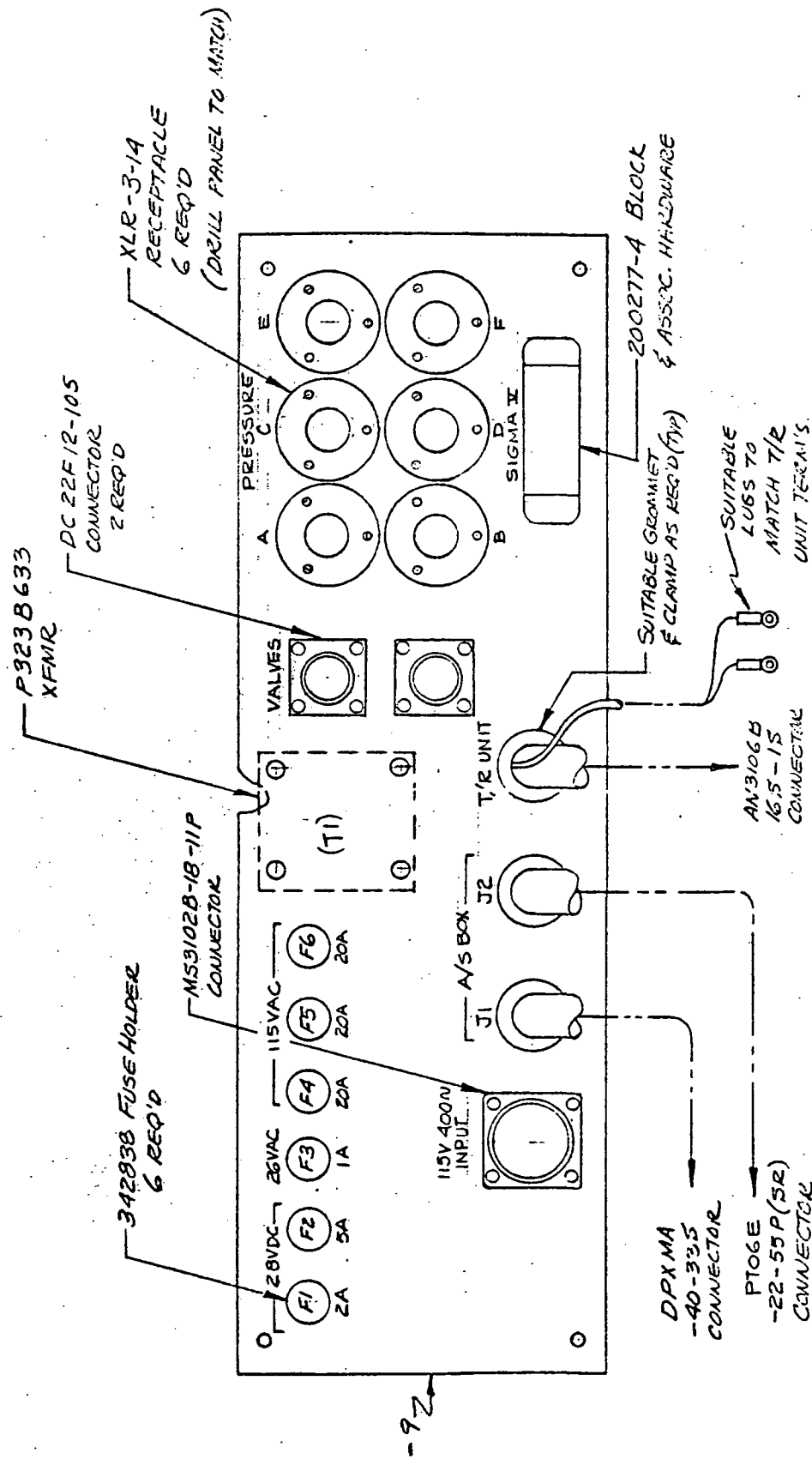
ENGINEERING ORDER

DAC 25-17088 (6-71)

DOUGLAS AIRCRAFT COMPANY
 LONG BEACH, CALIFORNIA
 MC DONNELL DOUGLAS
 2000 WEST 98th STREET
 TORRANCE, CALIFORNIA

15 Z 7935344

| SHEET | SIZE | DRAWING NUMBER |
|-------|---------------------|----------------|
| 1 | DRAWING CHANGED | |
| 2 | ADVANCE DWG CHG | |
| 3 | SERIAL EO | |
| 4 | NEW/REVISED RELEASE | NEW |
| 5 | REISSUE TO REVISE | R |

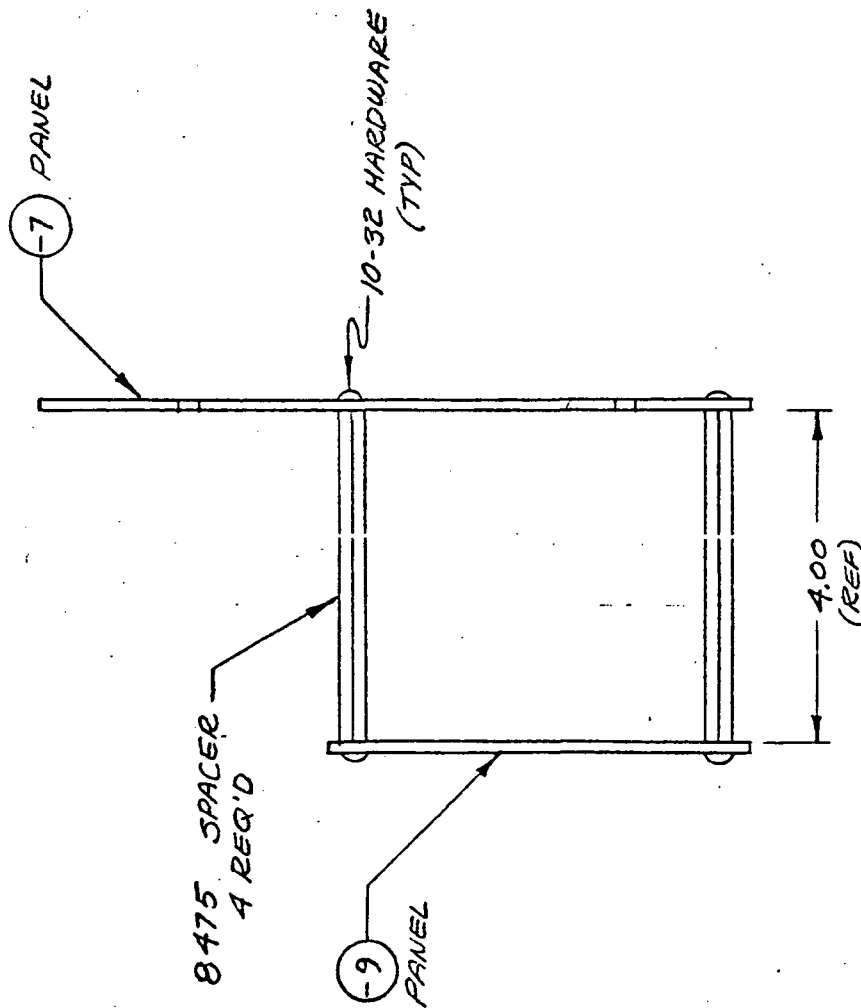


ENGINEERING ORDER

DAC 28-17098 (6-71)

DOUGLAS AIRCRAFT COMPANY
 1400 MARK BANGS
 MC DONNELL DOUGLAS
 GRAND AVENUE, ST. LOUIS, MISSOURI 63117

| | | | |
|----|-------|---------------------|----------------|
| 16 | SHEET | SIZE | DRAWING NUMBER |
| | 1 | DRAWING CHANGED | |
| | 2 | ADVANCE DWG CHG | |
| | 3 | SERIAL EO | |
| | 4 | NEW/REVISED RELEASE | NEED |
| | 5 | REISSUE TO REVISE | R |



DETAIL - REAR CONNECTOR PANEL MTG (SIDE VIEW)

-15 PANEL ASSY

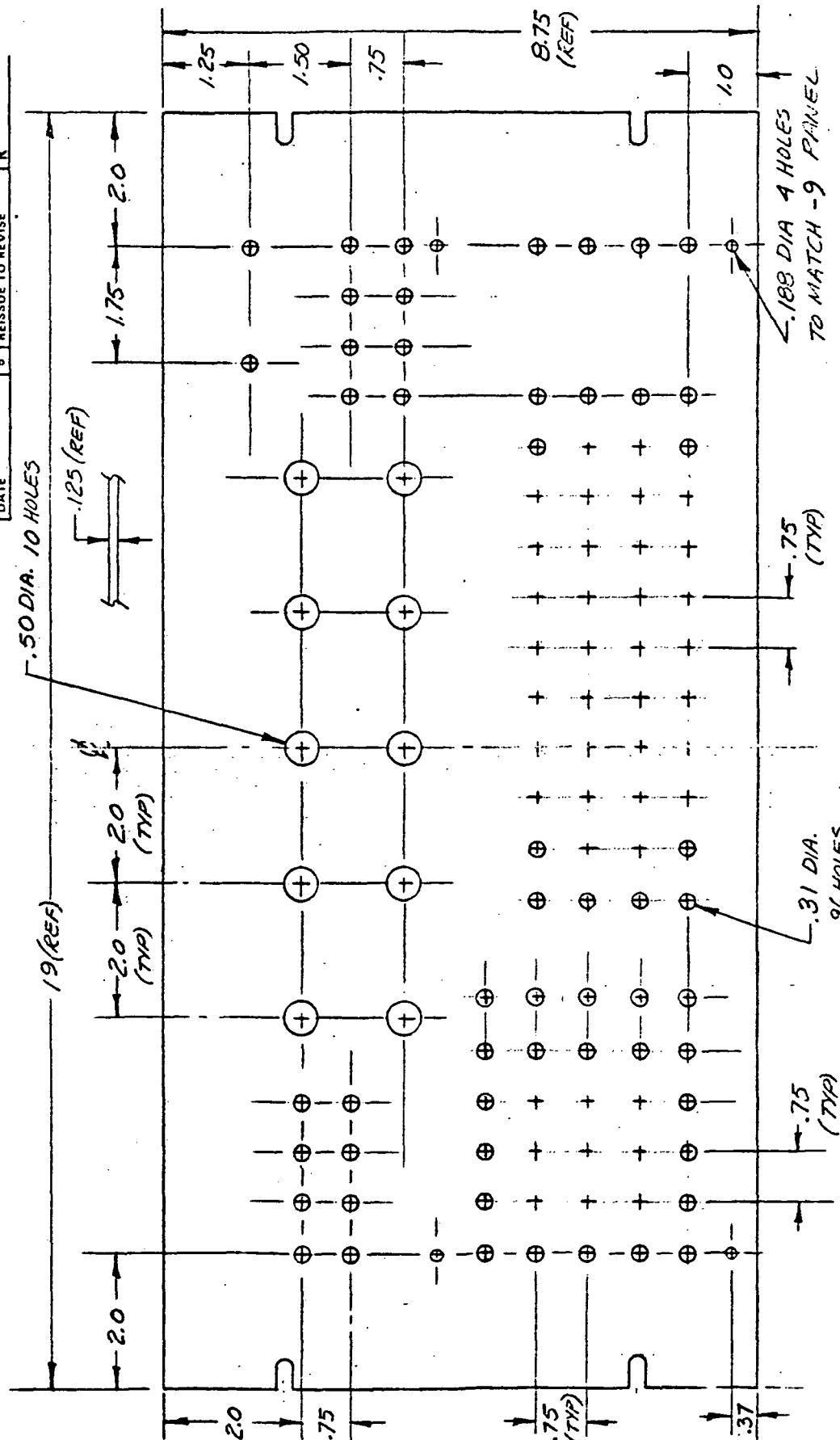
DWG NO. Z7935344

DOUGLAS AIRCRAFT COMPANY
1000 SANTA ANITA AVENUE
MCDONNELLA DOUGLAS
DOUGLAS FIELD NO. 2577
DOUGLAS FIELD

FOCUS GROUP NO. 050973

NOTES: 1. - 7 PANEL TO BE PAINTED LIGHT BEIGE ENAMEL. (BINGHAM BEIGE)

| | | | |
|----|-------|----------------|---------------------|
| 17 | SHEET | Z7935344 | |
| | SIZE | DRAWING NUMBER | |
| | DATE | 1 | DRAWING CHANGED |
| | DATE | 2 | ADVANCE DWG CHG |
| | DATE | 3 | SERIAL EO |
| | DATE | 4 | NEW/REVISED RELEASE |
| | DATE | 5 | REISSUE TO REVISE |
| | | | NEW |
| | | | R |



DETAIL - 7 PANEL

DWG
NO. E7935344

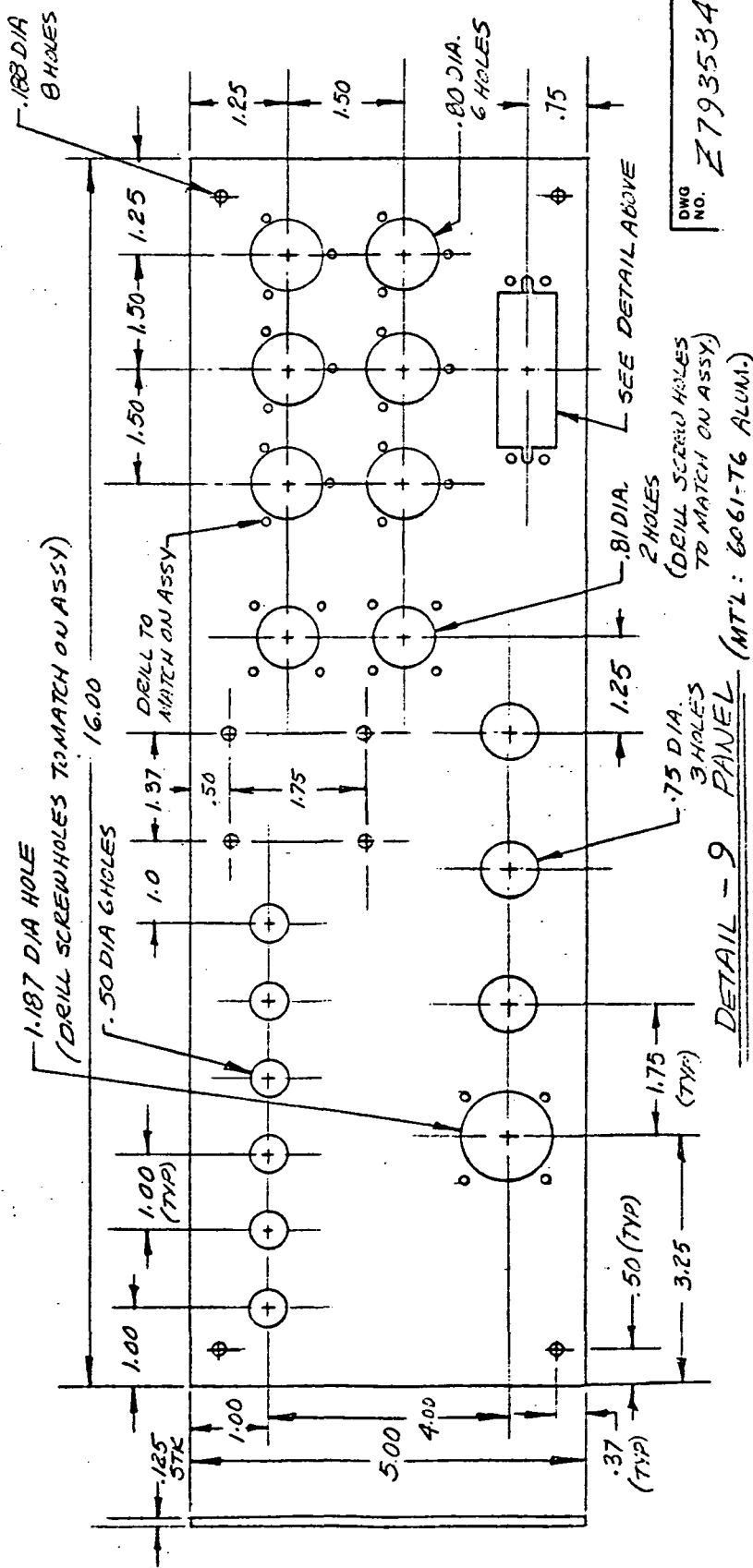
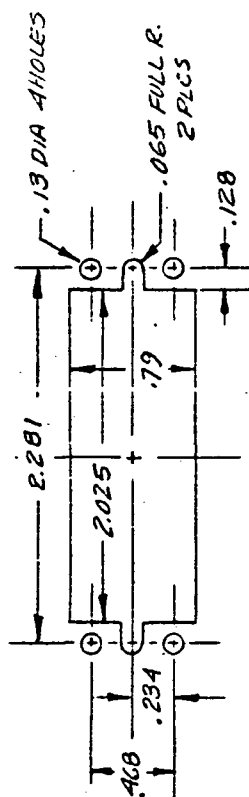
DOUGLAS AIRCRAFT COMPANY
LONG BEACH, CALIFORNIA
MACDONNELL DOUGLAS
GOOD MANY NO. 5277

Z7935344

18

SIZE | **DRAWING NUMBER**

| | | | |
|------|---|---------------------|-----|
| DATE | 1 | DRAWING CHANGED | |
| DATE | 2 | ADVANCE DWG CHG | |
| DATE | 3 | SERIAL EO | |
| DATE | 4 | NEW/REVISED RELEASE | NEW |
| DATE | 5 | REISSUE TO REVISE | R |



(DRILL SCREW HOLES
TO MATCH ON ASSY.)

DETAIL - 9 PANEL

DWG
NO. Z7935344

ENGINEERING ORDER

DAC 28-17088 (6-71)

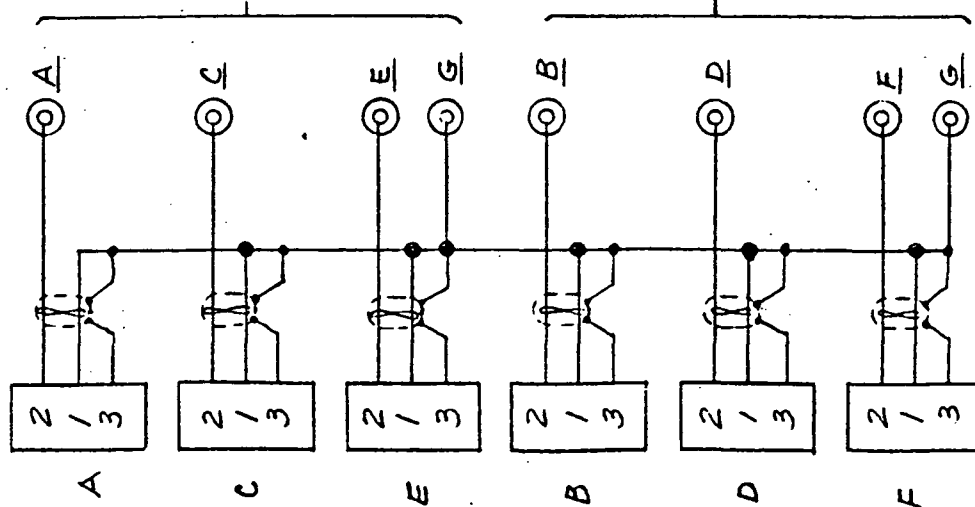
DOUGLAS AIRCRAFT COMPANY
 LONG BEACH, CALIFORNIA
 MC DONNELL DOUGLAS
 STANDARD NO. 1577

19 Z7935344

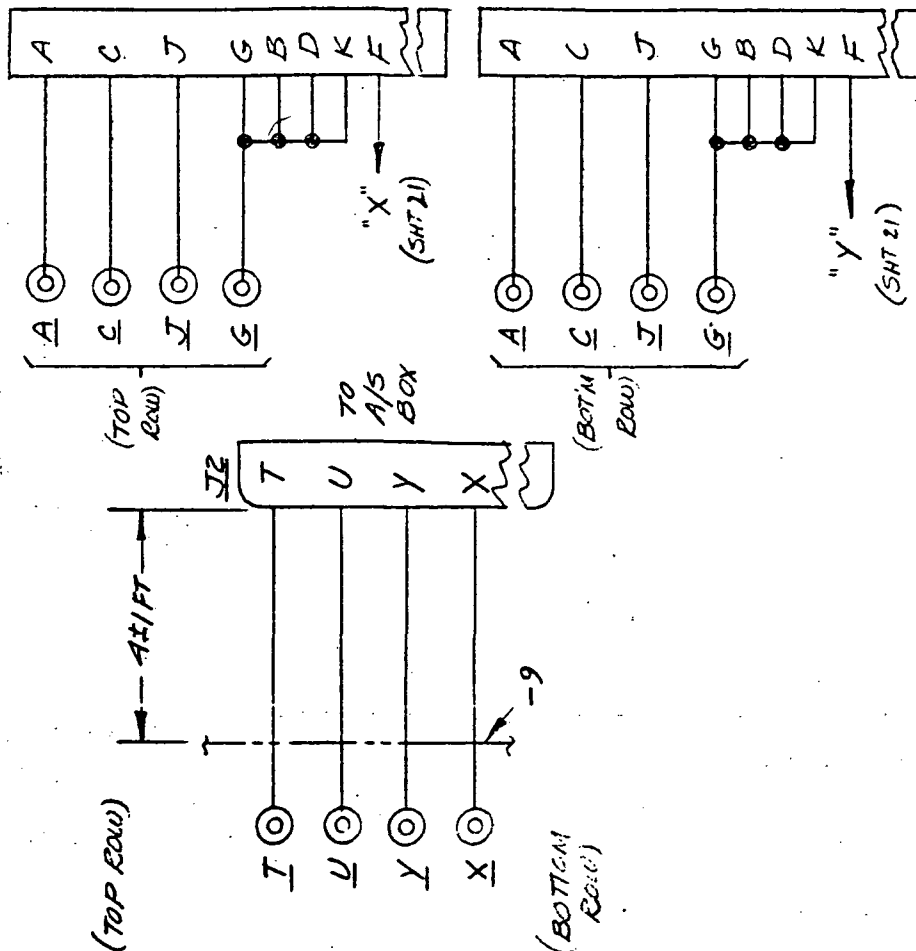
SHEET SIZE DRAWING NUMBER

| | | |
|------|---|---------------------|
| DATE | 1 | DRAWING CHANGED |
| DATE | 2 | ADVANCE DWG CHG |
| DATE | 3 | SERIAL EO |
| DATE | 4 | NEW/REVISED RELEASE |
| DATE | 5 | REISSUE TO REVISE |
| | | R |

PRESSURE



VALVES



WIRING DIAGRAM - 15 PANEL ASSY

(CONT'D ON SHEETS 20, 21)

DWG NO. Z7935344

ENGINEERING ORDER

DAC 25-17098 (8-71)

DOUGLAS AIRCRAFT COMPANY
LONG BEACH, CALIFORNIA
ROCKWELL DOUGLAS
FORM 25-17098 (8-71)

| | | | |
|----|---------------------|------|----------------|
| 20 | SHEET | SIZE | DRAWING NUMBER |
| 1 | DRAWING CHANGED | | |
| 2 | ADVANCE DWG CHG | | |
| 3 | SERIAL EO | | |
| 4 | NEW/REVISED RELEASE | | NEW |
| 5 | REISSUE TO REVISE | | R |

SIGMA I

| | |
|---|-------------|
| A | A-1 |
| B | A-2 |
| C | A-3 |
| D | A-4 |
| E | A-5 |
| F | A-6 |
| H | B-1 |
| J | B-2 |
| K | B-3 |
| L | B-4 |
| M | B-5 |
| N | B-6 |
| P | C-1 |
| R | C-2 |
| S | C-3 |
| T | C-4 |
| U | C-5 |
| V | C-6 |
| W | D-1 |
| X | D-2 |
| Y | D-3 |
| Z | D-4 |
| A | D-5 |
| B | D-6 |
| C | E-1 |
| D | E-2 |
| E | E-3 |
| F | E-4 |
| H | E-5 |
| J | E-6 |
| K | CHASSIS GND |

A/S BOX

| | |
|----|---|
| 7 | 0 |
| 8 | 0 |
| 9 | 0 |
| 10 | 0 |
| 11 | 0 |
| 12 | 0 |
| 13 | 0 |
| 14 | 0 |
| 15 | 0 |
| 16 | 0 |
| 17 | 0 |
| 18 | 0 |
| 20 | 0 |
| 21 | 0 |
| 22 | 0 |
| 23 | 0 |
| 24 | 0 |
| 25 | 0 |
| 26 | 0 |
| 27 | 0 |
| 30 | 0 |
| 31 | 0 |
| 32 | 0 |
| 33 | 0 |
| 35 | 0 |
| 36 | 0 |
| 37 | 0 |
| 38 | 0 |
| 39 | 0 |

-7 PANEL (REF)

4 ± 1 FT

(CONT'D ON SHEET 21)

TO
A/S
BOX

| |
|----|
| 35 |
| 36 |
| 37 |
| 38 |
| 39 |

WIRING DIAGRAM
-15 PANEL ASS'Y

DWG NO. Z7935344

(CONT'D ON SHEETS 19 & 21)

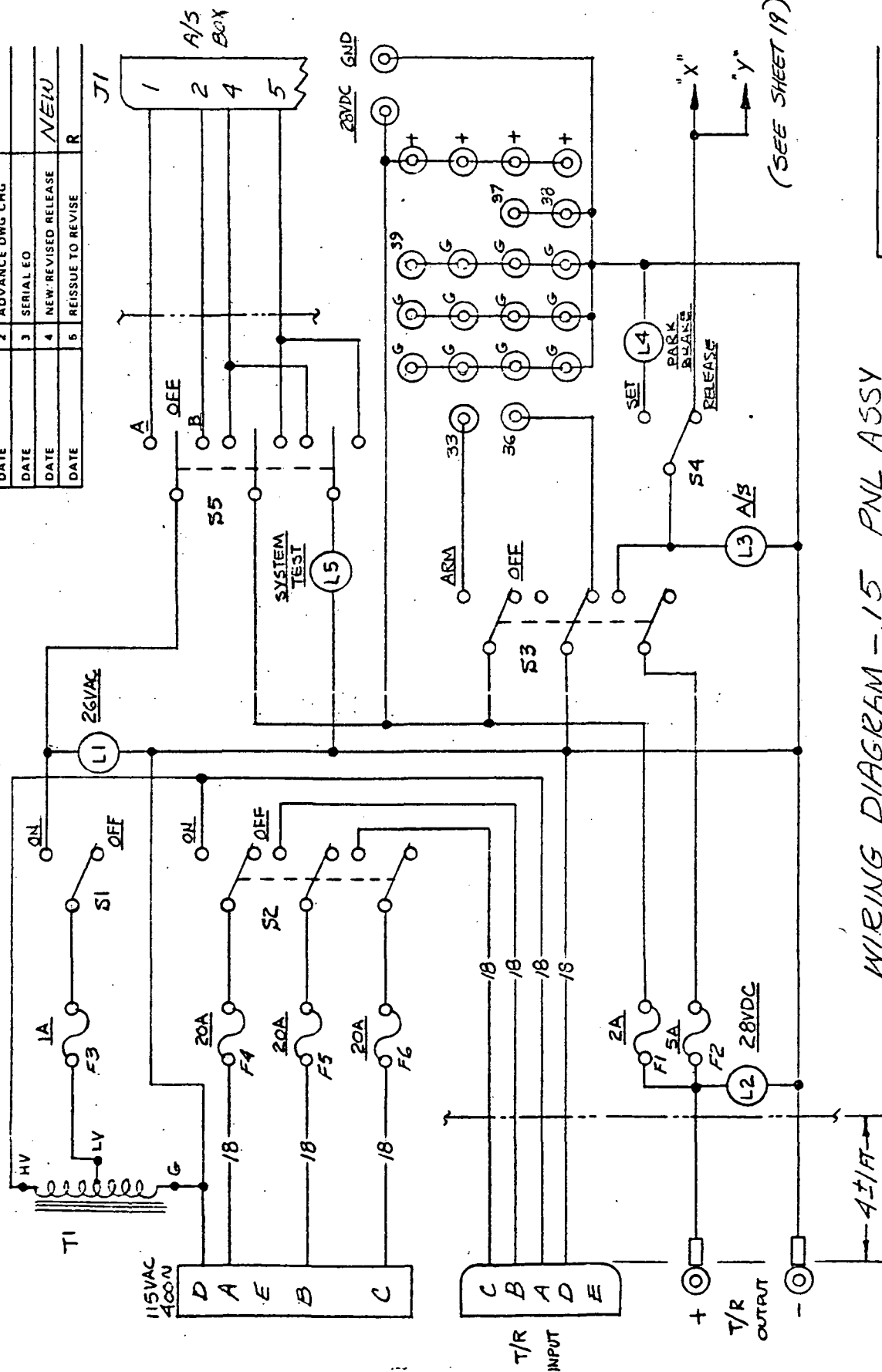
DOUGLAS AIRCRAFT COMPANY
LONG BEACH, CALIFORNIA
MCDONNELL DOUGLAS

DOUGLAS AIRCRAFT COMPANY
LONG BEACH, CALIFORNIA
MCDONNELL DOUGLAS

12

LEADS

| | | | |
|------|---|---------------------|-----|
| DATE | 1 | DRAWING CHANGED | |
| DATE | 2 | ADVANCE DWG CHG | |
| DATE | 3 | SERIAL EO | |
| DATE | 4 | NEW-REVISED RELEASE | NEW |
| DATE | 5 | REISSUE TO REVISE | R |



WIRING DIAGRAM - 15 PNL ASSY

(CONT'D ON SHTS 19, 20)

DWG
NO. Z 793534A

ENGINEERING ORDER

DAC 25-17098 (8-71)

DOUGLAS AIRCRAFT COMPANY
1500 SANTA ANITA AVENUE
MCDONNELL DOUGLAS
CHICAGO, ILL. 60646

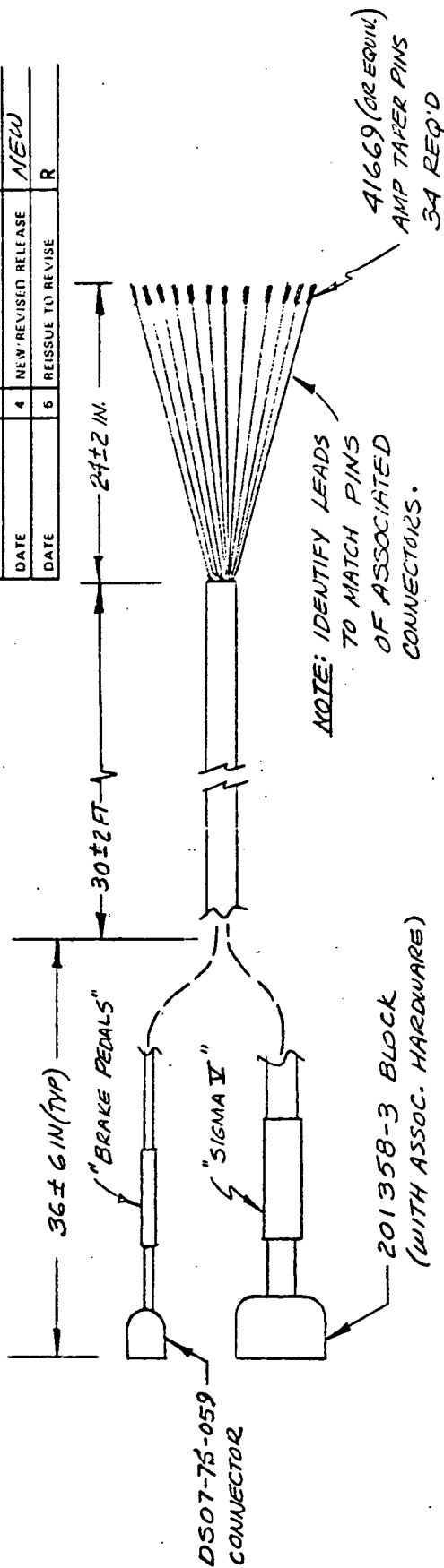
22

SHEET

SIZE

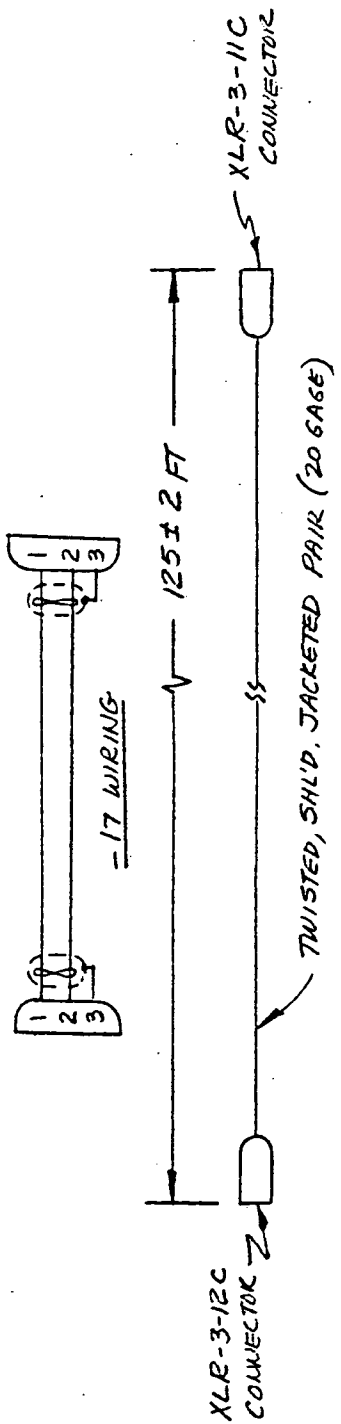
DRAWING NUMBER

| DATE | 1 | DRAWING CHANGED |
|------|---|---------------------|
| DATE | 2 | ADVANCE DWG CHG |
| DATE | 3 | SERIAL NO |
| DATE | 4 | NEW/REVISED RELEASE |
| DATE | 5 | REISSUE TO REVISE |
| | | R |



DETAIL -19 CABLE ASSY

(FOR WIRING, SEE SHEET 24)



DETAIL -17 CABLE ASSY

(6 REQ'D)

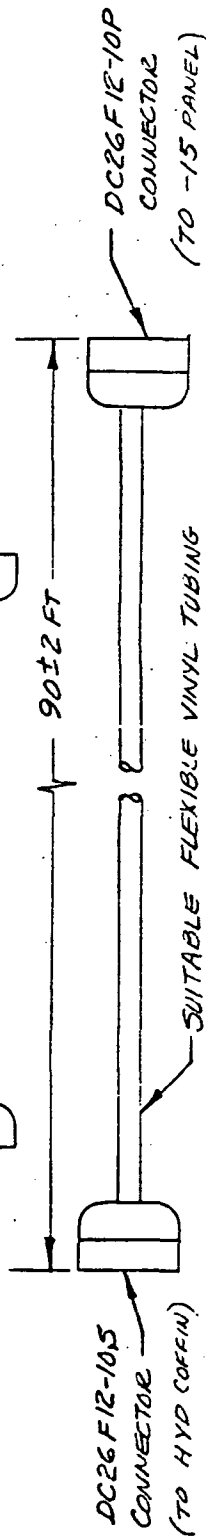
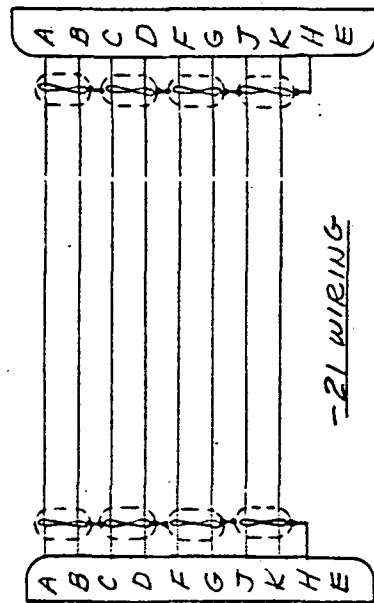
DWG NO. Z7935344

ENGINEERING ORDER

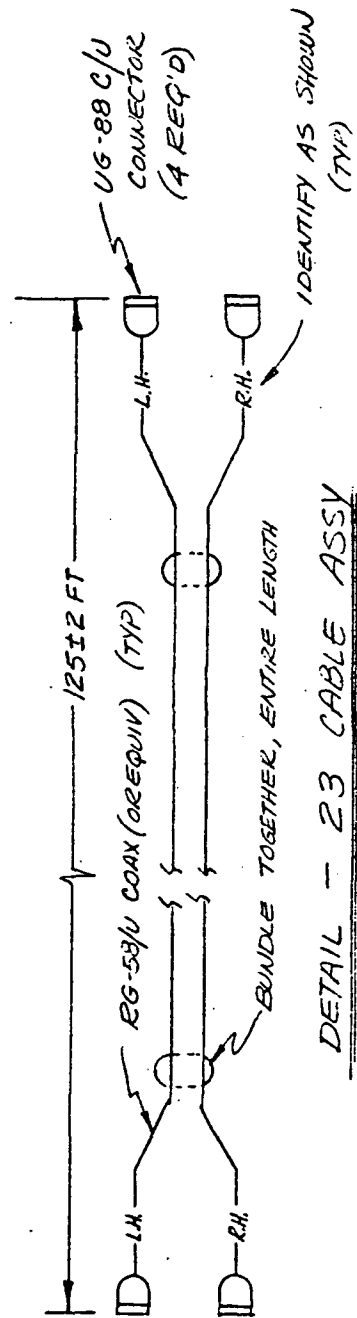
DAC 26-17098 (6-71)

DOUGLAS AIRCRAFT COMPANY
1800 JACKSON AVENUE
MCKINNEY, TEXAS 75069
FORM 0001/REV. 06-77

| DATE | SHEET | SIZE | DRAWING NUMBER |
|------|-------|---------------------|----------------|
| | 23 | | Z7935344 |
| DATE | 1 | DRAWING CHANGED | |
| DATE | 2 | ADVANCE DWG CHG | |
| DATE | 3 | SERIAL EO | |
| DATE | 4 | NEW REVISED RELEASE | NEW |
| DATE | 5 | REISSUE TO REVISE | R |



DETAIL - 21 CABLE ASSY (2 REQ'D)



DETAIL - 23 CABLE ASSY

ENGINEERING ORDER

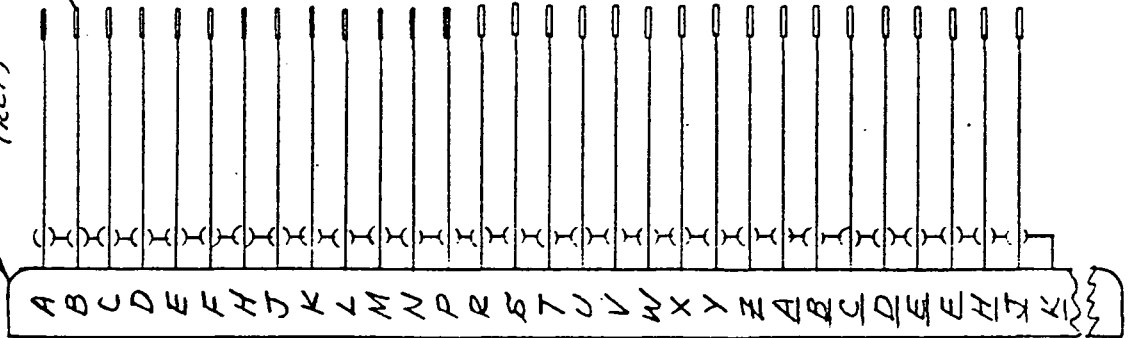
DAC 25-17098 (8-71)

DOUGLAS AIRCRAFT COMPANY
1800 FAIRFAX CALIFORNIA
MCDONNELL DOUGLAS
COMMUNICATIONS
FARM ROUTING UNIT

| DATE | SHEET | SIZE | DRAWING NUMBER |
|------|-------|---------------------|----------------|
| DATE | 24 | | Z 793534A |
| DATE | 1 | DRAWING CHANGED | |
| DATE | 2 | ADVANCE DWG CHG | |
| DATE | 3 | SERIAL EO | |
| DATE | 4 | NEW/REVISED RELEASE | NEW |
| DATE | 5 | REISSUE TO REVISE | R |

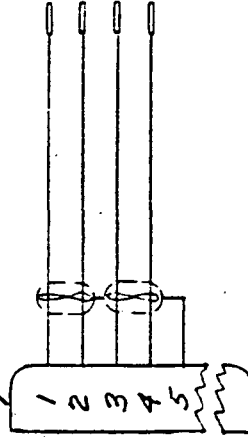
50-PIN AMP CONNECTOR
(REF)

AMP TAPER PN
(TYP)



SIGMA V

D507-75-059
(REF)



BRAKE
PEDALS

NOTE: ALL WIRE AWG 22

WIRING DIAGRAM -19 CABLE

DOUGLAS AIRCRAFT COMPANY
LONG BEACH, CALIFORNIA
MCDONNELL DOUGLAS
CASE NO. 117
DOUGLAS

2025 RELEASE UNDER E.O. 14176

✓ PARTS ARE IN HOUSE; SEE
DICK STORLEY OR BOB DEAN

| | | | | | |
|------|----|----------|-------|---------------------|----------------|
| | 25 | Z7935344 | SHEET | SIZE | DRAWING NUMBER |
| DATE | 1 | | | DRAWING CHANGED | |
| DATE | 2 | | | ADVANCE DWG CHG | |
| DATE | 3 | | | SERIAL EO | |
| DATE | 4 | | | NEW REVISED RELEASE | NEW |
| DATE | 5 | | | REISSUE TO REVISE | R |

| * USE EXISTING EQUIP. | | | | | | | | | |
|--|--------------------|---------------------|--|-------------------|--|---|--|--|--|
| ✓ PARTS ARE IN HOUSE; SEE DICK STOKLEY OR JOE DEAN | | | | | | | | | |
| DATE | | NEW REVISED RELEASE | | REISSUE TO REVISE | | R | | | |
| DATE | | NEW | | R | | | | | |
| PART NO. | PART NAME | VENDOR | | | | | | | |
| * 1 | SINGLE-BAY CABINET | HARRISON LABS | | | | | | | |
| 2 | MODEL 6299A | | | | | | | | |
| 1 | Z (TBD) | | | | | | | | |
| 1 | Z 4808926 | | | | | | | | |
| 1 | 7600 | PRESTON | | | | | | | |
| 6 | 8300 DO | PRESTON | | | | | | | |
| 6 | -17 | | | | | | | | |
| 1 | -19 | | | | | | | | |
| 2 | -21 | | | | | | | | |
| 1 | -23 | | | | | | | | |
| 1 | -13 | | | | | | | | |
| 1 | -15 | | | | | | | | |
| 1 | * 1 | G.E. | | | | | | | |
| 1 | 6RW176YN3 | | | | | | | | |
| 1 | * 1 | | | | | | | | |
| 6 | Z 4802188-553 | Z 7935344 | | | | | | | |

ENGINEERING ORDER

DAC 25-17088 (8-71)

DOUGLAS AIRCRAFT COMPANY
1805 BUCKLE, CALIFORNIA
MCDONNELL DOUGLAS
CORPORATION

26 Z 7935344

| SHEET | SIZE | DRAWING NUMBER |
|-------|------|----------------------|
| 1 | | DRAWING CHANGED |
| 2 | | ADVANCE DWG CHG |
| 3 | | SERIAL EO |
| 4 | | NEW, REVISED RELEASE |
| 5 | | REISSUE TO REVISE |

✓ PARTS ARE IN HOUSE; SEE
DICK STORLEY OR BOB DEAN

| | | PART NO. | PART NAME | VENDOR |
|-----|------|---------------|---|--------------|
| 11- | 1 | -3 | PANEL MAKE FROM CAL CHASSIS NO. PWA-12 (UNPAINTED ALUM) | |
| 81- | 1 | -5 | PANEL - .125 X 5 X 16.5 6061-T6 ALUM | |
| 51- | 1 | -7 | PANEL MAKE FROM CAL CHASSIS NO. PWA-14 (UNPAINTED ALUM) | |
| | 1 | -9 | PANEL - .125 X 5 X 16 6061-T6 ALUM | |
| | 1 | -11 | TIME DELAY ASSY | |
| | 4 | 8469 | SPACER | H.H. SMITH |
| | 46 | 8475 | SPACER | H.H. SMITH |
| | 2 | TY-53X | TRANSFORMER (T1, T2) | TRIAD |
| | 1 | P323BG33 | TRANSFORMER (115/26 V 400 W) | WESTINGHOUSE |
| | 1 | DPD-40-34P-1B | CONNECTOR (CONCOR) | ITT-CANNON |
| | 65 | 1498 (BLUE) | BANANA JACK | H.H. SMITH |
| | 36/0 | 1498 (GREEN) | " | " |
| | 51 | 1498 (RED) | " | " |
| | 30 | 1498 (YEL) | " | " |
| | | | | |

DWG NO. Z 7935344

ENGINEERING ORDER

DAC 25-17038 (6-71)

DOUGLAS AIRCRAFT COMPANY
1800 MAIN STREET
MCDONNELL DOUGLAS
CORPORATION
CROSS STREET NO. 2517

27 Z 7935344

SHEET SIZE DRAWING NUMBER

| | | |
|------|---|---------------------|
| DATE | 1 | DRAWING CHANGED |
| DATE | 2 | ADVANCE DWG CHG |
| DATE | 3 | SERIAL EQ |
| DATE | 4 | NEW/REVISED RELEASE |
| DATE | 5 | REISSUE TO REVISE |

NEW

| PART NO. | PART NAME | VENDOR |
|-----------------------|---|-------------|
| 1498 (BROWN) | EANANA JACK | H. H. SMITH |
| 1498 (BLACK) | " | " |
| MS24523-23 (OR EQUIV) | SPDT TOGGLE SW. -13: S2 THRU S5 -15: S1 & S4 | |
| MS24524-23 (OR EQUIV) | DIPDT " " S1 | |
| MS24525-23 (OR EQUIV) | APDT " " S2 & S3 | |
| MS24525-21 (OR EQUIV) | APDT (CENT OFF) " S5 | |
| MS25256-4-327 | LAMP ASSY (GREEN) L1 THRU L4 | |
| MS25256-2-327 | " " (YELLOW) L5 | |
| 342838 | FUSE HOLDER F1 THRU F6 | LITTELFUSE |
| 1A3AG | FUSE | |
| 2A3AG | " | |
| 5A3AG | " | |
| 20A3AG | " | |
| 31-010 | CONNECTOR (BULKHEAD BNC) | AMPHENOL |

DWG NO. Z 7935344

✓ PARTS IN HOUSE; SEE DICK STORLEY
OR BOB DEAN.

| | | |
|------|---|---------------------|
| DATE | 1 | DRAWING CHANGED |
| DATE | 2 | ADVANCE DWG CHG |
| DATE | 3 | SERIAL EO |
| DATE | 4 | NEW-REVISED RELEASE |
| DATE | 5 | REISSUE TO REVISE |

| DATE | | 5 | REISSUE TO REVISE | R |
|------------------|-----------------------------|------------------|-------------------|---|
| OR BOB DEAN. | | | | |
| PART NO. | PART NAME | VENDOR | | |
| MS3102B-18-11P | CONNECTOR | | | |
| DPAMA-40-33S | " | ITT/CANNON | | |
| PT06E-22-55P(SR) | " | BENDIX | | |
| AN3106B-16S-15 | " | | | |
| 200277-4 | BLOCK | A-NIP | | |
| XLP-3-14 | RECEPTACLE | ITT-CANNON | | |
| DC 22F 12-10S | CONNECTOR | BURBUDY | | |
| KHP17D11 | RELAY K1, K2 | POTTER-BRUNFIELD | | |
| 2N2324 | TRANSISTOR Q1, Q3 | G.E. | | |
| 2N2647 | TRANSISTOR Q2, Q4 | G.E. | | |
| 100Ω 1/2W | RESISTOR R4, R5, R9, R11 | | | |
| 150Ω 1/2W | RESISTOR R3, R10 | | | |
| 680Ω 1/2W | RESISTOR R6, R13 | | | |
| 15 MFD 50VDC | CAPACITOR C1 | | | |
| 9KH1 | RELAY SOCKET (POTTER-BRUN.) | | | |

DWG NO. Z 7935344

5

ENGINEERING ORDER

DAC 25-17088 (6-71)

DOUGLAS AIRCRAFT COMPANY
1800 WEST 10TH AVENUE
DENVER, COLORADO 80202

* 33K & 30K IN PARALLEL
PARTS IN HOUSE; SEE DICK STORLEY
OR BOB DEAN

29

Z7935344

| SHEET | SIZE | DRAWING NUMBER |
|-------|---------------------|----------------|
| 1 | DRAWING CHANGED | |
| 2 | ADVANCE DWG CHG | |
| 3 | SERIAL EQ | |
| 4 | NEW REVISED RELEASE | NEW |
| 5 | REISSUE TO REVISE | R |

| PART NO. | PART NAME | VENDOR |
|----------|----------------------------------|------------|
| 1 | CAPACITOR C2 | |
| 1 | POTENTIOMETER .1MEGΩ R1 | OHMITE |
| 1 | POTENTIOMETER .25MEGΩ R2 | OHMITE |
| 1 | RESISTOR R7 | |
| 1 | " R8 | |
| 1 | " R12 | |
| 1 | " R14 | |
| 1 | CIRCUIT BOARD (1/16 x 3 x 6 1/2) | VECTOR |
| 1 | CONNECTOR | ITT-CANNON |
| 1 | " | " |
| 1 | " | BURNDY |
| 1 | " | " |
| 4 | COAX COHN. (BNC) | |
| AS REQ | COAX CABLE | |

OWG NO. Z7935344

DOUGLAS AIRCRAFT COMPANY
LONG BEACH, CALIFORNIA
MCDONNELL DOUGLAS
C/REGISTRATION
5055 MOUNTAIN VIEW
50577

COPIES DESTROYED NO. 100071

✓ PARTS IN HOUSE; SEE DICK STOKLEY OR BOB DEAN.

| | | | |
|------|-------|---------------------|----------------|
| 30 | SHEET | Z 793534A | |
| | | SIZE | DRAWING NUMBER |
| DATE | 1 | DRAWING CHANGED | |
| DATE | 2 | ADVANCE DWG CHG | |
| DATE | 3 | SERIAL EO | |
| DATE | 4 | NEW/REVISED RELEASE | |
| DATE | 5 | REISSUE TO REVISE | |
| | | | NEW |
| | | | R |

| DATE | | 4 | 5 | 6 | 7 | 8 | 9 | 10 | 11 | 12 | 13 | 14 | 15 | 16 | 17 | 18 | 19 | 20 | 21 | 22 | 23 | 24 | 25 | 26 | 27 | 28 | 29 | 30 | 31 | 32 | 33 | 34 | 35 | 36 | 37 | 38 | 39 | 40 | 41 | 42 | 43 | 44 | 45 | 46 | 47 | 48 | 49 | 50 | 51 | 52 | 53 | 54 | 55 | 56 | 57 | 58 | 59 | 60 | 61 | 62 | 63 | 64 | 65 | 66 | 67 | 68 | 69 | 70 | 71 | 72 | 73 | 74 | 75 | 76 | 77 | 78 | 79 | 80 | 81 | 82 | 83 | 84 | 85 | 86 | 87 | 88 | 89 | 90 | 91 | 92 | 93 | 94 | 95 | 96 | 97 | 98 | 99 | 100 |
|------|------|---|---|---|---|---|---|----|----|----|----|----|----|----|----|----|----|----|----|----|----|----|----|----|----|----|----|----|----|----|----|----|----|----|----|----|----|----|----|----|----|----|----|----|----|----|----|----|----|----|----|----|----|----|----|----|----|----|----|----|----|----|----|----|----|----|----|----|----|----|----|----|----|----|----|----|----|----|----|----|----|----|----|----|----|----|----|----|----|----|----|----|----|----|----|----|----|-----|
| DATE | | 4 | 5 | 6 | 7 | 8 | 9 | 10 | 11 | 12 | 13 | 14 | 15 | 16 | 17 | 18 | 19 | 20 | 21 | 22 | 23 | 24 | 25 | 26 | 27 | 28 | 29 | 30 | 31 | 32 | 33 | 34 | 35 | 36 | 37 | 38 | 39 | 40 | 41 | 42 | 43 | 44 | 45 | 46 | 47 | 48 | 49 | 50 | 51 | 52 | 53 | 54 | 55 | 56 | 57 | 58 | 59 | 60 | 61 | 62 | 63 | 64 | 65 | 66 | 67 | 68 | 69 | 70 | 71 | 72 | 73 | 74 | 75 | 76 | 77 | 78 | 79 | 80 | 81 | 82 | 83 | 84 | 85 | 86 | 87 | 88 | 89 | 90 | 91 | 92 | 93 | 94 | 95 | 96 | 97 | 98 | 99 | 100 |
| DATE | DATE | 4 | 5 | 6 | 7 | 8 | 9 | 10 | 11 | 12 | 13 | 14 | 15 | 16 | 17 | 18 | 19 | 20 | 21 | 22 | 23 | 24 | 25 | 26 | 27 | 28 | 29 | 30 | 31 | 32 | 33 | 34 | 35 | 36 | 37 | 38 | 39 | 40 | 41 | 42 | 43 | 44 | 45 | 46 | 47 | 48 | 49 | 50 | 51 | 52 | 53 | 54 | 55 | 56 | 57 | 58 | 59 | 60 | 61 | 62 | 63 | 64 | 65 | 66 | 67 | 68 | 69 | 70 | 71 | 72 | 73 | 74 | 75 | 76 | 77 | 78 | 79 | 80 | 81 | 82 | 83 | 84 | 85 | 86 | 87 | 88 | 89 | 90 | 91 | 92 | 93 | 94 | 95 | 96 | 97 | 98 | 99 | 100 |
| DATE | DATE | 4 | 5 | 6 | 7 | 8 | 9 | 10 | 11 | 12 | 13 | 14 | 15 | 16 | 17 | 18 | 19 | 20 | 21 | 22 | 23 | 24 | 25 | 26 | 27 | 28 | 29 | 30 | 31 | 32 | 33 | 34 | 35 | 36 | 37 | 38 | 39 | 40 | 41 | 42 | 43 | 44 | 45 | 46 | 47 | 48 | 49 | 50 | 51 | 52 | 53 | 54 | 55 | 56 | 57 | 58 | 59 | 60 | 61 | 62 | 63 | 64 | 65 | 66 | 67 | 68 | 69 | 70 | 71 | 72 | 73 | 74 | 75 | 76 | 77 | 78 | 79 | 80 | 81 | 82 | 83 | 84 | 85 | 86 | 87 | 88 | 89 | 90 | 91 | 92 | 93 | 94 | 95 | 96 | 97 | 98 | 99 | 100 |
| DATE | DATE | 4 | 5 | 6 | 7 | 8 | 9 | 10 | 11 | 12 | 13 | 14 | 15 | 16 | 17 | 18 | 19 | 20 | 21 | 22 | 23 | 24 | 25 | 26 | 27 | 28 | 29 | 30 | 31 | 32 | 33 | 34 | 35 | 36 | 37 | 38 | 39 | 40 | 41 | 42 | 43 | 44 | 45 | 46 | 47 | 48 | 49 | 50 | 51 | 52 | 53 | 54 | 55 | 56 | 57 | 58 | 59 | 60 | 61 | 62 | 63 | 64 | 65 | 66 | 67 | 68 | 69 | 70 | 71 | 72 | 73 | 74 | 75 | 76 | 77 | 78 | 79 | 80 | 81 | 82 | 83 | 84 | 85 | 86 | 87 | 88 | 89 | 90 | 91 | 92 | 93 | 94 | 95 | 96 | 97 | 98 | 99 | 100 |
| DATE | DATE | 4 | 5 | 6 | 7 | 8 | 9 | 10 | 11 | 12 | 13 | 14 | 15 | 16 | 17 | 18 | 19 | 20 | 21 | 22 | 23 | 24 | 25 | 26 | 27 | 28 | 29 | 30 | 31 | 32 | 33 | 34 | 35 | 36 | 37 | 38 | 39 | 40 | 41 | 42 | 43 | 44 | 45 | 46 | 47 | 48 | 49 | 50 | 51 | 52 | 53 | 54 | 55 | 56 | 57 | 58 | 59 | 60 | 61 | 62 | 63 | 64 | 65 | 66 | 67 | 68 | 69 | 70 | 71 | 72 | 73 | 74 | 75 | 76 | 77 | 78 | 79 | 80 | 81 | 82 | 83 | 84 | 85 | 86 | 87 | 88 | 89 | 90 | 91 | 92 | 93 | 94 | 95 | 96 | 97 | 98 | 99 | 100 |
| DATE | DATE | 4 | 5 | 6 | 7 | 8 | 9 | 10 | 11 | 12 | 13 | 14 | 15 | 16 | 17 | 18 | 19 | 20 | 21 | 22 | 23 | 24 | 25 | 26 | 27 | 28 | 29 | 30 | 31 | 32 | 33 | 34 | 35 | 36 | 37 | 38 | 39 | 40 | 41 | 42 | 43 | 44 | 45 | 46 | 47 | 48 | 49 | 50 | 51 | 52 | 53 | 54 | 55 | 56 | 57 | 58 | 59 | 60 | 61 | 62 | 63 | 64 | 65 | 66 | 67 | 68 | 69 | 70 | 71 | 72 | 73 | 74 | 75 | 76 | 77 | 78 | 79 | 80 | 81 | 82 | 83 | 84 | 85 | 86 | 87 | 88 | 89 | 90 | 91 | 92 | 93 | 94 | 95 | 96 | 97 | 98 | 99 | 100 |
| DATE | DATE | 4 | 5 | 6 | 7 | 8 | 9 | 10 | 11 | 12 | 13 | 14 | 15 | 16 | 17 | 18 | 19 | 20 | 21 | 22 | 23 | 24 | 25 | 26 | 27 | 28 | 29 | 30 | 31 | 32 | 33 | 34 | 35 | 36 | 37 | 38 | 39 | 40 | 41 | 42 | 43 | 44 | 45 | 46 | 47 | 48 | 49 | 50 | 51 | 52 | 53 | 54 | 55 | 56 | 57 | 58 | 59 | 60 | 61 | 62 | 63 | 64 | 65 | 66 | 67 | 68 | 69 | 70 | 71 | 72 | 73 | 74 | 75 | 76 | 77 | 78 | 79 | 80 | 81 | 82 | 83 | 84 | 85 | 86 | 87 | 88 | 89 | 90 | 91 | 92 | 93 | 94 | 95 | 96 | 97 | 98 | 99 | 100 |
| DATE | DATE | 4 | 5 | 6 | 7 | 8 | 9 | 10 | 11 | 12 | 13 | 14 | 15 | 16 | 17 | 18 | 19 | 20 | 21 | 22 | 23 | 24 | 25 | 26 | 27 | 28 | 29 | 30 | 31 | 32 | 33 | 34 | 35 | 36 | 37 | 38 | 39 | 40 | 41 | 42 | 43 | 44 | 45 | 46 | 47 | 48 | 49 | 50 | 51 | 52 | 53 | 54 | 55 | 56 | 57 | 58 | 59 | 60 | 61 | 62 | 63 | 64 | 65 | 66 | 67 | 68 | 69 | 70 | 71 | 72 | 73 | 74 | 75 | 76 | 77 | 78 | 79 | 80 | 81 | 82 | 83 | 84 | 85 | 86 | 87 | 88 | 89 | 90 | 91 | 92 | 93 | 94 | 95 | 96 | 97 | 98 | 99 | 100 |
| DATE | DATE | 4 | 5 | 6 | 7 | 8 | 9 | 10 | 11 | 12 | 13 | 14 | 15 | 16 | 17 | 18 | 19 | 20 | 21 | 22 | 23 | 24 | 25 | 26 | 27 | 28 | 29 | 30 | 31 | 32 | 33 | 34 | 35 | 36 | 37 | 38 | 39 | 40 | 41 | 42 | 43 | 44 | 45 | 46 | 47 | 48 | 49 | 50 | 51 | 52 | 53 | 54 | 55 | 56 | 57 | 58 | 59 | 60 | 61 | 62 | 63 | 64 | 65 | 66 | 67 | 68 | 69 | 70 | 71 | 72 | 73 | 74 | 75 | 76 | 77 | 78 | 79 | 80 | 81 | 82 | 83 | 84 | 85 | 86 | 87 | 88 | 89 | 90 | 91 | 92 | 93 | 94 | 95 | 96 | 97 | 98 | 99 | 100 |
| DATE | DATE | 4 | 5 | 6 | 7 | 8 | 9 | 10 | 11 | 12 | 13 | 14 | 15 | 16 | 17 | 18 | 19 | 20 | 21 | 22 | 23 | 24 | 25 | 26 | 27 | 28 | 29 | 30 | 31 | 32 | 33 | 34 | 35 | 36 | 37 | 38 | 39 | 40 | 41 | 42 | 43 | 44 | 45 | 46 | 47 | 48 | 49 | 50 | 51 | 52 | 53 | 54 | 55 | 56 | 57 | 58 | 59 | 60 | 61 | 62 | 63 | 64 | 65 | 66 | 67 | 68 | 69 | 70 | 71 | 72 | 73 | 74 | 75 | 76 | 77 | 78 | 79 | 80 | 81 | 82 | 83 | 84 | 85 | 86 | 87 | 88 | 89 | 90 | 91 | 92 | 93 | 94 | 95 | 96 | 97 | 98 | 99 | 100 |
| DATE | DATE | 4 | 5 | 6 | 7 | 8 | 9 | 10 | 11 | 12 | 13 | 14 | 15 | 16 | 17 | 18 | 19 | 20 | 21 | 22 | 23 | 24 | 25 | 26 | 27 | 28 | 29 | 30 | 31 | 32 | 33 | 34 | 35 | 36 | 37 | 38 | 39 | 40 | 41 | 42 | 43 | 44 | 45 | 46 | 47 | 48 | 49 | 50 | 51 | 52 | 53 | 54 | 55 | 56 | 57 | 58 | 59 | 60 | 61 | 62 | 63 | 64 | 65 | 66 | 67 | 68 | 69 | 70 | 71 | 72 | 73 | 74 | 75 | 76 | 77 | 78 | 79 | 80 | 81 | 82 | 83 | 84 | 85 | 86 | 87 | 88 | 89 | 90 | 91 | 92 | 93 | 94 | 95 | 96 | 97 | 98 | 99 | 100 |
| DATE | DATE | 4 | 5 | 6 | 7 | 8 | 9 | 10 | 11 | 12 | 13 | 14 | 15 | 16 | 17 | 18 | 19 | 20 | 21 | 22 | 23 | 24 | 25 | 26 | 27 | 28 | 29 | 30 | 31 | 32 | 33 | 34 | 35 | 36 | 37 | 38 | 39 | 40 | 41 | 42 | 43 | 44 | 45 | 46 | 47 | 48 | 49 | 50 | 51 | 52 | 53 | 54 | 55 | 56 | 57 | 58 | 59 | 60 | 61 | 62 | 63 | 64 | 65 | 66 | 67 | 68 | 69 | 70 | 71 | 72 | 73 | 74 | 75 | 76 | 77 | 78 | 79 | 80 | 81 | 82 | 83 | 84 | 85 | 86 | 87 | 88 | 89 | 90 | 91 | 92 | 93 | 94 | 95 | 96 | 97 | 98 | 99 | 100 |
| DATE | DATE | 4 | 5 | 6 | 7 | 8 | 9 | 10 | 11 | 12 | 13 | 14 | 15 | 16 | 17 | 18 | 19 | 20 | 21 | 22 | 23 | 24 | 25 | 26 | 27 | 28 | 29 | 30 | 31 | 32 | 33 | 34 | 35 | 36 | 37 | 38 | 39 | 40 | 41 | 42 | 43 | 44 | 45 | 46 | 47 | 48 | 49 | 50 | 51 | 52 | 53 | 54 | 55 | 56 | 57 | 58 | 59 | 60 | 61 | 62 | 63 | 64 | 65 | 66 | 67 | 68 | 69 | 70 | 71 | 72 | 73 | 74 | 75 | 76 | 77 | 78 | 79 | 80 | 81 | 82 | 83 | 84 | 85 | 86 | 87 | 88 | 89 | 90 | 91 | 92 | 93 | 94 | 95 | 96 | 97 | 98 | 99 | 100 |
| DATE | DATE | 4 | 5 | 6 | 7 | 8 | 9 | 10 | 11 | 12 | 13 | 14 | 15 | 16 | 17 | 18 | 19 | 20 | 21 | 22 | 23 | 24 | 25 | 26 | 27 | 28 | 29 | 30 | 31 | 32 | 33 | 34 | 35 | 36 | 37 | 38 | 39 | 40 | 41 | 42 | 43 | 44 | 45 | 46 | 47 | 48 | 49 | 50 | 51 | 52 | 53 | 54 | 55 | 56 | 57 | 58 | 59 | 60 | 61 | 62 | 63 | 64 | 65 | 66 | 67 | 68 | 69 | 70 | 71 | 72 | 73 | 74 | 75 | 76 | 77 | 78 | 79 | 80 | 81 | 82 | 83 | 84 | 85 | 86 | 87 | 88 | 89 | 90 | 91 | 92 | 93 | 94 | 95 | 96 | 97 | 98 | 99 | 100 |
| DATE | DATE | 4 | 5 | 6 | 7 | 8 | 9 | 10 | 11 | 12 | 13 | 14 | 15 | 16 | 17 | 18 | 19 | 20 | 21 | 22 | 23 | 24 | 25 | 26 | 27 | 28 | 29 | 30 | 31 | 32 | 33 | 34 | 35 | 36 | 37 | 38 | 39 | 40 | 41 | 42 | 43 | 44 | 45 | 46 | 47 | 48 | 49 | 50 | 51 | 52 | 53 | 54 | 55 | 56 | 57 | 58 | 59 | 60 | 61 | 62 | 63 | 64 | 65 | 66 | 67 | 68 | 69 | 70 | 71 | 72 | 73 | 74 | 75 | 76 | 77 | 78 | 79 | 80 | 81 | 82 | 83 | 84 | 85 | 86 | 87 | 88 | 89 | 90 | 91 | 92 | 93 | 94 | 95 | 96 | 97 | 98 | 99 | 100 |
| DATE | DATE | 4 | 5 | 6 | 7 | 8 | 9 | 10 | 11 | 12 | 13 | 14 | 15 | 16 | 17 | 18 | 19 | 20 | 21 | 22 | 23 | 24 | 25 | 26 | 27 | 28 | 29 | 30 | 31 | 32 | 33 | 34 | 35 | 36 | 37 | 38 | 39 | 40 | 41 | 42 | 43 | 44 | 45 | 46 | 47 | 48 | 49 | 50 | 51 | 52 | 53 | 54 | 55 | 56 | 57 | 58 | 59 | 60 | 61 | 62 | 63 | 64 | 65 | 66 | 67 | 68 | 69 | 70 | 71 | 72 | 73 | 74 | 75 | 76 | 77 | 78 | 79 | 80 | 81 | 82 | 83 | 84 | 85 | 86 | 87 | 88 | 89 | 90 | 91 | 92 | 93 | 94 | 95 | 96 | 97 | 98 | 99 | 100 |
| DATE | DATE | 4 | 5 | 6 | 7 | 8 | 9 | 10 | 11 | 12 | 13 | 14 | 15 | 16 | 17 | 18 | 19 | 20 | 21 | 22 | 23 | 24 | 25 | 26 | 27 | 28 | 29 | 30 | 31 | 32 | 33 | 34 | 35 | 36 | 37 | 38 | 39 | 40 | 41 | 42 | 43 | 44 | 45 | 46 | 47 | 48 | 49 | 50 | 51 | 52 | 53 | 54 | 55 | 56 | 57 | 58 | 59 | 60 | 61 | 62 | 63 | 64 | 65 | 66 | 67 | 68 | 69 | 70 | 71 | 72 | 73 | 74 | 75 | 76 | 77 | 78 | 79 | 80 | 81 | 82 | 83 | 84 | 85 | 86 | 87 | 88 | 89 | 90 | 91 | 92 | 93 | 94 | 95 | 96 | | | | |

DWG
NO. Z 7955344

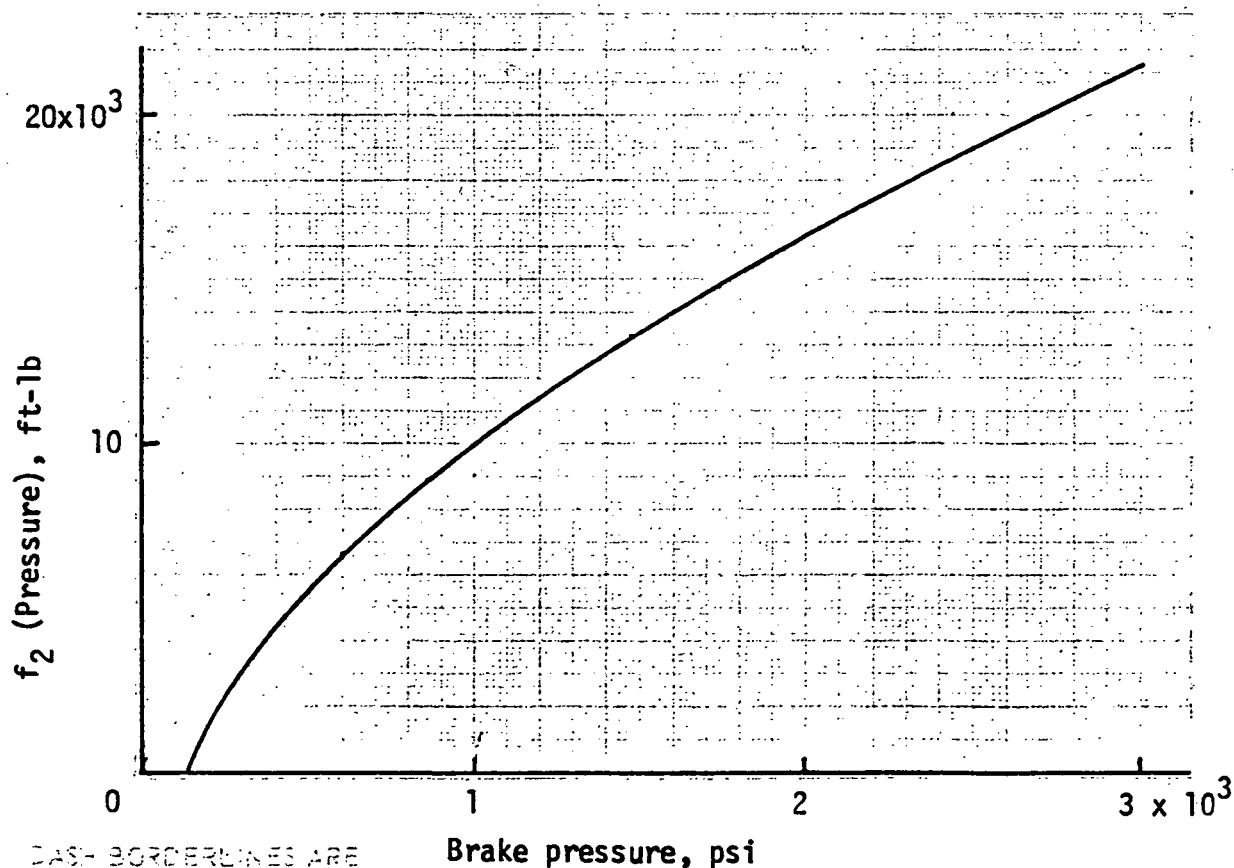
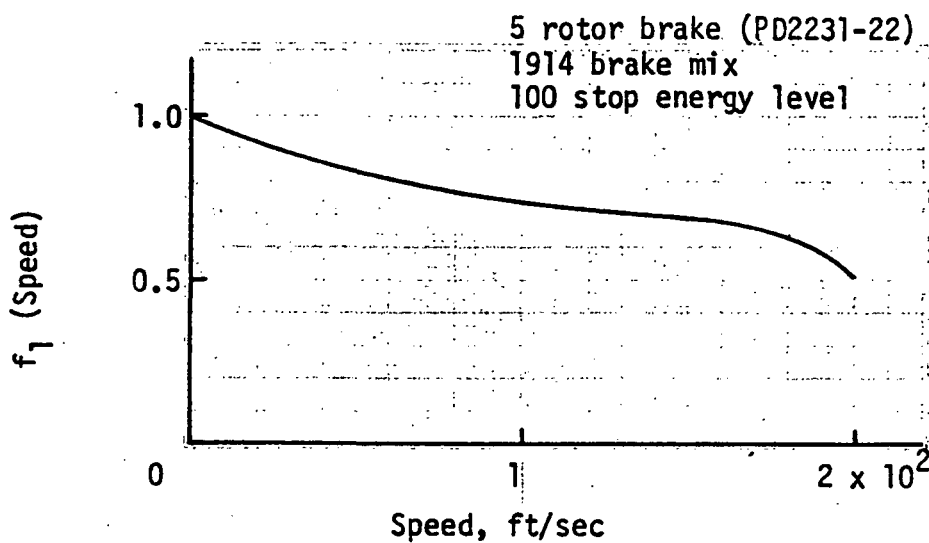
Section 5. ANALOG ANTISKID SIMULATOR VALIDATION

The validation consisted of matching Langley test-track test data (NASA TN D-8332) on the antiskid simulator.

The test conditions (speed, vertical load, maximum coefficient of friction, tire yaw angle, and commanded brake pressure) were set up on the simulator and runs were made. The drag loads decelerating the aircraft were adjusted to give the same deceleration and the torque gain was adjusted to give the same skid pressure level as on the test data. The brake characteristics utilized are shown in Figure C-5.

Two of the Langley tests were selected for correlation. The time history for the first, in which the tire was unyawed, is shown in Figure C-6. The actual test conditions are denoted on the figure. Figure C-7 presents the simulator run for the same conditions. The degree of correlation between the simulator and test data can be seen by comparing these two figures. Note the similarity in skid depth and in the levels of the brake pressure, brake torque and drag coefficient of friction just prior to the skids. The correlation between the simulator and test data is good, except that the pressure recovery immediately following a skid was quicker on the simulator. The time history of the second test, in which the tire was yawed 6°, is shown in Figure C-8 and the corresponding simulator run is shown in Figure C-9. Here, particularly note how well μ_s correlates, both unbraked and with 2000 psi applied (slip ratio = 10%). The comments made above about the degree of correlation for the other case apply here also for the initial skid. The subsequent shallow skids shown in the test data weren't duplicated on the simulator. These deep skids on the simulator are probably due to the adjustments made to achieve rougher cockpit motion.

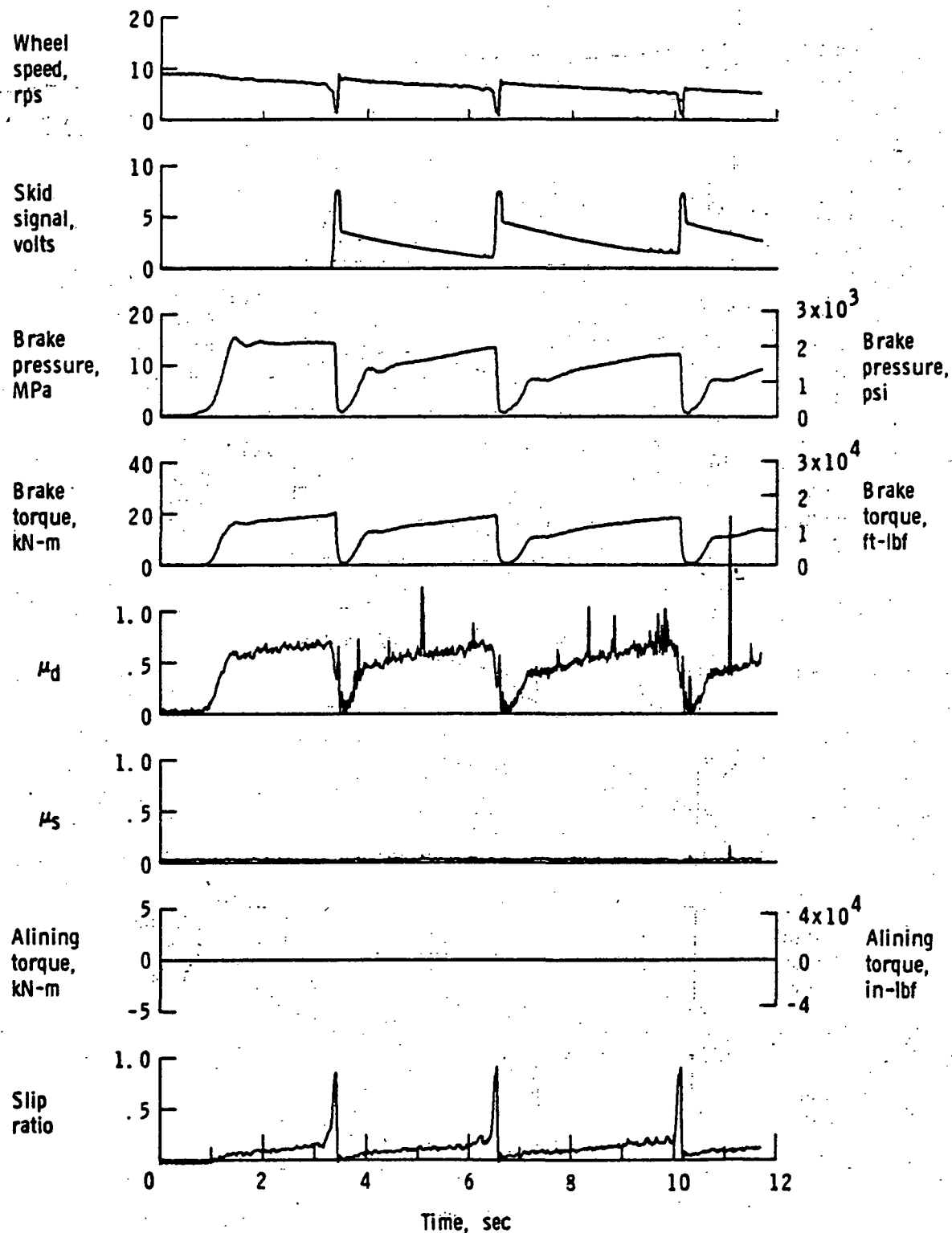
$$\text{Brake torque} = f_1 (\text{Speed}) \times f_2 (\text{Pressure})$$



DASH-BORDERLINES ARE

Brake pressure, psi

FIGURE C-5 BRAKE TORQUE/PRESSURE/SPEED RELATIONSHIP



Time histories for run 2; nominal carriage speed, 44 knots; vertical load, 59.6 kN (13 400 lbf); yaw angle, 0° ; surface condition, dry; tire condition, new; brake pressure, 14 MPa (2000 lbf/in²).

FIGURE C-6 TEST TIME HISTORY SELECTED FOR ANTISKID SIMULATOR VALIDATION -- UNYAWED TIRE

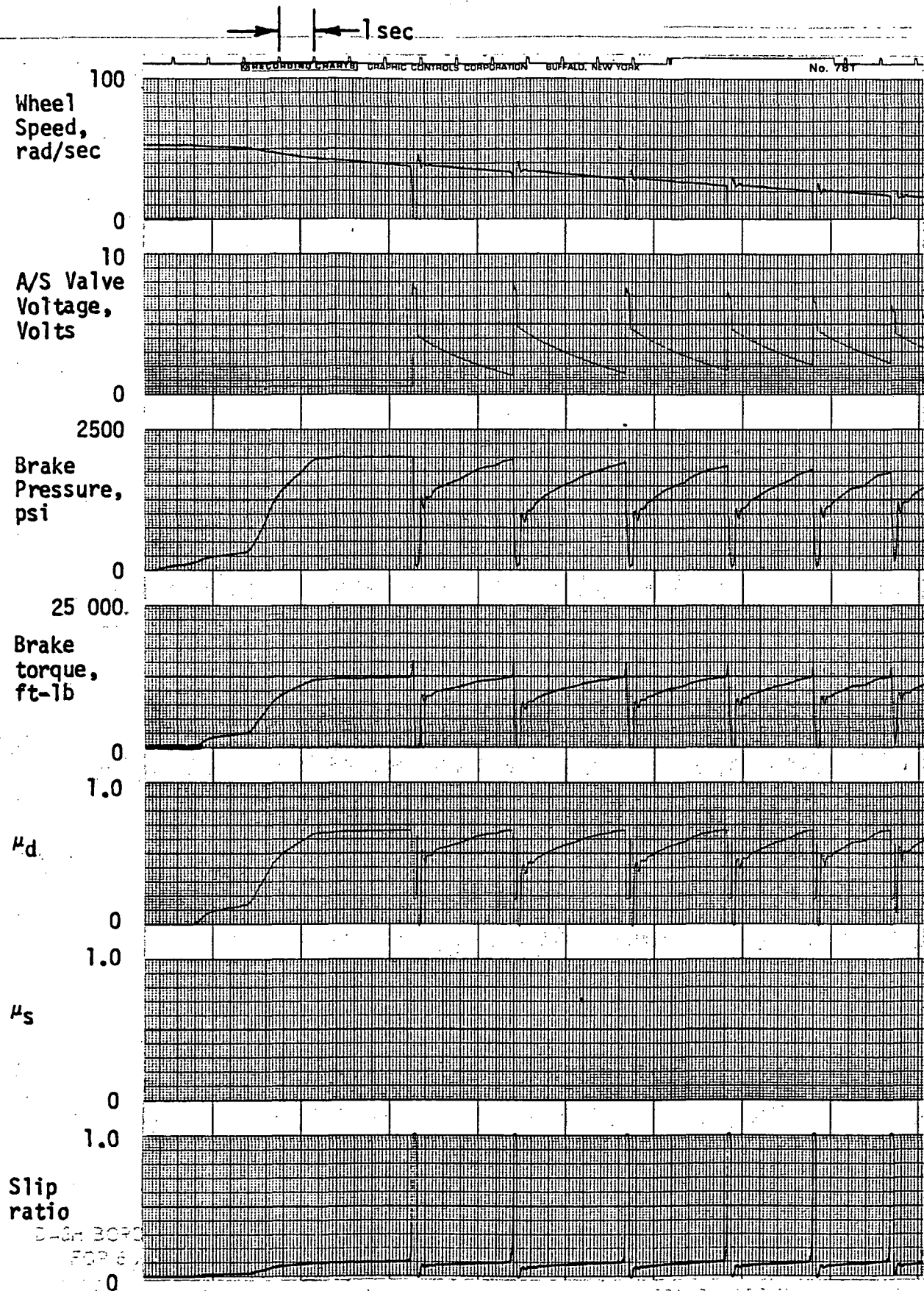
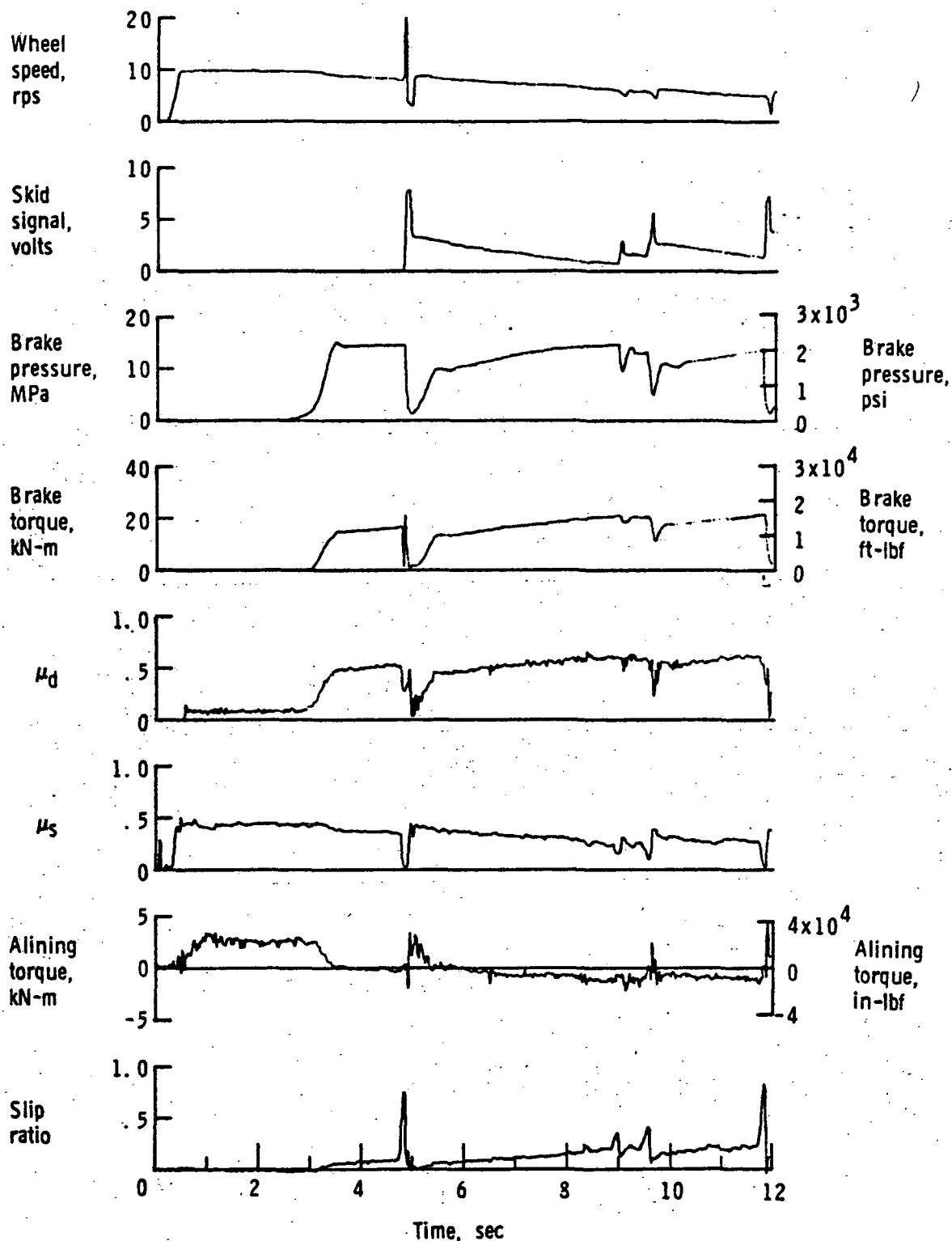


FIGURE C-7 ANTISKID SIMULATOR TIME HISTORY -- UNYAWED TIRE



Time histories for run 36; nominal carriage speed, 46 knots; vertical load, 83.6 kN (18 800 lbf); yaw angle, 6° ; surface condition, dry; tire condition, new; brake pressure, 14 MPa (2000 lbf/in²).

FIGURE C-8 TEST TIME HISTORY SELECTED FOR ANTISKID SIMULATOR VALIDATION -- YAWED TIRE

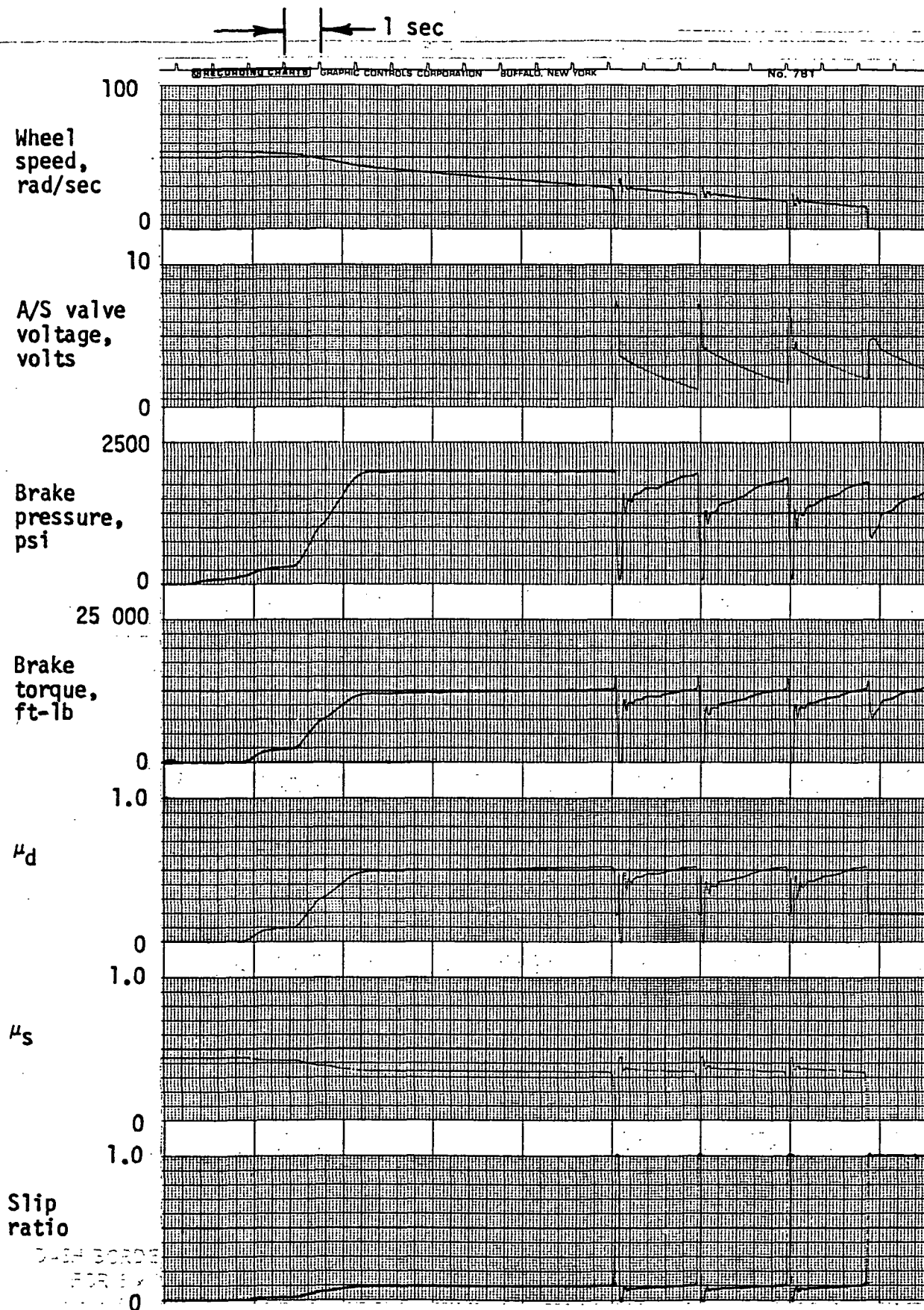


FIGURE C-9 ANTISKID SIMULATOR TIME HISTORY -- YAWED TIRE

APPENDIX D
COCKPIT SIMULATOR

The cockpit mounted on the motion base platform is sized and configured as a DC-10. This appendix outlines those changes that were made to the cockpit to more closely represent the DC-9 for the ground handling study.

Flight Instruments

DC-9 type instruments were installed on the Captain's side. These instruments were all types normally used in DC-9's except the vertical speed indicator which was a DC-10 type. The three DC-10 engine N_1 indicators were replaced with two DC-9 type EPR indicators. See Table D1 for list of instruments used. The First Officer's side remained in the DC-10 configuration.

Pilot Controls

The only changes made to the pilot controls were changes in the force gradients and the removal of the number three engine control lever. Figures D1 through D4 show the force versus position curves of the column, wheel, rudder pedals and toe brakes.

The spring rates of the column and wheel were changed to more closely match the DC-9. The force gradient of the rudder pedals was left the same as the DC-10. The force gradient of the toe brakes was adjusted using test pilot's comments. The curve shown is the gradient actually used.

As mentioned the number three (farthest right) engine control lever was removed leaving numbers one and two for independent twin engine control. A reverse thrust detent was added for the ground handling study. This addition is described in Appendix A Section 3 "Engine Model."

Pitch trim was provided through a thumb activated switch on the left hand side of the Captain's wheel and the right hand side of the First Officer's wheel.

Pilot Controls (Continued)

The speed brake and flap controls were DC-10 types but were active with the exception that the speed brake lever did not move with auto ground spoilers.

The nose wheel steering side controller "tiller" was not active for this study.

See Appendix A Section 2 "Aero and Control Systems" for additional descriptions of pilot controls.

Outside Visual Scene

The outside visual scene was provided by a Redifon Visual Flight Attachment (VFA). At the cockpit the VFA image is presented to the pilot by a T.V. monitor through large collimating lenses. The faces of the T.V. monitors are masked to provide the proper pilot eye cut off angle. For the DC-9 this angle is about 15.5° down from horizontal and was obtained in the DC-10 cockpit by moving the masks on the monitors up to a point where the cut off angle is correct, provided the eye is in the designated position. (See Figure D5.)

NOTE: It is very important for those "flying" the simulator (and the aircraft for that matter) to have their eyes in the proper position!

TABLE D1
EQUIPMENT USED FOR DC-9

| <u>VENDOR PART NO.</u> | <u>SERIAL NO.</u> | <u>NAME</u> | <u>VENDOR</u> |
|---------------------------|-------------------|--|---------------|
| 2067635-0701 TYPE 1NA-51A | 7526 | RADIO ALTIMETER IND. | BENDIX |
| 522-3907-001 TYPE 329B-7M | 666 | ALTITUDE INDICATOR (FLT DIR. INDICATOR) | COLLINS |
| 522-3875-002 TYPE 33/A-6K | E-5 | HOR. SITUATION IND. (COURSE INDICATOR) | COLLINS |
| A50D-10D KIT | 4191 | SIMULATED ALTIMETER | AEROSONIC |
| MS-45-1D KIT | 8252 | SIM. MACH/AIRSPD. IND. | MIDWAY |
| JG298H1 | B-416 | EPR INDICATOR | HONEYWELL |
| | B-432 | EPR INDICATOR | HONEYWELL |
| 2594468-902 | 2090895 | VERTICAL SPD. IND. | SPERRY |

DC-9 BRAKE SIMULATION MBS



FIG. 01

MODEL DC9-30

ESTIMATED WHEEL FORCE AS FUNCTION OF

WHEEL POSITION

$V_0 = 185 \text{ KTS} (1.31g + 5 \text{ KTS})$ CG @ 20.5% MAC

$\delta_T = 50^\circ/\text{EXT}$

APPROACH

NOTE AERODYNAMIC LOAD IS INCLUDED

AERO ESTIMATED CURVE

ACTUAL ON MBS

WHEEL FORCE, FW (LB)

δ_W (DEG)

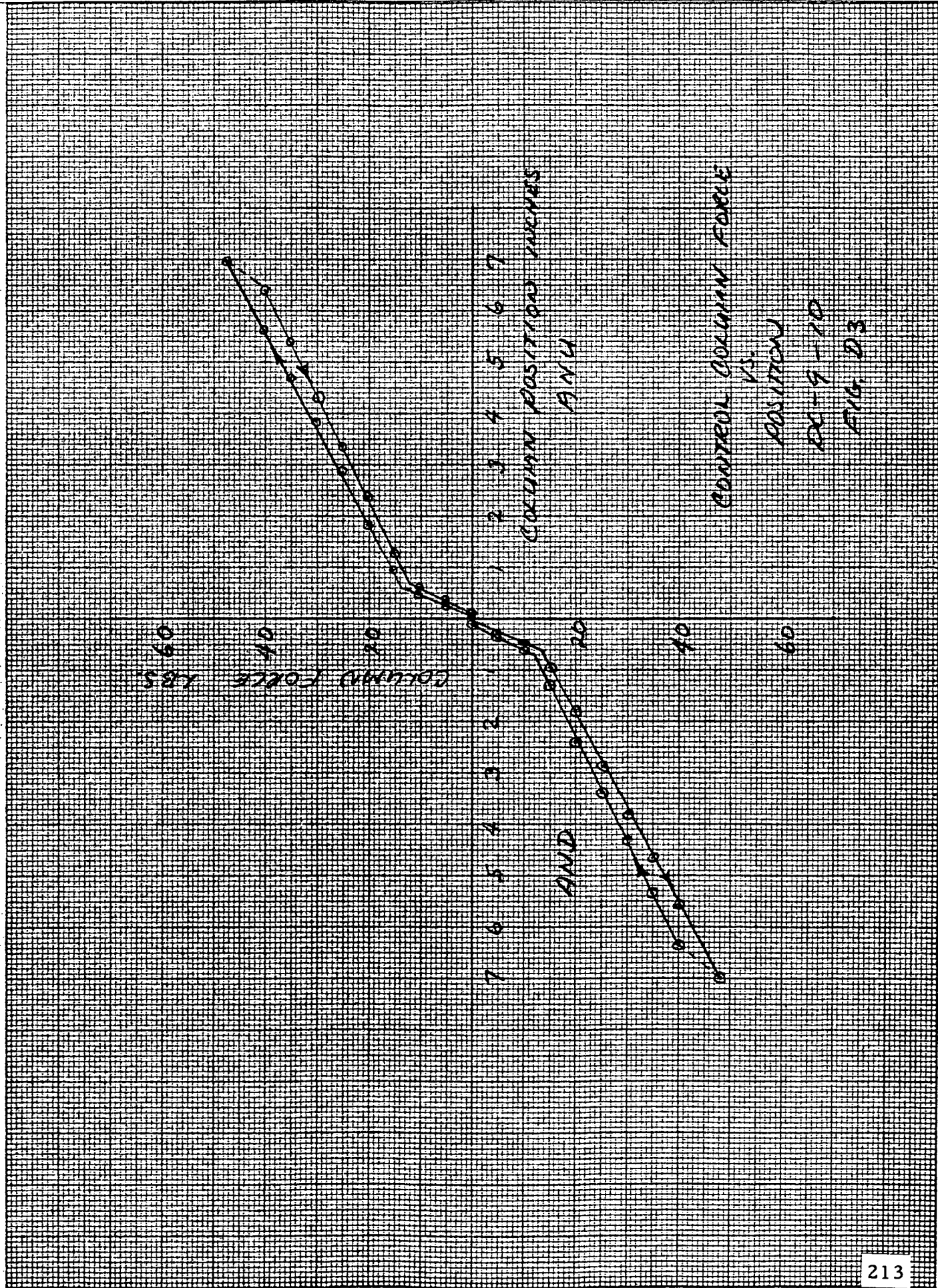
WHEEL POSITION

ROLL AXIS - MGT BASE SIM
DC-9 CONFIG - RED SPRINGS
AIL TAB THROW: $\pm 29^\circ$
T/E AIL, SURFACE THROW: $12^\circ \text{ UP}, 15^\circ \text{ DOWN}$

SYSTEM FRICTION: $\sim \frac{3}{4} \text{ \#}$

SIMULATION GOOD TO $\pm 50^\circ$ WHEEL
SC HLTZ 3/24/97

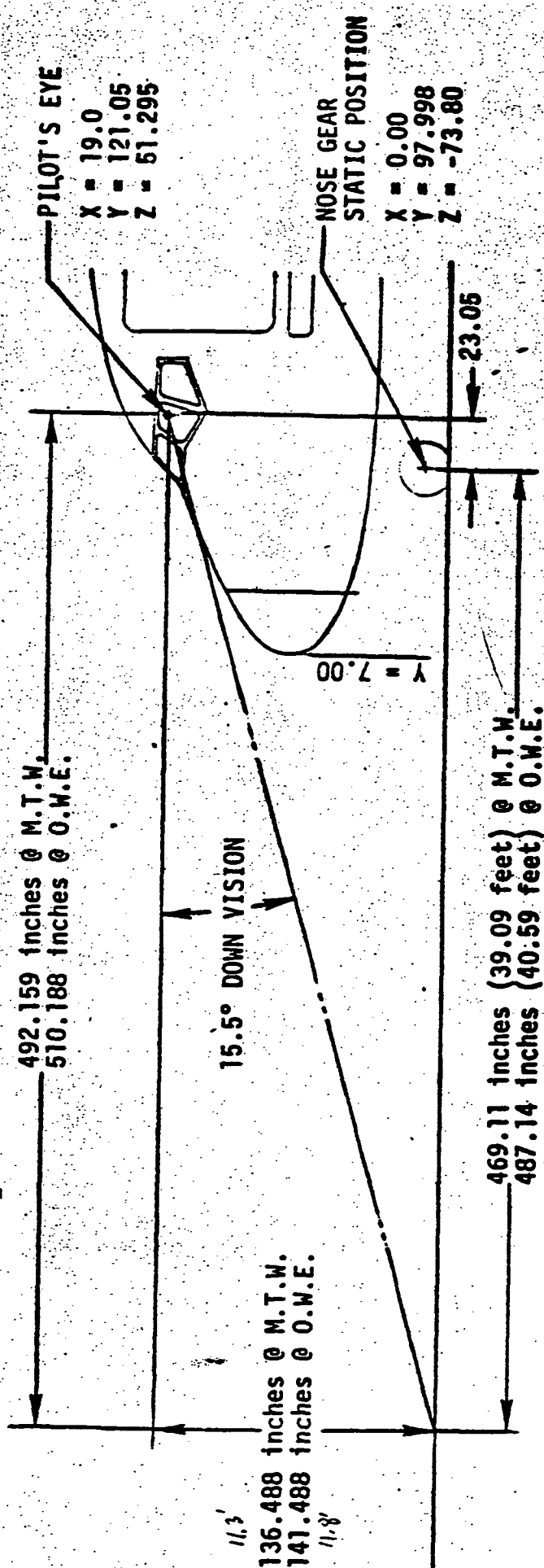
FIG. 02



CONTROL COLUMN FORCE
VS
POSITION
DC-9-10
FIG. D3



DC9-40 DISTANCE FROM
NOSE LANDING GEAR TO PILOT'S FORWARD VISION
CUT-OFF POINT



O.W.E. = OPERATING WEIGHT EMPTY
M.T.W. = MAXIMUM TAXI WEIGHT

DIMENSIONS ARE IN INCHES OR FEET

FIGURE D5

APPENDIX E
PROGRAMMING CONSIDERATIONS

This appendix covers some considerations in programming a digital computer to form a real-time solution to the airframe model. The term "real-time" in this context means that vehicle command inputs must be received and "next" airframe state variables calculated fast enough so that the various pilot displays can be updated with no perceptable "steps."

The DC-9-10 airframe model was programmed on the Systems Simulation Sigma V digital computer. An extended version of Fortran was used extensively as the programming language. All of the algorithms associated with the airframe simulation were solved at least once every 50 milli seconds. The single exception was a section of the strut routine (STRUTS) which was solved 7 times faster. The execution of the program took almost 100% of the 50 milli second frame.

When the simulation program was first assembled it took a few milli seconds longer than 50 to solve. This "overframing" condition was rectified by the following procedures:

- 1) All routines not specifically needed for RDC were taken out;
- 2) The beam noise was eliminated from the ILS model;
- 3) The turbulence filter parameters, which normally vary with speed and altitude, were calculated for a nominal speed and altitude and held constant during the real-time sequence. (See Sppendix A, Section 4 for description of the turbulence model);
- 4) The choice of 7 iterations per frame for a segment of the strut routine was due in part to timing considerations. (See Appendix A, Section 5);
- 5) Some other minor simplifications were made to the strut routine. (The statements preceded by an "X" in the Fortran listing of the STRUTS routine were left out).

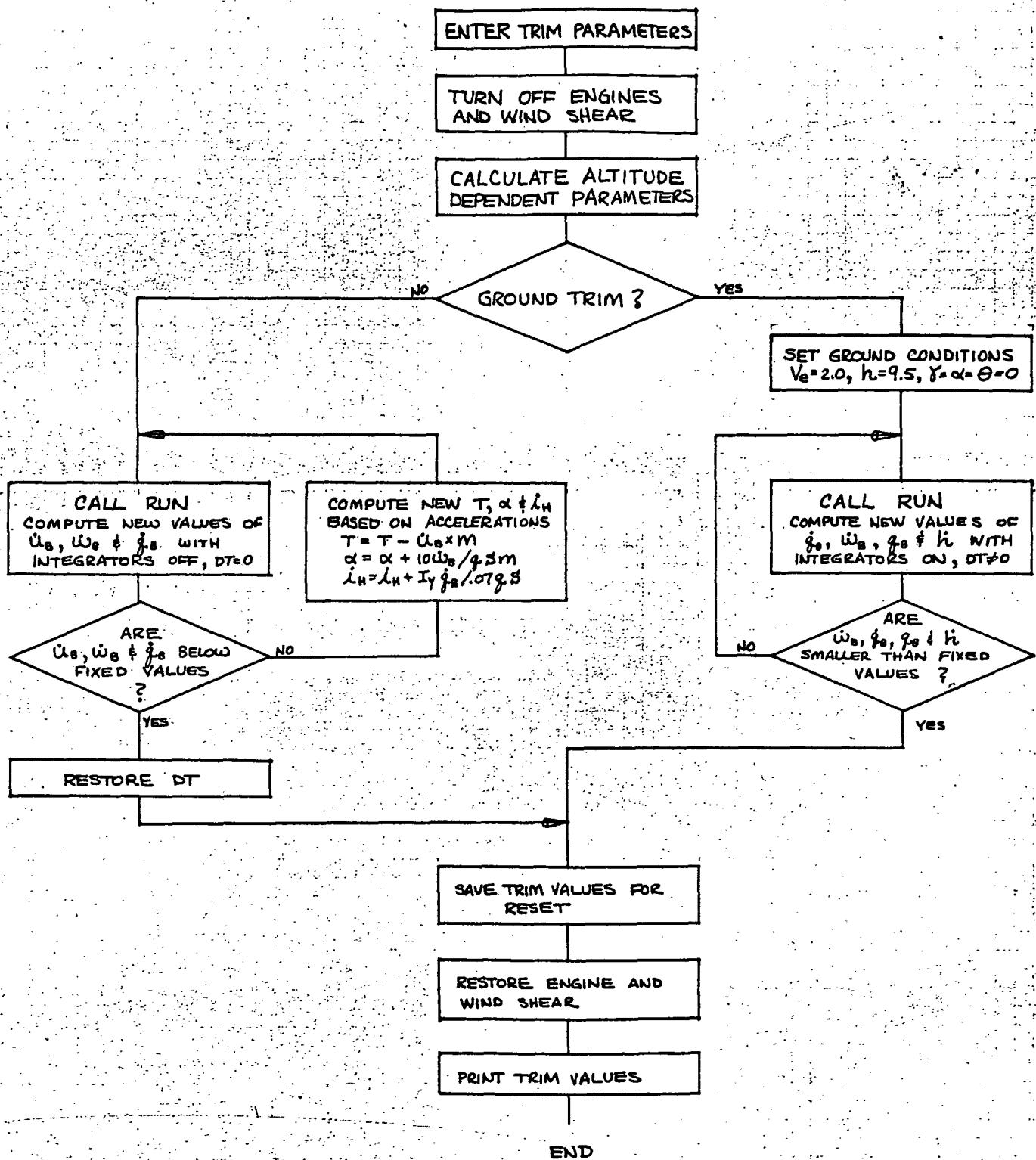
The above five items were specific things done to the RDC program to make it "fit" in the frame time. Some general techniques used by the Douglas Systems Simulation group to effect time saving are described below:

- Simple Euler integration is used throughout the program with the only exception being some linear transfer funtions where finite difference equations are used.

- A special limited range arc tangent routine was implemented. This routine, which is good for resultant angles between ± 20 degrees, was used for solving angle of attack, side slip angle and the ILS deviations.
- No matrix arithmetic or general matrix subroutines are used for real-time calculations.
- An attempt is made to minimize subroutine CALL's. Fortran CALL statements invoke linkage routines which can be time consuming.
- A careful check is made to be sure that all calculations of constants are done "outside" the real-time loop.

Another point of interest to programmers is that in the solving of the X and Z axes moments of the aircraft a cross inertia term must be dealt with. (See Appendix A, Section 1, Figure 1.2). For the RDC DC-9 model the \dot{P} and \dot{r} equations were solved using Cramer's rule to eliminate the "cross" terms. This technique seems to work quite well. However, in previous airframe simulations this same situation was handled by simply using the "past" value of one of the dot terms in the solution of current value of the other. This method also gave satisfactory results.

An important aspect of simulating an aircraft is providing the capability to place the simulated vehicle in different initial positions. A "trimming" process is necessary if it is desired to start the test run with the forces and moments balanced. A special trimming routine was implemented for this purpose. The desired aircraft configuration and position is input at the beginning of a series of runs. The calculations were made to trim the aircraft. These trim values were saved so each time the simulator was put in the reset mode they could be entered as initial conditions to the equations. A flow chart of the "trim" procedure is shown in Figure 1E.



VOLUME II REFERENCES

1. Expansion of Flight Simulator Capability for Study and Solution of Aircraft Directional Control Problems on Runways, Phase I, MDC Report A3304.
2. Expansion of Flight Simulator Capability for Study and Solution of Aircraft Directional Control Problems on Runways, Phase II, NASA CR-145044.
3. Russell V. Parrish, James E. Dieudonne, and Dennis J. Martin, Jr., 'Motion Software for a Synergistic Six-Degree-Of-Freedom Motion Base,' NASA TND-7350, 1973.
4. Harry Passmore and C. R. Korba, 'DC-9 Landing Gear Math Model for Directional Control on Runway Flight Simulation,' MDC Report A4816, 1977.
5. Sandy M. Stubbs and John A. Tanner, 'Behavior of Aircraft Antiskid Braking Systems on Dry and Wet Runway Surfaces,' NASA TND-8332, 1976.
6. Douglas Report No. LB-31624, 'Estimated Aerodynamics Data For Stability and Control Calculations, Model DC-9 Jet Transport, Series 10,' dated December 31, 1964 with latest revision February 23, 1967.
7. N. M. Barr, D. Gangass and D. R. Schaeffer, 'Wind Models for Flight Simulation and Certification of Landing and Approach Guidance and Control Systems,' Report No. FAA-RD-74-206 by Boeing Commercial Airplane Co., for U.S. Dept. of Transportation, December, 1974.
8. R. E. McFarland: NASA-Ames Program Specification, titled "Wind," Part No. NAPS-80, Computer Sciences Corporation NASA-Ames Site Operation.
9. R. V. Parrish, J. D. Rollins and Dennis J. Martin, Jr.: 'Visual/Motion Simulation of CTOL Flare and Touchdown Comparing Data Obtained from Two Model Board Display Systems,' AIAA Paper No. 76-010, April 26-28, 1976.
10. Redifon Report No. SD/846/S Issue 3, 'Requirements for the Compatibility of a McDonnell Douglas Corporation Flight Simulator to the Redifon Rigid Model Visual Flight Attachment,' January 12, 1971.

VOLUME II - REFERENCES (Cont'd)

11. E. A. Mechtly, "The International System of Units, Physical Constants and Conversion Factors," second revision, NASA Report No. SP-7012, 1973.